Multi-taxic palaeohistological analyses of vertebrates originating from the Upper Triassic at Krasiejów (SW Poland) and an assessment of growth patterns in comparative taxa

Dissertation
zur
Erlangung des Doktorgrades (Dr. rer. nat.)
der
Mathematisch-Naturwissenschaftlichen Fakultät
der
Rheinischen Friedrich-Wilhelms-Universität Bonn

von
Elżbieta M. Teschner
aus
Jastrzębie-Zdrój, Polen

Bonn, 2022

Angefertigt mit Genehmigung der Mathematisch-Naturwissenschaftlichen Fakultät
der Rheinischen Friedrich-Wilhelms-Universität Bonn

Gutachter: Prof. Dr. Thomas Martin
Gutachterin: Prof. Dr. Elena Yazykova

Tag der Promotion: 24.03.2023
Erscheinungsjahr: 2023

Acknowledgements

During the last few years, especially while I was working on this doctoral thesis, I have met an uncountable number of people at conferences, during research stays and on other formal and informal events - thank you for your support and fruitful discussions. I am endlessly grateful to Dorota Konietzko-Meier, who first offered me to work with temnospondyls under her supervision during my Master's thesis, and to whom I later presented the idea of this thesis. She supported me at every stage of the PhD, celebrated with me the successes and helped during the more challenging parts. I would like to thank the supervisors and commission members, especially Thomas Martin and Elena Yazykova, who have reviewed this work. I wish to thank my colleagues at the Institute of Geosciences in Bonn and the Institute of Biology in Opole for their support, many conversations and stimulating discussions. The Polish National Science Centre enabled me to do all the field work without which the sampling and laboratory work would not have been possible. I would like thank all my co-authors, from whom I learned a lot, for their patience and the possibility to work on joint projects. Over the years I have received support from my friends who had an open ear, motivated me, and distracted me when it was needed. Finally, my deepest thanks are dedicated to my family, especially my parents and siblings, and to Patrick, for their support, encouragement and understanding.

Summary

Palaeohistology is a useful tool for gaining direct information on skeletochronology, metabolic rate, growth rate or mode of life of extinct vertebrates. Moreover, the histological framework can also be applied for indirect reconstructions of palaeoenvironments and implications about palaeoclimate. The Upper Triassic at Krasiejów, in south-western Poland, preserves a unique bonebed in terms of quality and quantity of the material recovered. The taxa studied herein include the aquatic temnospondyl amphibians *Metoposaurus krasiejowensis*, and *Cyclotosaurus intermedius*, the aquatic to semi-aquatic phytosaur *Parasuchus* cf. *arenaceus*, the terrestrial aetosaur *Stagonolepis olenkae* and the volant proterosaur *Ozimek volans*. Of all taxa, humeri and femora were sampled in order to study histological growth. Moreover, it was tested if the observed growth pattern was either linked with phylogenetic position or ontogenetic stage, or if it showed influence of external signals, e.g., environmental and/or climatic factors. In addition to the temnospondyl amphibian *M.* krasiejowensis, the histological growth of the other taxa sampled herein was studied for the first time. Moreover, the histological growth pattern of *C. intermedius* described in this thesis, is the first description of a cyclotosaurid in general. Although, on the morphological level temnospondyl humeri from Krasiejów show only little distinction, on the histological level, the growth pattern of the *Cyclotosaurus* humerus differs distinctly from that of *Metoposaurus*. Thus, the histological variation within *Metoposaurus* humeri observed by Teschner et al. (2018), visible as two distinctly growing histotypes (histotype I and II), was not interspecific as previously assumed, but is rather linked with interspecific variation. Therefore, histotype I is the growth pattern of *Metoposaurus* and histotype II represents *Cyclotosaurus*. All sampled taxa from Krasiejów, independent of their phylogenetic placement or ontogenetic stage, have a lamellar-zonal bone type (LZB) built of parallel-fibred bone with various organisation level of collagen fibres, occasionally grading into lamellar bone. The growth marks are always preserved in the form of alternating vascularised zones and almost avascular annuli. Striking is the lack of the deposition of Lines of Arrested Growth (LAGs) in the cortex. The vascularisation varies between taxa and also between skeletal elements, but is mostly preserved in the form of simple vascular canals in younger individuals, and with increasing ontogenetic stage, it becomes intermixed with primary and secondary osteons. The older the specimen, the more erosion cavities are preserved and the more remodelled the primary tissue becomes. Surprisingly, both the amphibians and reptiles grew in a similar fashion, despite their distant phylogenetic relationship. This implies that the influence of external features on the growth pattern was stronger than the primary phenotypic signal. The only taxon from Krasiejów in which growth was different, *O. volans*, retains thin lamellae building the cortex and show deposition of LAGs, beside cyclical deposition of zones and annuli. However, this unique framework is rather linked with the biomechanical bone adaptation to the gliding mode of life, than implying an environmental and/or climatic signal. The comparative taxa used from other localities, such as the phytosaur *Nicrosaurus* sp. and the aetosaur *Aetosaurus ferratus*, both from southern Germany, and the temnospondyl amphibian *Panthasaurus maleriensis* from India, showed that the animals had the same tissue type as the Polish taxa during growth, but either revealed deposition of LAGs e.g., in *Nicrosaurus* or demonstrated that the taxa were ontogenetically too young, e.g., *Aetosaurus* to be able to deposit growth marks. Further, a comparison with literature data has shown, that growth in aetosaur and phytosaur taxa from North and South America was characterised by a more rapidly deposited fibro-lamellar bone type than in Polish taxa, but still show the deposition of LAGs, which is distinctly different from the specimens sampled herein. Moreover, the temnospondyl amphibian from Morocco, *Dutuitosaurus ouazzoui*, grew with LZB, similar to the taxa sampled herein, but preserved extraordinarily expressed, multiple LAGs. This suggests that the climate between Europe and Asia and that of North and South America and Africa was different during the Late Triassic, and this had a strong influence on the growth pattern of taxa belonging to the same family (e.g., *Metoposaurus* and *Panthasaurus* vs. *Dutuitosaurus*), and occupying the same ecological niche but separated geographically; similar to aetosaurs and phytosaurs. This is the first study to sample phylogenetically distant taxa from the same locality, yielding new insights into the biology of animals that shared a complex ecosystem. Since previous studies typically only use single taxa and/or elements, this comprehensive comparative analysis on a complete ecosystem, took into account possible alteration of growth pattern such as bone adaptation, phylogenetic relationship or ontogenetic stage.

Structure of the dissertation

This dissertation consists of seven chapters. Chapter 1 provides an overview of the research problem, i.e., the influence of external factors on the growth pattern; it also provides an introduction into palaeohistology, the geological background of the sampling locality and summarizes previous palaeohistological analyses.

Chapters 2 and 4 have already been published in international peer-reviewed journals. Chapter 2 was published in *PeerJ* and Chapter 4 in *Contributions to Zoology*. According to the regulations, both chapters appear only in a summarized form in this dissertation, and the original published papers can be found in the appendices (Appendix A and Appendix B), with page format and page numbering matching dissertation style.

Chapters 3, 5 and 6 are finished manuscripts, submitted to peer-reviewed scientific journals (*Acta Palaeontologica Polonica*, *Journal of Vertebrate Paleontology* and *Palaeontology* respectively) and are currently under review. They follow the individual journal styles and the only modification applied herein is the change of figure numbering to adapt to the dissertation style.

For Chapters 2–6 author contributions were provided at the beginning of each separate section.

Chapter 7 gives an insight into the influence of external factors on growth pattern modification by taking into consideration various factors, e.g., genetic constraint, ontogeny or phylogenetic signal. It summarizes the growth of sampled taxa from Krasiejów and compares the growth of other, closely related taxa known from the literature. Moreover, it discusses future perspectives and possibilities of applying palaeohistological methods on similar case studies worldwide.

Contents

Chapter 1

General Introduction

1.1 Taxonomic Review of the Triassic Krasiejów fauna and flora

Krasiejów is an exceptional Upper Triassic paleontological locality in south-western Poland with thousands of fossil bones preserved (Dzik et al. 2000). The macro fauna is morphologically well studied, and represents both amniotes and non-amniotes. The vast majority of the skeletal elements belongs to the aquatic temnospondyl amphibian *Metoposaurus krasiejowensis* Sulej, 2002 (Fig. 1.1). Moreover, there is also a second, aquatic temnospondyl amphibian *Cyclotosaurus intermedius* Sulej and Majer, 2005, however it occurs less commonly in comparison to *M. krasiejowensis*. Further, the reptile fauna is represented by the semi-aquatic to aquatic phytosaur *Parasuchus* cf. *arenaceus* (Dzik, 2001), the terrestrial aetosaur *Stagonolepis olenkae* Sulej, 2010 and silesaurid *Silesaurus opolensis* Dzik, 2003. Less commonly found, there are cranial remains and teeth of the large terrestrial rauisuchid *Polonosuchus silesiacus* (Sulej, 2005). The small gliding protorosaur *Ozimek volans* Dzik and Sulej, 2016 is known from few skeletal elements preserved in few blocks.

Figure 1.1 Picture of the in-situ preserved Upper Triassic bonebed in Krasiejów. All visible material belongs to the temnospondyl amphibian *Metoposaurus krasiejowensis*. Most abundant skeletal elements in the picture are skulls and vertebrae, moreover, there are lower jaws, clavicles and interclavicle; note, that all material is disarticulated. Scale bar equals 20 cm.

The vertebrate micro fauna is mostly known from small-sized teeth, tooth plates or scales, but shows a higher taxonomic diversity (Skrzycki 2015, 2016; Antczak and Bodzioch 2018; Kowalski et al. 2019; Sulej et al. 2021). The aquatic fauna is represented by hybodont sharks, palaeoniscids, semionotids, redfieldiids, dipnoan and ganoid fishes, and unidentified temnospondyl amphibians (Skrzycki 2015, 2016; Antczak and Bodzioch 2018; Kowalski et al. 2019). The terrestrial micro fauna is represented by cynodonts, rhynchocephalian lepidosauromorphs and several small archosauromorphs, e.g., protorosaurians, pseudosuchians, theropod dinosaur and most probably a basal sauropodomorph and a crocodylomorph (Kowalski et al. 2019; Sulej et al. 2021).

The invertebrates are represented mostly by bivalves, especially *Silesunio parvus* Skawina and Dzik, 2011, a crab-like crustacean *Opolanka decorosa* Dzik, 2008, spinicaudatan crustaceans (Olempska 2004), ostracods and phyllopods (Dzik 2008). Coleopteran beetles described from this locality were found in coprolite material (Qvarnström et al. 2019).

Plant remains are not abundant and poorly preserved in the sediments from Krasiejów, however, the most abundant are charophytes, a green algae group from the family Porocharaceae (Zatoń et al. 2005). Moreover, *Neocalamites merianii* and *Sphenopteris* sp. were documented in the Krasiejów bonebed (Pacyna 2019).

1.2 Geological Background of the Krasiejów deposit

The geologic age of the Krasiejów site is still controversial, based on biostratigraphy and the correlation with beds in Southern Germany, a Carnian age was first proposed (Dzik et al. 2000). On the other hand, a Norian age was proposed according to lithostratigraphic, sedimentologic and taphonomic studies (Szulc 2005; Bodzioch and Kowal-Linka 2012; Szulc and Racki 2015; Szulc et al. 2015, 2017; Racki et al. 2017; Jewuła et al. 2019). The origin of the accumulation is reconstructed as having formed after a catastrophic event (Bodzioch and Linka, 2012). Further, Jewuła et al. (2019) reconstructed the Krasiejów area during the Upper Triassic as a fresh water reservoir resembling a modern gilgai realm. This is in contradiction to the previously proposed lacustrine origin of the sediments (Dzik et al. 2000; Dzik 2003).

The Late Triassic climatic conditions in general are being reconstructed as similar to today's monsoonal climate with seasonal fluctuations of dry and rainy episodes (Dubiel et al. 1991; Dickins 1993; Parrish 1993). Most probably it also applied to the Upper Triassic at Krasiejów (Jewuła et al. 2019). Moreover, based on mineralogical analysis, an arid to semi-arid climate was proposed (Zatoń et al. 2005). Additionally, first histological data on animals recovered from the Krasiejów site also showed cyclical growth in long bones, which most probably correspond to the seasonal fluctuations of the climate (Konietzko-Meier and Klein 2013; Konietzko-Meier and Sander 2013).

1.3 Palaeohistology of previously sampled taxa from Krasiejów

Palaeohistology provides information about the animals individual age, diet, metabolic rate and even the habitat or the relative climatic conditions (Francillon-Vieillot et al. 1990; de Buffrénil et al. 2021). A complete growth cycle consists of a zone, an annulus and a Line of Arrested Growth (LAG) (Francillon-Vieillot et al. 1990). Zones represent phases of fast bone deposition with vascularised, less organized bone tissue, whereas annuli are slowly deposited, highly organised and avascular bone structure (Francillon-Vieillot et al. 1990; de Buffrénil et al. 2021; Fig. 1.2). Zones can be correlated with active growth phases when there was enough nutrition, water, etc. to keep the animal alive during a favourable season, whereas annuli indicate episodes of slowed-down phases of growth with less food availability and generally harsher conditions, deposited during an unfavourable season. LAGs indicate a complete cessation of growth, and are correlatable with biological factors, but can also be climatic indicators for very drastic and extremely unfavourable conditions (Francillon-Vieillot et al. 1990; Steyer et al. 2004).

The two main bone tissue types are lamellar zonal bone (LZB) or fibro-lamellar bone (FLB; Francillon-Vieillot et al. 1990; de Buffrénil et al. 2021). LZB is characterized by the deposition of parallel-fibred and lamellar bone at a rather lower growth rate, and a low to moderate vascularisation density and stratification by growth marks (Francillon-Vieillot et al. 1990). Contrary to that FLB is characterised by a fast deposition rate of woven bone and parallel-fibred bone with high vascularisation density and almost uninterrupted bone deposition (Francillon-Vieillot et al. 1990). LZB is associated with exothermic animals e.g., Temnospondyli (de Ricqlès 1979; Steyer et al. 2004; Ray et al. 2009; Witzmann 2009; Mukherjee et al. 2010; Sanchez et al. 2010a, b; Sanchez and Schoch 2013; Konietzko-Meier and Klein 2013; Konietzko-Meier and Sander 2013; McHugh 2014), whereas FLB is typically found in endothermic animals e.g. most dinosaurs and mammals (Francillon-Vieillot et al. 1990; Horner et al. 2000; Horner and Padian 2004; Sander and Andrassy 2006; Klein and Sander 2007; Köhler et al. 2012; Fig. 1.2). FLB deposition was also observed in basal Archosauria (de Ricqlès et al. 2003, 2008), however, pseudosuchian archosaurs show a varied tissue type deposition across a clade and can even change within a family (de Ricqlès et al. 2003, 2008; Klein et al. 2017; Teschner et al. 2022; Fig. 1.2).

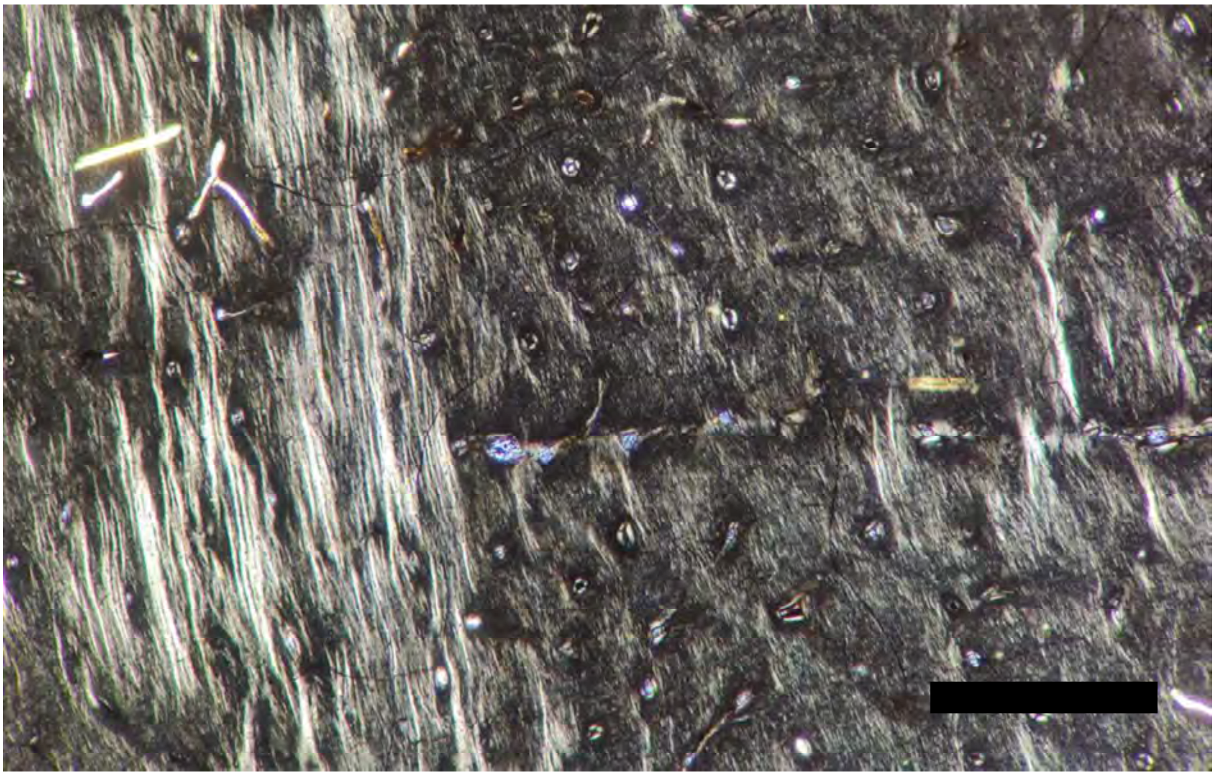

Figure 1.2 Histological section of *Stagonolepis olenkae* humerus (UOPB 00120) from Krasiejów locality in polarized light. The section is divided in higher organized collagen fibres forming parallel-fibred bone grading into lamellar bone (corresponding with an annulus) on the left and less organized collagen fibres forming parallel-fibred bone (corresponding with a zone) on the right. The bone grows with a lamellar-zonal bone tissue. Scale bar equals 0.5 mm.

Palaeohistological analyses are destructive in nature, therefore, the acquisition of material can be problematic. The Upper Triassic at Krasiejów on the other hand, due to the high quantity and quality of fossil finds (Fig. 1.1), enables palaeohistological analyses on multiple elements but also on various taxa. The most abundant and the best studied taxon from Krasiejów is *M. krasiejowensis,* as the cranium (Gruntmejer et al. 2016, 2019a; Konietzko-Meier et al. 2018), lower jaw (Gruntmejer et al. 2019b; 2021), the pectoral girdle and ribs (Gądek 2012; Kalita et al. 2022), vertebrae (Konietzko-Meier et al. 2012, 2014) and even long bones (Konietzko-Meier and Klein 2013; Konietzko-Meier and Sander 2013; Teschner et al. 2018) were studied.

All bones of *M. krasiejowensis* grow with a lamellar-zonal bone pattern and they show the deposition of parallel-fibred bone of varying degree of fibres organisation, and with lamellar bone, and a varying density of vascular canals (Gądek 2012; Gruntmejer et al. 2016, 2019a, 2019b, 2021; Kalita et al. 2022; Konietzko-Meier and Klein 2013; Konietzko-Meier and Sander

2013; Konietzko-Meier et al. 2012, 2014, 2018; Teschner et al. 2018). Moreover, the long bones show a cyclical growth deposition of vascularised zones and avascularised annuli (Konietzko-Meier and Klein 2013; Konietzko-Meier and Sander 2013; Konietzko-Meier et al. 2012, 2014, 2018; Teschner et al. 2018). In the *M. krasiejowensis* femora, additionally incipient fibro-lamellar bone was observed in the juvenile individuals (Konietzko-Meier and Sander 2013). From the *Metoposaurus* vertebrae mostly the intercentrum is preserved, it consists of endochondral and periosteal domain. The latter grows also with parallel-fibred bone, showing similar structure to that preserved in long bones. In endochondral domain the most characteristic feature is the preservation of calcified cartilage (Konietzko-Meier et al. 2012, 2014).

The cyclically growing long bones or vertebrae are of endochondral origin, whereas dermal bones form during the intramembranous ossification, and therefore, preserve different histological structures (de Buffrénil et al. 2021).

The dermal bones of *M. krasiejowensis* consist of a compact external cortex, a spongious inner region and a compact inner cortex (Gądek 2012; Gruntmejer et al. 2016, 2019a, 2019b, 2021; Kalita et al. 2022; Konietzko-Meier et al. 2018). The microstructure and histology of cranial bones is a good source of information about the biomechanical processes as the bone reacts on local stress by increasing or decreasing its porosity; this principle was applied for the reconstruction of the feeding behaviour of *M. krasiejowensis* (Gruntmejer et al. 2016, 2019a, 2019b, 2021). Most recent study showed, that dermal bones are also a good source of information regarding the mode of life (Kalita et al. 2022). However, dermal bones are not useful for the reconstruction of skeletochronology, due to the different bone origin between long bones and dermal bones (Klein et al. 2009; Hayashi et al. 2013).

The second taxon from Krasiejów studied palaeohistologically is the silesaurid *Silesaurus opolensis* (Fostowicz-Frelik and Sulej 2010). The sampled femora, tibiae, a metatarsal and ribs belonged to ontogenetically different individuals, however, not all samples were taken from the histological midshaft, which most probably altered the signal observed. The bones grew with fibro-lamellar bone with a dense network of longitudinal vascular canals, moreover, the bones grow with almost no interruption by annuli or LAGs, and show no signs of remodelling (Fostowicz-Frelik and Sulej 2010). Only one tibia (ZPAL ab III/1885) of *S. opolensis* showed LAGs in the outermost cortex and a decreasing vascularisation density towards the outer cortex surface (Fostowicz-Frelik and Sulej 2010). Fostowicz-Frelik and Sulej (2010) interpreted the growth of *S. opolensis* as a dinosaur-like pattern, and a probably endothermy in this animal. Interestingly, LAGs are absent in the previously sampled

Metoposaurus bones from the Krasiejów bonebed (Konietzko-Meier and Klein 2013; Konietzko-Meier and Sander 2013; Teschner et al. 2018).

1.4 The influence of external factors on the growth pattern

The variation of histological growth observed within the humeri belonging to the temnospondyl amphibian *Metoposaurus krasiejowensis* was unexpected (Teschner et al. 2018). A histological study of 12 humeri has shown that despite a rather uniform morphology, the bones grow histologically with two distinct growth patterns. Therefore, the Histotype I (H1) showed a cyclic growth with broad phases of rapid growth with less organised bone structure and high vascularisation, and phases deposited as similarly sized or thinner, avascular and highly organised bone (Teschner et al. 2018). Histotype II (H2), on the contrary, showed an extremely broad phase of rapid growth with numerous vascular canals in a less organised bone matrix, and only very thin, and occurring in the outer cortex, highly organised and avascular rings. Moreover, after the comparison of the same bone length, the H1 shows signs of remodelling, whereas H2 bone remodelling is almost absent (Teschner et al. 2018).

The preliminary explanation, why the histotypes occurred within the *M. krasiejowensis* humeri, was two-fold, namely, it was either intraspecific variation, or interspecific variation (Teschner et al. 2018). In terms of intraspecific variation, the occurrence of two different species was hypothesised, however, it was rendered as unlikely, although, the Krasiejów locality preserves a second temnospondyl amphibian, namely *C. intermedius* (Teschner et al. 2018). Moreover, at that time, no histological growth of a cyclotosaurid long bone was known. The interspecific variation was proposed to be either connected with a population separation, this could be geographic and/or time separation, or with the presence of sexual dimorphism (Teschner et al. 2018). In order to explain better the occurrence of H1 and H2 in *M. krasiejowensis* humeri (Teschner et al. 2018), more material was sampled and examined within this thesis.

1.5 Aim of dissertation

The focus of this dissertation is to test palaeohistologically, how does external factors alter the individual growth pattern of various taxa. The novelty of this study relies on sampling a complete ecosystem including both, amniotes and non-amniotes, that lived near-by and therefore, were most probably exposed on the same climatic conditions. In addition, the sampled bones belong to animals originating from one locality, however occupying various habitats e.g., terrestrial, semi-aquatic, aquatic and gliding forms. Krasiejów bonebed, due to the numerous finds, gives the opportunity to sample multiple skeletal elements from various taxa.

1.6 Description of chapters

Chapter 2 discusses the histological growth of *Panthasaurus maleriensis*, a metoposaurid from the Late Triassic Maleri Formation in India. Several long bones (two humeri, a femur, a tibia and an ulna), a rib and an intercentrum were sampled histologically. All studied bones originated from the same locality, and are housed at the Indian Statistical Institute in Kolkata. As and approach towards the explanation of the two Histotypes *sensu* Teschner et al. (2018), observed in *Metoposaurus krasiejowensis* from Poland, a comparison of growth patterns between these two taxa was made. Moreover, the literature data for the femora of the Moroccan metoposaurid *Dutuitosaurus ouazzoui* were used for comparison. All bones grew with lamellar-zonal bone, and showed the deposition of alternating growth cycles including zones and annuli, and only the Moroccan taxon showed LAGs in the cycle, indicating harsher climatic conditions in Morocco during the Late Triassic. Moreover, the *P. maleriensis* humeri show, with increasing ontogeny, prominent thinning of zone thickness towards the outermost cortex, a similar scenario was previously observed in *D. ouazzoui* femora (no humeri were sectioned from this taxon until now).

Chapter 3 describes the growth between two exceptionally large humeri, until now the largest known from Krasiejów. Both bones are of nearly the same size and are morphologically almost uniform, however, histologically, the humeri grow with two strikingly different growth patterns. Therefore, the alternating growth with the zones becoming distinctly thinner towards the outermost cortex is assumed to represent *Metoposaurus krasiejowensis*, whereas the other specimen with still thick zones and very thin annuli and a low degree of remodeling belongs to *Cyclotosaurus intermedius*, and therefore, provides the first description for humeral growth for a *Cyclotosaurus.* This study shows also, that the morphological shape among Stereospondyli does not differ much, and within a disarticulated bonebed with multiple temnospondyl taxa, makes is almost impossible to distinguish even on a generic level.

Chapter 4 represents the first histological growth description of *Stagonolepis olenkae* and *Parasuchus* cf. *arenaceus* humeri and femora from Krasiejów. The former being a terrestrial aetosaurs and the latter a semi-aquatic to aquatic phytosaurs. For comparison of the growth pattern, a phytosaur *Nicrosaurus* femur from the German Heslach locality, of a similar geologic age (Norian) and of a similar size/length as the Polish *Parasuchus*. The main focus lies on the comparison of growth between taxa not closely related but originating from the same locality (*Stagonolepis* vs. *Parasuchus*), and taxa closely related (*Parasuchus* vs. *Nicrosaurus*) but originating from different localities, in order to see how the growth pattern gets influenced by the phylogenetic signal, different niche occupation and the geographic separation. Stunningly, the growth pattern of *Stagonolepis* and *Parasuchus* are very similar, beside the different niche occupation, thus a different mode of life, and a more distant phylogenetic relationship, those two taxa from Krasiejów show a very similar growth pattern. More interestingly, both taxa do not show clear LAGs, and only show rest lines. However, the *Nicrosaurus* femur from Germany, beside the close phylogenetic relationship with *Parasuchus* shows a more varied growth pattern, remodelling pattern in the inner cortex which is probably influenced by the niche occupation, and it shows one LAG in the outer cortex. It seems, that the external factors, e.g., climatic conditions, had a major influence on the growth pattern, even if the animals are not closely related.

Chapter 5 gives insight into the growth of juvenile aetosaurs *Aetosaurus ferratus* from the Late Triassic (middle Norian) Kaltental from Germany. The sampled humeri originate from an astonishing accumulation of 24 small-sized aetosaurs. The comparison was made to see how the early ontogenetic stage looks histologically, and if it is possible to find out, if *Aetosaurus* is a juvenile stage or a dwarfed species. The study shows, that *A. ferratus* is an early ontogenetic stage, showing locally growth lines, which might represent a hatchling bone, and thus it is the first report of such for aetosaurs. Moreover, it shows possible evidence of gregarious behaviour among pseudosuchians.

Chapter 6 provides the first histological description of *Ozimek volans* long bones, the gliding representative from the Krasiejów bonebed. It gives the first attempt to tests histologically if *O. volans* was able to perform gliding flight. This is the only taxon from Krasiejów sampled herein, showing the deposition of LAGs. However, the LAGs deposition is most probably connected with the specialized niche occupation and thus the histological framework is an adaptation to withstand the biomechanical stress generated during the gliding flight, rather than is linked with climatic conditions.

Chapter 7 discusses the influence of external conditions, e.g., environmental or climatic influence. The most important factors to consider during the interpretation of data, is the comparison between the same elements. Further, the ontogenetic stage of the sampled should be considered, thus a juvenile specimen might show different features than an adult specimen. Next, the phylogenetic signal or the genetic constraint might be stronger and therefore, the growth pattern by not get altered by the external factors. The climatic and environmental conditions, had a major influence on the growth pattern, on both, amniotes and non-amniotes taxa from Krasiejów.

Chapter 2

Climatic influence on the growth pattern of *Panthasaurus maleriensis* from the Late Triassic of India deduced from paleohistology

2.1 Authors and their contributions

Teschner, E. M., Chakravorti, S., Sengupta, D. P., and D. Konietzko-Meier. 2020. Climatic influence on the growth pattern of *Panthasaurus maleriensis* from the Late Triassic of India deduced from paleohistology. *PeerJ*, 8: e9868.

EMT and DK-M designed the study; SC and DPS provided material; EMT selected the material, took photographs and micrographs and prepared thin-sections in the laboratory; EMT and DK-M analysed the thin-sections; EMT wrote the manuscript draft and prepared figures; SC wrote parts of the *Geology* section; DK-M critically revised the first draft; EMT revised the manuscript; All authors accepted the final version for submission. The doctoral student and the supervisor confirm that all co-authors are in agreement with the publication being used for the doctoral thesis.

2.2 Article Summary

Temnospondyli Zittel, 1888 are a wide clade of extinct amphibians, ranging from the Early Carboniferous to Early Cretaceous (Holmes and Carroll 1977; Warren et al. 1997), and are preserved worldwide (Schoch 2013). Stereospondyli Zittel, 1888 is a group of temnospondyl amphibians, in which the family Metoposauridae Watson, 1919 is placed (Schoch 2013). The stratigraphic range of metoposaurids is limited to the Late Triassic (Norian-Carnian) and their geographic occurrence is almost global, except for Australia and Antarctica (Schoch 2003, 2013). Metoposaurids, especially the species *Metoposaurus krasiejowensis* Sulej, 2002 is a well-studied group, in terms of the phylogenetic position (morphology, morphometrics), mode of life (computer modelled biomechanics) and even histological growth (palaeohistology). *Panthasaurus maleriensis* Chakravorti and Sengupta, 2019 is the southernmost record of Metoposauridae occurring in the Maleri Formation inside the Pranhita-Godavari basin in Central India (Roychowdhury 1965; Sengupta 2002), and until now it was not studied histologically. Beside the bonebed in the Grabowa Formation in south-western Poland, including *M. krasiejowensis* from Krasiejów (Racki et al. 2017), the Argana Basin in the south-western part of Morocco, preserves *Dutuitosaurus ouazzoui* Dutuit, 1976 (Sulej 2007; Steyer et al. 2004). However, as for *M. krasiejowensis* almost every skeletal element was studied histologically (Gądek 2012; Gruntmejer et al. 2016, 2019a, 2019b, 2021; Kalita et al. 2022; Konietzko-Meier and Klein 2013; Konietzko-Meier and Sander 2013; Konietzko-Meier et al. 2012, 2014, 2018; Teschner et al. 2018), for *D. ouazzoui* only femora were sectioned (Steyer et al. 2004). Herein, we studied histologically long bones (humeri, femur, tibia and ulna), a rib, an ilium and an intercentrum, belonging most likely to eight individuals ranging from different ontogenetic stages. The main aim of the study was to analyse the intraspecific variability and the relationship between the observed growth pattern and climatic and/or environmental conditions. Further, the newly studied material of *P. maleriensis* was compared to the bone growth of *M. krasiejowensis* and *D. ouazzoui*. All *Panthasaurus* samples show a lamellar-zonal tissue type with primary cortex built of parallel-fibred bone consisting various degrees of fibre organisation. *P. maleriensis* long bones grow uniformly, and no varied growth pattern is observed, contrary to the histotypes observed in *M. krasiejowensis* humeri (Teschner et al. 2018). Moreover, the long bones and the rib show a cyclical growth with the deposition of vascularised zones (with lower organisation degree of fibres) and avascular annuli (with higher organisation degree of fibres). The ilium is highly remodelled and preserves a metaplastic-like structure, whereas the intercentrum preserves an endochondral and periosteal domain. With increasing ontogenetic stage, in the long bones towards the outermost cortex surface, the thickness of zones is decreasing, whereas annuli become thicker or grow with the same thickness. Lines of Arrested Growth (LAGs) are absent in the Indian sample, instead only multiple resting lines are preserved in the outer annuli, in both, the limb bones and the rib section. The occurrence of rest lines might be connected with climatic and environmental influence and not with ontogeny, as the rest lines occur inside the annulus, therefore, during the unfavourable season. Since a similar histological framework, without the deposition of LAGs, was observed in *M. krasiejowensis* (Konietzko-Meier and Klein 2013; Konietzko-Meier and Sander 2013; Teschner et al. 2018), the local climate was presumably relatively mild in India and Poland during the Late Triassic. In contrast to that is Morocco during the Late Triassic, with most probably a harsher climatic condition, since the femora of *D. ouazzoui* preserve numerous, regularly deposited LAGs throughout the ontogeny (Steyer et al. 2004).

Chapter 3

Palaeohistology helps reveal taxonomic variability in exceptionally large temnospondyl humeri from the Late Triassic Krasiejów deposit (SW Poland)

3.1 Authors and their contributions

Teschner, E. M., Garbay, L., Janecki, P., and D. Konietzko-Meier. Palaeohistology helps revealing taxonomic variability in exceptionally large temnospondyl humeri from the Late Triassic Krasiejów deposit (SW Poland). Submitted to *Acta Palaeontologica Polonica* on September 30th, 2022; 1st revision submitted on November 25th, 2022; 2nd revision submitted on December 7th 2022.

EMT and DK-M designed the study; EMT selected the material and prepared thin-sections in the laboratory; EMT and DK-M analysed the thin-sections; LG and PJ analysed the bone morphology; PJ partially prepared figure 3.4; EMT took photographs and micrographs, wrote the manuscript draft and prepared the final figures; LG measured the bones and wrote the *Morphology* section; DK-M critically revised the first draft; EMT revised the manuscript; All authors accepted the final version for submission. The doctoral student and the supervisor confirm that all co-authors are in agreement with the publication being used for the doctoral thesis.

3.2 Abstract as submitted to *Acta Palaeontologica Polonica*

For more than twenty years, palaeontological excavations have been carried out at the Late Triassic site of Krasiejów (south-west Poland), providing thousands of skeletal elements belonging to various tetrapod groups. However, almost all bones are preserved in a disarticulated state. This generates problems in taxonomic assignment among closely related groups, e.g., temnospondyl amphibians. As far as cranial elements, the pectoral girdle bones and the intercentra are very diagnostic, all other remaining skeletal elements are difficult to unambiguously assign between either the trematosaurid *Metoposaurus krasiejowensis* or the capitosaurid *Cyclotosaurus intermedius*, both originating from Krasiejów. Especially, since comparative postcranial material from other Late Triassic localities worldwide is very rare or even absent, making the assignment on a genus level even more problematic. With the help of bone histology, we tested the taxonomic assignment of two exceptionally large humeri with only marginally differing morphology. Both humeri show lamellar-zonal bone and preserve

between four to seven visible growth cycles, but with a markedly different amount of primary tissue, a varying degree of remodelling and a distinct growth pattern. Considering the fact that both humeri are almost the same size, they show a different histological ontogenetic stage, implying an assignment to two different genera. Therefore, the specimen UOBS 02431 shows advanced remodelling, residuals of primary bone, distinctly decreasing thickness of zones towards the outer cortex, and thick annuli and is assigned to *M. krasiejowensis*. Whereas the specimen UOBS 02116 shows limited remodelling, with large amount of primary bone preserved as alternating thick zones and thin annuli, it is considered to represent *C. intermedius*. This study shows that temnospondyl amphibians might show only minor differences in humeral morphology, making histology an even more valuable tool for taxonomic assignment at a genus level.

3.3 Introduction

Temnospondyli Zittel, 1888 is one of the largest non-amniote tetrapod orders, distributed globally with a wide stratigraphic occurrence ranging from the Early Carboniferous to the Early Cretaceous (Holmes and Carroll 1977; Warren et al. 1997). The systematics of Temnospondyli are based almost exclusively on cranial characters (Schoch 2013). Articulated postcranial material of Mesozoic temnospondyls is very rare, e.g., *Dutuitosaurus ouazzoui* (Dutuit, 1976), *Paracyclotosaurus davidi* Watson, 1958, and therefore intraspecific variability at the generic level is not well understood. This makes the assignment of disarticulated bones to a specific genus or species even more difficult and problematic when at least two temnospondyl amphibian species co-occur together in a single locality. This scenario applies to the Polish Late Triassic (Norian) Krasiejów clay pit, preserving at least two temnospondyl amphibians, the capitosaurid *Cyclotosaurus intermedius* Sulej and Majer, 2005 and a trematosaurid *Metoposaurus krasiejowensis* (Sulej, 2002).

The family Capitosauroidae Shishkin, 1964 includes eight valid *Cyclotosaurus* Fraas, 1889 taxa with a narrow stratigraphic occurrence (Carnian-Rhaetian), mainly known from European localities such as Germany, Poland, France, Luxembourg, Greenland (Meyer and Pleninger 1844; Fraas 1913; Kuhn 1932; Kuhn 1942; Buffetaut and Wouters 1986; Milner et al. 1996; Sulej and Majer 2005; Marzola et al. 2017; Witzmann et al. 2016; Konietzko-Meier et al. 2019), but also from Thailand (Ingavat and Janvier 1981). As far as cyclotosaurid cranial material is diagnostic, e.g., closed otic notch and the position of the orbits (Damiani 2000;

Schoch and Milner 2000), the postcranial material is very scarce, and thus not considered as taxonomically valuable. The Polish (Krasiejów) *C. intermedius* is the first species for which, in addition to the skulls and mandibles, a scapulocoracoid, an interclavicle, a fragmentary clavicle, a cleithrum and a humerus have been described (Sulej and Majer 2005). The only other published morphological description of a cyclotosaurid long bone is based on the German (Bonenburg) cf. *Cyclotosaurus* humerus (Konietzko-Meier et al. 2019).

The family Metoposauridae includes 10 valid species known from almost all continents except Australia and South America (Gee and Jasinski 2021). Although *D. ouazzoui* is the only articulated metoposaurid species, *M. krasiejowensis* and *Panthasaurus maleriensis* (Roychowdhury, 1965) are known from numerous skeletal elements, including long bones (Roychowdhury 1965; Sengupta 2002; Sulej 2007), which were also studied at the histological level (Konietzko-Meier and Klein 2013; Konietzko-Meier and Sander 2013; Teschner et al. 2018, 2020).

Although the vertebral shape and the ornamentation pattern of the shoulder girdle elements of *Cyclotosaurus* are characteristic and differ from *Metoposaurus* (Sulej and Majer 2005; Sulej 2007), it is difficult to distinguish the long bone morphology between these two taxa. A *C. intermedius* humerus described by Sulej and Majer (2005) possesses a broad proximal and distal head, a weakly defined deltopectoral crest and supinator process, a thin entepicondyle and a pronounced ectepicondyle. Sulej (2007) described the *M. krasiejowensis* humerus as a short bone with wide proximal and distal end with a clear torsion, and a pronounced ectepicondyle with a short and thin supinator process, whereas the entepicondyle is thicker than the supinator process. Barycka (2007) described a series of *M. krasiejowensis* humeri as well-ossified bones with well-developed processes, e.g., supinator process, wide and flattened ends, small degrees of torsion unrelated to the bone length, generally obliquely positioned radial condyles, and less prominent deltopectoral crests. Moreover, Barycka (2007) noted, that the smallest bones possess smooth surfaces and weakly developed processes, crests and tuberositae, but a well-developed supinator process, deltopectoral crest and medial epicondyle. In contrast, the lattisimi process, subcoracoscapular process and lateral epicondyle are well-defined in the larger forms. In general, both authors point to high morphological variation within the metoposaurid humeri, and thus, clear diagnostic features are not well defined (Barycka 2007; Sulej 2007). Therefore, the distinction between trematosaurids and cyclotosaurids is problematic at the morphological level, especially with disarticulated material, as the characters might change during ontogeny.

Until now, size was also used as a proxy for genus determination, i.e., small-sized bones were attributed to *Metoposaurus*, whereas larger-sized specimens were attributed to *Cyclotosaurus*, based on the known skull length (small- to middle-sized *Metoposaurus* crania and large-sized *Cyclotosaurus* crania known from Krasiejów) (Sulej and Majer 2005; Sulej 2007). However, large metoposaurid skulls are known for *D. ouazzoui* (67 cm, Dutuit 1976), and a large (ca. 75 cm long) *Metoposaurus* skull was excavated from Krasiejów during the 2021 field campaign, so the taxonomic assignment of the postcrania is very doubtful based solely on the size. The lack of comparative *Cyclotosaurus* material and thus the unknown ontogenetic variation among humeri makes the final determination impossible.

A histological study conducted on a series of *M. krasiejowensis* humeri revealed the presence of two histotypes (Teschner et al. 2018). Histotype I showed a growth pattern of alternating growth cycles composed of a moderately vascularised zone and an avascular annulus together, both of a similar thickness and progressing remodelling with ontogeny, whereas histotype II represented humeri growing with a very thick, highly vascularised zone and a very thin annulus and only marginal remodelling. Teschner et al. (2018) primarily proposed that the observed difference in the humeral growth pattern could be the result of various populations separated in time and/or space, and therefore showing a different growth pattern due to variation in local environmental conditions. However, an affiliation to two different taxonomic groups was not ruled out (Teschner et al. 2018). Later, the histology of a cf. *Cyclotosaurus* humerus from Bonenburg showed a clear difference in the growth pattern between *M. krasiejowensis* and cf. *Cyclotosaurus*, making the histology of the latter similar to histotype II observed in *M. krasiejowensis* humeri (Teschner et al. 2018; Konietzko-Meier et al. 2019). Hence, the high variation in morphological characters in *M. krasiejowensis* humeri and the occurrence of two histological growth patterns could be linked to an interspecific variation rather than to an intraspecific variation.

The aim of this study is to find out whether the differences in the amphibian humeral morphology and histology indeed reflect the intraspecific variability in the Krasiejów assemblage. Here we describe for the first time the histology and the growth pattern of two exceptionally large humeri, initially assigned to *Cyclotosaurus intermedius*, from the Late Triassic of Krasiejów. We compared it with the known histological growth pattern of *Metoposaurus krasiejowensis*, another temnospondyl amphibian co-occurring at this site. Moreover, we test whether the humeral microstructure provides information about environmental adaptation and allows us to distinguish the mode of life between *Metoposaurus* and *Cyclotosaurus*.

Institutional abbreviations

UO – University of Opole, Opole, Poland; **IGPB** – University of Bonn, Institute of Geosciences, Section Palaeobiology, Bonn, Germany; **LWL-MFN P** – Landschaftsverband Westfalen-Lippe, Museum für Naturkunde, Abteilung Paläontologie, Münster, Münster, Germany; **UOBS** – old collection catalogue; University of Opole, Biosystematics, Opole, Poland; **UOPB** – new collection catalogue; University of Opole, Palaeobiology, Opole, Poland; **ZPAL** – collection of the Institute of Palaeobiology, Polish Academy of Sciences, Warsaw, Poland.

Other abbreviations

An – annulus; **EFS** – External Fundamental System; **LAG** – Line of Arrested Growth; **Zo** – zone.

3.4 Material and Methods

3.4.1 Material

The sectioned material includes two large temnospondyl humeri, UOBS 02116 (146.4 mm; Figs. 1A-D; Table 1) and UOBS 02431 (141.6 mm; Fig. 2A-D; Table 1), belonging to two temnospondyl amphibians, initially assigned to *Cyclotosaurus intermedius*. Both bones originated from the Late Triassic (Norian) Krasiejów locality in southwestern Poland (Bodzioch and Kowal-Linka 2013; Jewuła et al. 2019) and are housed at the Institute of Biology, University of Opole. The material was the subject of a muscle reconstruction study; however, no morphological description was published along with this, and the taxonomic assignment was based solely on the large size of the humeri (Lech 2010). In addition, two *M. krasiejowensis* humeri (UOPB 00109 representing Histotype I and UOBS 00547 representing histotype II *sensu* Teschner et al. (2018) and cf. *Cyclotosaurus* LWL-MNF P 64371 humerus (Konietzko-Meier et al. 2019) were used for bone compactness analyses (Table 1).

3.4.2 Methods

Both specimens were measured using a sliding calliper with precision of 0.05mm. The histological samples were taken from the histological midshaft of both humeri (Figs. 1-3) yielding the most complete growth record (Konietzko-Meier and Klein, 2018; Teschner et al. 2018). The taken samples were processed into standard petrographic thin-sections in the laboratory of the Institute of Geosciences (IGPB) at the University of Bonn (Germany) applying the technique described in Klein and Sander (2007). Wet silicon carbide (SiC) abrasive powders with grit sizes of 600 and 800 were used to grind and polish to a final thin-section thickness ranging from 25 to 40 micrometres. Osteohistological examination was performed with a *Leica DM LP* polarising light microscope and photographs were taken with a *Leica DFC 420* camera attached to the microscope. The overview pictures in polarised light were merged using *Photoshop 5*. For the microanatomical analyses of specimens UOBS 02116 and 02431, the thin-sections were scanned (Fig. 3A-B; Table 1) with an *Epson Perfection 750V PRO* scanner and transformed into black (bone) and white (cavities) images (Fig. 4A-F; Table 1). In order to measure the bone compactness, the *bw-counter* pixel counting software developed by ©Peter Göddertz (IGPB) was used to measure the ratio of compact bone vs. cavities (Table 1). The detailed morphology and histology of the additional specimens used bone compactness analyses (UOPB 00109, UOBS 00574 and LWL-MNF P 64371) described previously in Konietzko-Meier et al. (2019) and Teschner et al. (2018). The morphological nomenclature follows Barycka (2007) and Sulej (2007) and the histological nomenclature follows Francillon-Vieillot et al. (1990) and de Buffrénil et al. (2021). It is important to mention that metaplastic bone forms in bone of dermal origin, however, and the herein studied long bones are of a periosteal origin (de Buffrénil et al. 2021). The term 'metaplastic-like bone' used in this study is not linked to the bone origin but is referred exclusively as a structural resemblance noted previously in Temnospondyli (Konietzko-Meier et al. 2019; Teschner et al. 2020) and therefore, does not represent a true metaplastic bone.

3.5 Results

3.5.1 Morphological description

Specimen UOBS 02116 is 141.6 mm long (Fig. 1A-D; Table 1), has a short shaft (40 mm) and a slender proximal end (50 mm) compared to its wide distal end (86 mm). Anteriorly, the distal end has a pronounced 6.3 mm long ectepicondyle (*epicondylus lateralis sensu* Barycka 2007) and 10.9 mm long supinator process (Fig. 1A-B). Proximally, the ectepicondyle proceeds into the radial crest (adductor crest *sensu* Barycka 2007) before ending in the 28.5 mm long latissimi process (Fig. 1A). Anterior to the ectepicondyle, the short supinator process is located dorsally, the supinator process is longer than the ectepicondyle and extends proximally into the deltopectoral crest (Fig. 1A-B). Posteriorly, the humeroradial tuberosity (Fig. 1) is located dorsally, with its rugose insertion of the grand pectoral muscle (Dutuit 1976) or biceps brachii

Figure 3.1 Morphology of *Cyclotosaurus intermedius* UOBS 02116 in A: dorsal view; B: ventral; C: proximal; D: distal view. Scale bar equals 20 mm. Abbreviations: de – epicondylar depression; dp – deltopectoral crest; ec – ectepicondyle; en – entepicondyle; hr – humeroradial tuberosity; lp – lattisimi process; rc – radial crest; sp – supinator process.

(Ochev 1972). The epicondylar depression forms a groove between the supinator process and ectepicondyle, and is 14.5 mm wide (Fig. 1A). On the opposite side of the distal end, the entepicondyle (medial epicondyle *sensu* Barycka 2007) proceeds proximally (16.4 mm), and is wider than the supinator process. The postero-dorsal depression forming a groove between the latissimi process and subcoracoscapular process is 12.8 mm wide. Despite four processes, the proximal end is compact and thick, with an oval-shaped scapulocoracoid articular facet (a major axis of 25.5 mm and a minor axis of 22 mm). In comparison, the distal end shows a 14 mm thin rectangular shape antero-posteriorly with only the ectepicondyle and supinator process disrupting the shape. The proximal and the distal articulation facets form an angle of 55° (Table 1).

Specimen UOBS 02431 is 146.4 mm long (Fig. 2A-D; Table 1) and has a short and slender shaft of the same width as the proximal end (48 mm), whereas the distal end is wider (84 mm). Anteriorly, the distal end shows a pronounced 11.1 mm long ectepicondyle and a 15.8 mm long supinator process (Fig. 2A-B). Proximally, the ectepicondyle proceeds into the radial crest and ends in a 21 mm long latissimi process (Fig. 2A). Anterior to the ectepicondyle, the short, dorsally situated supinator process is longer than the ectepicondyle and extends proximally into the deltopectoral crest (Fig. 2A-B). Posteriorly, the humeroradial tuberosity (Fig. 2A) with a rugose insertion of the grand pectoral muscle (Dutuit 1976) or biceps brachii

Table 1. Measurements of known humeri of *Cyclotosaurus* and *Metoposaurus krasiejowensis*.

Character	Taxon	Total length [mm]	Midshaft width [mm]	Distal width [mm]	Proximal width [mm]	Torsion [°]	Compactness [%]	Reference
Specimen								
UOBS 02116	*Cyclotosaurus intermedius**	141.6	40	86	50	55	85	this study
UOBS 02431	*Metoposaurus krasiejowensis*	146.4	48	84	48	83	71	this study
UOBS 00574	*Cyclotosaurus intermedius**	65.4	20.5	36.1	24	65	82	Teschner et al. 2018
UOPB 00109	*Metoposaurus krasiejowensis*	69.2	22.1	43.4	26.5	75	66	Teschner et al. 2018, this study
LWL-MFN P 64371	cf. *Cyclotosaurus*	167	50	87	50	34	78	Konietzko-Meier et al. 2019, this study
ZPAL Ab III 887/3	*Cyclotosaurus intermedius*	130	32	62	48	70	–	Sulej and Majer 2005, this study

*Originally published as *Metoposaurus krasiejowensis* (Lech, 2010; Teschner et al. 2018), herein revised as *Cyclotosaurus intermedius*

(Ochev 1972) is preserved. The epicondylar depression is 18 mm wide and forms a groove between the supinator process and ectepicondyle (Fig. 2A). On the opposite side of the distal end, the entepicondyle proceeds proximally into the 20.7 mm wide subcoracoscapular process, being thicker than the supinator process. The postero-dorsal depression forming a groove between the latissimi process and subcoracoscapular process, is 14.6 mm wide. Despite four processes, the proximal end is compact and thick, with an oval-shaped scapulocoracoid articular facet (a major axis of 45 mm and a minor axis of 29 mm). In comparison, the distal end shows a 13.5 mm thin rectangular shape with only the ectepicondyle and supinator process disrupting the shape. The proximal and distal articulation facet form an angle of 83° (Table 1).

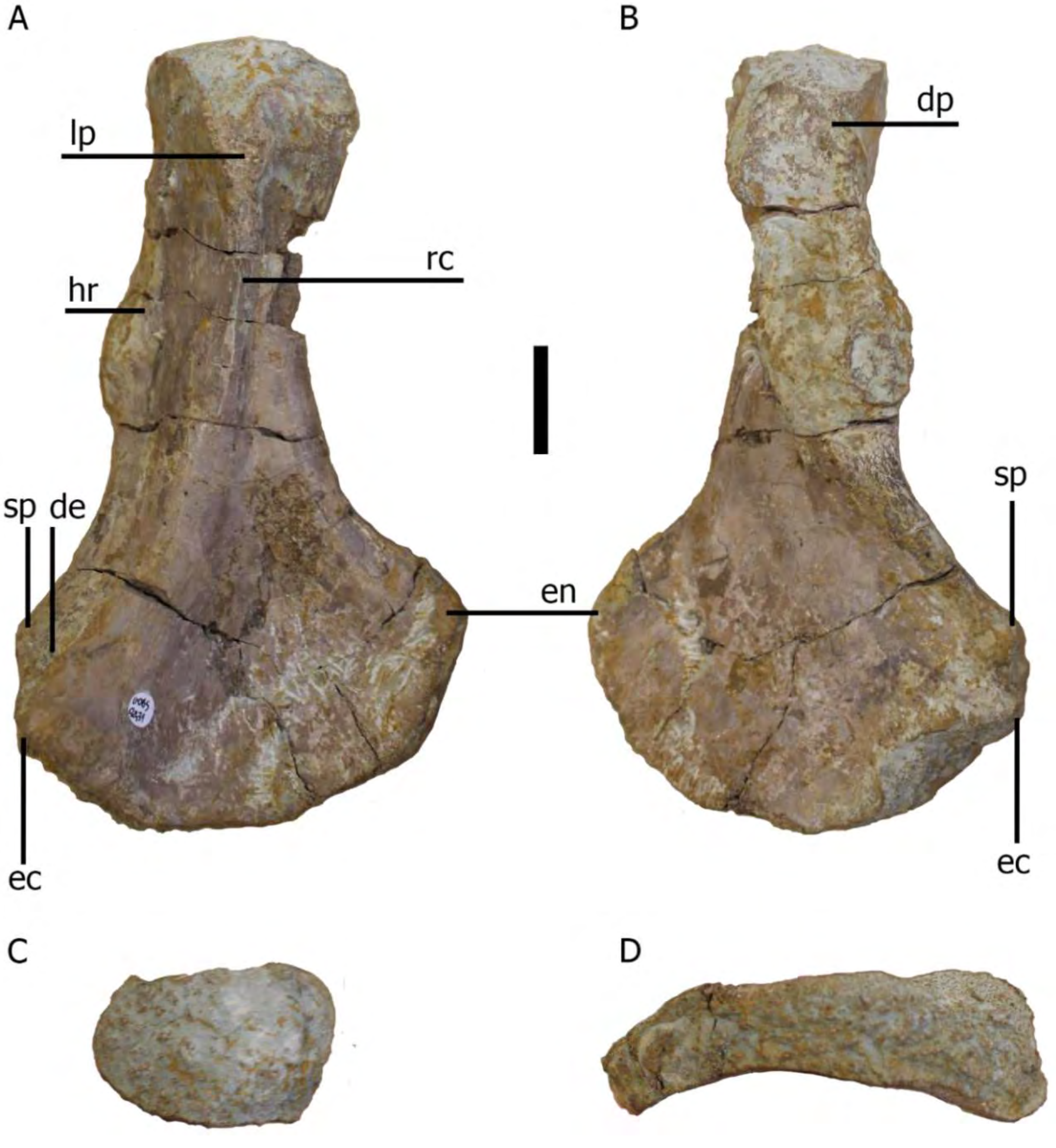

Figure 3.2: Morphology of *Metoposaurus krasiejowensis* UOBS 02431 in A: dorsal; B: ventral; C: proximal; D: distal view. Scale bar equals 20 mm. Abbreviations: de – epicondylar depression; dp – deltopectoral crest; ec – ectepicondyle; en – entepicondyle; hr – humeroradial tuberosity; lp – lattisimi process; rc – radial crest; sp – supinator process.

3.5.2 Microstructure

Specimen UOBS 02116 (Fig. 3A$_{1\text{-}2}$; Table 1) represents a humerus sectioned at the histological midshaft with the nutrient canal preserved on the ventral side, whereas humerus UOBS 02431 (Fig. 3B$_{1\text{-}2}$; Table 1) has the nutrient canal positioned on the dorso-lateral side. Both humeri are triangular in cross-section and the apex of the humerus, which corresponds with the radial crest (Figs. 1-2), is on the dorsal side of the bone. The UOBS 02116 specimen is prominently flattened (Fig. 3A$_{1\text{-}2}$). In specimen UOBS 02116 the shorter flange borders the lateral side and the longer flange runs towards the medial side. In the specimen UOBS 02431 the flanges are of almost equal length (Fig. 3B$_{1\text{-}2}$). The bone compactness value equals 85 % for specimen UOBS 02116 (Table 1; Fig. 4A and 71 % for specimen UOBS 02431 (Table 1; Fig 4B). The bone compactness for the *M. krasiejowensis* specimen UOPB 00109 is 66% (Table 1; Fig. 4C) and 82 % for UOBS 00574 (Table 1; Fig. 4D). For the specimen LWL-MFN P 64371 cf. *Cyclotosaurus* the bone compactness is 78% (Table 1; Fig. 4E).

3.5.3 General histology

Neither of the two humeri, UOBS 02116 and 02431, shows a medullary cavity (Fig. 3A-B), instead the perimedullary region is developed in both individuals. The boundary between the perimedullary region, composed of secondary trabeculae, and the primary cortex is gradual, without a sharp border (Fig. 3A-B). The primary cortex preserved around the section in both specimens consists of parallel-fibred bone with varying degrees of collagen fibres organisation (Fig. 5A-K). On the medial side of the section UOBS 02116, the tissue becomes less unorganized and fibrous, resembling a ‘metaplastic-like tissue’, which reaches up to the outermost surface of the bone (Fig. 5C-D). The vascular density is moderate to high in both sections (Fig. 5A-K). The vascular canals in the primary cortex are mostly longitudinal primary osteons (Fig. 5A-B, E-F). The simple, longitudinal vascular canals are scattered in the inner cortex, whereas towards the outermost cortex they are arranged in rows (Fig. 5J-K). Secondary osteons are preserved in both sections; however, they are more numerous in the section UOBS 02431 than in section UOBS 02116 (Fig. 5E-F, H-K). Osteocyte lacunae are not common in both sections; however, they are more numerous in specimen UOBS 02116 than in specimen UOBS 02431 (Fig. 5J-K). Moreover, they are larger in specimen UOBS 02116 and possess well-developed canaliculi (Fig. 5G), whereas the osteocytes in the section UOBS 02413 lack canaliculi (Fig. 5H). There are regions of well-vascularised but less organised parallel-fibred bone, referred as zones (zo; Fig. 5J-K), and regions of well-organized parallel-fibred bone without or only with few vascular canals, referred as annuli (an; Fig. 5J-K).

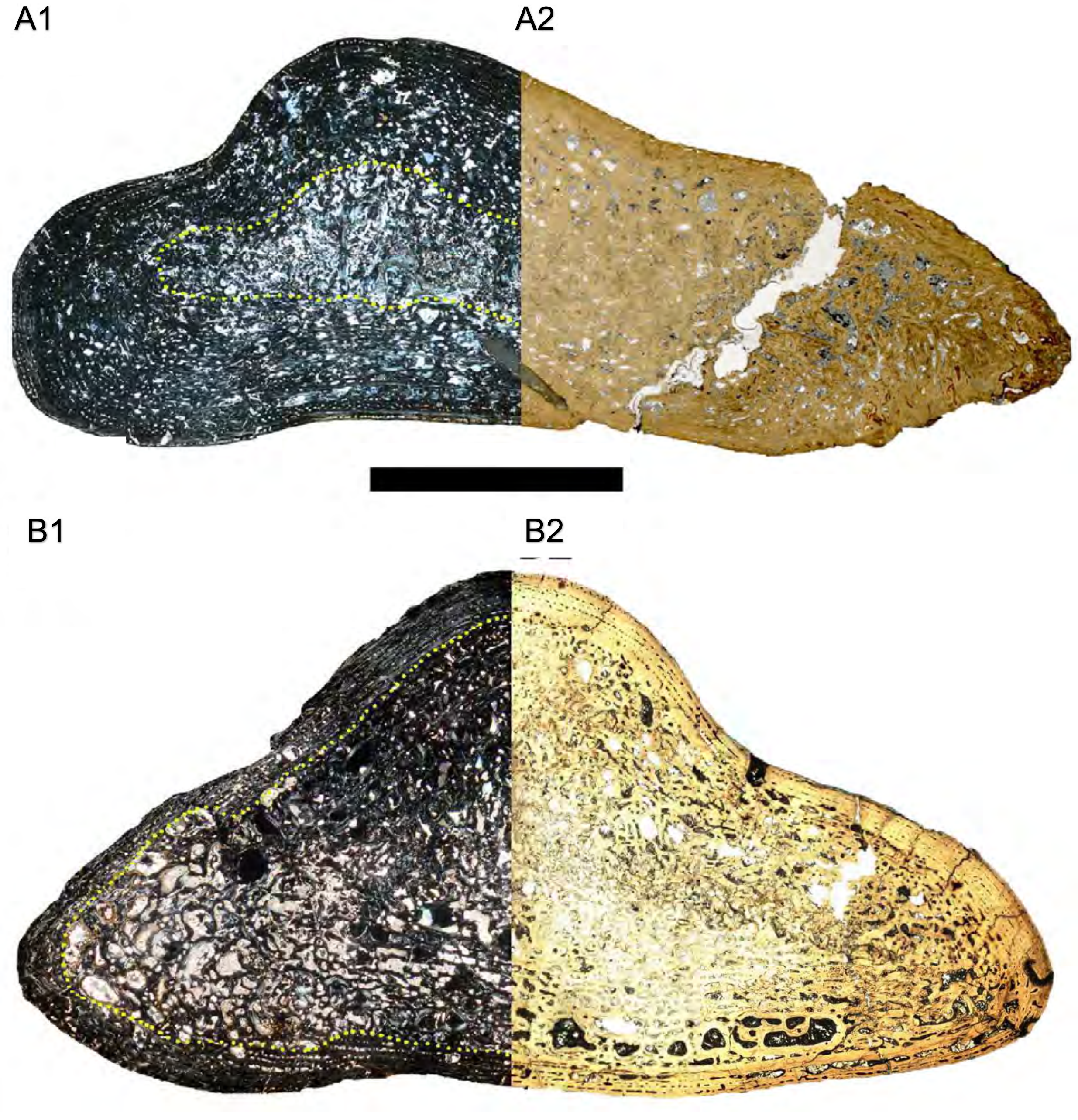

Figure 3.3: Histology of *Cyclotosaurus intermedius* humerus in A1: polarized light and A2: normal transmitted light; and *Metoposaurus krasiejowensis* humerus in B1: polarized light and B2: normal transmitted light. Scale bar equals 10 mm. The dashed line marks the border between the perimedullary region (internal) and the primary cortex (external). Scale bar equals 10 mm.

3.5.4 Growth pattern

Specimen UOBS 02116

The innermost part of the section preserves crushed secondary trabeculae (Figs. 3A; 5K). The primary matrix reaches very deep into the section (Figs. 2A$_{1-2}$, 5K) and the primary tissue is distributed almost throughout the section. In the inner part of the cortex, the erosion cavities are numerous, unorganized, and vary in shape and size (Figs. 4A-B, 5H). The erosion cavities are lined by lamellar bone, and are embedded in a less organised primary parallel-fibred bone matrix, with remains of the remodelled thick, first zone (Figs. 5A-B, K). This is followed by a remodelled and thin, first annulus (Fig. 5K). The second zone (Fig. 5K) consists of a combination of elongated primary osteons, secondary osteons, and a few large, scattered erosion cavities; however, towards the outer cortex, they are more organized and primarily arranged in rows. Next, a thin, avascular layer is present, resembling the second annulus (Fig. 5K). The third zone (Fig. 5K) is similar in thickness to the second zone, but with a lower number of large erosion cavities, but with numerous primary osteons. Further, a thick, third annulus is preserved in the outer cortex (Fig. 5K). In the outermost cortex a thin, fourth zone consisting of one row of primary osteons embedded in a higher organized parallel-fibred bone is

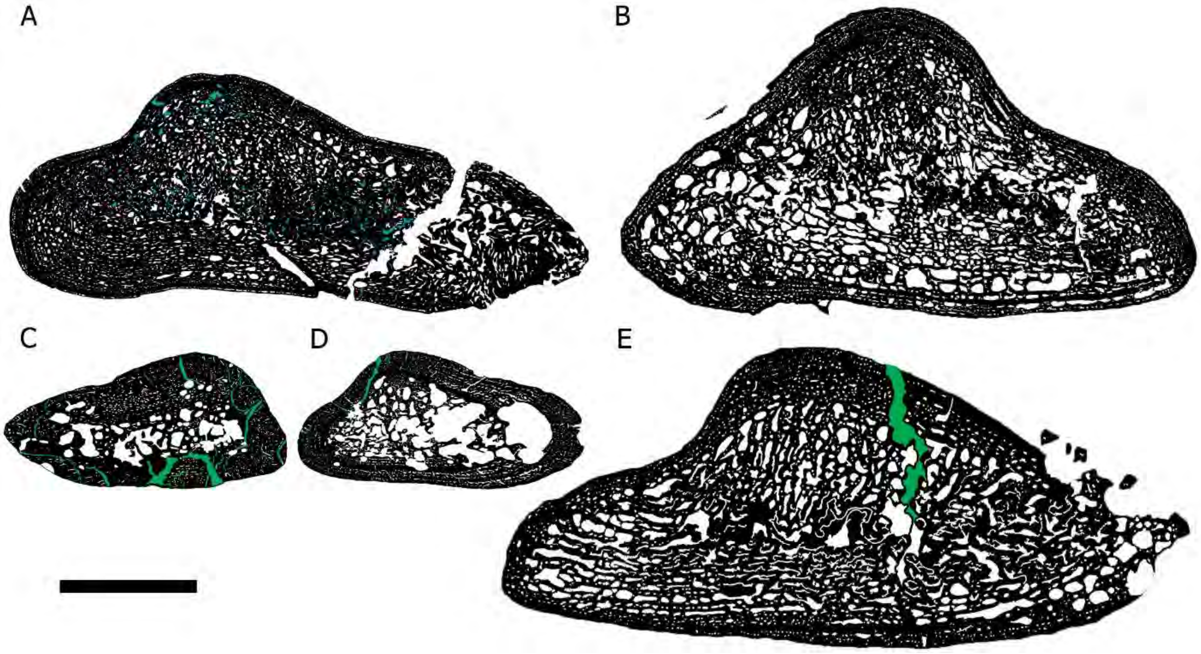

Figure 3.4: Microanatomy of A: *Cyclotosaurus intermedius* UOBS 02116; B: *Metoposaurus (Figure 3.4 continuation from previous page) krasiejowensis* UOBS 02431; C: *Cyclotosaurus intermedius* UOBS 00574 (histotype II *sensu* Teschner et al. 2018); D: *Metoposaurus krasiejowensis* UOPB 00109 (histotype I *sensu* Teschner et al. 2018) E: cf. *Cyclotosaurus* LWL-MFN P 64371. Black colour corresponds with the bone, white colour corresponds with pores, blue and green colour corresponds with diagenetic cracks. Scale bar equals 10 mm.

preserved (Fig. 5K). The primary osteons are not roundish but elongated (parallel to the surface), and only in the region of the radial crest do the canals become more radial. Prominent rest lines occur only in the outermost cortex, inside the thin, fourth annulus (Fig. 5K). Clear LAGs or an EFS are absent in this section. Generally, the zones are distinctly thicker than the annuli and no thinning of the zones towards the outer cortex is observed in this sample.

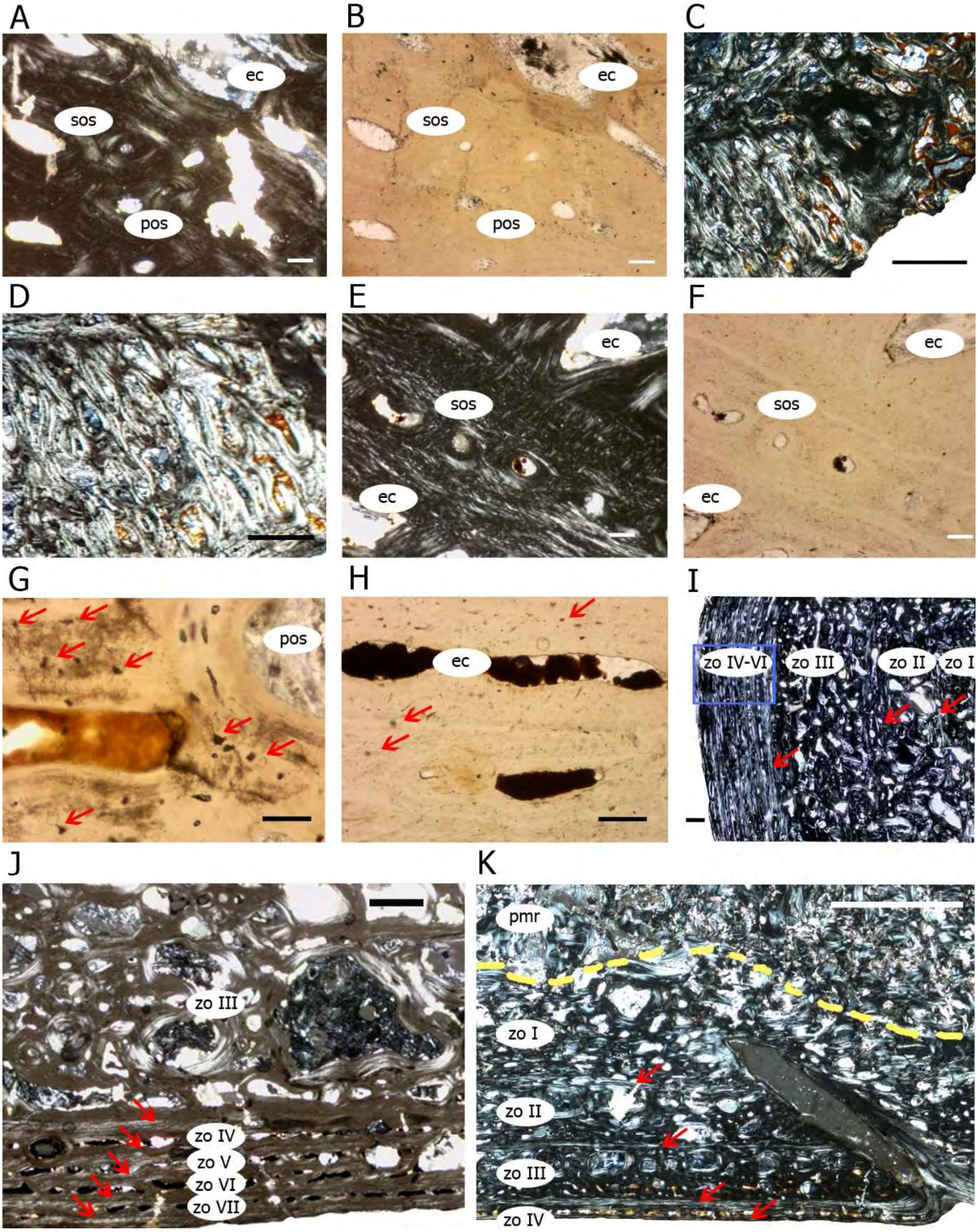

Figure 3.5: Detailed histology of the humeri of *Cyclotosaurus intermedius* UOBS 0216 (A–D, G, K)

(*Figure 3.5 continuation from previous page*) and *Metoposaurus krasiejowensis* UOBS 02431 (E–F, H–J); A–B: close-up of the primary cortex consisting of less-organised parallel-fibred bone; C: fibrous, 'metaplastic-like tissue' on the medial bone side; D: close-up from C of the unorganized, fibrous ‘metaplastic-like tissue’; E–F: close-up of the primary cortex consisting of less-organised and better-organised parallel-fibred bone; G: osteocyte lacunae with well-preserved canaliculi; H: osteocyte lacunae lacking canaliculi; I–J: growth pattern with preserved residuals of the thick annuli and zones (zo I – zo III) and thin annuli and zones (zo IV – zo VII); K: growth pattern with preserved thin annuli and thick zones (zo I – zo IV), the dashed line marks the border between the perimedullary region and the cortex. A, C–D, F–H in polarized light and B, E in normal transmitted light. Arrows in G–H indicate osteocyte lacunae and in H–K indicate the annuli. Scale bar equals 1 mm for A–B, E–F, 0.5 mm for C, I-K and 0.2mm for D, G–H. Abbreviations: an – annulus; ec – erosion cavity; pmr – perimedullary region pos – primary osteon; sos – secondary osteon; zo – zone.

Specimen UOBS 02431

The central most part of the section consists of diagenetically crushed secondary trabeculae (Figs. 4B$_{1\text{-}2}$, 5I-J), and together with large erosion cavities they represent the perimedullary region. In the inner part of the cortex, on the dorso-medial side, a highly remodelled layer with large erosion cavities is present, resembling the first zone (Fig 5I). Between the erosion cavities, remains of more organized parallel-fibred bone are visible, resembling a thick, first annulus (Fig. 5I). Next, a thick, extensively remodelled second zone with multiple, scattered erosion cavities is present (Fig 5I). Following that the residual of the second, thick annulus is preserved (Fig 5I), and further a thick, third zone is deposited (Fig. 5I-J). The third annulus is thin and avascular (Fig. 5I-J). Zones four to seven are very thin and consist of a single row of simple vascular canals and primary and secondary osteons, which become more remodelled towards the section centre (Fig. 5I-J). They are best to observe on the ventral side (Fig. 5J). In the outermost cortex, the thin and avascular annuli (fourth to seventh) are present (Fig 5J); moreover, each of the annuli contains a prominent rest line. Generally, the zones become distinctly thinner towards the outermost cortex (Fig. 5I-J).

3.6 Discussion

3.6.1 Morphological and ontogenetic variation

The humeri sectioned herein are exceptionally large (Figs. 1-2; Table 1) compared to the other amphibian humeri originating from the Krasiejów deposit (Barycka 2007; Sulej 2007; Teschner et al. 2018); however, they are morphologically very similar to each other. The most striking differences are the degree of torsion between the distal and proximal head in specimen UOBS

02116 (55°) and UOBS 02431 (83°) and the thickness of the ectepicondyle, which is almost twice larger in the specimen UOBS 02431 than in specimen UOBS 02116 (Table 1). These two characters make the specimen UOBS 02116 thinner and flatter in the lateral view than specimen UOBS 02431.

However, it is not clear how important these characters are in the context of taxonomic assignment. Sulej & Majer (2005) provided the degree of torsion between the proximal and distal head of 70° for *C. intermedius* (130 mm; Table 1), while the only other known cyclotosaurid humerus of cf. *Cyclotosaurus* (167 mm, Table 1) shows a torsion of 34° (Konietzko-Meier et al. 2019). Barycka (2007) noted a degree of torsion ranging from 22° to 40° for *M. krasiejowensis* (59.8-107.5 mm). Sulej (2007) did not provide measurements, but pointed out that torsion vary greatly, with the angle even exceeding 90°. Teschner (2015) measured additional *M. krasiejowensis* humeri (65.4-82.6 mm), which also showed strong torsional variability (55°-85°) that was not related to ontogenetic development. Based on the data for metoposaurids, it is not possible to state how important torsion is for a taxonomic diagnosis. Sulej (2007) observed that the ectepicondyle is very pronounced in *M. krasiejowensis* humeri.

Other morphological features that are helpful in distinguishing *Cyclotosaurus* from *Metoposaurus* are the shape of the proximal head and the anterior edge (Sulej and Majer 2005; Barycka 2007; Sulej 2007). Sulej (2007) notes that the proximal head in *C. intermedius* is slender and has a narrower ectepicondyle and much shorter anterior edge of the shaft than that of *M. krasiejowensis* (Sulej, 2007). However, Sulej (2007) emphasises that the length of the anterior margin is variable in *Metoposaurus*, making the latter feature doubtful and non-diagnostic.

After comparing the above-mentioned features with the bones described herein, the humerus UOBS 02116 has significantly less torsion and a thinner ectepicondyle than the specimen UOBS 02431, but the proximal flange is wide in both specimens. Both humeri have the same shape of the anterior margin of the shaft and both lack a pronounced supinator process (Table 1). Nevertheless, it is important to point out that the strong torsion of humerus UOBS 02431 makes estimation of the shape of the anterior margin more difficult. Therefore, taxonomic assignment of the humeri to a certain genus based solely on morphology is doubtful, as the range of ontogenetic variability in *Cyclotosaurus* is unknown due to the lack of comparative material. Furthermore, no large *M. krasiejowensis* humeri are known, neither from

Krasiejów nor from other locality worldwide, hence no ontogenetic series are known and no further studies on morphological development have been conducted.

Nevertheless, some of the humeri published earlier as *M. krasiejowensis* show similar characters to *C. intermedius*, e.g., weakly developed supinator process and an overall slim shape; however, all were significantly smaller than the herein studied *C. intermedius* humeri (Sulej 2007; Barycka 2007; Teschner et al. 2018). Due to the very small number of known humeri of *Cyclotosaurus*, it cannot be ruled out that some of the bones examined so far and assigned to *Metoposaurus* based on their small size (Sulej 2007; Barycka 2007; Teschner et al. 2018) indeed represent juvenile *Cyclotosaurus* humeri (Table 1). Especially, since *M. krasiejowensis* humeri are exceptionally variable morphologically (Sulej 2007; Barycka 2007). The high variability among *M. krasiejowensis* (Barycka 2007; Sulej 2007) might thus be related to interspecific, rather than intraspecific variation. Therefore, a revision of the morphological characters of the stereospondyl postcranial material is necessary.

Since there are only two large humeri assigned to *Cyclotosaurus* (*C. intermedius* and cf. *Cyclotosaurus*) and no other comparative material is available worldwide, bone histology might shed new light on the biology of the animals and help with taxonomic assignment.

3.6.2 Histology and growth pattern

The thin-sections of both humeri are triangular in cross-section, however the specimen UOBS 02116 is much flatter (Fig. 3A-B). The nutrient canal enters from the dorso-lateral side in specimen UOBS 02431 (Fig. 3B), whereas it enters from the ventral side in section UOBS 02116 (Fig. 3A). Further, the section UOBS 02116 possesses a distinct 'metaplastic-like structure' on the medial side, corresponding with the deltopectoral crest (Figs. 3B, 4A, 5C).

At the histological level, both humeri show a lamellar-zonal bone tissue composed of parallel-fibred bone with similar vascular density and preservation of alternating growth marks (zones and annuli; Figs. 3A-B; 5A, D, F-H. However, the zones in specimen UOBS 02431 are mostly preserved only in the outermost portion of the cortex and consist only of one row of vascular canals, separated by thin avascular annuli (Fig. 5I-J). Moreover, only residuals of the primary tissue are still preserved locally, next to the lateral margin in the deeper part of the cortex (Fig. 3B). In this region, the presence of thick annuli alternating with thinner zones is preserved. In specimen UOBS 02116, on the other hand, the alternating growth marks are visible throughout the entire section and can be followed into the deeper parts of the cortex

(Figs.3A; 5H). The zones are of an equal thickness and are separated by thin annuli. Interestingly, LAGs are not preserved in either sample, which might be related to climatic and/or environmental influence and confirms a rather mild climate during the Late Triassic in Krasiejów, as previously suggested for other taxa from this locality (Teschner et al. 2020, 2022). Only in specimen UOBS 02431, in the external most cortex, few rest lines occur, indicating slowed growth (Francillon-Vieillot et al. 1990; de Buffrénil et al. 2021). Moreover, specimen UOBS 02116 does not show a clear trend of decreasing thickness of growth marks towards the outer cortex; instead the bone was still actively growing as expressed by the presence of thick zones (Fig. 5K).

Ontogenetic age is related to bone remodelling, thus, the older the specimen the more remodelled the tissue (Klein and Sander 2008; Konietzko-Meier et al. 2012; Mitchell et al. 2017). The most striking difference between these two bones is the degree of remodelling (Fig. 3A-B). Considering that both bones are of similar size, the amount of the primary tissue in specimen UOBS 02116 is large and is still preserved in the deeper portion of the cortex (Fig. 3A$_1$), whereas in specimen UOBS 02431 it is limited only to the outer cortex (Fig. 3B$_1$). The distinctly extensive remodelling and a clear decrease of growth rate observed in the humerus UOBS 02431, indicates an older ontogenetic stage of that bone when compared to the second humerus UOBS 02116, which was still actively growing. The growth pattern of the histologically older bone (UOBS 02431) resembles the pattern known for *Metoposaurus krasiejowensis* long bones, growing with unusually thick annuli (Konietzko-Meier and Klein 2013; Konietzko-Meier and Sander 2013). The humerus (120 mm) of the metoposaurid *P. maleriensis* shows extensive remodelling and a similar thinning of the zones towards the outer cortex (Teschner et al 2020). Unfortunately, no humeri of the metoposaurid *D. ouazzoui* from Morocco were examined, however, the femora (79-157 mm) show a similar growth pattern to *M. krasiejowensis*, except for the deposition of distinct LAGs in the Moroccan taxon, which are absent in the Polish taxon (Steyer et al. 2004). Additionally, a similar position of the nutrient canal entering from the dorso-lateral side was observed in specimen UOPB 00109 of *M. krasiejowensis* (Teschner et al. 2018). Further, the specimen UOBS 02431 and the *M. krasiejowensis* humeri studied in Teschner et al. (2018) do not show a similar 'metaplastic-like structure'.

The only other histologically examined cyclotosaurid humerus was described by Konietzko-Meier et al. (2019). Unfortunately, the growth pattern of cf. *Cyclotosaurus* (LWL-MFN P 64371) was not described, nevertheless, the observation made on the available material shows a lot of primary tissue also preserved in the inner portion of the bone, whereas the growth marks contain a thin annulus and a thick zone (Konietzko-Meier et al. 2019), similar to the growth pattern present in the humerus UOBS 02116 (Figs. 3A; 5H). Further, the latter specimen shows a distinct 'metaplastic-like structure' in the region corresponding with the deltopectoral crest on the medial side (Fig. 5C-D), similar to the tissue observed in the cf. *Cyclotosaurus* humerus from Bonenburg (Konietzko-Meier et al. 2019). Unfortunately, the cf. *Cyclotosaurus* specimen from Bonenburg was not sectioned at the exact midshaft plane, and therefore, the nutrient canal is not visible in this thin-section (Konietzko-Meier et al. 2019).

The difference in the ontogenetic stage in the sampled bones is significant (Fig. 3A-B) as it would not be expected for bones of similar size. The age, together with the different histological characters, strongly suggests that the observed variability is related to the presence of two different taxa and does not represent intraspecific variation. Thus, the older bone belongs to a very large and old *Metoposaurus* (UOBS 02431; Figs. 2A-D; 3B; 4B; 5F-G), while the younger bone represents a medium-sized humerus of *Cyclotosaurus* (UOBS 02116; Figs. 1A-D; 3A; 4A; 5H).

If growth pattern is a reliable indicator for taxonomic differences, the question arises whether the previously observed histotypes in *M. krasiejowensis* humeri actually represent an intraspecific variation or rather express an interspecific variation (Teschner et al. 2018). Therefore, the assumption previously applied to the long bones from Krasiejów that small-sized animals belong to *Metoposaurus* and large-sized humeri belong to *Cyclotosaurus* is thus invalid. After the re-evaluation of the humeri described in Teschner et al. (2018) we can certainly state that humeri described as histotype I, e.g., UOPB 00109 (Fig. 4D), growing with alternating zones and annuli represent small- to medium-sized *M. krasiejowensis* humeri. In contrast, humeri described as histotype II, e.g., specimen UOBS 00574 (Fig. 4C), outlying by its growth with a very thick zone and only one, extremely thin annulus and a high degree of vascularisation (Teschner et al. 2018), represents a juvenile *Cyclotosaurus* humerus. Moreover, the specimen UOBS 00574 proposed herein to be a juvenile *Cyclotosaurus*, does not show a distinct torsion between the distal and proximal head, and despite its high vascularity, the bone compactness value is 82 % (Table 1; Fig. 4C). In contrast, the compactness of the *M. krasiejowensis* humeri sampled by Teschner et al. (2018) ranges between 55-76% and for specimen UOPB 00109 it is 66% (Table. 1; Fig. 4D). The cyclotosaurid, cf. *Cyclotosaurus* from Bonenburg (Konietzko-Meier at al. 2019) shows a similar growth pattern as the specimen UOBS 02116, which is proposed herein to represent a *Cyclotosaurus*. Moreover, the bone compactness of the cyclotosaurid LWL-MFN P 64371 is also relatively high with 78% (Table. 1; Fig. 4E).

3.6.3 Mode of life as deduced from bone compactness

Only a few humeri from Mesozoic Temnospondyli have been examined histologically. Sanchez et al. (2010) sampled the capitosaurid *Mastodonsaurus giganteus*, however, the authors did not provide a detailed description of the histology nor figured the section, therefore, comparison of the growth pattern nor of the bone compactness is possible. The Indian capitosaurids *Paracyclotosaurus crookshanki* and *Cherninia denwai* (Mukherjee et al. 2020) show a varied growth pattern within the sampled bones, and a preservation of various bone tissues (woven fibred bone in juveniles and later an incipient fibro-lamellar bone with the tendency to parallel-fibred and lamellar bone later in ontogeny). Mukherjee at al. (2020) proposed a different niche occupation for the examined taxa, a passive benthic predation for *Cherninia*, and a shallow water predation with a possible terrestrialisation for *Paracyclotosaurus*. Moreover, *P. crookshanki* shows a clear torsion in the bones whereas in *C. denwai* this character is variable (Mukherjee et al. 2020).

In general, specimen UOBS 02431, referred here as *Metoposaurus*, shows a higher degree of vascularisation and therefore has a less compact cortex (bone compactness value of 71%; Table 1; Fig. 4B). Specimen UOBS 02116 has a more compact cortex (bone compactness value of 85 %; Table 1; Fig. 4A) which could indicate occupation of different ecological niches in the water column. Therefore, the more compact bone observed for *Cyclotosaurus* could be an adaptation to a lifestyle close to the water surface and a possible degree of terrestrialisation, as in the modern giant salamanders *Andrias* or as proposed for *P. crookshanki* (Mukherjee et al. 2020), while the lower bone porosity value of UOBS 02431 indicates a more active swimming lifestyle as proposed previously for metoposaurids (Kalita et al. 2022). However, even if the animals have similar bone lengths, they do not represent an ontogenetically corresponding stage, but rather represent two different species. Therefore, the reflected change in bone density (85% for UOBS 02116 and 71% for UOBS 02431; Fig. 4A-B; Table 1) does not represent an environmental signal or a mode of life. Instead, the tendency of increasing porosity in the older specimen, as observed herein in specimen UOBS 02431, was described in *M. krasiejowensis* dermal bones of the pectoral girdle (Kalita et al. 2022). Thus, no information about the mode of life and or niche occupation, based on the bone compactness study, can be provided.

3.7 Conclusions

The fossil record of the stereospondyl postcranial skeleton is rarely preserved in the fossil record. Herein sectioned two humeri, despite their similar bone length and a uniform morphology, show a different growth pattern at the histological level. Therefore, the described specimens are assigned to two different temnospondyl genera. The humerus UOBS 02116, shows a low degree of torsion between the proximal and distal end, and it is attributed to *Cyclotosaurus*. On the other hand, the specimen UOBS 02431, with a prominent degree of torsion between the proximal and distal head of 83°, is attributed to *Metoposaurus*. Histologically, the specimen UOBS 02116 shows more compact bone than the specimen UOBS 02431. Both humeri show a slightly varied growth pattern, with the *Cyclotosaurus* humerus showing four visible cycles and the *Metoposaurus* humerus preserving seven visible growth cycles. Despite a similar bone length, specimen UOBS 02116 represents a histologically younger individual than specimen UOBS 02431. The older age of the latter is reflected by the distinctive thinning of zones and thickening of annuli towards the outer cortex, as well as advanced remodelling. The absence of clear LAGs in both specimens suggests that the climate in Krasiejów was rather mild during the Late Triassic, as previously proposed. Furthermore, this study indicates that capitosaurids and trematosaurids share a similar humeral morphology and therefore assignment at the genus level based on disarticulated material is problematic, but bone histology is a valuable tool in the taxonomic assignment of Temnospondyli.

3.8 Acknowledgements

Olaf Dülfer (University of Bonn), Krzysztof Książkiewicz (University of Wrocław) are thanked for the preparation of the specimens. Tomasz Szczygielski and Tomasz Sulej (Institute of Paleontology, Polish Academy of Sciences) are thanked for proving access to the collection with comparative material. Sudipta Kalita (University of Bonn) is acknowledged for the preparation of figures for the bone compactness analysis. We are also grateful to the Editor Daniel E. Barta, and the Reviewers Damien Germain and Justyna Słowiak-Morkovina for their helpful comments and suggestions. This research has been funded by the Polish National Science Centre (NCN) grant number: UMO-2016/23/N/ST10/02179.

Chapter 4

Growth and limb bone histology of aetosaurs and phytosaurs from the Late Triassic Krasiejów locality (SW Poland) reveals strong environmental influence on the growth pattern

4.1 Authors and their contributions

Teschner, E. M., Konietzko-Meier, D., and N. Klein. 2022. Growth and limb bone histology of aetosaurs and phytosaurs from the Late Triassic Krasiejów locality (SW Poland) reveals strong environmental influence on growth pattern. *Contributions to Zoology*, 91(3): 199-232.

EMT, DK-M and NK designed the study; EMT selected the material and prepared thin-sections in the laboratory; EMT, DK-M and NK analysed the thin-sections; EMT took photographs and micrographs, prepared the figures, and wrote the manuscript draft; DK-M and NK critically revised the first draft; EMT revised the manuscript; All authors accepted the final version for submission. The doctoral student and the supervisor confirm that all co-authors are in agreement with the publication being used for the doctoral thesis.

4.2 Article Summary

Beside temnospondyl amphibians, the Late Triassic (Norian) Krasiejów bonebed preserves also a reptile fauna, including a phytosaur *Parasuchus* cf. *arenaceus* (Dzik, 2001) and an aetosaur *Stagonolepis olenkae* Sulej, 2010. Although these two groups are not closely related, they both are archosaurs and belong to the clade Archosauriformes Gauthier, 1986. The phytosaur occupied an aquatic to semi-aquatic niche, whereas the aetosaur was a terrestrial, heavily armoured herbivores to omnivores (Desojo et al. 2013). From those two genera, *S. olenkae* and *P.* cf. *arenaceus*, femora and humeri were sectioned histologically. Moreover, for comparison of growth pattern, a similarly-sized femur of the phytosaur *Nicrosaurus* sp. Fraas, 1866 from the German Heslach locality was sampled. Even though *Nicrosaurus* originates from a geographically more distant locality, it originates from similarly aged beds (Norian; Wild 1989) and it is phylogenetically more closely related to *Parasuchus* from Krasiejów, than *Parasuchus* to *Stagonolepis*. The main aim of this study was to analyse the growth pattern of animals originating from one locality, but occupying different ecological niche, and between animals closely related but originating from different localities. Additionally, a comparison of the growth pattern with literature data on previously histologically examined aetosaurs and phytosaurs long bones from North America (*Rutiodon* sp., Phytosauria indet., *Desmatosuchus* sp., *Calyptosuchus* sp., *Typothorax* sp., *Coahomasuchus chathamensis*; de Ricqlès et al. 2003; Hoffman et al. 2019), South America (*Aetosauroides scagliai*; Ponce et al. 2022), and Europe (*Mystriosuchus steinbergeri*; Butler et al. 2019) was performed. All three, newly sectioned taxa display lamellar-zonal bone build of parallel-fibred bone with various collagen fibres organisation and show a low to moderate vascular density. Both, femora and humeri, show a rather diffuse growth pattern, however, areas of lower organised fibres (zones) and higher organised fibres (annuli) occur, and sometimes are visible only locally. Clear Lines of Arrested Growth (LAGs) are absent for the samples from Krasiejów and in the *Nicrosaurus* femur one LAG was observed in the outermost cortex. Interestingly, towards the outer cortex the annuli thickness increases and in the outermost cycles they become distinctly wider than the zones. Instead of LAGs, the Krasiejów taxa display multiple rest lines and sub-cycles in the cortex. The phytosaurs (*Rutiodon* sp., Phytosauria indet.) and aetosaurs (*Desmatosuchus* sp., *Calyptosuchus* sp., *Typothorax* sp., *C. chathamensis*) from North America grow with the fast-growing fibro-lamellar bone and in the later phase of growth the change into slow-growing lamellar-zonal bone (de Ricqlès et al. 2003; Hoffman et al. 2019). Moreover, the South American aetosaur *A. scagliai* also exhibits a phase of fast-growing fibro-lamellar bone and later in the ontogeny it changes into lamellar-zonal bone (Ponce et al. 2022). Further, all taxa from North and South America show the deposition of LAGs and grow with parallel-fibred bone intermixed with woven bone, which are both absent in the samples from Krasiejów (de Ricqlès et al. 2003; Hoffman et al. 2019; Ponce et al. 2022). The marine phytosaurs *M. steinbergeri* from Austria, grows similar to the herein studied samples from Poland and Germany, only with lamellar-zonal bone consisting of parallel-fibred and lamellar bone, without the woven bone component (Butler et al. 2019). However, *M. steinbergeri* shows the deposition of LAGs (Butler et al. 2019), which is absent in the samples from Krasiejów (Poland). The very similar growth pattern was observed between *S. olenkae* and *P.* cf. *arenaceus* from Krasiejów, despite the different phylogenetic position and the occupation of different life styles (terrestrial vs. semi-aquatic). Therefore, the absence of LAGs but the occurrence of rest lines might be connected with special local environmental conditions in Krasiejów during the Late Triassic period, which were rather mild.

Chapter 5

Triassic nursery? Evidence of gregarious behavior in juvenile pseudosuchian archosaurs as inferred by humeral histology of *Aetosaurus ferratus* (Norian; southern Germany)

5.1 Authors and their contributions

Teschner, E. M., Konietzko-Meier, D., Desojo, J.B., Schoch, R.R., and N. Klein. Triassic nursery? Evidence of gregarious behavior in juvenile pseudosuchians archosaurs as inferred by humeral histology of *Aetosaurus ferratus* (Norian; southern Germany). Submitted to *Journal of Vertebrate Paleontology* on August 3rd, 2022; 1st revision submitted on November 4th; 2nd r revision submitted on December 7th, 2022.

EMT, DK-M and NK designed the study; RRS provided the material; EMT selected the material and prepared thin-sections in the laboratory; EMT and DK-M scanned the bones in a micro-CT; EMT, DK-M and NK analysed the thin-sections; EMT took photographs and micrographs, prepared the figures, and wrote the manuscript draft; DK-M, NK and JBD critically revised the first draft; EMT revised the manuscript; All authors accepted the final version for submission. The doctoral student and the supervisor confirm that all co-authors are in agreement with the publication being used for the doctoral thesis.

5.2 Abstract as submitted to *Journal of Vertebrate Paleontology*

The taxon *Aetosaurus ferratus* was erected on the basis of a unique accumulation of 24 small-sized skeletons (20 to 82 cm body length) from the Late Triassic Kaltental locality (southern Germany). The histology of two humeri of *A. ferratus* belonging to the smallest and largest individual of the Kaltental assemblage reveals parallel-fibered bone, with relatively densely scattered simple vascular canals arranged reticularly to radially. The larger specimen preserves few, small primary osteons. Both specimens show residuals of an avascular tissue with zonation, which most likely represent hatchling bone. No signs of remodeling in form of secondary osteons or resorption are present in neither specimen. Annual growth marks are absent too in both individuals. Comparing tissue type of both analyzed humeri with long bone histology of large-sized aetosaurs from other localities worldwide, implies a juvenile stage for both Kaltental specimens, and thus, provides a juvenile stage for all specimens of the assemblage. An accumulation of so many juveniles of a similar size is a novelty for aetosaurs,

and might indicate a gregarious behavior in early ontogenetic stages to overcome predation or might be the result of environmental conditions such as a drought.

5.3 Introduction

Aetosauria are a clade of quadrupedal, armored archosaurs whose terrestrial ecology is inferred as including both herbivory and omnivory (Desojo et al., 2013). Aetosaurs achieved a nearly global geographic distribution, whereas they are stratigraphically restricted to the Upper Triassic (Carnian-Rhaetian) (Desojo et al., 2013; Biacchi Brust et al., 2018). Most aetosaur taxa reach a total body length between three and six meters (Desojo et al., 2013). The only exceptions are the relatively small *Coahomasuchus* spp. from North America (approx. 150 cm total body length) and *Aetosaurus ferratus* Fraas, 1877 from Germany (between 20 to 150 cm) (Schoch 2007). *A. ferratus* is best known from an accumulation of 24 individuals (20 to 82 cm) excavated in Kaltental near Stuttgart (Lower Stubensandstein), but is also reported by single *Aetosaurus* specimens from Pfaffenhofen (Middle Stubensandstein) (Fraas, 1877; Schoch, 2007) and Eibensbach (Lower Stubensandstein) (Wild, 1989). Also from the area of Stuttgart (Heslach, Murrhardt), a second, nearly complete specimen of the aetosaur *Paratypothorax andressorum* (Long and Ballew, 1985) is approximately 200 cm in length (Schoch and Desojo, 2016).

The *A. ferratus* osteology from Kaltental was first studied by Fraas (1877) and later in more detail by Schoch (2007) with comparisons to other *Aetosaurus* material from the vicinity of Stuttgart and to *Stagonolepis robertsoni* Walker, 1961 from Scotland. Based on the general low degree of ossification (e.g., unfused caudal neural arches, poorly pronounced fourth trochanter, and thin and slender osteoderms with a weakly developed ornamentation), the *A. ferratus* material was interpreted as most certainly juvenile (Schoch, 2007). Study of the additional specimen of *P. andressorum* (Schoch and Desojo, 2016) also addressed the question of whether the *A. ferratus* accumulation represents a small-sized species or a collection of juveniles. The small size of *A. ferratus*, its geographical proximity to the *P. andressorum* material, as well as the morphological similarities between these two aetosaur taxa, constitutes some level of support that *Aetosaurus* represent a juvenile stage of this larger taxon (Schoch and Desojo, 2016). To test this hypothesis further and more directly utilizing long bone paleohistology, as the histological growth pattern, the tissue type and the growth mark deposition, thus it informs about the ontogenetic stage (de Buffrénil et al., 2021).

Previous histological study of *A. ferratus* (SMNS 12670) and *P. andressorum* (SMNS 91551) examined two paramedian osteoderm fragments (Scheyer et al., 2014). In *A. ferratus*, both cortices are thin and consist of lamellar bone, but with a highly vascularized (primary vascular canals) external cortex lacking growth marks (Scheyer et al., 2014). The external cortex of the *P. andressorum* osteoderm, in contrast, consists of a low vascularized (scattered primary vascular canals) lamellar-zonal bone (LZB) containing coarse Sharpey's fibers as well as few secondary osteons (Scheyer et al., 2014). The inner region is highly remodeled and the basal cortex consists of LZB with only a few simple primary vascular canals. In the thickest area of the basal cortex, 17 growth cycles are preserved as alternating zones and lines of arrested growth (LAGs) (Scheyer et al., 2014). Thus, the osteoderm histology supports an estimated age of one year for *A. ferratus* (specimen SMNS 12670, which was not part of the herein sampled *Aetosaurus* accumulation) and at least 17 years for *P. andressorum* (Scheyer et al., 2014).

There are a few published studies that examine the long bone histology of various North American (possibly *Calyptosuchus, Desmatosuchus* and *Typothorax*; de Ricqlès et al., 2003; *Coahomasuchus*; Hoffman et al., 2019), South American (*Aetosauroides*; Ponce et al., 2022), and Polish (*Stagonolepis*; Teschner et al., 2022) aetosaur taxa. Long bones of North and South American taxa show fibro-lamellar bone (FLB) in the inner cortex with a change to LZB in the outer cortex, with well-developed growth marks in form of LAGs (de Ricqlès et al., 2003; Hoffman et al., 2019; Ponce et al., 2022). The Polish *Stagonolepis olenkae*, however, shows only LZB with alternating zones, annuli, and absence of LAGs (Teschner et al., 2022). The smallest-known, sampled aetosaur humerus is that of *Aetosauroides scagliai*, which measures approximately 11.5 cm (Ponce et al., 2022) and is thus nearly triple the size as the herein studied *A. ferratus* humeri.

We studied the humeral histology of two specimens from the *Aetosaurus ferratus* assemblage from Kaltental (S Germany) in order to address the question, whether the small size of *A. ferratus* reflects an early ontogenetic stage or is diagnostic of the species.

Institutional Abbreviations—IGPB Bonn, Institute of Geosciences, Division of Palaeontology, University of Bonn, Bonn, Germany; **SMNS**, State Museum of Natural History, Stuttgart, Germany.

5.4 Material and Methods

The two sampled humeri belong to the Kaltental assemblage from the Lower Stubensandstein (Löwenstein Formation, middle Norian, Upper Triassic) near Stuttgart and are stored at the German State Museum of Natural History Stuttgart (SMNS) under the repository number SMNS 5770. The humeri are from the smallest (SMNS 5770-21; 3.1 cm humerus length; Fig. 1A) and one of the largest (SMNS 5770-2; 5.3 cm humerus length; Fig. 1B) individuals of the accumulation and were isolated mechanically from the slab. Before thin-sectioning, both were cast and later molded with plaster. µCT scans (www.morphosource.org/projects/000477738) were obtained with v|tome|x scanner manufactured by GE phoenix|X-ray, housed at the Institute of Geosciences in Bonn, Germany (IGBP), in order to determine the most suitable sampling area (i.e., the growth center) yielding the most complete growth record. It was identified as the area with the smallest medullary cavity and thickest cortex in cross section, which corresponds herein with the mid-diaphysis (Fig. 1A-J). Thin-sections were prepared according to the method described in Klein and Sander (2007) and are deposited under www.morphosource.org/projects/000477738. The histological study was performed with a Leica DM LP microscope, the pictures were obtained with a Leica DFC 420 camera. For the microstructural studies, the thin-sections scans were converted into binary images (black=bone, white=porosity; Fig 1C, G) and the porosity was measured with the software *BoneProfileR* (web server version v. 2.4 build 766; Gônet et al., 2022). The histological nomenclature follows Francillon-Vieillot et al. (1990) and de Buffrénil et al. (2021).

5.5 Results

The cross-section of the smaller specimen SMNS 5770-21 (3.7 mm midshaft diameter; Fig. 1G-J) is narrow elliptical as it is medio-laterally crushed post-mortally, whereas the cross-section of the larger specimen SMNS 5770-2 (5.3 mm midshaft diameter; Fig 1C-F) is broad elliptical. Both sections show a central medullary cavity, which is larger in SMNS 5770-21 (Fig. 1C-F) compared to SMNS 5770-2 (Fig. 1G-J); the cortex, however, is thicker in specimen SMNS 5770-2. The medullary cavity is bordered directly by the primary periosteal cortex in both specimens. No endosteal bone is present in SMNS 5770-21 (Figs. 1C-F; 2A-B), whereas in SMNS 5770-2 a thin layer of endosteal lamellar bone is lining the medullary cavity (Figs. 1H-J; 2C-D). No signs of remodeling are visible in either specimen, instead, only the primary, periosteal cortex is preserved, consisting of parallel-fibered bone. Locally, a higher organization of fibers is preserved in both sections (Fig. 1E-F, I-J; 2E-F); however, they are not traceable throughout the cortices. On the medial side in both specimens, a highly organized and almost avascular tissue is preserved (Figs. 1D-F, H-J; 2E-F); however, in SMNS 5770-2, a clear zonation, in form of thin layers of higher organized tissue, is preserved additionally (Figs.1H-J; 2F). The vascular density is moderate to high in both samples. In SMNS 5770-21, it is regularly dense until the outermost cortex, where the vascular density slightly decreases with an overall cortex compactness value of 94% (Fig. 1C). In SMNS 5770-2, the vascular density is high throughout the section, the cortex compactness value is 83% (Fig. 1I). In SMNS 5770-

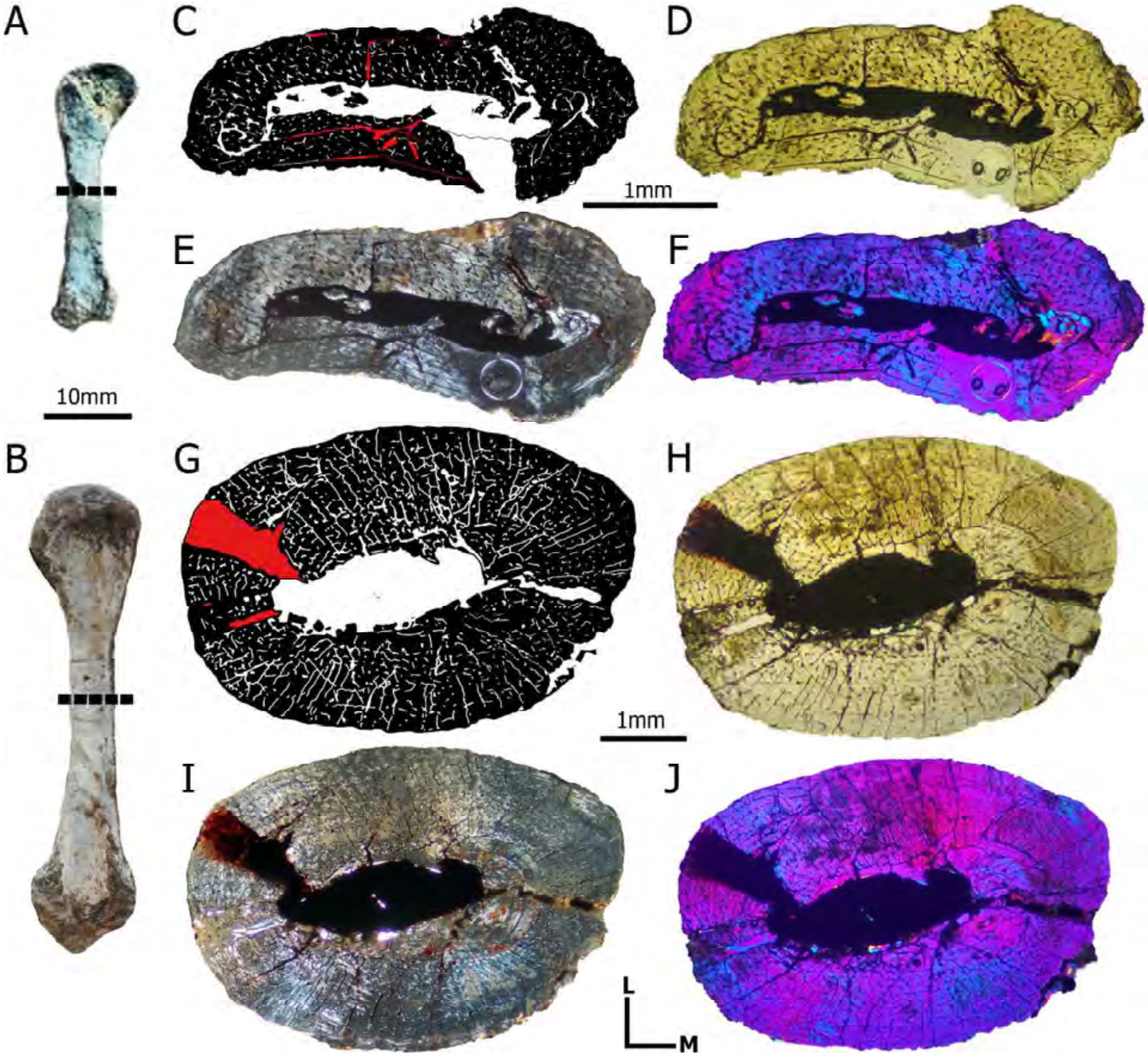

Figure 5.1: *Aetosaurus ferratus* humerus morphology of **A**, SMNS 5770-21 and **B**, SMNS 5770-2; **C**, bone microstructure of SMNS 5770-21; **D**, cross-sections of SMNS 5770-21 in normal transmitted and **E**, **F**, cross-polarized light; **G**, bone microstructure of SMNS 5770-2, **H**, cross-sections of SMNS 5770-2 in normal transmitted light and **I**, **J**, cross-polarized light. Scale bar for **A** and **B** equals 10 mm.

21, the simple vascular canals are reticularly oriented; additionally, radial simple vascular canals are preserved mostly at the lateral and medial bone side (Figs. 1C-J; 2A-B, E). In SMNS 5770-2, the simple vascular canals are mostly arranged in radial and reticular orientation, preserved equally throughout the cortex (Figs. 1G-J; 2C-D, F). Moreover, very few, scattered, small primary osteons are present in the SMNS 5770-2 section (Figs.1I-J; 2D, F). Osteocyte lacunae are more numerous in the smaller SMNS 5770-21, whereas in the larger SMNS 5770-2 they are almost absent (Fig. 2A-B). Similarly, SMNS 5770-21 shows few Sharpey's fibers, whereas they are absent in SMNS 5770-2. Secondary osteons, erosion cavities or annual growth marks are absent in both samples.

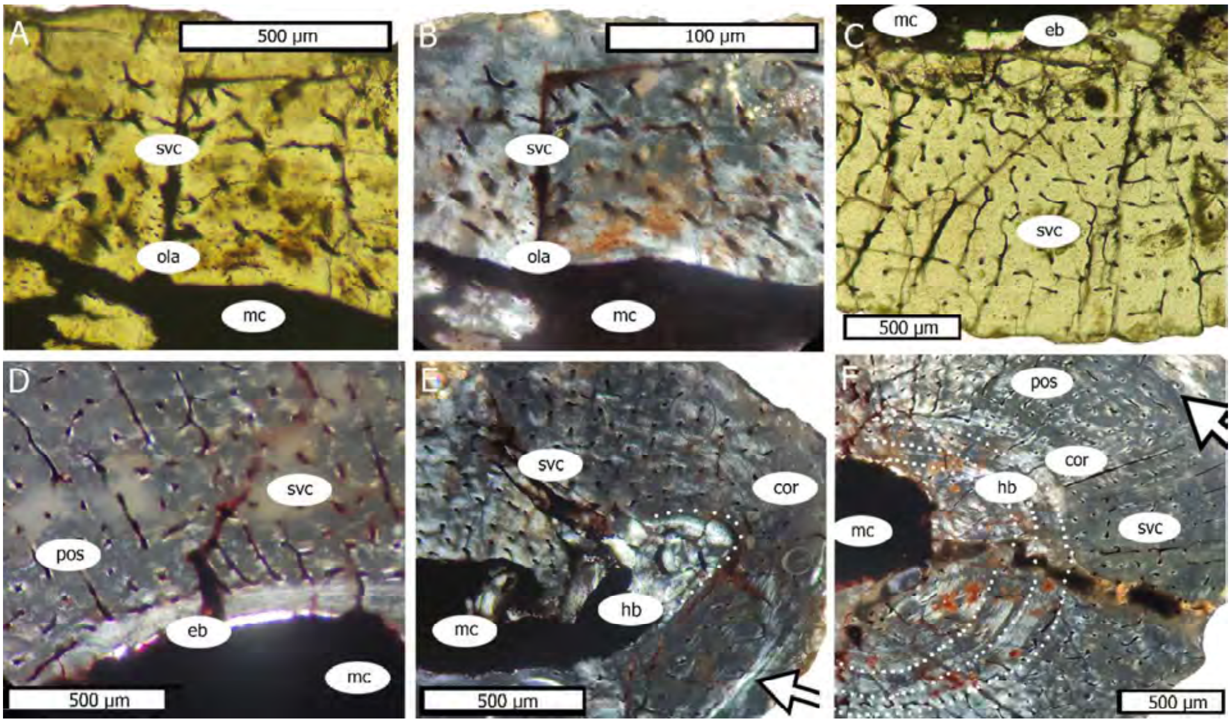

Figure 5.2: Detailed histology of *Aetosaurus ferratus* humerus **A**, **B**, **E**, SMNS 5770-21 and **C**, **D**, **F**, SMNS 5770-2. Arrows in **E**, and **F**, indicate the areas with higher organized tissue. **cor**= cortex; **eb**= endosteal bone; **hb**= hatchling bone; **mc**= medullary cavity; **ola**= osteocyte lacunae; **pos**= primary osteons; **svc**= simple vascular canals.

5.6 Discussion

5.6.1 Ontogenetic Stage

Both specimens grew with a parallel-fibered bone and show a similar vascular density; however, abundant radial vascular canals preserved in both sections indicate a fast growth rate (de Margerie et al., 2002). The highly organized, almost avascular tissue in the innermost cortex with preserved zonation (only in SMNS 5770-2; Figs. 1H-J; 2F) most likely represents hatchling bone (Klein and Griebeler, 2018). The cortex thickness, which is thinner in the smaller SMNS 5770-21, correlates with the increasing bone length. Also, the larger SMNS 5770-2 shows deposition of an endosteal bone layer around the medullary cavity, which is absent, or not yet developed, in the smaller specimen. Although the tissue is relatively highly organized, both specimens are attributed to an early ontogenetic stage based on the lack of annual growth marks and the absence of remodeling or resorption, as seen in other aetosaur limb bone samples (de Ricqlès et al., 2003; Hoffman et al., 2019; Ponce et al., 2022; Teschner et al., 2022). Because no annual growth marks are discernible, the age of both individuals are estimated as less than one year. Although dermal bone and long bone histology are difficult to compare directly (Klein et al., 2009), the age estimation of a maximum of one year for the *A. ferratus* osteoderm (Scheyer et al., 2014) fits well to our age estimation for *A. ferratus* humeri, implying a juvenile stage for all sampled elements of *Aetosaurus*. Based on our histological results (no erosion, higher vascular density, no annual growth marks) and together with the morphological evidence (Schoch, 2007) we conclude, that sampled elements of *A. ferratus* (Scheyer et al., 2014) represent an early ontogenetic stage: i.e., represents juvenile individuals. To test the hypothesis that all specimens of *A. ferratus* are juvenile more samples of larger *A. ferratus* individuals are needed.

5.6.2 Histological Growth

Previous histological studies of limb bones from various aetosaur taxa (de Ricqlès et al., 2003; Hoffman et al., 2019; Ponce et al., 2022; Teschner et al., 2022) included only long bones distinctly larger than our specimens. Aetosaur long bones from North and South America always show a phase of rapid deposition of highly vascularized FLB (woven bone intermixed with parallel-fibered bone) and later in ontogeny a phase of slower bone deposition consisting of low vascularized LZB (lamellar bone intermixed with parallel-fibered bone) (de Ricqlès et al., 2003; Hoffman et al., 2019; Ponce et al., 2022). Moreover, all studied taxa from North and South America show woven bone in their inner cortex, a tissue which indicates fast deposition and is thus assumed to indicate an early ontogenetic stage (de Ricqlès et al., 2003; Hoffman et al., 2019; Ponce et al., 2022). However, *Stagonolepis olenkae* humeri from Poland show no deposition of woven bone and thus no deposition of FLB. Interestingly, *S. olenkae* grew only with LZB throughout their preserved ontogeny, and furthermore, it shows no clear LAGs but instead displays a rather diffuse stratification by zones and annuli (Teschner et al., 2022).

However, the sampled size range of *Stagonolepis* humeri was between 21.6-24 cm and none of the samples from Poland belong to a very small/young individual (Teschner et al., 2022). Thus, we cannot exclude that earlier ontogenetic stages might have displayed woven bone that was subsequently removed by remodeling in these larger specimens.

The smallest Kaltental specimens (3.1-5.3 cm) lack any woven bone component, and the deposited parallel-fibered tissue is already well organized. This could either be because the juveniles start with slow growth as observed in some pachypleurosaurs (Klein and Griebeler, 2018), which continue later with fast growing tissue, or they were in general restricted to slow growth with a highly organized parallel-fibered bone throughout ontogeny, as described for a marine phytosaur from Austria (Butler et al., 2019). Given what we know from aetosaur growth from *S. olenkae*, the latter explanation is reasonable, although this is atypical for an archosaur (de Ricqlès et al., 2003; 2008; Klein et al., 2017). The closely related aetosauriform *Revueltosuchus callenderi* grows also only with slow-growing LZB but the growth is interrupted by several LAGs (Parker et al., 2022). Klein et al. (2017) summarized the deposition of various bone tissues (LZB, FLB or first growth with LZB and a later turnover to FLB) within a phylogenetic context. However, none of the previously sampled pseudosuchians showed the deposition of LZB and a later turnover into FLB (de Ricqlès et al., 2003; 2008; Klein et al., 2017; Ponce et al., 2022; Teschner et al., 2022). Moreover, the previous attempts to correlate the growth pattern observed in appendicular bones (e.g., deposition of slow-, fast-growing bone tissue or a mix of both) with phylogeny did not show a clear trend, as it varies across genera (de Ricqlès et al., 2003; 2008; Klein et al., 2017).

5.6.3 Paleobiological Implications

The Kaltental individuals range in size from 20 to 82 cm but the smallest and largest humeri, based on histological evidence, are both less than one year old. With 24 individuals, this accumulation could represent a single clutch, when assuming different growth rates e.g., due to intraspecific, and/or sex differences; however, this is speculative. If correct, this would imply that the clutch members stayed together, for an extended period, weeks if not months, after hatching. Extant reptile species are highly variable in terms of how long clutch members stay together, if at all, ranging from several days to several years (e.g., sea turtles vs. crocodiles) (Gans and Tinkle, 1978; Thorbjarnarson and Hernández, 1993). Nonetheless, we infer that the *A. ferratus* juveniles from Kaltental form a biologic rather than a taphonomic accumulation. It was proposed for *A. ferratus* (SMNS 5770), that the association was due to fluvial processes (Fraas, 1877). Arguments against a solely taphocoenosis include the lack of evidence for post-mortem transportation, and an overall high degree of skeletal articulation. Moreover, the specimens do not show a preferred orientation, such as a sub-parallel side-by-side alignment indicative of transportation flow (Abdala et al., 2006). They instead, point in different directions and lie on the same ground level. There is also no evidence that the specimens were mired in sediment, which is another potential mechanism explaining the origin of this accumulation (Sander, 1992). In any case, the Kaltental specimens could represent an age aggregation of juveniles. Herd behavior can be excluded, as no large specimens were found in the nearest proximity of the association or locality. This accumulation might have formed during a period of drought as observed for modern vertebrates in Africa (Shipman, 1975); however, under this hypothesis one would expect preservation of different ontogenetic stages and/or other taxa, neither of which are present at Kaltental. If the animals did die during a single catastrophic event, then the Kaltental assemblage could reflect gregarious behavior. A juvenile only assemblage of Early Cretaceous *Psittacosaurus* from China was interpreted to reflect anti-predation social behavior (Zhao et al., 2013). Moreover, a mono-taxic aggregation of nine adults of the prestosuchid *Decuriasuchus quartacolonia* from the Middle Triassic of Santa Maria Formation in southern Brazil were reported (França et al., 2011) as representing a possible social grouping, a behavior well-supported among dinosaurs (e.g., Cotton et al., 2008; Zhao et al., 2013; Pol et al., 2021). Nesbitt et al. (2020) described at least three similarly sized specimens of the loricate *Heptasuchus clarki* from the ?Mid-Upper Triassic from Central Wyoming (USA). Most recently, Parker et al. (2022) described a grouping of 12 individuals of the aetosauriformes *Revueltosaurus callenderi* from the Upper Triassic Chinle Formation in Arizona (USA), that based on long bone histology, represent late juvenile to sub-adult animals.

5.7 Conclusions

The long bone histology of two *A. ferratus* specimens from Kaltental clearly shows an early ontogenetic stage (i.e., juveniles) based on their tissue type and the absence of growth marks and erosion. Moreover, the humeri preserve a tissue resembling hatchling bone. The Kaltental slab contains an assemblage of juveniles, which formed more likely biologically than taphonomically. The individuals had gathered for whatever reason, possibly as a single clutch, and likely died during a single catastrophic event (e.g., drought). Since the smallest and largest

A. ferratus humerus from the association do not exceed one year at death, the SMNS slab would preserve a multiple juvenile assemblage rather than a small-sized species. Therefore, we cannot exclude the possibility that the *Aetosaurus* and *Paratypothorax*, both originating from the Stubensandstein (Löwenstein Formation), may represent one taxon and different ontogenetic stages, as proposed previously. Furthermore, the *Aetosaurus ferratus* aggregation indicates the first evidence of gregarious behavior among aetosaurs.

5.8 Acknowledgements

We thank I. Rosin (SMNS Stuttgart) and O. Dülfer (IGBP Bonn) for preparation of the material and the production of the thin-sections; F. Miedema for the discussion and linguistic improvement of the former version of the manuscript; and P. Jiménez-Huidobro for the assistance during µCT scanning. Editor G. Bever and reviewers B. Parker, R. Irmis, and anonymous provided constructive suggestions which improved the manuscript.

Chapter 6

The unique long bone histology of *Ozimek volans* from the Late Triassic of Poland

6.1 Authors and their contributions

Konietzko-Meier, D, Teschner, E.M., Tańczuk, A., and P.M. Sander. Unique long bone histology of *Ozimek volans* from the Late Triassic of Poland. Submitted to *Palaeontology* on September 14th, 2022.

EMT and DK-M designed the study; EMT selected the material and prepared thin-sections in the laboratory; EMT, DK-M and PMS analysed the thin-sections; EMT took micrographs; DK-M and PMS performed SEM analyses; DK-M took photographs, prepared the final figures, and wrote the manuscript draft; EMT, AT and PMS revised the first draft; All authors accepted the final version for submission. The doctoral student and the supervisor confirm that all co-authors are in agreement with the publication being used for the doctoral thesis.

6.2 Abstract as submitted to *Palaeontology*

Ozimek volans is one of the most mysterious representatives of the Late Triassic fauna of Krasiejów, Poland. Phylogenetically, it belongs to the "protorosaurs", but the elongated limbs and presumed gliding abilities are not known in this group, making *Ozimek* more similar to Pterosauria rather than to other protorosaurs. Therefore, it is interesting to see if the unusual lifestyle for protorosaurs is reflected in the bone histology. The goal of this study is to investigate whether the bones of *Ozimek* exhibit any specific histological adaptations to gliding in addition to morphological limb elongation. Two long bones from *Ozimek* (femur and humerus) were sectioned to obtain details about the histological framework. A large medullary cavity and thin walls built of lamellar bone with rare simple vascular canals are visible in both bones. However, the most characteristic feature of the cortex are the numerous lamellae visible as regular, densely packed rings around the entire section. *Ozimek* bones histologically resemble those of small bats with their compact structure, little to moderate vascularisation, and slow remodelling, contrary to birds and pterosaurs growing with highly vascularised fibro-lamellar bones. It is likely that bats, as well as *Ozimek*, grew too slowly to form a lamellar bone, instead, a thin, compact and poorly vascularised cortex might be well suited to handle a high load while

limiting overall weight. In this case, well-ordered collagen fibres in successive lamellae appear to be a key adaptation for better distribution of the load generated during gliding along the bone.

6.3 Introduction

One of the most enigmatic members of the Late Triassic fauna from the Krasiejów site is *Ozimek volans* Dzik and Sulej, 2016, a small reptile with very long and graceful fore- and hind limb bones (Dzik and Sulej 2016). The unique anatomy of *Ozimek* makes it difficult to determine its phylogenetic position. *Ozimek* was originally classified as a member of the Sharovipterygidae Tatarinov 1989 within Archosauromorpha Huene 1946 (Dzik and Sulej 2016). The first phylogenetic analysis that included *Ozimek* determined it to be a member of Tanystropheidae, a clade within Protorosauria, and a close relative of *Langobardisaurus* and *Tanytrachelos* (Pritchard and Sues 2019). In the most recent study (Spiekman et al. 2021), *Ozimek* is placed in the Archosauromorpha, but its exact position is unclear, either being included in Tanystropheidae or being the sister group to that clade.

Regardless of the exact phylogenetic position, the extremely elongated limbs are not known at all in "protorosaurs" (*sensu* Spiekman et al. 2021), and appear to be a unique adaptation of *Ozimek*. In terms of morphology, the skeleton of *Ozimek* shows similarity to that of *Sharovipteryx mirabilis* (Sharov 1971; Gans et al. 1987; Unwin et al. 2000), known from its soft part preservation including a flight membrane extending to the tip of its hind legs (Sharov 1971; Gans et al. 1987; Unwin et al. 2000). Thus, Dzik and Sulej (2016) reconstructed *O. volans* in a similar manner, with a flight membrane that served as gliding surfaces and were stretched between elongated fore- and hind limbs.

The elongated extremities and the postulated presence of the flight membranes make the Bauplan of *Ozimek* more similar to Pterosauria than to any other protorosaur. The question arises whether *Ozimek* was actually able to glide or the graceful limbs are an expression of a different mode of life than has been hypothesized. The ability to fly in pterosaurs and volant birds is not only reflected in their morphology through lengthening and slimming of the limb bones, but also required numerous adaptations at the histological level to produce a lightweight skeleton. The most important adaptation is the postcranial skeletal pneumaticity (PSP), (Martin and Palmer 2014). Through PSP, the heavy marrow in the interior of the bones is replaced by air. In addition to their extremely thin bone walls, key features of pterosaur and bird bones include rapid growth, manifested by the deposition of fibro-lamellar bone tissue (FLB) and lamellar bone endosteum lining the large and empty medullary cavity (de Ricqlès et al. 2000; de Margerie 2002; de Margerie et al. 2005; Steel 2008; Prondvai et al. 2012; Martin-Silverstone et al. 2016). Dzik and Sulej (2016) have previously mentioned the presence of thin bone walls in *Ozimek*, noting the similarity to flying taxa, but have not provided details on the histology of this taxon. Therefore, it is important to examine histologically whether the unusual lifestyle proposed for *Ozimek* is also reflected in the internal structure of the bones.

The objective of this work thus is to histologically examine two long bones, a humerus and a femur, derived from association of bones, to answer the question of the ability of *Ozimek* long bones to withstand the biomechanical stress associated with gliding.

6.4 Material and Methods

Five thin sections were prepared and examined for this study: three sections (a cross, a longitudinal, and an oblique tangential) from humerus UOPB 1148a (Fig. 6.1A) and a cross and a longitudinal section from the midshaft of femur UOPB 1148b (Fig. 6.1B). Both bones were preserved close to each other in one block, and were already published under the collection number UOPB 1148 (Dzik and Sulej 2016). To avoid misunderstanding, the letters a and b respectively for the humerus and the femur were added to the collection number. The anatomical orientation of bones and following thin-sections was performed based on the reconstruction from Dzik and Sulej (2016).

Figure 6.1: Long bones of *Ozimek volans* from the Late Triassic of Krasiejów (Poland). A, left humerus in proximal view. B, right femur in anterior view. Scale bars equal 10 mm. The white lines mark the cutting planes (1-cross section; 2-longitudinal section and 3-oblique tangential).

Thin sections were made in the laboratory of the Institute of Geosciences of the University of Bonn, Germany (IGPB), using the standard petrographic methods modified from Lamm (2013) and Stein and Sander (2009). A Leica DM EP light microscope with normal transmitted light and cross-polarized light was used to evaluate the sections and attached camera. In addition, a cross-section from the humerus was examined using the TESCAN Vega 4 SEM available at the IGPB. The sample, before being coated with gold, was etched with 10% HCl for a few seconds and rinsed with water. In this way, in addition to the lamellae, it was possible to visualize the osteocyte lacunae and tubules, which were naturally filled with the adhesive during the preparation of the thin section.

Histological nomenclature follows Francillon-Vieillot et al. (1990) and de Buffrénil et al. (2021).

6.5 Results

The detailed morphology of the humerus and femur was described previously (Dzik and Sulej 2016). Both bones (Fig. 6.1) are extremely long, with the humerus being 49 mm long (the largest known humerus, ZPAL AbIII/2511, is 61 mm long - Dzik and Sulej 2016), while the femur is almost twice as long (97 mm, the femur studied herein is the longest known).

The humerus (UOPB 1148a) is 4.2 mm in diameter, and the cortex is approximately 0.5 mm thick (Fig. 6.2A-D). The medullary cavity accounts for 42% of the surface area of the section (Fig. 6.2A-D). A strong regional differentiation of organisation can be observed in the cortex (Fig. 6.2D). The posterior part of the innermost cortex consists of lamellar bone with clearly visible lamellae forming an area without vascular canals, identified as the first annulus (Fig. 6.2E-G). A distinct line of arrested growth (LAG) separates the first annulus from the first zone, preserved as an area consisting of less organized, parallel-fibred tissue with only a few longitudinal, simple vascular canals. The first zone ends with a reversal line followed by the second annulus consisting of lamellar bone tissue and hosting two closely spaced LAGs (Fig. 6.2E-G). On the anterior side of the section, the innermost growth mark (annulus only) is only rudimentarily preserved (Fig. 6.2H-J). The growth record begins with the first zone, which is moderately vascularised by longitudinal primary osteons. The first zone is followed by the second, avascular annulus, which is separated from the first zone by a distinct reversal line. In the second annulus, three LAGs are visible separated by slow-growing lamellar bone (Fig. 6.2H-J). However, the most conspicuous structure preserved on the anterior side, is a distinct

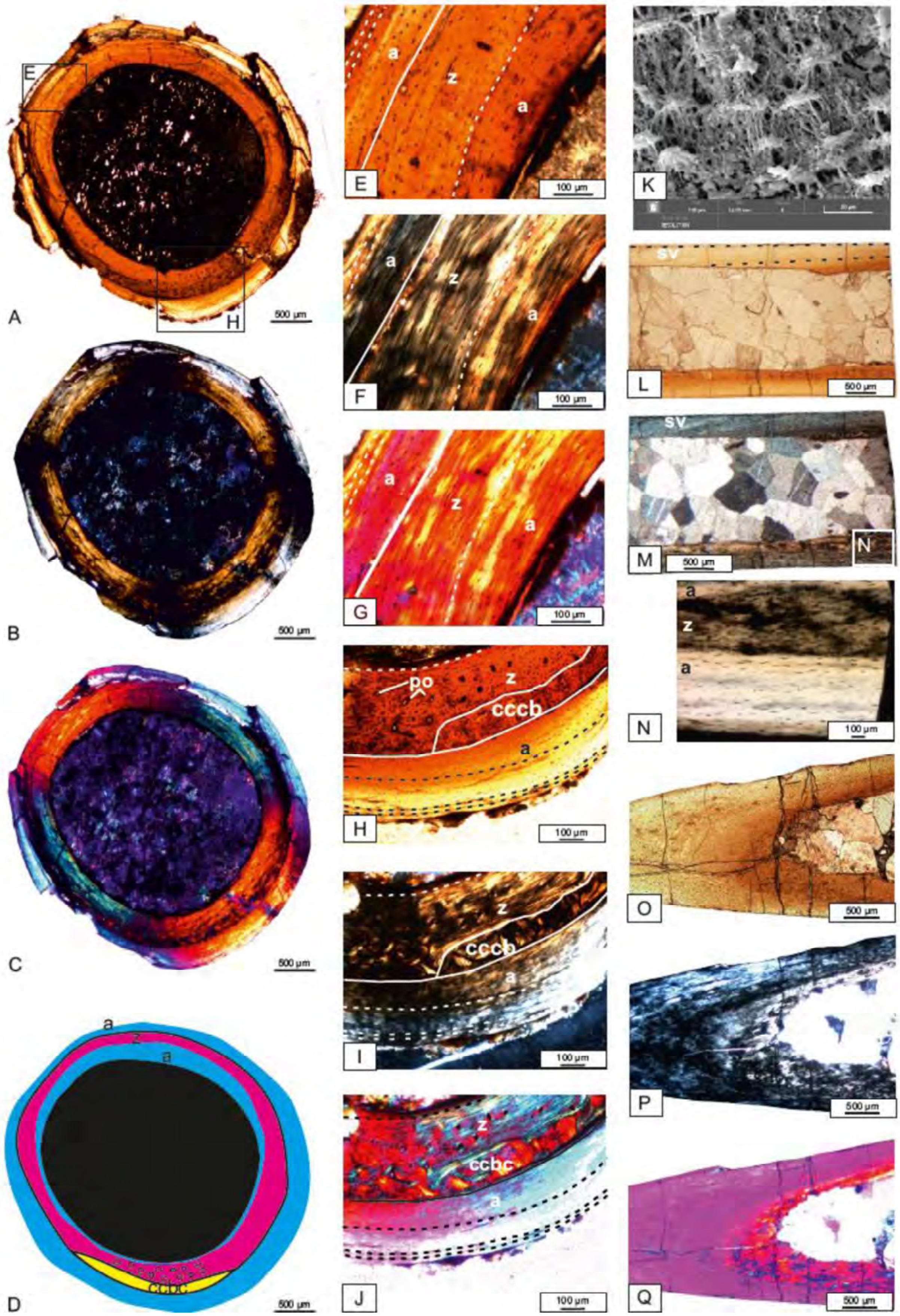

Figure 6.2: Microstructure and histology of the humerus midshaft of *Ozimek volans* from the Late Triassic of Krasiejów (Poland). A-C, the overview of the histological framework visible in the cross

(*Figure 6.2 continuation from previous page*) section in normal light (A), polarised light (B) and with lambda filter (C). D, the schema of the distribution of the growth marks visible in the cross section of humerus midshaft. E-G, close-up of the posterior part of cortex with well visible lamellae and growth marks in normal light (E), polarised light (F) and with lambda filter (G). H-J, close-up of the anterior fragment of cortex with visible island of coarse compact cancellous bone and growth marks in normal light (H), polarised light (I) and with lambda filter (J). K, SEM photography showing the osteocyte lacunae surrounded by net of canaliculi. L-M, the overview of the histological framework visible in the longitudinal section in normal (L) and polarised (M) light; the arrow marks the vascular canal. N, close up pf the fragment of cortex visible in the longitudinal section in polarised light. O-Q, the overview of the histological framework visible in the oblique tangential section in normal light (O), polarised (P) light and with lambda filter (Q). Continues lines always indicate the reversal lines, dashed lines mark the Lines of Arrested Growth. Abbreviations: A - annulus, cccb - coarse compact cancellous, po - primary osteon, sv - simple vascular canal, z - zone.

patch in the middle part of the cortical bone, consisting of an accumulation of the coarse compact cancellous bone (CCCB), separated from the inner zone by a reversal line and bounded externally by the second annulus, separated as well as by a reversal line (Fig. 6.2H-J). In all regions of the lamellar bone, the individual lamellae are very well defined (Fig. 6.2E-G). The osteocyte lacunae are very flat in the lamellar portions, whereas the shape of the osteocytes in the parallel-fibred matrix is more rounded (Fig. 6.2E). The osteocyte lacunae are always surrounded by a well-preserved network of canaliculi (Fig. 6.2K).

In the longitudinal section, a partially preserved zone is visible, framed internally and externally by lamellar annuli; the last one with two LAGs present (Fig. 6.2L-N). The simple vascular canals are observable as oblique structures intersecting the cortex (Fig. 6.2N).

In the oblique tangential section, the thin layer of lamellar bone followed by unorganized bone is visible in the innermost cortex (Fig. 6.2O-Q). In this section, the distribution of collagen fibres in the adjacent lamellae can be followed; the orientation of collagen fibres in each individual layer is not very different and they always show no colour distinction under microscopic observation with lambda filter while section rotation (Fig. 6.2Q).

In a femur (UOPB 1148b) the diameter of the femoral shaft measures 3.3 mm, with a cortical thickness of 0.2 mm (Fig. 6.3A-C). Extensive resorption of the medullary margin is visible, with a large medullary cavity accounting for 51% of the surface area of the sections (Fig. 6.3A-C). The femur has a less complex histological structure compared with the humerus. Most of

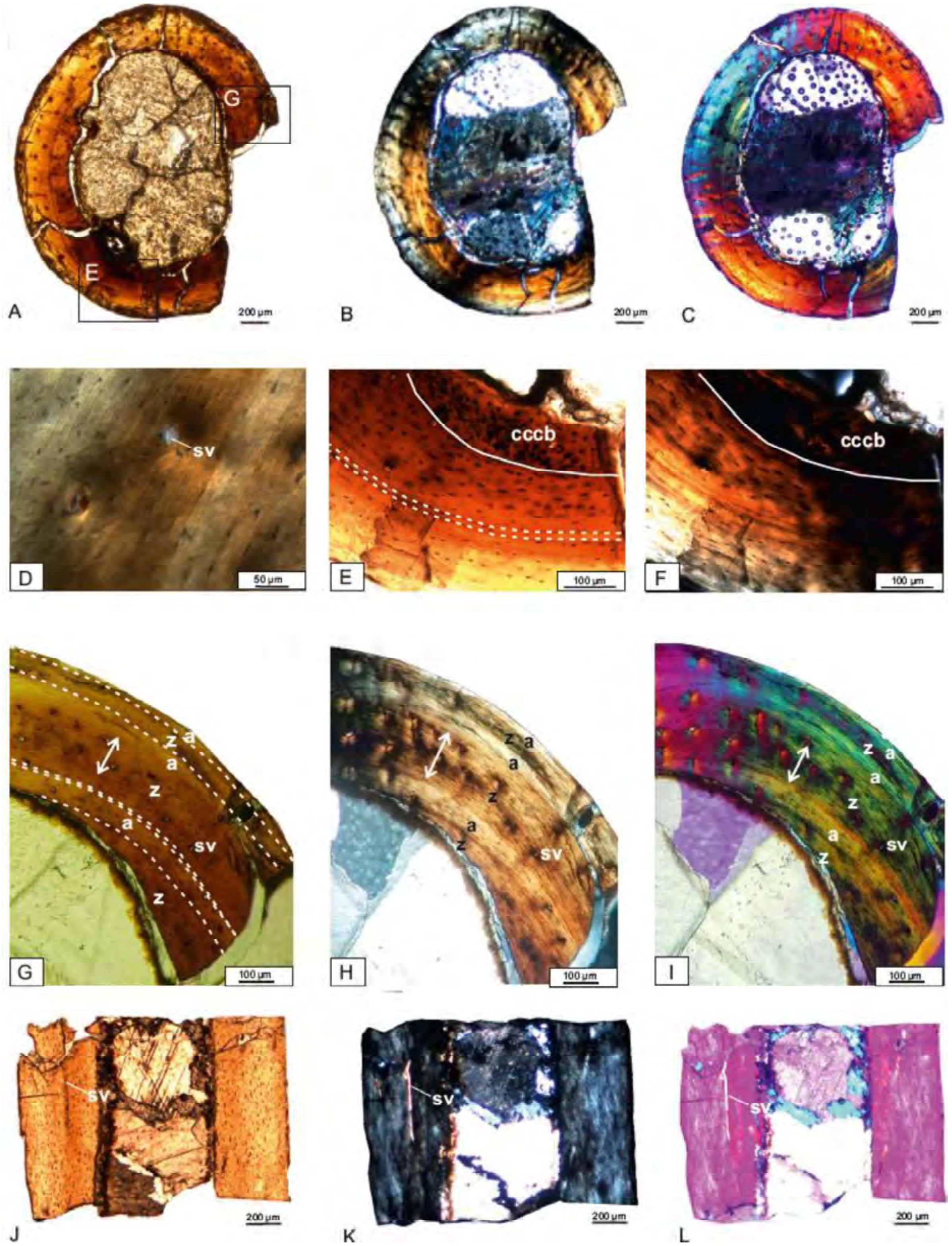

Figure 6.3: Microstructure and histology of the femur midshaft of *Ozimek volans* from the Late Triassic of Krasiejów (Poland). A-C, overview of the histological framework visible in the cross section in normal light (A), polarised light (B) and with lambda-filter (C). D, close-up if the cortex with visible well-organized lamellae system, image in polarized light. E-F, close-up of the cortex with preserved fragments of coarse compact cancellous bone in normal (E) and polarized (F) light. G-I, close-up of the anterior fragment of cortex with visible growth marks in normal light (G), polarised light (H) and with lambda filter (I), the arrow indicates the second zone. J-L, the overview of the histological framework visible in the longitudinal section in normal (J), polarised (K) light and with lambda filter (L). Continues

(*Figure 6.3 continuation from previous page*) lines always indicate the reversal lines, dashed lines mark the Lines of Arrested Growth. Abbreviations: a - annulus, cccb - coarse compact cancellous, dL – double LAG, sv – simple vascular canal, z - zone.

the cortex is composed of lamellar bone (Fig. 6.3A-C), with rare simple longitudinal vascular canals (Fig. 6.3D). The most characteristic cortex feature are the numerous lamellae, visible as regular, densely packed rings around the entire section, with the course of these lines changing slightly around the vascular canals (Fig. 6.3D). A small patch of CCCB is present at the margin of the medullary region, separated from the cortex by a reversal line (Fig. 6.3E-F). The most pronounced growth-related features are preserved at the anterior margin of the section, with the visible innermost remnant of the first zone, followed by the first LAG and first annulus (Fig. 6.3G-I). The first annulus terminates with a second distinct, double LAG. The adjoining second zone is much thicker than the first annulus and preserves most of the vascularisation, mostly represented by the simple canals and few primary osteons. The second zone merges into the second annulus with no clearly visible LAG in between. The second annulus ends again with a LAG (the third) adjacent to the third, thin zone followed by the fourth LAG. The last two LAGs join in parts of the section and form a double LAG. The entire growth sequence ends with the third annulus (Fig. 6.3G-I).

The longitudinal section of the femur also shows the lamellar structure of the cortex with few vascular canals (Fig. 6.3J-L). Growth marks corresponding to the pattern in the transverse section are only weakly recognisable, whereas LAGs are not visible (Fig. 6.3J-L).

6.6 Discussion

6.6.1 Ontogenetic development and growth pattern of Ozimek volans based on histology.

Morphologically, Dzik and Sulej (2016) reconstructed *Ozimek* with a femur that is approximately 1.3 times longer than the humerus, noting that the anterior limbs are much shorter in the juvenile stage compared to the hind limbs. However, the morphology of *Ozimek* was reconstructed based on composite skeletons, derived from bone assemblages in several blocks, what can lead to errors, as there is no certainty that elements in one block belong to one individual (Dzik and Sulej 2016). As noted above, the femur described in the current study is the longest known and was described by Dzik and Sulej (2016) as an adult, whereas the humerus from the same association, also examined herein, was determined by the same authors to be a juvenile based on the spherical shape of the proximal head and prominent dorsal crest (Dzik and Sulej 2016). Dzik and Sulej (2016) also noted these inconsistencies in size determination; they explained this by ontogenetic variation or incomplete preservation. The method which can help to confirm the ontogenetic stage is palaeohistology.

In the humerus, two annuli and one zone are preserved, with the second annulus being exceptionally thick (Fig. 6.2E-J), with one episode of growth cessation (LAG) visible in the innermost annulus at the end of the event, and three in the outer layer in some regions (Fig. 6.2E-J). In the femur, three well-preserved growth cycles are visible, each consisting of a fast-growing zone and a slow-growing annulus (Fig. 6.3G-I). However, the distribution of the LAGs varies strongly. The innermost, first annulus is enclosed between two LAGs, indicating cessation of growth at the beginning and end of the phase of slower growth, whereas in the second annulus, cessation of growth occurs only at the end of the phase, and the third annulus begins with a LAG again (Fig. 6.3G-I). Despite the not symmetrical occurrence of growth cessations which can reflect the seasonal environmental variation of the local conditions, the growth pattern of the femur is relatively clear. Based on the amount of growth marks (only a zone and an annulus) the estimated minimal age of the femur is three years.

Using the same proxy, the estimated minimal age of the humerus is only two years. However, in the humerus the meaning of the growth pattern preserved in the cortex following the reversal line is difficult to explain. Three LAGs are visible there, with the innermost being separated from the following two by a thick tissue layer, whereas the last two lines are relatively close to each other (Fig. 6.2H-J). Thus, these structures could represent two seasonal changes with a weakly differentiated zone in between. Nevertheless, it cannot be excluded that these lines represent three annual episodes of growth interruption or that they are just resting lines, rather than annual LAGs, that occur during one season. The last scenario is commonly known in other taxa from Krasiejów and described for the temnospondyl amphibian *Metoposaurus krasiejowensis* (Konietzko-Meier and Klein 2013; Konietzko-Meier and Sander 2013; Teschner et al. 2018), the aetosaur *Stagonolepis olenkae* and the phytosaur *Parasuchus* cf. *arenaceus* (Teschner et al. 2022). In that case, the thick external annulus with numerous growth lines is interpreted as a single growth event that occurred during a relatively long but mild dry season. Thus, the age of the humerus can be estimated to be two to five years, depending on which scenario is considered, and makes the humerus either older than? the femur or younger.

Features common in both bones are remnants of CCCB separated from the rest of the cortex by an extensive reversal line. The highly pronounced reversal line indicates resorption of the outer bone surface, which is necessary for the change in shape of the bone. In the humerus, this line is preserved throughout the entire section (Fig. 6.2D), whereas, in the femur, it is visible only in a small area of the section (Fig. 6.3E). In addition, the remnants of CCCB visible in the midshaft region of both bones indicate, that the length growth was rapid, resulting in a displacement of metaphyseal structures toward the diaphysis as growth and remodelling occurred (Steel et al. 2005). If these two elements represent an important break in the growth history, then the entire cortex of the femur corresponds only with the outer portion of the humeral cortex. It suggests, that in the humerus the innermost edge of the cortex is significantly less resorbed preserving earlier ontogenetic events. This, together with the fact that femur is much longer than the humerus, seems to confirm the more juvenile status of the humerus compared to the femur. However, it is important to state, that due to lack of comparative material, it is impossible to objectively determine the ontogenetic stage of both bones.

6.6.2 Does bone histology of Ozimek reflect phylogeny or lifestyle adaptation?

The bone histology of the taxa phylogenetically closest to *Ozimek*, namely *Tanystropheus* and *Macrocnemus*, show no similarity to *Ozimek*. Instead, the two taxa exhibit a relatively thick cortex with lamellar-zonal bone consisting of primary lamellar to parallel-fibred tissue of periosteal origin. The medullary cavity contains cancellous bone of secondary trabeculae surrounding a central cavity (Jaquier and Scheyer 2017). This implies, if the phylogenetic placement of *Ozimek* is correct, that its bone structure may be determined more strongly by its adaptation to a specific lifestyle-gliding, rather than by phylogenetic relationship.

Gliding is indeed a form of flight, which has been broadly defined as any locomotor behaviour in air that involves active control of aerodynamic forces (Dudley et al. 2007). However, gliders share almost no single anatomical or behavioural feature, and some species are unspecialized for gliding, producing aerodynamic forces using posture and orientation alone (Socha et al. 2015). Analyses based on extant mammal taxa support the theory that gliders should have long humeri and femora to improve aspect ratio, and that larger gliders should have relatively longer limb bones than smaller gliders to minimize drag and patagial loading at greater body masses (Runestad and Ruff 1995). There is not much known about the microanatomy and histology of long bones of gliders. Amson and Bibi (2021) suggest a tendency among scaly tailed squirrels and gliding squirrels to have a light-weight humerus and more circular diaphysis in cross-section compared to non-avian taxa, as an adaptation to resist torsional loads and/or to a multidirectional bending environment.

Flapping flight evolved in only three vertebrate groups: pterosaurs, birds, and bats. In all these three groups, bones with large medullary cavities and thin walls are present (Currey and Alexander 1985; Cubo and Casinos 1998). However, at the histological level, all volant birds and pterosaurs typically contain highly vascularised FLB tissue, with the lamellar bone never being developed as a dominant periosteal bone type and pneumatisation of the skeleton (de Ricqlès et al. 2000; Padian et al. 2004; Steel 2008; Martin and Palmer, 2014; Prondvai et al. 2012; Lee and Simons 2015; Martin-Silverstone et al. 2016). Moreover, the feature that makes the bones of larger, taxonomically derived pterosaur groups histologically unique is a "plywood-like" tissue composed of multiple layers of bone tissue, each with a different orientation of collagen fibres (Quekett 1849; de Ricqlès et al. 2000; Sayão 2003; Steel 2003, 2008; Chinsamy et al. 2009; Prondvai et al. 2012). None of these characters are present in *Ozimek*. The only volant group lacking the FLB tissue over a wide phylogenetic and body size range are bats (de Ricqlès et al. 2000; Padian et al. 2004; Steel 2008; Lee and Simons 2015). All of the humeri of small chiropterans examined, exhibit an avascular to poorly vascularised cortex with readily visible lamellae (see Lee and Simons 2015 - Fig. 4). *Ozimek* bones are in some way rather similar to small bat bones at the histological level, sharing a compact structure, low to moderate vascularisation, and slow remodelling. Lee and Simons (2015) suggested that the vascular disparity between the humeri of bats and birds may be related to differences in somatic growth rate, where bats grow approximately four times slower than birds of comparable size. Therefore, bats, as well as *Ozimek*, grow too slowly to form FLB, instead a compact, low-vasculature cortex might be well adapted to handle high stress while limiting weight (Lee and Simons 2015). However, a proper biomechanical analysis addressing the link between histology, microanatomy, and morphology of bat bones is lacking.

6.6.3 Lamellar bone as a specific biomechanical adaptation to flying.

Lamellar bone is one of the major bone tissue types found in vertebrates. It is a slowly depositing, highly organized tissue that forms in a dynamic osteogenetic process (Prondvai et al. 2014) and occurs mainly in primary or secondary osteons, but can also form a large part of primary compacta in some bradymetabolic vertebrates, in small-bodied mammals, and even is often deposited centripetally as endosteal bone and secondary trabeculae (Marotti et al. 1999;

Ferretti et al. 2002; Lamb 2013 and reference therein). The specific orientation of collagen fibres in successive lamellae gives a typical image of lamellar bone under the microscope in cross-polarized light: with the distinct banded or alternating pattern and in structures with a circular orientation of the lamellae, i.e., osteons, a dark "Maltese cross" effect (Bromage et al. 2003; Mitchell and van Heteren 2017).

What makes bones of *Ozimek* unique is their osteon-like structure with the “Maltese cross” effect, which results from the extremely well-developed lamellae (Figs. 6.2C and 6.3C). Similar, well-preserved structural lamellae are not known from appositionally growing cortex of any fossil tetrapod; moreover, such structure is usually restricted to the centripetally filled-in secondary osteons of modern mammals (Georgiadis et al. 2016; Stockhausen et al. 2021) and dinosaurs (Mitchell and van Heteren 2017). This raises the question of the cause and the role of the extremely well-developed lamellae in the bone cortex of *Ozimek*.

If the proposed lifestyle (Dzik and Sulej 2016) - gliding flight - was correct, then the long bones may have been subjected to high stresses. Insights from the biomechanics of secondary osteons may be informative here. The well-ordered collagen fibres in successive lamellae appear to be an important adaptation for better distribution of load along the bone. Studies by Ascenzi and Bonucci (1967, 1968, 1972) and Ascenzi et al. (2003, 2008) showed that different secondary osteons with well-visible lamellae are linked to different mechanical constraints. They showed that in humans secondary osteons with more longitudinally oriented collagen fibres, remaining dark in polarized light, have higher tensile strength (Ascenzi and Bonucci 1967), and that the elastic modulus is greatest in osteons with more transversely oriented fibres, appearing brightest under polarized light (Ascenzi and Bonucci 1968). Stockhausen et al. (2021) confirmed that the bright osteons are found in areas of compressive loading and the dark osteons are predominantly found in regions of a higher degree of stiffness, are required to be subjected to uniaxial loading, either compression or tension.

In the *Ozimek* extremities, the collagen fibres in the respective layers are oriented only longitudinally and diverge little between layers, so that the structure of the complete bone is more similar to the light osteons, which can decisively increase the compressive strength of the bone and elastic modulus (Stockhausen et al. 2021), what makes the bone especially suitable to resist torsional loads and multidirectional bending originating during gliding (Amson and Bibi 2021).

6.7 Conclusions

It seems that in the case of *Ozimek*, the observed histological structure is a clear respond to biomechanical stress connected with the gliding, rather than the representation of phylogenetic relation. The unique histological framework of long bones with extremely well-expressed lamellae is not a common adaptation known among avian animals, but with the combination with a low body weight, the limbs can contribute as a good support for a gliding animal. The slightly different histological structure of the humerus compared to the femur, especially the thicker cortical bone of the former, could indicate a different loading of the forelimb. However, since the bone is probably ontogenetically much younger than the femur, it cannot be excluded that this is related to ontogeny and indicates a change in loading mode due to development and growth. If yes, then bones coming from the same block do not belong to the same individual and cannot be taken as a proxy for morphological reconstruction. *Ozimek*, with thin-walled but biomechanically resistant bones and morphological adaptations, appears to be well adapted to gliding flight, although active flying does not appear likely due to the peculiar structure of the pectoral girdle.

6.8 Acknowledgements

We thank Olaf Dülfer for preparing thin-sections and Georg Oleschinski for photos (both University of Bonn). Adam Bodzioch from University of Opole is thanked for access and permission for sectioning of the material. We thank both reviewers and editor for all comments which greatly improved the previous version of this manuscript.

Chapter 7

Synthesis

The previous chapters have described the histological growth pattern of various taxonomic groups, including both amniotes and non-amniotes. Under careful examination, the same skeletal elements for every sampled group, namely humeri and femora, were prepared. Moreover, the ontogenetic stage was also considered during evaluation, in order to avoid misinterpretations while directly comparing specimens of different ontogenetic age with features not developed or already remodelled. Importantly, all sampled material originated from a single locality (Krasiejów), although the animals occupied different ecological niches. Therefore, the influence of various modes of life that could possibly overprint growth patterns, was also considered during the comparison between taxa.

Astonishingly, the growth pattern seems to be shared by most of the taxa originating from Krasiejów, and at least between the temnospondyl amphibians, aetosaurs and phytosaurs, despite their distant phylogenetic relationship. Therefore, for a better explanation of this phenomenon, the main idea was to compare the taxa occurring in Krasiejów with closely related taxa living in the same geological time interval but from geographically distant localities and thus exposed to possibly different (local) environmental and/or climatic conditions.

7.1 Histological growth of temnospondyl amphibians

In *Metoposaurus krasiejowensis* long bones have a lamellar-zonal tissue consisting of parallel-fibred bone with alternations of lamellar bone preserved (Konietzko-Meier and Klein 2013; Konietzko-Meier and Sander 2013). Growth marks in the form of zones and annuli are preserved (Konietzko-Meier and Klein 2013; Konietzko-Meier and Sander 2013; Teschner et al. 2018, 2020). Konietzko-Meier and Klein (2013) also note, that the thickness of annuli is unusually broad and occasionally of the same thickness as the corresponding zones. Strikingly, LAGs were absent in the Krasiejów samples.

The present comparison with the metoposaurid *Panthasaurus maleriensis* from India has shown a similar growth pattern as in *M. krasiejowensis*. Two humeri ISIA 70 and ISIA 73 (65 mm and 120 mm), and a femur, ISIA 83 (140 mm), revealed that with increasing length (i.e., the ontogenetic stage), the growth marks, especially the zones, become thinner towards the outer cortex and the annuli become ever thicker (Teschner et al. 2020). Moreover, the Indian sample also lacks deposition of LAGs, similar to samples from Krasiejów (Teschner et al. 2020). Steyer et al. (2004) sectioned femora of the Moroccan metoposaurid *Dutuitosaurus ouazzoui* and noted that the animals grew also with a lamellar-zonal pattern, deposit zones and annuli, however, they also deposit clear LAGs. Therefore, after comparing the taxa within one family, of similar geological age but inhabiting geographically distant places, we proposed that climatic conditions had an impact on the growth pattern. It follows that the climate in Morocco during the Late Triassic was much harsher than in Poland or India (Teschner et al. 2020).

Further, humeri of a second temnospondyl amphibian from Krasiejów, namely *Cyclotosaurus intermedius*, were sectioned. Both humeri (UOBS 02116 and UOBS 02431) were exceptionally large (141.6 mm and 146.4 mm) for Krasiejów. Based on their size they were assumed to belong to *Cyclotosaurus* and herein we tested the taxonomic affiliation of two large bones with a near uniform morphology. Palaeohistology has revealed that despite the almost identical shape and length, the bones document two distinct growth patterns. Moreover, the bones rather reflected the histotypes raised previously by Teschner et al. (2018) for *M. krasiejowensis* humeri. Both bones grew with lamellar-zonal bone and deposit growth marks in the form of zones and annuli, and again lack the deposition of LAGs. Astonishingly, despite being of the same length, both humeri showed a distinctly different ontogenetic age. Specimen UOBS 02431 showed a prominent thinning of zones towards the outer cortex and a highly advanced bone remodelling, almost copying the growth pattern of humerus ISIA 73 of *P. maleriensis*. However, specimen UOBS 02116 grew still with very thick zones and only showed thin annuli, and only a little bone remodelling. Therefore, humerus UOBS 02431 would represent an adult *M. krasiejowensis* whereas specimen UOBS 02116 would represent *C. intermedius*. Since postcranial material of cyclotosaurids is very rare, there is no material to compare the growth with. The only other sectioned humerus belongs to cf. *Cyclotosaurus* from the German Bonenburg locality and shows a similar growth pattern to humerus UOBS 02116, sectioned herein (Konietzko-Meier et al. 2019).

7.2 Histological growth of aetosaurs

Of the terrestrial aetosaur *Stagonolepis olenkae* ten humeri and two femora from Krasiejów were sectioned. The humeri grow rather uniformly with a lamellar-zonal bone consisting of parallel-fibred bone of various collagen fibre organisation. Thus, the zones are less organized on the tissue level and the annuli show more highly organized fibres. The growth pattern becomes more diffuse, with the occurrence of sub-cycles in the cortex. Further, *Stagonolepis* does not show LAGs. Despite a low size range (216-240 mm), the counted growth cycles (two to six), and thus the relative age, is not correlatable with bone length. The femora of *Stagonolepis* (330 mm and 370 mm) are completely remodelled and thus show no growth marks anymore.

There are histologically sectioned long bones of taxa from the USA (*Desmatosuchus* sp.*,* *Calyptosuchus* sp., *Typothorax* sp.; de Ricqlès et al. 2003; *Coahomasuchus chathamensis* Hoffman et al. 2019) and Argentina (*Aetosauroides scagliai*; Ponce et al. 2022) in the literature. The North American and South American aetosaurs show two phases of growth; first a fast-growth consisting of highly vascularised fibro-lamellar bone built of parallel-fibred and woven component, and later in the ontogeny of a slowed-down growth consisting of lamellar-zonal bone built of parallel-fibred and lamellar bone. Additionally to zones and annuli, the sectioned long bones from the USA and Argentina also show deposition of clear LAGs (de Ricqlès et al. 2003; Hoffman et al. 2019; Ponce et al. 2022).

For comparative purposes *Aetosaurus ferratus* from the Norian of Kaltental in Germany was sectioned, this is geographically closer to Krasiejów and thus potentially was exposed to similar climatic conditions. The material of *A. ferratus* originates from an accumulation of 24 small-sized individuals. Therefore, it is important to consider the ontogenetic age, and thus, a strict comparison between *Stagonolepis* and *Aetosaurus* should not be performed at this stage, because ontogeny might show a stronger palaeohistological signal.

Nevertheless, the humeri of *A. ferratus* reveal a very juvenile tissue built of parallel-fibred bone, lacking the woven component. Locally, the tissue preserves more organized fibres; these, might represent a hatchling bone. However, no clear zones, annuli or LAGs can be distinguished.

7.3 Histological growth of phytosaurs

Of the semi-aquatic to aquatic taxon *Parasuchus* cf. *arenaceus* one humerus (193 mm) and three femora (250-390 mm) were sampled. All samples have a lamellar-zonal bone consisting of parallel-fibred bone with various degrees of collagen fibres organisation. The growth marks, preserved in the form of zones and annuli are recognizable; however, LAGs are absent, but instead multiple rest lines occur. As assumed for taxa originating from Krasiejów, and described above, the unusually mild climate should be visible in the growth pattern of phytosaurs. For comparison, a closely related, but geographically distant phytosaur, *Nicrosaurus* sp. was sampled. The sectioned femur, of a similar size (295 mm), reveals the disposition of lamellar-zonal bone, consisting of parallel-fibred bone. However, the alternation of zones and annuli is better visible in this sample. Moreover, the femur of *Nicrosaurus* shows one clear LAG in the outer cortex. This indicates that environmental and/or climatic conditions in southern Germany during the Norian differed from those at Krasiejów.

Other histologically sectioned long bones of phytosaurs include taxa from the USA (Phytosauria indet., *Rutiodon* sp.; de Ricqlès et al. 2003) and Austria (*Mystriosuchus steinbergeri*; Butler et al. 2019). Similar to North American aetosaur taxa, phytosaur growth has two phases; a first with a rapidly deposited fibro-lamellar bone and a subsequent one with a more slowly deposited lamellar-zonal bone (de Ricqlès et al. 2003). Moreover, they exhibit clear growth marks in the form of zones, annuli and LAGs (de Ricqlès et al. 2003).

The Austrian taxon, however, grows only with lamellar-zonal bone consisting merely of parallel-fibred and lamellar bone, also lacking the woven component. *Mystriosuchus* is distinct from *Parasuchus* by deposition of LAGs, absent in the latter. Thus, again it was assumed, that the lack of LAGs in the taxa sampled from Krasiejów reflected the influence of climate, and thus would hint at a fairly mild, but still seasonal climate, during the Norian in the area of today's Krasiejów.

7.4 Histological growth of the protorosaur *Ozimek volans*

The sole gliding member of the Krasiejów fauna, *Ozimek volans*, shows a highly unique growth pattern. The sectioned femur and humerus display very thin lamellae. The tissue is rather avascular and consists mainly of lamellar bone and parallel-fibred bone. Growth marks in the form of zones and annuli are preserved, and even LAGs occur. The biomechanical constraint of the bone is very unique. No other extinct group shows a similar growth pattern. Tanystropheids or pterosaurs grow typically with fibro-lamellar bone, and especially pterosaurus, show a typical "plywood- like" tissue, which is lacking in *Ozimek* (de Ricqlès et al. 2000; Sayão 2003; Steel 2003, 2008; Chinsamy et al. 2009; Prondvai et al. 2012; Jaquier and Scheyer 2017). A growth pattern similar to that of *Ozimek* is visible in small modern birds (Lee and Simons 2015); however, these two groups are phylogenetically very distant. Therefore, the histological structure of *Ozimek* rather does not reflect climatic conditions, but is a response to the biomechanical loading connected with its mode of life.

7.5 Future perspectives

This study shows that animals, even phylogenetically distant from each other, and occupying different ecological niches, show very similar tissue deposition. All taxa from Krasiejów reveal growth pattern that indicates that there were no harsh climatic conditions. The only exception is *Ozimek*; however, its different type of bone architecture reflects an adaptation to a gliding mode of life, and thus, the differences are rather connected to biomechanics and not to climatic influence. It is astonishing that external drivers (environmental and/or climatic factors) overprint the phylogenetic signal in the Krasiejów faunal assemblage. This was previously noted by Fostowicz-Frelik and Sulej (2010) in long bones of the silesaurid *Silesaurus opolensis*, where only one tibia showed a weakly visible LAG in the outermost cortex, whereas the other bones showed uninterrupted growth. Even though *Silesaurus* is assumed to have been endotherm, and thus, would have had a “dinosaur-like” growth pattern without clear cyclical deposition of growth marks (zones, annuli and LAGs), it is remarkable, that the animal does not show any deposition of LAGs. However, this might be connected with the expression of the phylogenetic signal.

In future work it is important to study how the growth pattern changes in various elements of the Moroccan metoposaurid *D. ouazzoui*. Do the humeri also show two histotypes, similar to the patterns observed in *M. krasiejowensis* (Teschner et al. 2018)? Does the Argana Basin also preserves postcranial material of *Cyclotosaurus* or other temnospondyl amphibians? Moreover, would other skeletal elements of *Dutuitosaurus* also preserve LAGs, similar to studied ontogenetic series of femora (Steyer et al. 2004), or is LAGs deposition linked with specific skeletal elements in Temnospondyli? Moreover, long bones of the North American taxa should be studied in a greater detail.

Regarding aetosaurs and phytosaurs, it would be interesting to sample a complete ontogenetic series, which is not possible at the moment with material from Krasiejów. The main question regarding bone growth of the juvenile *A. ferratus* is whether the stratified bone observed locally in the inner cortex represents a hatchling bone or if it already shows growth marks in the primary cortex. Moreover, would *Aetosaurus* continue growing with a slowed-down growth and the occurrence of possible LAGs? And, further, would *Aetosaurus* be growing with woven bone, which is absent in the *Stagonolepis* bones but present in all taxa from North and South America? Additionally, was woven bone in long bones of *Stagonolepis* not deposited at all or was it already remodelled in the sampled material?

Further, it would be interesting to study the growth pattern of the phytosaur *Parasuchus hislopi* from India, which co-occurred with *P. maleriensis* in the Maleri Formation of Central India. It would be also important to compare the material with other phytosaurs, but more importantly, to compare with other faunal components from the Maleri Formation.

In general, it is also important to investigate further the drivers behind the various types of tissue deposition, which applies to both groups, Aetosauria and Phytosauria. Thus, why do the lamellar-zonal bone deposits occur solely in the European taxa and why do the bones from American taxa exhibit both, fibro-lamellar and lamellar-zonal bone? How much does this depend of genetic constraint and metabolic rate, or is it solely taxon specific or even climatic dependent?

Complete Literature List

Abdala, N.F., Cisneiros, J.C., and R.M.H. Smith. 2006. Faunal aggregation in the Early Triassic Karoo Basin: earliest evidence of shelter sharing behavior among tetrapods? *Palaios*, 21: 507–512.

Antczak, M., and A. Bodzioch. 2018. Diversity of fish scales in Late Triassic deposits of Krasiejów (SW Poland). *Paleontological Research*, 22(1): 91–100.

Amson, E., and F. Bibi. 2021. Differing effects of size and lifestyle on bone structure in mammals. *BMC Biology*, 19: 1–18.

Ascenzi, A., and E. Bonucci. 1967. The tensile properties of single osteons. *The Anatomical Record*, 158: 375–386.

Ascenzi, A., and E. Bonucci. 1968. The compressive properties of single osteons. *The Anatomical Record*, 161: 377–391.

Ascenzi, A., and E. Bonucci. 1972. The shearing properties of single osteons. *The Anatomical Record*, 172: 499–510.

Ascenzi, M.G., Ascenzi, A., Benvenuti, A., Burghammer, M., Panzavolta, S., and A. Bigi. 2003. Structural differences between "dark" and "bright" isolated human osteonic lamellae. *Journal of Structural Biology*, 141: 22–33.

Ascenzi, M.G., Gill, J., and A. Lomovtsev. 2008. Orientation of collagen at the osteocyte lacunae in human secondary osteons. *Journal of Biomechanics*, 41: 3426–3435.

Barycka, E. 2007. Morphology and ontogeny of the humerus of the Triassic temnospondyl amphibian *Metoposaurus diagnosticus*. *Neues Jahrbuch für Geologie und Paläontologie Abhandlungen*, 243: 351–361.

Biacchi Brust, A.C., Desojo, J.B., Schultz, C.L., Paes-Neto, V.D., and Á.A.S Da-Rosa. 2018. Osteology of the first skull of *Aetosauroides scagliai* Casamiquela 1960 (Archosauria: Aetosauria) from the Upper Triassic of southern Brazil (Hyperodapedon Assemblage Zone) and its phylogenetic importance. *PLoS One*, 13(8): e0201450.

Bodzioch, A., and M. Kowal-Linka 2012. Unraveling the origin of the Late Triassic multitaxic bone accumulation at Krasiejów (S Poland) by diagenetic analysis. *Palaeogeography, Palaeoclimatology, Palaeoecology*, 346: 25–36.

Bromage, T.G., Goldman, H.M., McFarlin, S.C., Warshaw, J., Boyde, A., and C.M. Riggs. 2003. Circularly polarized light standards for investigations of collagen fiber orientation in bone. *The Anatomical Record Part B: The New Anatomist: An Official Publication of the American Association of Anatomists*, 274: 157–168.

Buffetaut, E., and G. Wouters. 1986. Amphibian and reptile remains from the Upper Triassic of Saint-Nicolas-de-Port (eastern France) and their biostratigraphic significance. *Modern Geology*, 10: 133–145.

Butler, R.J., Jones, A.S., Buffetaut, E., Mandl, G.W., Scheyer, T.M., and O. Schultz. 2019. Description and phylogenetic placement of a new marine species of phytosaur (Archosauriformes: Phytosauria) from the Late Triassic of Austria. *Zoological Journal of the Linnean Society*, 187(1): 198–228.

Chakravorti, S., and D.P. Sengupta, 2019. Taxonomy, morphometry and morphospace of cranial bones of *Panthasaurus* gen. nov. *maleriensis* from the Late Triassic of India. *Journal of Iberian Geology*, 45(2): 317–340.

Chinsamy, A., Codorniu, L., and L. Chiappe. 2009. Palaeobiological implications of the bone histology of *Pterodaustro guinazui*. *The Anatomical Record: Advances in Integrative Anatomy and Evolutionary Biology*, 292: 1462–1477.

Cotton, W. D., Cotton, J. E., and A. P. Hunt. 2008. Evidence for social behavior in ornithopod dinosaurs from the Dakota Group of northeastern New Mexico, USA. *Ichnos: An International Journal of Plant & Animal Traces*, 6(3): 141–149.

Cubo, J., and A. Casinos. 1998. The variation of the cross-sectional shape in the long bones of birds and mammals. *Annales des Sciences Naturelles: Zoologie et Biologie Animale*, 19: 51–62.

Currey, J.D., and R.M. Alexander. 1985. The thickness of the walls of tubular bones. *Journal of Zoology*, 206: 453–468.

Damiani, R.J. 2001. A systematic revision and phylogenetic analysis of Triassic mastodonsauroids (Temnospondyli: Stereospondyli). *Zoological Journal of the Linnean Society*, 133: 379–482.

De Buffrénil, V., de Ricqlès, A.J., Zylberberg, L., and K. Padian. 2021. *Vertebrate Skeletal Histology and Paleohistology*, pp. 838. CRC Press, Boca Raton and London.

De Margerie, E. 2002. Laminar bone as an adaptation to torsional loads in flapping flight. *Journal of Anatomy*, 201: 521–526.

De Margerie, E., Cubo, J., and J. Castanet. 2002. Bone typology and growth rate: testing and quantifying 'Amprino's rule' in the mallard (*Anas platyrhynchos*). *Comptes Rendus Biologies*, 325: 221–230.

De Margerie, E., Sanchez, S., Cubo, J., and J. Castanet. 2005. Torsional resistance as a principal component of the structural design of long bones: comparative multivariate evidence in birds. *The Anatomical Record Part A: Discoveries in Molecular, Cellular, and Evolutionary Biology: An Official Publication of the American Association of Anatomists*, 282: 49–66.

De Ricqlès, A.J. 1979. Relations entre structures histologiques, ontogenese, strategies demographiques et modalites evolutives: le cas des reptiles captorhinomorphes et des stegocephales temnospondyles. *Comptes Rendus de l'Academie des Sciences Paris, Serie D*, 288: 1147–1150.

De Ricqlès, A.J, Padian, K., Horner, J.R. and H.E. Francillon-Vieillot. 2000. Palaeohistology of the bones of pterosaurs (Reptilia: Archosauria): anatomy, ontogeny, and biomechanical implications. *Zoological Journal of the Linnean Society*, 12: 349–385.

De Ricqlès, A.J., Padian, K., and J.R. Horner. 2003. On the bone histology of some Triassic pseudosuchian archosaurs and related taxa. *Annales de Paléontologie*, 89: 67–101.

De Ricqlès, A.J., Padian, K., Knoll, F., and J.R. Horner. 2008. On the origin of high growth rates in archosaurs and their ancient relatives: complementary histological studies on Triassic archosauriforms and the problem of a "phylogenetic signal" in bone histology. *Annales de Paléontologie*, 94: 57–76.

Desojo, J.B., Heckert, A.B., Martz, J.W., Parker, W.G., Schoch, R.R., Small, B.J., and T. Sulej. 2013. Aetosauria: a clade of armoured pseudosuchians from the Upper Triassic continental beds. *Geological Society London*: *Special Publications*, 379(1): 203–239.

Dickins, J.M. 1993. Climate of the late Devonian to Triassic. *Palaeogeography, Palaeoclimatology, Palaeoecology*, 100(1-2): 89–94.

Dubiel, R.F., Parrish, J.T., Parrish, J.M., abd Good, S.C. 1991. The Pangaean megamonsoon: evidence from the Upper Triassic Chinle Formation, Colorado Plateau. *Palaios*, 6(4): 347–370.

Dudley, R., Byrnes, G., Yanoviak, S.P., Borrell, B., Brown, R.M., and J.A. McGuire. 2007. Gliding and the functional origins of flight: biomechanical novelty or necessity? *Annual Review of Ecology, Evolution, and Systematics*, 38:179–201.

Dutuit, J.M. 1976. Introduction à l'étude paléontologique du Trias continental marocain. Description des premiers stegocephales recueillis dans le couloir d'Argana (Atlas occidental). *Mémoires du Museum national d'histoire naturelle Série C*, 36: 1–253.

Dzik, J. 2001. A new *Paleorhinus* fauna in the early Late Triassic of Poland. *Journal of Vertebrate Paleontology*, 21(3): 625–627.

Dzik, J. 2003. A beaked herbivorous archosaur with dinosaur affinities from the early Late Triassic of Poland. *Journal of Vertebrate Paleontology*, 23(3): 556–574.

Dzik, J. 2008. Gill structure and relationships of the Triassic cycloid crustaceans. *Journal of Morphology*, 269(12): 1501–1519.

Dzik, J., and T. Sulej. 2016. An early Late Triassic long-necked reptile with a bony pectoral shield and gracile appendages. *Acta Palaeontologica Polonica*, 61: 805–823.

Dzik, J., Sulej, T., Kaim, A., and R. Niedźwiedzki. 2000. Późnotriasowe cmentarzysko kręgowców lądowych w Krasiejowie na Śląsku Opolskim. *Przegląd geologiczny*, 48(3): 226–235.

Ferretti, M., Palumbo, C., Contri, M., and G. Marotti. 2002. Static and dynamic osteogenesis: two different types of bone formation. *Anatomy and Embryology*, 206: 21–29.

Fostowicz-Frelik, Ł., and T. Sulej 2010. Bone histology of *Silesaurus opolensis* Dzik, 2003 from the Late Triassic of Poland. *Lethaia*, 43(2): 137–148.

Fraas, O. 1866. Vor der Sündfluth! Eine Geschichte der Urwelt, pp. 516. Hoffmann'sche Verlags-Buchhandlung, Stuttgart.

Fraas, O. 1877. *Aëtosaurus ferratus* Fr. *Die gepanzerte Vogel-Echse aus dem Stubensandstein bei Stuttgart*, pp. 21. Schweizerbart, Stuttgart.

Fraas, E. 1889. Die Labyrinthodonten der schwäbischen Trias. *Palaeontographica*, 36: 1–158.

Fraas, E. 1913. Neue Labyrinthodonten aus der schwäbischen Trias. *Palaeontographica*, 60: 275–294.

França, M.A.G., Ferigolo, J., and M.C. Langer. 2011. Associated skeletons of a new middle Triassic "Rauisuchia" from Brazil. *Naturwissenschaften*, 98: 389–395.

Francillon-Vieillot, H.E., de Buffrénil, V., Castanet, J., Géraudie, J., Meunier, F.J., Sire, J.Y., Zylberg L., and A. de Ricqlès. 1990. Microstructure and mineralization of vertebrate skeletal tissues. *Skeletal Biomineralization: Patterns, Processes and Evolutionary Trends*, 1: 471–530.

Gądek, K. 2012. Palaeohistology of ribs and clavicle of *Metoposaurus diagnosticus* from Krasiejów (Upper Silesia, Poland). *Opole Scientific Society Natural Journal*, 45: 39–42.

Gans, C., and D.W. Tinkle 1978. *Biology of the Reptilia. Volume 7. Ecology and Behaviour A*, pp. 720. Academic Press, London, New York, and San Francisco.

Gans, C., Darevski, I., and L.P. Tatarinov. 1987. *Sharovipteryx*, a reptilian glider? *Paleobiology*, 13: 415–426.

Gauthier, J. 1986. Saurischian monophyly and the origin of birds. *Memoirs of the California Academy of sciences*, 8: 1–55.

Gee, B.M., and S.E. Jasinski. 2021. Description of the metoposaurid *Anaschisma browni* from the New Oxford Formation of Pennsylvania. *Journal of Paleontology*, 95: 1061–1078.

Georgiadis, M., Müller, R., and P. Schneider. 2016. Techniques to assess bone ultrastructure organization: orientation and arrangement of mineralized collagen fibrils. *Journal of the Royal Society Interface*, 13(119): 20160088.

Gônet, J., Laurin, M., and M. Girondot. 2021. BoneProfileR: The next step to quantify, model, and statistically compare bone section compactness profiles. Palaeontologia Electronica 25(1): a12 doi.org/10.26879/1194

Gruntmejer, K., Konietzko-Meier, D., and A. Bodzioch. 2016. Cranial bone histology of *Metoposaurus krasiejowensis* (Amphibia, Temnospondyli) from the Late Triassic of Poland. *PeerJ*, 4: e2685.

Gruntmejer, K., Konietzko-Meier, D., Bodzioch, A., and J. Fortuny. 2019a. Morphology and preliminary biomechanical interpretation of mandibular sutures in *Metoposaurus krasiejowensis* (Temnospondyli, Stereospondyli) from the Upper Triassic of Poland. *Journal of Iberian Geology*, 45(2): 301–316.

Gruntmejer, K., Konietzko-Meier, D., Marcé-Nogué, J., Bodzioch, A., and J. Fortuny. 2019b. Cranial suture biomechanics in *Metoposaurus krasiejowensis* (Temnospondyli, Stereospondyli) from the upper Triassic of Poland. *Journal of Morphology*, 280(12): 1850–1864.

Gruntmejer, K., Bodzioch, A., and D. Konietzko-Meier. 2021. Mandible histology in *Metoposaurus krasiejowensis* (Temnospondyli, Stereospondyli) from the Upper Triassic of Poland. *PeerJ*, 9: e12218.

Hayashi, S. Houssaye, A., Nakajima, Y., Chiba, K., Ando, T., Sawamura, H., Inuzuka, N., Kaneko, N. and Osaki, T. 2013. Bone inner structure suggests increasing aquatic adaptations in Desmostylia (Mammalia, Afrotheria). *PLoS One*, 8(4): e59146.

Hoffman, D.K., Heckert, A.B., and L.E. Zanno. 2019. Disparate growth strategies within Aetosauria: novel histologic data from the aetosaur *Coahomasuchus chathamensis*. *The Anatomical Record*, 302: 1504–1515.

Holmes, R., and R. Carroll. 1977. A temnospondyl amphibian from the Mississippian of Scotland. *Bulletin of the Museum of Comparative Zoology*, 147: 489–511.

Horner, J.R., Padian, K., and A.J. de Ricqlès. 2000. Long bone histology of the hadrosaurid dinosaur *Maiasaura peeblesorum*: growth dynamics and physiology based on an ontogenetic series of skeletal elements. *Journal of Vertebrate Paleontology*, 20: 115–129

Horner, J.R., and K. Padian. 2004. Age and growth dynamics of *Tyrannosaurus rex*. *Proceedings of the Royal Society, London B Biological Sciences*, 271: 1875–1880.

Huene, F. 1946. Die grossen Stämme der Tetrapoden in den geologischen Zeiten. *Biologisches Zentralblatt*, 65: 268–275.

Ingavat, R., and P. Janvier. 1981. *Cyclotosaurus* cf. *posthumus* Fraas (Capitosauridae, Stereospondyli) from the Huai Hin Lat Formation (Upper Triassic), Northeastern Thailand: with a note on capitosaurid biogeography. *Geobios*, 14: 711–725.

Jaquier, V.P., and T.M. Scheyer. 2017. Bone histology of the Middle Triassic longnecked reptiles *Tanystropheus* and *Macrocnemus* (Archosauromorpha, Protorosauria). *Journal of Vertebrate Paleontology*, 37: e1296456.

Jewuła, K., Matysik, M., Paszkowski, M., and J. Szulc. 2019. The late Triassic development of playa, gilgai floodplain, and fluvial environments from Upper Silesia, southern Poland. *Sedimentary Geology*, 379: 25–45.

Kalita, S., Teschner, E.M., Sander, P.M., and D. Konietzko-Meier. 2022. To be or not to be heavier: the role of dermal bones in the buoyancy of the Late Triassic temnospondyl amphibian *Metoposaurus krasiejowensis*. *Journal of Anatomy*, 241: 1459–1476.

Klein, N., and P.M. Sander. 2007. Bone histology and growth of the prosauropod dinosaur *Plateosaurus engelhardti* von Meyer, 1837 from the Norian bonebeds of Trossingen (Germany) and Frick (Switzerland). *Special Papers in Palaeontology*, 77: 169–206.

Klein, N. and P.M. Sander. 2008. Ontogenetic stages in the long bone histology of sauropod dinosaurs. *Paleobiology*, 34(2): 247–263.

Klein, N., Scheyer, T.M., and T. Tütken. 2009. Skeletochronology and isotopic analysis of a captive individual of *Alligator mississippiensis* Daudin, 1802. *Fossil Record*, 12: 121–131.

Klein, N., Foth, C., and R.R. Schoch. 2017. Preliminary observations on the bone histology of the Middle Triassic pseudosuchian archosaur *Batrachotomus kupferzellensis* reveal fast growth with laminar fibrolamellar bone tissue. *Journal of Vertebrate Paleontology*, 37: e1333121.

Klein, N., and E.M. Griebeler. 2018. Growth patterns, sexual dimorphism, and maturation modelled in Pachypleurosauria from Middle Triassic of central Europe (Diapsida: Sauropterygia). *Fossil Record*, 21: 137–157.

Köhler, M., Marin Moratalla, N., Jordana, X., and R. Aanes. 2012. Seasonal bone growth and physiology in endotherms shed light on dinosaur physiology. *Nature*, 487: 358–361.

Konietzko-Meier, D., Bodzioch, A., and P.M. Sander. 2012. Histological characteristics of the vertebral intercentra of *Metoposaurus diagnosticus* (Temnospondyli) from the Upper Triassic of Krasiejów (Upper Silesia, Poland). *Earth and Environmental Science Transactions of the Royal Society of Edinburgh*, 103(3-4): 237–250.

Konietzko-Meier, D., and N. Klein. 2013. Unique growth pattern of *Metoposaurus diagnosticus krasiejowensis* (Amphibia, Temnospondyli) from the Upper Triassic of Krasiejów, Poland. *Palaeogeography, Palaeoclimatology, Palaeoecology*, 370: 145–157.

Konietzko-Meier, D., and P.M. Sander. 2013. Long bone histology of *Metoposaurus diagnosticus* (Temnospondyli) from the Late Triassic of Krasiejów (Poland) and its paleobiological implications. *Journal of Vertebrate Paleontology*, 33: 1003–1018.

Konietzko-Meier, D., Danto, M., and K. Gądek. 2014. The microstructural variability of the intercentra among temnospondyl amphibians. *Biological Journal of the Linnean Society*, *112*(4), 747–764.

Konietzko-Meier, D., Gruntmejer, K., Marcé-Nogué, J., Bodzioch, A., and J. Fortuny. 2018. Merging cranial histology and 3D-computational biomechanics: a review of the feeding ecology of a Late Triassic temnospondyl amphibian. *PeerJ*, 6: e4426.

Konietzko-Meier, D., Werner, J.D., Wintrich, T., and P.M. Sander. 2019. A large temnospondyl humerus from the Rhaetian (Late Triassic) of Bonenburg (Westphalia, Germany) and its implications for temnospondyl extinction. *Journal of Iberian Geology*, 45: 287–300.

Kuhn, O. 1932. Labyrinthodonten und Parasuchier aus dem mittleren Keuper von Ebrach in Oberfranken. *Neues Jahrbuch für Mineralogie, Geologie und Paläontologie*, 69: 94–144.

Kuhn, O. 1942. Über *Cyclotosaurus hemprichi* Kuhn und einige weitere Tetrapodenreste aus dem Keuper von Halberstadt. *Beiträge zur Geologie von Thüringen*, 6: 181–197.

Lamb, H.H. 2013. Climate: present, past and future (Routledge revivals), Volume 2. In: *Climatic history and the future*, pp. 870. Routledge and CRC Press, London.

Lamm, E.-T. 2013. Preparation and sectioning of specimens. In: K. Padian and E.-T. Lamm (eds.). *Bone Histology of Fossil Tetrapods: Advancing Methods, Analysis, and Interpretation*, pp. 55–160. University of California Press, Los Angeles.

Lech, K.A. 2010. Reconstruction of forelimb musculature of temnospondyl amphibian *Cyclotosaurus intermedius* Sulej and Majer, 2005 from the Late Triassic of Poland. In*:* D. Nowakowski (Ed.), *Morphology and Systematics of Fossil Vertebrates*, pp. 52–66. DN Publisher, Wroclaw.

Lee, A.H., and E.L. Simons. 2015. Wing bone laminarity is not an adaptation for torsional resistance in bats. *PeerJ*, 3: e823.

Long, R.A., and K.L. Ballew. 1985. Aetosaur dermal armor from the Late Triassic of southwestern North America, with special reference to material from the Chinle Formation of Petrified Forest National Park. *Museum of Northern Arizona Bulletin*, 47: 45–68.

Marotti, G., Ferretti, M., Palumbo, C., and M. Benincasa. 1999. Static and dynamic bone formation and the mechanism of collagen fiber orientation. *Bone*, 25: 156.

Martin, E.G., and C. Palmer. 2014. Air space proportion in pterosaur limb bones using computed tomography and its implications for previous estimates of pneumaticity. *PloS One*, 9(5): e97159.

Martin-Silverstone, E., Witton, M.P., Arbour, V.M., and P.J. Currie. 2016. A small azhdarchoid pterosaur from the latest Cretaceous, the age of flying giants. *Royal Society Open Science*, 3(8): 160333.

Marzola, M., Mateus, O., Shubin, N.H., and L.B. Clemmensen. 2017. *Cyclotosaurus naraserluki*, sp. nov., a new Late Triassic cyclotosaurid (Amphibia, Temnospondyli) from the Fleming Fjord Formation of the Jameson Land Basin (East Greenland). *Journal of Vertebrate Paleontology*, 37(2): e1303501.

McHugh, J.B. 2014. Paleohistology and histovariability of the Permian stereospondyl *Rhinesuchus*. *Journal of Vertebrate Paleontology*, 34(1): 59–68.

Meyer, von, H., and T. Plieninger. 1844. *Beiträge zur Paläontologie Württembergs, enthaltend die fossilen Wirbeltierreste aus den Triasgebilden mit besonderer Rücksicht auf die Labyrinthodonten des Keupers*, pp. 132. Schweizerbart, Stuttgart.

Milner, A.R., Duffin, C., and D. Delsate. 1996. Plagiosaurid and capitosaurid amphibian material from the Late Triassic of Medernach, Grand-Duchy of Luxembourg: preliminary note. *Bulletin de la Sociètè Belge de Gèologie*, 104: 42–53.

Mitchell, J., and A.H.van Heteren. 2017. A literature review of the spatial organization of lamellar bone. *Comptes Rendus Palevol*, 15: 23–31.

Mitchell, J., Sander, P.M., and K.H. Stein. 2017. Can secondary osteons be used as ontogenetic indicators in sauropods? Extending the histological ontogenetic stages into senescence. *Paleobiology*, 43(2): 321–342.

Mukherjee, D., Ray, S., and D.P. Sengupta. 2010. Preliminary observations on the bone microstructure, growth patterns, and life habits of some Triassic temnospondyls from India. *Journal of Vertebrate Paleontology*, 30(1): 78–93.

Mukherjee, D., Sengupta, D.P., and N. Rakshit. 2020. New biological insights into the Middle Triassic capitosaurs from India as deduced from limb bone anatomy and histology. *Papers in Palaeontology*, 6: 93–142.

Nesbitt, S.J., Zawiskie, J.M., and R.M. Dawley. 2020. The osteology and phylogenetic position of the loricatan (Archosauria: Pseudosuchia) *Heptasuchus clarki*, from the? Mid-upper Triassic, southeastern big Horn Mountains, Central Wyoming (USA). *PeerJ*, 8: e10101.

Ochev, V.G. 1972. *Capitosauroid labyrinthodonts from the southeastern European part of the USSR*, pp. 269. Saratov State University, Saratov. [in Russian].

Olempska, E. 2004. Late Triassic spinicaudatan crustaceans from southwestern Poland. *Acta Palaeontologica Polonica*, 49(3): 429–442.

Pacyna, G. 2019. Sphenopsid and fern remains from the Upper Triassic of Krasiejów (SW Poland). *Annales Societatis Geologorum Poloniae*, 89(3): 307–316.

Padian, K., Horner, J.R., and A.J. de Ricqlès. 2004. Growth in small dinosaurs and pterosaurs: the evolution of archosaurian growth strategies. *Journal of Vertebrate Paleontology*, 24: 555–571.

Parker, W.G., Nesbitt, S.J., Irmis, R.B., Martz, J.W., Marsh, A.D., Brown, M.A., Stocker, M.R., and S. Werning. 2022. Osteology and relationships of *Revueltosaurus callenderi* (Archosauria: Suchia) from the Upper Triassic (Norian) Chinle Formation of Petrified Forest National Park, Arizona, United States. *Anatomical Record*, 305: 2353–2414.

Parrish, J.T. 1993. Climate of the supercontinent Pangea. *The Journal of Geology*, 101(2): 215–233.

Pol, D., Mancuso, A. C., Smith, R. M., Marsicano, C. A., Ramezani, J., Cerda, I. A., Otero, A., and V. Fernandez. 2021. Earliest evidence of herd-living and age segregation amongst dinosaurs. *Scientific Reports*, 11(1): 1–9.

Ponce, D.A., Desojo, J.B., and I.A. Cerda. 2022. Palaeobiological inferences of the aetosaur *Aetosauroides scagliai* (Archosauria: Pseudosuchia) based on microstructural analyses of its appendicular bones. *Historical Biology*, doi.org/10.1080/08912963.2022.2035728.

Pritchard, A.C., and H.-D. Sues. 2019. Postcranial remains of *Teraterpeton hrynewichorum* (Reptilia: Archosauromorpha) and the mosaic evolution of the saurian postcranial skeleton. *Journal of Systematic Palaeontology*, 17: 1745–1765.

Prondvai, E., Stein, K.H., Ősi, A., and P.M. Sander. 2012. Life history of *Rhamphorhynchus* inferred from bone histology and the diversity of pterosaurian growth strategies. *PLoS One*, 7(2): e31392.

Prondvai, E., Stein, K.H., de Ricqlès, A.J., and J. Cubo. 2014. Development-based revision of bone tissue classification: the importance of semantics for science. *Biological Journal of the Linnean Society*, 112: 799–816.

Quekett, J. 1849. On the intimate structure of bone, as composing the skeleton, in the four great classes of animals, viz., mammals, birds, reptiles, and fishes, with some remarks on the great value of the knowledge of such structure in determining the affinities of minute fragments of organic remains. *Transactions of the Microscopical Society of London*, 2: 46– 58.

Qvarnström, M., Wernström, J. V., Piechowski, R., Tałanda, M., Ahlberg, P. E., and G. Niedźwiedzki. 2019. Beetle-bearing coprolites possibly reveal the diet of a Late Triassic dinosauriform. *Royal Society Open Science*, 6(3): e181042.

Racki, G. 2017. Portal prezentujący kościonośny kajper Górnego Śląska w świetle wyników grantu N307 11703. *Przegląd Geologiczny*, 65: 275–281.

Ray, S., Mukherjee, D., and S. Bandyopadhyay. 2009. Growth patterns of fossil vertebrates as deduced from bone microstructure: case studies from India. *Journal of Biosciences*, 34(5): 661–672.

Roychowdhury, T. 1965. A new metoposaurid amphibian from the Upper Triassic Maleri Formation of Central India. *Philosophical Transactions of the Royal Society of London. Series B, Biological Sciences,* 250: 1–52.

Runestad, J.A., and C.B. Ruff. 1995. Structural adaptations for gliding in mammals with implications for locomotor behavior in paromomyids. *American Journal of Physical Anthropology*, 98: 101–119.

Sanchez, S., de Ricqlès, A.J., Schoch, R. R., and J.-S. Steyer 2010a. Developmental plasticity of limb bone microstructural organization in *Apateon*: Histological evidence of paedomorphic conditions in branchiosaurs. *Evolution and Development*, 12(3), 315–328.

Sanchez, S., Steyer, J. S., Schoch, R. R., and de Ricqlès, A.J. 2010b. Palaeoecological and palaeoenvironmental influences revealed by long-bone palaeohistology: the example of the Permian branchiosaurid *Apateon*. *Geological Society London: Special Publications*, 339(1): 139–149.

Sanchez, S., Germain, D., de Ricqlès, A.J., Abourachid, A., Goussard, F., and P. Tafforeau. 2010c. Limb-bone histology of temnospondyls: implications for understanding the diversification of palaeoecologies and patterns of locomotion of Permo-Triassic tetrapods. *Journal of Evolutionary Biology*, 23: 2076–2090.

Sanchez, S., and R.R. Schoch. 2013. Bone histology reveals a high environmental and metabolic plasticity as a successful evolutionary strategy in a long-lived homeostatic Triassic temnospondyl. *Evolutionary Biology*, 40(4): 627–647.

Sander, P.M. 1992. The Norian *Plateosaurus* bonebeds of central Europe and their taphonomy. *Palaeogeography, Palaeoclimatology, Palaeoecology*, 93: 255–299.

Sander, P.M., and P. Andrassy. 2006. Lines of arrested growth and long bone histology in Pleistocene large mammals from Germany: what do they tell us about dinosaur physiology? *Palaeontographica Abteilung A*, 227: 143–159.

Sayão, J.M. 2003. Histovariability in bones of two pterodactyloid pterosaurs from the Santana Formation, Araripe Basin, Brazil: preliminary results. *Geological Society London: Special Publications*, 217: 335–342.

Scheyer, T.M., Desojo, J.B., and I.A. Cerda. 2014. Bone histology of phytosaur, aetosaur, and other archosauriform osteoderms (Eureptilia, Archosauromorpha). *Anatomical Record*, 297: 240–260.

Schoch, R.R. 2003. Early larval ontogeny of the Permo-Carboniferous temnospondyl *Sclerocephalus*. *Palaeontology*, 46(5): 1055–1072.

Schoch, R.R. 2007. Osteology of the small archosaur *Aetosaurus* from the Upper Triassic of Germany. *Neues Jahrbuch für Geologie und Paläontologie, Abhandlungen*, 246: 1–35.

Schoch, R.R. 2013. The evolution of major temnospondyl clades: An inclusive phylogenetic analysis. *Journal of Systematic Palaeontology*, 11: 673–705.

Schoch, R.R., and J.B. Desojo. 2016. Cranial anatomy of the aetosaur *Paratypothorax andressorum* Long and Ballew, 1985, from the Upper Triassic of Germany and its bearing on aetosaur phylogeny. *Neues Jahrbuch für Geologie und Paläontologie, Abhandlungen*, 279: 73–95.

Schoch, R.R., and A.R. Milner. 2000. *Stereospondyli. Encyclopedia of palaeoherpetology Part 3B*, pp. 220. Verlag Dr. Friedrich Pfeil, Munich.

Sengupta, D.P. 2002. Indian metoposaurid amphibians revised. *Paleontological Research*, 6: 41–65.

Sharov, A.G. 1971. New flying reptiles from the Mesozoic of Kazakhstan and Kyrgyzstan. *Trudy Paleontologicheskogo Instituta AN SSSR*, 130: 104–113. [in Russian].

Shipman, P.A.T. 1975. Implications of drought for vertebrate fossil assemblages. *Nature*, 257: 667–668.

Shishkin, M.A. 1964. Suborder Stereospondyli. In*:* Y.A. Orlov (ed.). *Amphibia, Reptilia, Aves*, pp. 83–122. *Osnovy Paleontologii*, Moscow. [in Russian].

Skawina, A., and J. Dzik. 2011. Umbonal musculature and relationships of the Late Triassic filibranch unionoid bivalves. *Zoological Journal of the Linnean Society*, 163(3): 863–883.

Skrzycki, P. 2015. New species of lungfish (Sarcopterygii, Dipnoi) from the Late Triassic Krasiejów site in Poland, with remarks on the ontogeny of Triassic dipnoan tooth plates. *Journal of Vertebrate Paleontology*, 35(5): e964357.

Skrzycki, P. 2016. The westernmost occurrence of *Gnathorhiza* in the Triassic, with a discussion of the stratigraphic and palaeogeographic distribution of the genus. *Fossil Record*, 19(1): 17–29.

Socha, J.J., Jafari, F., Munk, Y., and G. Byrnes. 2015. How animals glide: from trajectory to morphology. *Canadian Journal of Zoology*, 93: 901–924.

Spiekman, S.F.N., Fraser, N.C., and T.M. Scheyer. 2021. A new phylogenetic hypothesis of Tanystropheidae (Diapsida, Archosauromorpha) and other “protorosaurs”, and its implications for the early evolution of stem archosaurs. *PeerJ*, 9: e11143.

Steel, L. 2003. The John Quekett sections and the earliest pterosaur histological studies. *Geological Society London: Special Publications*, 217: 325–334.

Steel, L. 2008. The palaeohistology of pterosaur bone: an overview. *Zitteliana*, 28: 109–125.

Steel, L., Martill, D.M., Unwin, D.M., and J.D. Winch. 2005. A new pterodactyloid pterosaur from the Wessex Formation (Lower Cretaceous) of the Isle of Wight, England. *Cretaceous Research*, 26: 686–698.

Stein, K.H., and P.M. Sander. 2009. Histological core drilling: A less destructive method for studying bone histology. In: M.A. Brown, J.F. Kane, and W.G. Parker. (Eds.). *Methods In*

Fossil Preparation: Proceedings of the First Annual Fossil Preparation and Collections Symposium, pp. 69–80. Petrified Forest National Park, Arizona.

Steyer, J.S., Laurin, M., Castanet, J., and A.J. de Ricqlès. 2004. First histological and skeletochronological data on temnospondyl growth: palaeoecological and palaeoclimatological implications. *Palaeogeography, Palaeoclimatology, Palaeoecology*, 206: 193–201.

Stockhausen, K.E., Qwamizadeh, M., Wölfel, E.M., Hemmatian, H., Fiedler, I.A.K., Flenner, S., Longo, E., Amling, M., Greving, I., Ritchie, R.O., Schmidt F.N., and B. Busse. 2021. Collagen fiber orientation is coupled with specific nano-compositional patterns in dark and bright osteons modulating their biomechanical properties. *ACS Nano*, 15: 455–467.

Sulej, T. 2002. Species discrimination in the Late Triassic labyrinthodont *Metoposaurus*. *Acta Palaeontologica Polonica*, 47: 535–546.

Sulej, T. 2005. A new rauisuchian reptile (Diapsida: Archosauria) from the Late Triassic of Poland. *Journal of Vertebrate Paleontology*, 25(1): 78–86.

Sulej, T. 2007. Osteology, variability, and evolution of *Metoposaurus*, a temnospondyl from the Late Triassic of Poland. *Palaeontologia Polonica*, 64: 29–139.

Sulej, T. 2010. The skull of an early Late Triassic aetosaur and the evolution of the stagonolepidid archosaurian reptiles. *Zoological Journal of the Linnean Society*, 158(4): 860–881.

Sulej, T., and D. Majer. 2005. The temnospondyl amphibian *Cyclotosaurus* from the Late Triassic of Poland. *Palaeontology*, 48: 157–170.

Sulej, T. Kowalski, J., Bodzioch, A., and E. Hara. 2021. Eucynodont teeth from the Late Triassic of Krasiejów, Southern Poland. *Historical Biology*, 33(12): 3633–3640.

Szulc, J. 2005. Sedimentary environments of the vertebrate-bearing Norian deposits from Krasiejów, Upper Silesia (Poland). *Hallesches Jahrbuch der Geowissenschaften*, 19, 161–170.

Szulc, J. and G. Racki. 2015. Formacja grabowska: podstawowa jednostka litostratygraficzna kajpru Górnego Śląska. *Przegląd Geologiczny*, 63(2): 103–113.

Szulc, J., Racki, G., Jewuła, K., and J. Środoń. 2015. How many Upper Triassic bone–bearing levels are there in Upper Silesia (southern Poland)? A critical overview of stratigraphy and facies. *Annales Societatis Geologorum Poloniae*, 85(4): 587–626.

Szulc, J., Racki, G., and A. Bodzioch. 2017. Comment on "An early Late Triassic long-necked reptile with a bony pectoral shield and gracile appendages" by Jerzy Dzik and Tomasz Sulej. *Acta Palaeontologica Polonica*, 62(2): 287–288.

Tatarinov, L.P. 1989. On the Taxonomic Position and Mode of Life of the Problematic Upper Triassic Reptile *Sharovipteryx mirabilis*, *Paleontologicheski Zhurnal*, 2: 110–112. [in Russian].

Teschner, E.M., Sander, P.M., and D. Konietzko-Meier. 2018. Variability of growth pattern observed in *Metoposaurus krasiejowensis* humeri and its biological meaning. *Journal of Iberian Geology*, 44: 99–111.

Teschner, E.M., Chakravorti, S., Sengupta, D.P., and D. Konietzko-Meier. 2020. Climatic influence on the growth pattern of *Panthasaurus maleriensis* from the Late Triassic of India deduced from paleohistology. *PeerJ*, 8: e9868.

Teschner, E.M., Konietzko-Meier, D., and N. Klein. 2022. Growth and limb bone histology of aetosaurs and phytosaurs from the Late Triassic Krasiejów locality (SW Poland) reveals strong environmental influence on growth pattern. *Contributions to Zoology*, 91: 199– 232.

Thorbjarnarson, J.B., and G. Hernández. 1993. Reproductive ecology of the Orinoco crocodile (*Crocodylus intermedius*) in Venezuela. I. Nesting ecology and egg and clutch relationships. *Journal of Herpetology*, 27(4): 363–370.

Unwin, D.M., Alifanov, V.R., and M.J. Benton. 2000. *Enigmatic small reptiles from the Middle–Late Triassic of Kyrgyzstan*. In: M.J. Benton, M.A., Shishkin, D.M. Unwin, and E.N. Kurochkin (Eds.). *The Age of Dinosaurs in Russia and Mongolia*, pp. 177–186. Cambridge University Press, Cambridge.

Walker, A.D. 1961. Triassic reptiles from the Elgin area: *Stagonolepis*, *Dasygnathus* and their allies. *Philosophical Transactions of the Royal Society of London. Series B, Biological Sciences*, 244: 103–204.

Warren, A., Rich, T.H., and P. Vickers-Rich. 1997. The last labyrinthodonts. *Palaeontographica A*, 247: 1–24.

Watson, D.M.S. 1919. The structure, evolution and origin of the amphibia. The orders Rachitomi and Stereospondyli. *Philosophical Transactions of the Royal Society of London. Series B, Containing Papers of a Biological Character*, 209(360): 1–73.

Watson, D.M.S. 1958. A new labyrinthodont (*Paracyclotosaurus*) from the Upper Trias of New South Wales. *Bulletin of the British Museum of Natural History, London (Geology)*, 3: 233–263.

Wild, R. 1989. Aetosaurus (Reptilia: Thecodontia) from the Upper Triassic (Norian) of Cene near Bergamo, Italy, with a revision of the genus, *Rivista del Museo Civico di Scienze Naturali*, 14: 1–24.

Witzmann, F. 2009. Comparative histology of sculptured dermal bones in basal tetrapods, and the implications for the soft tissue dermis. *Palaeodiversity*, 2: 233–270.

Witzmann, F., Sachs, S., and C. Nyhuis. 2016. A new species of *Cyclotosaurus* (Stereospondyli, Capitosauria) from the Late Triassic of Bielefeld, NW Germany, and the intrarelationships of the genus. *Fossil Record*, 19: 83–100.

Zatoń, M., Piechota, A., and E. Sienkiewicz. 2005. Late Triassic charophytes around the bone-bearing bed at Krasiejów (SW Poland)–palaeoecological and environmental remarks. *Acta Geologica Polonica*, 55(3): 283–293.

Zhao, Q., Benton, M.J., Xu, X., and P.M. Sander. 2013. Juvenile-only clusters and behaviour of the Early Cretaceous dinosaur *Psittacosaurus*. *Acta Palaeontologica Polonica*, 59: 827–833.

Zittel, K.A. 1888. Vertebrata (Pisces, Amphibia, Reptilia, Aves). In*: Handbuch der Palaeontologie, Abteilung: Palaeozoologie*, pp. 598. Oldenbourg, Munich.

List of Figures

List of Tables

Appendices

Appendix A: A1– A34

Teschner, E. M., Chakravorti, S., Sengupta, D. P., and D. Konietzko-Meier. 2020. Climatic influence on the growth pattern of *Panthasaurus maleriensis* from the Late Triassic of India deduced from paleohistology. *PeerJ*, 8: e9868.

Appendix B: B1– B34

Teschner, E. M., Konietzko-Meier, D., and N. Klein. 2022. Growth and limb bone histology of aetosaurs and phytosaurs from the Late Triassic Krasiejów locality (SW Poland) reveals strong environmental influence on growth pattern. *Contributions to Zoology*, 91(3): 199-232.

Climatic influence on the growth pattern of *Panthasaurus maleriensis* from the Late Triassic of India deduced from paleohistology

Elżbieta M. Teschner[1,2], Sanjukta Chakravorti[3], Dhurjati P. Sengupta[3] and Dorota Konietzko-Meier[1,2]

[1] Institute of Biology, University of Opole, Opole, Poland
[2] Section Paleontology, Institute of Geosciences, University of Bonn, Bonn, Germany
[3] Geological Studies Unit, Indian Statistical Institute, Kolkata, West Bengal, India

ABSTRACT

Metoposaurids are representatives of the extinct amphibian clade Temnospondyli, found on almost every continent exclusively in the Late Triassic deposits. Osteohistologically, it is one of the best-known temnospondyl groups, analyzed with a wide spectrum of methods, such as morphology, morphometry, bone histology or computed modelling. The least known member of Metoposauridae is *Panthasaurus maleriensis* from the Pranhita-Godavari basin in Central India, being geographically the most southern record of this family. For the first time the bone histology of this taxon was studied with a focus on the intraspecific variability of the histological framework and the relationship between the observed growth pattern and climatic and/or environmental conditions. The studied material includes thin-sections of five long bones, a rib, an ilium and an intercentrum belonging most likely to eight individuals ranging from different ontogenetic stages. All bones have a large medullary region with progressively increasing remodeling, surrounded by a lamellar-zonal tissue type. The primary cortex consists of parallel-fibered matrix showing various degrees of organization, less organized collagen fibers in the zones and higher organized in the annuli. Growth marks occur in the form of alternating zones and annuli in every bone except the ilium and the intercentrum. The vascularity becomes less dense towards the outermost cortex in all sampled limb bones. Towards the outermost cortex the zone thickness is decreasing, in contrast to the avascular annuli, that become thicker or are of the same thickness. The growth pattern of *P. maleriensis* is uniform and represents changes in ontogenetic development. Multiple resting lines are prominent in the outer annuli of the limb bones and the rib and they presumably indicate climatic and environmental influence on the growth pattern. Therefore, a prolonged phase of slowed-down growth occurred during the unfavorable phase, but a complete cessation of growth indicated by Lines of Arrested Growth (LAGs) is not recorded in the studied samples. Based on the histological framework we conclude that the climate had an impact on the growth pattern. As we do not see any LAGs in the Indian metoposaurid, we assume that the local climate was relatively mild in India during the Late Triassic. A similar prolonged phase of slowed down growth without the occurrence of LAGs was observed in *Metoposaurus krasiejowensis* from the Late Triassic of Krasiejów (Poland). This is in contrast to Moroccan metoposaurid *Dutuitosaurus*

Submitted 16 March 2020
Accepted 13 August 2020
Published 8 September 2020

Corresponding author
Elżbieta M. Teschner,
eteschner@uni.opole.pl

Academic editor
Christopher Noto

Additional Information and Declarations can be found on page 24

DOI 10.7717/peerj.9868

How to cite this article Teschner EżM, Chakravorti S, Sengupta DP, Konietzko-Meier D. 2020. Climatic influence on the growth pattern of *Panthasaurus maleriensis* from the Late Triassic of India deduced from paleohistology. *PeerJ* **8**:e9868 http://doi.org/10.7717/peerj.9868

ouazzoui from the Late Triassic of Argana Basin, where LAGs are regularly deposited throughout ontogeny indicating most likely harsher climatic conditions.

Subjects Paleontology, Zoology, Histology
Keywords *Panthasaurus maleriensis*, Temnospondyli, Late triassic, Paleohistology, Histovariability, Climatic influence

INTRODUCTION

Bone histology is a powerful tool which allows scientists to study various, morphologically often not accessible, aspects of extinct animals' biology. Through the microstructural framework and histological characters ontogeny, phylogeny, biomechanics, and environment could be revealed (*Horner, de de Ricqlès & Padian, 1999*; *Horner, de de Ricqlès & Padian, 2000*; *de Ricqlès et al., 2001*; *Padian, de de Ricqlès & Horner, 2001*; *Padian & Lamm, 2013*). The effects of the local environmental conditions are especially important for ectothermic animals e.g., amphibians, as for them the ambient environment has a direct influence on the formation of the bone tissue (*Padian & Lamm, 2013*). For ectothermic animals, the growth rate is directly related to environment. i.e., during favorable conditions, the bone deposition rate is usually higher, whereas during unfavorable conditions growth rate is relatively low or even cessation of growth could be observed (*Francillon-Vieillot et al., 1990*). Thus, based on the sequences of zones, annuli and lines of arrested growth (LAGs), a conclusion about the conditions in which the animal was living is possible. However, the histological bone framework is modified not only by the external factors, but is also biologically determined by ontogeny or genetic preconditions resulting in the process of developmental plasticity. For fossil taxa the direct determination which factors play more important role in creating the final bone structure and distinguishing between the influence of the internal and external factors on the development is extremally difficult, due to the lack of most of the biological information. The only possibility to determine the influence of the local conditions on the growth pattern are indirect methods based on the combination of the geological and histological information. To conduct such a study, a taxon with a wide geographical distribution, recognized geological setting and a well-known histological record is necessary. An ideal model for such test is the temnospondyl amphibian family occurring in the Late Triassic, namely Metoposauridae.

Temnospondyli and Metoposauridae

Temnospondyli *Zittel, 1888* is a large clade of extinct amphibians and their fossil remains can be found worldwide. It is represented by diverse groups with a notable variation in skull shape and body size. Their stratigraphical occurrence ranges from the Early Carboniferous (*Holmes & Carroll, 1977*) to the Early Cretaceous (*Milner, 1990*; *Warren, Rich & Vickers-Rich, 1997*). They occupied various ecological niches e.g., aquatic, semi-aquatic and terrestrial (*Lindeman, 1991*; *Pawley & Warren, 2004*; *Schoch, 2014*). The Metoposauridae is a group placed within the Stereospondyli clade (*Schoch, 2014*; *Fortuny et al., 2018*) with a stratigraphic appearance restricted to the Late Triassic (*Schoch,* 2003; Schoch, 2013). The group includes the European genera *Metoposaurus diagnosticus* (Von Meyer, 1842) (Germany), *Metoposaurus krasiejowensis* (Sulej, 2002) (Poland) and *Metoposaurus algarvensis* Brusatte et al., 2015 (Portugal), the African taxa from Morocco *Dutuitosaurus ouazzoui* (Dutuit, 1976), *Arganasaurus lyazidi* (Dutuit, 1976), *Arganasaurus azerouali* (Dutuit, 1976), and those from Madagascar _*Metoposaurus hoffmani* Dutuit, 1978, *nomen dubium* (Fortuny et al., 2019). Finally, in North America metoposaurids are represented by *Koskinonodon perfectus* (Case, 1922), *Anaschisma browni* (Branson, 1905) and *Apachesaurus gregorii* Hunt, 1993. From Asia, the Indian taxon *Panthasaurus maleriensis* (Roychowdhury, 1965) is known from the Late Triassic (Carnian to Norian) Maleri Formation (Roychowdhury, 1965; Sengupta, 2002; Chakravorti & Sengupta, 2019) based on multiple skeletal elements and from the Late Triassic (Carnian to Norian) Tiki Formation (Sengupta, 1992) based on only fragmentary preserved skull material. For a long time, *P. maleriensis* represented the most mysterious and least known taxon among all metoposaurids due to the unclear taxonomic relationship and its preservation state (Roychowdhury, 1965).

Geology, environment and climatic conditions of the Maleri Formation

The Pranhita-Godavari Basin is one of the rift basins that were actively filled by the sediments when the Indian landmass was a part of the southern supercontinent Gondwana. The material used in this study originates from the Late Triassic Maleri Formation located within the Pranhita-Godavari Basin of Central India. The formation can be divided into lower and upper section (Kutty & Sengupta, 1988). However, no radiometric dating has been carried out so far. Biostratigraphically, the faunal assemblage of the Lower and Upper Maleri Formation is distinctive and non-overlapping (Datta, Ray & Bandyopadhyay, 2019). The Lower Maleri is considered Carnian in age based on the following index taxa viz. phytosaurs *Parasuchus hislopi* (Chatterjee, 1978) and *Volcanosuchus statisticae* Datta, Ray & Bandyopadhyay, 2019, the metoposaur *Panthasaurus maleriensis* (Roychowdhury, 1965), the rhynchosaur *Hyperodapedon huxleyi* (Mukherjee & Ray, 2014) a traversodontid *Exaeretodon statisticae* (Chatterjee, 1982) and a cynodont *Deccanodon maleriensis* (Nath & Yadagiri, 2007). The Upper Maleri fauna is assigned to the Norian age based on the occurrence of the chigutisaurs: *Compsocerops cosgriffi* and *Kuttycephalus triangularis* (Sengupta, 1995) more derived, phytosaurs cf. *Leptosuchus* (Novas et al., 2010), sauropodomorphs (Bandyopadhyay, 2011; Bandyopadhyay & Ray, 2020; Kutty et al., 2007) and the general disappearance of rhynchosaurs, metoposaurs as well as basal phytosaurs. Identical to other Gondwana basins, the Maleri Formation is dominated by a sandstone-mudstone alternation with occasional calcirudites. Dasgupta, Ghosh & Gierlowski-Kordesch (2017) recently suggested the presence of small, ephemeral and vegetated swamps or ponds along the flow path of the channels in both formation units. Sedimentological evidence of the deposition of parallel-laminate and cross-bedded sheet sandstone within the thick succession of mudstones proves a fluvial environment of the Maleri Formation (Robinson, 1970; Sarkar, 1988; Dasgupta, Ghosh & Gierlowski-Kordesch, 2017). The early Late Triassic climate of the supercontinent Pangea is said to be arid to semi-arid in the interior of Gondwana (*Mueller, Krystyn & Kürschner, 2016*). *Robinson (1970)* suggested a warm and humid climate of the Maleri Formation due to the presence of red mudstones, although the presence of red color in mudstones is not a sufficient indicator for the paleoenvironment. According to *Smoot & Olsen (1988)*, red and massive mudstones can be deposited under dry to wet conditions and their variation can be only understood by the preservation of texture; however, according to *Patranabish-Deb & Fukuoka (1998)*, it is more likely that the dissolution of ferric illite from the abundant Proterozoic rocks surrounding the Pranhita Godavari Basin contributed towards the red coloration of the mudstones in the Maleri Formation. *Kutty (1971)* pointed out that the presence of unioids at the junction of the Lower and Upper Maleri Formation represents a well-watered swamp-like environment indicating prevalent humid paleoclimate. *Sarkar (1988)* showed the presence of high smectite content (48–75%) through Differential Thermal Analysis (DTA) and X-ray analysis, which indicated some amount of rainfall. On the other hand, the sporadic presence of barite coupled with the occurrence of displacive and replacive calcite cements together with caliches indicate a warm to hot climate with low seasonal rainfall (*Sarkar, 1988*). Overall, according to *Sarkar (1988)*, the predominance of smectite in the sediment, the poor floral content of the Maleri Formation, and the paucity of evaporites point to a low seasonal rainfall in a semi-arid environment. However, an array of aquatic fauna, including the metoposaurids, chigutisaurids and phytosaurs, present within the Maleri Formation does not support this. Most of these analyses were done on the Maleri Formation as a whole without distinguishing its bordering (upper and lower) parts. Detailed changes in the paleoenvironment of the Maleri Formation from Carnian to Norian is a work in progress. The excavated spiral and non-spiral coprolites produced by fishes and piscivorous animals yielded gymnosperm pollen, apiculate trilete spores produced by pteridophytes and sparse fungal and algal spores together with an admixture of wood shreds, amorphous vegetable matter and fungal remains (*Vijaya, Prasad & Singh, 2009*). Hence there is an indirect evidence of vegetation from coprolites as well as from the presence of herbivores such as the rhynchosaurs or dicynodonts (*Nath & Yadagiri, 2007*; *Mukherjee & Ray, 2014*; *Bandyopadhyay & Ray, 2020*). Moreover, according to the latest work by *Dasgupta, Ghosh & Gierlowski-Kordesch (2017)* the climate was warm with seasonal rainfall, which lead to the production of the large amount of mud aggregates and vertic soils and a semi-humid or semi-arid setting has been proposed with prominent seasonality for the Late Triassic Maleri Formation.

General temnospondyl osteohistology

The most suitable bones for osteohistological studies from the postcranial material are the limb bones sectioned at the midshaft plane, since they contain the most complete bone growth record as those elements ossify early in ontogeny (*Ricqlès, 1983*; *Francillon-Vieillot et al., 1990*; *Chinsamy, 1993*; *Erickson & Tumanova, 2000*; *Horner, Ricqlès & Padian, 2000*; *Sander, 2000*). During the last two decades many osteohistological studies on various postcranial elements from various temnospondyl clades were published e.g., *de Ricqlès (1979)* and *de Ricqlès (2001)* described the general histological growth briefly concluding that temnospondyl bones preserve lamellar-zonal tissue; *Damiani (2000)* studied Triassic temnospondyl femora from Australia showing that they possess a large medullary region filled by trabeculae and remains of calcified cartilage, highly vascularized primary bone tissue with an alternation of thick zones built by parallel-fibered bone and thin, avascular annuli built by lamellar tissue, and the absence of LAGs; *Witzmann (2009)* studied the histological growth pattern of the dermal bones of various temnospondyl groups; *Sanchez et al. (2010a)* and *Sanchez et al. (2010b)* focused on bone histology of the small-sized *Apateon* from the Permian resembling a thin, almost avascular cortex consisting of lamellar bone and a large open medullary cavity, moreover, they indicated a strong paleoenvironmental and paleoecological influence reflected in its growth; *Witzmann & Soler-Gijon (2010)* analyzed osteoderms of various temnospondyl amphibians and *Bystrowiella* showing a metaplastic development in *Plagiosuchus*, and in *Gerrothorax* and dissorophids periosteal ossification; *Konietzko-Meier & Schmitt (2013)* studied a Middle Triassic *Plagiosuchus* femur and observed a small medullary cavity, surrounded by endosteal bone, a thick but porous cortex and an incipient fibro-lamellar bone gradually passing into parallel-fibered bone, and towards the outermost cortex more lamellar bone and five LAGs; *Konietzko-Meier, Shelton & Sander (2016)* studied North American stegocephalians including *Eryops, Archeria* and *Diadectes* from the Briar Creek bonebed, which revealed a different growth pattern resembling five different histotypes explained by interspecific or intraspecific variability. It seems that the clade Metoposauridae is the best studied due to its preservation and a generous number of various skeletal elements is available for histological studies. Femora of the metoposaurid *Dutuitosaurus ouazzoui* have been studied by *Steyer et al. (2004)*, observing fast initial growth rate concluded on the basis of wide and densely vascularized zones in juvenile individuals and a decrease of growth rate in adult specimens indicated by a decrease in vascular density and thickness of zones. The sexual maturity was estimated for the seventh year of life (*Steyer et al., 2004*) and the growth pattern was linked with the local seasonal environment changes. The osteohistological growth of almost every skeletal element of *Metoposaurus krasiejowensis* has been studied, e.g., limb bones (*Konietzko-Meier & Klein, 2013*; *Konietzko-Meier & Sander, 2013*; *Teschner, Sander & Konietzko-Meier, 2018*). In general, the growth of *Metoposaurus krasiejowensis* consists of primary cortex built up of parallel-fibered bone, and sometimes even incipient fibro-lamellar bone (*Konietzko-Meier & Sander, 2013*), which might be exclusively deposited in juvenile individuals (*Konietzko-Meier & Sander, 2013*). There is also a rich data set published on dermal bones in order to infer information about feeding ecology based on biomechanical reconstruction of metoposaurid skull (*Gruntmejer, Konietzko-Meier & Bodzioch, 2016*; *Gruntmejer et al., 2019a*; *Gruntmejer et al., 2019b*; *Konietzko-Meier et al., 2018*). Analyzes of vertebrae helped to establish histological ontogenetic stages, a method which allows a relative determination of individual age, based on various histological and microstructural characters of vertebrae, when the classical growth cycles are not developed (*Konietzko-Meier, Bodzioch & Sander, 2012*) and showed the variability between different temnospondyl groups which may be taxonomically important (*Konietzko-Meier, Danto & Gądek, 2014*). Various groups studied in *Konietzko-Meier, Danto & Gądek (2014)* seem to have an individual histological framework, however in Stereospondyli the calcified cartilage is preserved a long time in all ontogenetic stages, contrary to Dvinosauria and Eryopoidae which ossify early in ontogeny. The preliminary analysis on ribs (*Gądek, 2012*) showed a very avascular primary tissue. *Gee, Parker & Marsh (2017)* studied vertebrae of the North American metoposaurids *Koskinonodon perfectus* and *Apachesaurus gregorii* confirming a uniform growth among all metoposaurid intercentra.

Studies including osteohistological research on Indian temnospondyls are rare (*Ray, Mukherjee & Bandyopadhyay, 2009*; *Mukherjee, Ray & Sengupta, 2010*; *Mukherjee, Sengupta & Rakshit, 2020*). *Ray, Mukherjee & Bandyopadhyay (2009)* provided preliminary results on the osteohistology of limb bones, ribs, and intercentra of three temnospondyl taxa from different Indian Triassic localities. They studied a trematosaurid from the Early Triassic (Panchet Formation, Damodar Basin), a paracyclotosaurid from the Middle Triassic (Denwa Formation, Satpura Basin), and a chigutisaurid from the Late Triassic (Maleri Formation, Pranhita-Godavari Basin). The conclusion from *Ray, Mukherjee & Bandyopadhyay (2009)* paper was that the examined taxa show distinct growth patterns: the trematosaurid exposed a thick layer of avascular lamellar bone at the periphery, towards the inner cortex a fibro-lamellar bone tissue, the absence of annuli or LAGs except for one humerus, and a woven fibered bone matrix in the ribs; the paracyclotosaurid were characterized by lamellar bone, high vascularity in the humerus and low vascularity in the femur and tibia, the ribs exhibited woven fibered bone matrix, and annuli and LAG were absent except for three LAGs in an intercentrum; the chigutisaurid shows a predominantly lamellar tissue in the long bones, woven fibered matrix in the rib, absence of growth rings in rib and intercentrum but presence of three LAGs in the humerus. The general conclusion was that the Early Triassic trematosaurids had an overall fast growth, in contrast to that of the Middle and Late Triassic temnospondyls (*Ray, Mukherjee & Bandyopadhyay, 2009*). *Mukherjee, Ray & Sengupta (2010)* restudied the material used in *Ray, Mukherjee & Bandyopadhyay (2009)*, and they described the histology of bones from the families Trematosauridae (Early Triassic; humerus and femur), Paracyclotosauridae (Middle Triassic; humerus, femur, tibia, rib and intercentra), Chigutisauridae (Late Triassic; humerus, rib and intercentrum) and an indeterminate temnospondyl (Early Triassic; humerus and ribs) from India. In general, all samples showed a relatively compact cortex surrounding a well-differentiated central medullary region, the occurrence of predominantly longitudinal canals, a decreasing vascularity towards the outer cortex until an avascular outer cortex and the absence of growth rings except for three samples. In conclusion, a change of growth, during the ontogeny, from well-vascularized fibro-lamellar bone to peripheral lamellar bone and LAGs was observed in the Early Triassic trematosaurid, in contrast to the Middle Triassic paracyclotosaurid and Late Triassic chigutisaurid (predominance of lamellar bone), where the growth was cyclical but slow. In conclusion, the rapid growth in trematosaurids was explained as an adaptation to the free niche after the Permo-Triassic extinction event. Based on the growth pattern, the low to moderate cortical porosity in the Early Triassic taxon was linked with a terrestrial lifestyle, and due to a high cortical porosity and extensive medullary spongiosa observed in the analyzed chigutisaurid, a semi-aquatic to aquatic life mode was assumed. The varying cortical thickness in the paracyclotosaurid was explained with different biomechanical adaptation. No conclusions on the influence from the climate were drawn in that study.

In the study by Mukherjee, Sengupta & Rakshit (2020), a larger dataset was analyzed histologically including 17 limb bones ranging from juvenile to adult ontogenetic stages. The studied taxa included Middle Triassic capitosaurids, such as *Cherninia denwai* (nine limb bones), *Paracyclotosaurus crookshanki* (five limb bones) and an indetermined capitosaurid (five limb bones). The analyzes showed differences in paleobiology and lifestyle adaptations. The deposition of incipient fibro-lamellar bone tissue in temnospondyls was linked with the rapid achievement of a large body sizes. *C. denwai* shows first highly vascularized woven fibered bone tissue and later in ontogeny incipient fibrolamellar bone tissue with visible growth marks. The change in tissue type was linked to the achievement of the sexual maturity. The limb bones of *P. crookshanki* consist of parallel-fibered bone and azonal lamellar bone tissue during the entire ontogeny, implying a slow growth. For the life habitat reconstruction *C. denwai* is proposed to be a passive predator living on the bottom of the water reservoir, whereas *P. crookshanki* was reconstructed as a shallow water predator with certain level of terrestriality.

However, a clear correlation between osteohistology and the climatic influence was pointed out only in few papers. Sanchez & Schoch (2013) combined paleoecological and paleohistological analyses on the Triassic taxon *Gerrothorax* from two German localities and concluded an ecological flexibility and evidence of developmental and metabolic plasticity in the taxon. Konietzko-Meier & Klein (2013) and Konietzko-Meier & Sander (2013) observed an unusual alternation of fast (zones) and slow (annuli containing multiple resting lines) growth phases of almost the same thickness in *Metoposaurus krasiejowensis*, corresponding with the favorable and unfavorable seasons. Moreover, Konietzko-Meier & Klein (2013) compared the histological pattern known from femora of *M. krasiejowensis* with the results published for *Dutuitosaurus ouazzoui* in Steyer et al. (2004). The most characteristic difference is the structure of annuli and presence of typical LAGs in the African specimen. According to Konietzko-Meier & Klein (2013), this results from the occurrence of different local conditions, the climate in Morocco was harsh with distinct dry seasons resulting in a clear cessation of growth creating LAGs. In contrast, the mild climate in Krasiejów allowed the animals to grow almost the entire time and only a little influence of the dry period is observable as a decrease in growth rate. McHugh (2014) studied the Late Permian stereospondyl *Rhinesuchus* which shows a seasonal growth with a moderate remodeling, fibro-lamellar and lamellar bone tissue and zones and annuli of a various thickness. Moreover, the preservation of multiple resting lines in the annuli indicates slower metabolism during harsh climatic periods and a possible reason for Stereospondyli to overcome the Permo-Triassic extinction. McHugh (2015) analyzed humeri of *Micropholis stowi* (Dissorophoidea) and *Lydekkerina huxleyi* (Lydekkerinidae) from South Africa showing a convergent occurrence of fibro-lamellar tissue and the absence of LAGs and a suggestion of a terrestrial lifestyle for *M. stowi* due to a free medullary cavity, an azonal tissue, suggesting an adaptation to the dry and hot environmental conditions during the Early Triassic. Canoville & Chinsamy (2015) reported on the histological growth of *Lydekkerina huxleyi* concluding an overall faster growth in early ontogeny linked with a faster attended sexual maturity, moreover, the limb bone microanatomy and histology reveals an empty medullary cavity and a thick cortex implying an amphibious lifestyle with a tendency to more terrestrial or occasionally fossorial lifestyle probably as an adaptation to the harsh environmental conditions.

Aim of the study

This study focuses on the change of the histological growth pattern within one species, namely *Panthasaurus maleriensis* originating from the Lower Maleri Formation in India. It is, so far, the only known metoposaurid from the southern hemisphere. The osteohistological growth of *P. maleriensis* has not yet been described and therefore the growth development within different skeletal elements in different ontogenetic stages of a single taxon is studied here. The Indian taxon is interesting for histological studies, as it was paleogeographically separated from other metoposaurid taxa and the climatic conditions based on geological studies are well-known (*Dasgupta, Ghosh & Gierlowski-Kordesch, 2017*). It allows us to test to what degree the osteohistology among metoposaurids is plastic and reflects the environmental condition. The comparison of the histological framework of three taxa, namely *P. maleriensis*, *M. krasiejowensis* and *D. ouazzoui* can help to answer the question about limits of developmental plasticity of bone structure among metoposaurids.

MATERIAL & METHODS

Material

The sampled material belongs to the Indian representative of metoposaurids *Panthasaurus maleriensis* (*Roychowdhury, 1965*). The material was excavated near the Aigerapalli village in the Lower Maleri Formation from the Late Triassic (*Sengupta, 1995*; *Sengupta, 2002*; *Sengupta, 2003*; *Chakravorti & Sengupta, 2019*). Morphologically, the cranial and postcranial material of *Panthasaurus maleriensis* were described in detail first in *Roychowdhury (1965)* and later in *Sengupta (2002)*. The here analyzed samples are restricted mostly to limb bones including two humeri, one femur, a tibia and a fragmentary ulna. In addition, a rib, an ilium, and an intercentrum of *P. maleriensis* were sectioned. Both humeri studied here are from the left body size, where the smaller humerus (ISIA 73) measures 65 mm in length with a diameter of 24 mm, and the larger humerus (ISIA 70) measures 120 mm in length, and 35 mm in midshaft diameter. The femur (ISIA 83) is from a left limb and has a total length of 140 mm and a midshaft width of 26 mm. The tibia (ISIA 98) has a length of 62 mm and the fragmentary preserved (posterior portion) ulna (ISIA 200) measured 32 mm in length. The reconstructed approximate length of the entire bone is 64 mm. In addition, we studied a left ilium (ISIA 87) measuring 51 mm in length and a fragmentary rib (ISIA 199) with a preserved length of 37 mm. No proxy is available for a total length reconstruction of the rib. The intercentrum (ISIA 198) has a height of 41 mm and a width of 40 mm. The material is stored in the collection of the Indian Statistical Institute (ISI) in Kolkata. All studied bones are listed in Table 1. The maximal known size of a *P. maleriensis* femur is 140 mm (ISIA 83), of a humerus is 144 mm (ISIA 68), of an ulna is 78 mm (ISIA 97) and of a tibia is 65 mm (ISIA 99).

Methods

Table 1 Measurements taken from the the sectioned bones of *Panthasaurus maleriensis*.

Skeletal element of *Panthasaurus maleriensis*	Specimen number	Total length	Percentage of largest bone	Midshaft width	Visible cycles	Estimated cycles
Humerus (L)	ISIA 73	65	45%	24	1,5	1,5
Humerus (L)	ISIA 70	120	83%	35	3	4
Femur (L)	ISIA 83	140	100%	26	4	5
Ulna (R) fragm.	ISIA 200	64[a]	82%[a]	11	2	3
Tibia (R)	ISIA 98	62	95%	12	3	4
Rib fragm.	ISIA 199	37	–	14	3	–
Ilium (L)	ISIA 87	51	56%	13	–	–
Intercentrum	ISIA 198	41	–	43	–	–

Notes.

L, left; R, right; fragm., fragmentary.

[a] estimated length.

All taken measurements of Panthasaurus maleriensis bones are in millimeters.

Thin-sectioning

The thin-sections have been prepared in the laboratory of the Institute of Geosciences at the Rheinische Friedrich-Wilhelms-Universität Bonn, Germany. All bones were sectioned according to *Stein & Sander (2009)* and *Lamm (2013)*, however, their technique was slightly modified. Wet silicon carbide (SiC) grinding powder with grit sizes of 600 and 800 were used for grinding and polishing the thin-sections. All limb bone sections were cut at the midshaft plane. A sagittal section of the intercentrum was made. The osteohistological analysis was performed with a LEICA DM LP polarizing light microscope and the photographs were taken with a LEICA DFC 420 camera attached to the microscope. The sections were scanned with an EPSON PERFECTION 750V PRO scanner in order to gain microstructural overview.

Measurements of the growth cycles thickness

For the estimation of the width of the growth cycles (= zone +) we calculated separately the relative percentage thickness for the zones and annuli in correlation to the total cortex width (Table 2).

Terminology

The morphological description follows the nomenclature used in *Sulej (2007)*, where the osteohistological nomenclature is based on *Francillon-Vieillot et al. (1990)*. Here, we distinguish between two types of Sharpey's fibers, first representing long fibers reaching deep into the cortex, being most probable muscle and tendon attachments (*Francillon-Vieillot et al., 1990*) and second, short fibers arranged in bundles, existing only close to the periosteal surface, being probably attachments of the periosteum (*Witzmann, 2009*; *Konietzko-Meier & Sander, 2013*). The meaning of zone and annulus in the current study follows *Konietzko-Meier & Sander (2013)*. The zone is a highly vascularized layer, with lower organization of collagen fibers in contrast to the term annulus, which refers to the layer without or low number of vascular canals and higher organization of collagen fibers. In the studied material no annual LAGs occur, instead, adjacent to the annuli, numerous lines

Table 2 Percentage thickness of the individual annuli and zones of Panthasaurus maleriensis limb bones.

***Panthasaurus maleriensis* skeletal element vs. growth cycle**	**Humerus ISIA 73**		**Humerus ISIA 70**		**Femur ISIA 83**		**Ulna ISIA 200**		**Tibia ISIA 98**	
	zo	**an**	**zo**	**an**	**zo**	**an**	**zo**	**an**	**zo**	**an**
1st cycle	40	10	-*	-*	-*	-*	-*	-*	-*	-*
2nd cycle	50		53	13	35	5	59	4	54	19
3rd cycle			6	**14**	7	**7**	8	**29**	5	**12**
4th cycle			6	**8**	7	**18**			5	**5**
5th cycle					7	**14**				

Notes.
zo, zone; an, annulus.
*estimated length
All values are calculated in % as a proportion of the individual width of every zone and annulus versus the total cortex width; bold are marked all ratios where the annulus is thicker than the zone in one growth cycle.

are present, which are referred to in this paper as resting lines (for details see Discussion section and paper by *Konietzko-Meier & Sander, 2013*). The count of the annual growth cycles (= age in years) is based on a sequence of a zone and an annulus.

RESULTS

General osteohistology of *Panthasaurus maleriensis*

The innermost part of every sectioned bone (Table 1) is built up by secondary trabecular bone, which is followed by a perimedullary region consisting of a mix of primary and secondary bone. The border between the medullary region, perimedullary region and the cortex is not well defined (Fig. 1A). The primary cortex is preserved throughout the complete section in every specimen, although the bone remodeling is in different stages. The primary matrix consists of parallel-fibered bone with various degrees of collagen-fibers organization (Figs. 1B–1C). Vascularization varies from secondary osteons and/or resorption cavities visible in the deep layers of the cortex (Figs. 1B–1C) and towards the periosteal margin it is present as simple vascular canals and/or primary osteons in the outermost part of the cortex. The orientation of the vascular canals varies from longitudinal and reticular in the innermost cortex to longitudinal canals arranged in rows towards the outermost cortex (Figs. 1D–1J) in all samples. Usually, only zones (with lower organized collagen fibers and numerous vascular canals) and annuli (with higher organized collagen fibers and limited amount of vascular canals) occur as growth marks, and a complex build of a zone and an annulus is counted here as one annual growth cycle (Figs. 1G–1H). No classical LAGs are observed. Osteocyte lacunae are numerous in every section.

Detailed osteohistologicial description

Humeri –Humerus ISIA 73 represents a small-sized humerus consisting of 45% of the maximal length of the largest known humerus (ISIA 68). The cross-section is triangular in shape (Fig. 1A). The medullary region is filled with secondary trabeculae (Figs. 1B–1C). The perimedullary region is rather thin in comparison to the cortical thickness and still preserves a relatively large amount of primary tissue. The erosion cavities are larger on the

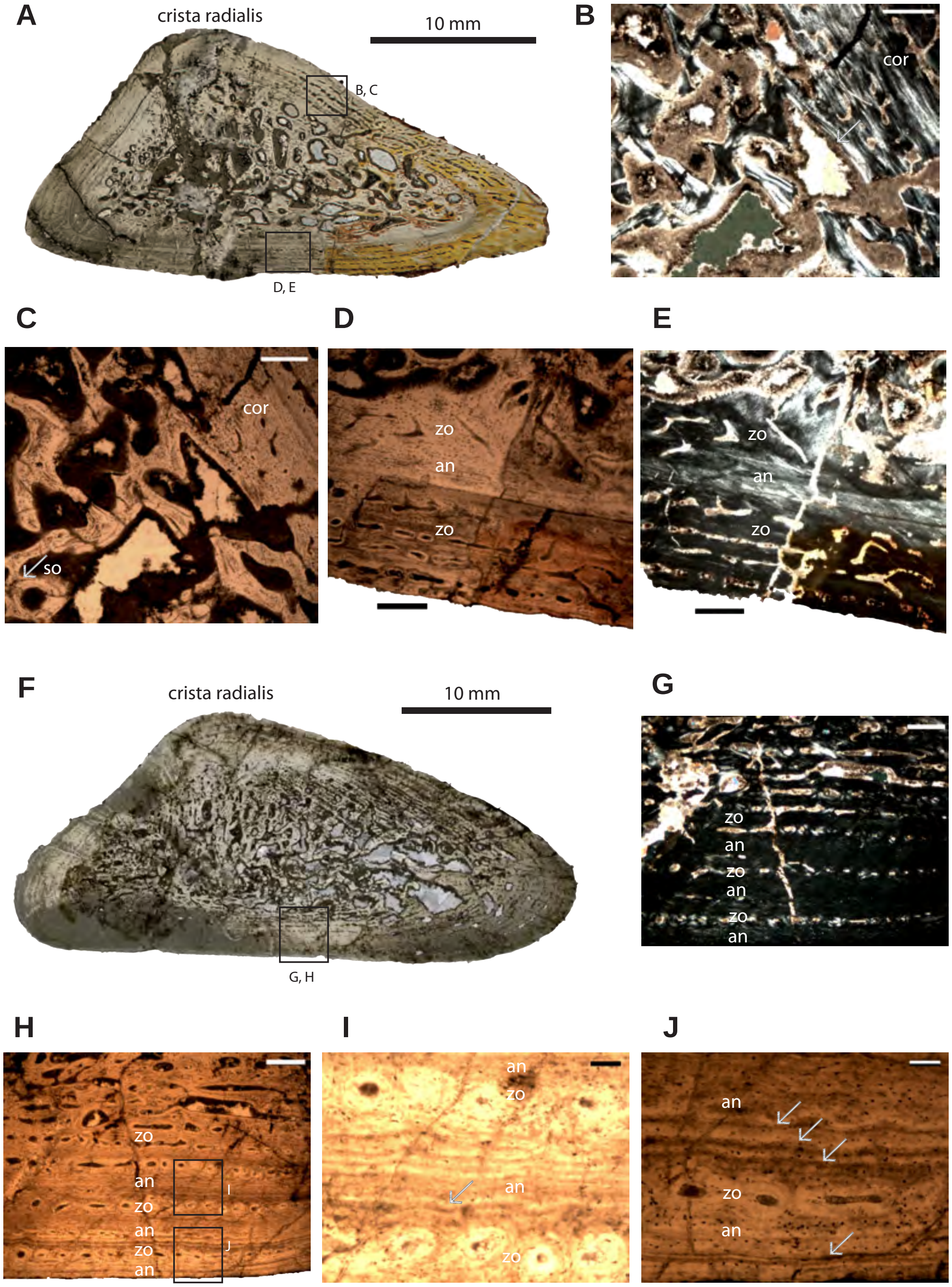

Figure 1 **Microstructure and histology of the humeri of *Panthasaurus maleriensis*.** (A) microstructure of the small-sized humerus ISA 73. (B) the unsharp border between the cortex (cor) and the perimedullary cavity, the secondary osteon (so) is indicated by an arrow; in normal transmitted light. (C) the same picture as in (B) but in polarized light. (D) border between the innermost cortex, a thin annulus and the outermost cortex; a change of vascularization from reticular to longitudinal towards the (continued on next page…)

Full-size DOI: 10.7717/peerj.9868/fig-1

Figure 1 (...continued)
periosteal surface can be observed; in normal transmitted light. (E) the same picture as in (D) but in polarized light. (F) microstructure of the large-sized humerus ISA 70. (G) section showing the alternation of zones and annuli; perimedullary region showing large erosion cavities; towards the cortical surface the vascular canals show a change in shape, from longitudinal to reticular; the width of the annuli increases towards the sections surface; in normal transmitted light. (H) the same picture as in (G) but in polarized light. (I) enlargement of (H) showing two zones consisting of single vascular rows and an annulus with multiple resting lines; in normal transmitted light. (J) enlargement of (H) showing a wide annulus, a zone with a single row of vascular canals and the outermost annulus; the multiple resting lines are indicated by arrows; in normal transmitted light. Scale bar: (B, C, D, G), 500 µm; (I and J), 100 µm. Abbreviations: cor, cortex; so, secondary osteon; zo, zone; an, annulus.

anterior side. The bone matrix is dominated by highly organized parallel-fibered tissue. In the innermost part of the section vascular canals are longitudinal to reticular. Towards the outer cortex a change of simple vascular canals shape is visible (Figs. 1D–1E); the canals are longitudinal. On the ventral side, the canals become radial in shape. Primary osteons dominate in this specimen. A sequence built of the first, innermost zone and an annulus is followed by a second, outermost zone (Figs. 1D–1E, Table 2). Generally, the zones are wider than the annulus in this specimen. The first visible zone has almost been destroyed by remodeling (40% of the cortex, Table 2). The following first avascular annulus is thin (10% of the cortex, Table 2). The second visible zone is thicker than the first zone (50% of the cortex, Table 2) and it possesses rows of longitudinal and reticular vascular canals. No LAGs or resting lines are observed in this section. Short Sharpey's fibers are present, and they occur close to the sections' surface, mostly on the posterior and anterior tip of the bone, although they are not very abundant.

Humerus ISIA 70 represents a large-sized humerus consisting of 83% of the maximal length (ISIA 68). The cross-section is triangular in shape (Fig. 1F) and the nutrient canal is visible on the ventral side. The resorption is extensive and the perimedullary region is well developed (Fig. 1F). Deep in the primary cortex, a mix of longitudinal and reticular vascular canals is preserved, and towards the outer cortex the canals become more longitudinal, are sometimes connected to each other, and are arranged in rows (Figs. 1G–1H). In the region of the *crista radialis*, the vascular canals are mostly reticular in shape. In this specimen the zones and annuli vary in thickness (Table 2). Three growth cycles can be distinguished, and after the first cycle a change of growth rate is visible (Figs. 1G–1H). The innermost first visible zone is wide (53% of the cortex, Table 2) and highly vascular but contains also numerous erosion cavities. Following this the first visible, thin annulus (13% of the cortex, Table 2) with a few resting lines (Fig. 1I) is laid down and the second zone comprising of only one row of longitudinal vascular canals (6% of the cortex, Table 2) is deposited. It is followed by a thick (13% of the preserved cortex, Table 2) second annulus (Figs. 1G–1J), which shows multiple resting lines (Fig. 1J). Towards the subperiosteal surface the third, thin zone containing only one row of vascular canals occurs (6% of the cortex, Table 2). The third annulus is again thick (8% of the cortex, Table 2) and it possesses multiple resting lines (Fig. 1J). The Sharpey's fibers are not very prominent in this section, although they occur close to the cortical surface on the dorsal side.

Femur –The cross-section of specimen ISIA 83 belongs to the largest preserved femur in the ISI collection. The section is oval in shape (Fig. 2A). The medullary region is large, with a few secondary trabeculae preserved inside (Figs. 2A–2F). The perimedullary region is distinct and possesses many erosion cavities due to progressed process of remodeling. The vascular canals are mostly longitudinal (Fig. 2B) and the number of canals decreases towards the cortical surface. The primary osteons (Fig. 2C) are dominant in this section and they are arranged in rows. The section preserved also secondary osteons (Fig. 2D). Four annual growth cycles were observed (Table 2). After the appearance of a thick, first zone (35% of the cortex, Table 2), the thickness of the following zones decreases distinctly, whereas the annuli increase their thickness compared to the associated zones and become even distinctly thicker (Figs. 2E–2F; Table 2). In the first visible innermost zone (7% of the cortex, Table 2) the vascularization is very high and the organization level of the tissue is very low. The structure of tissue resembles the incipient fibro-lamellar bone (Fig. 2B). The following first visible annulus is very thin and avascular (5% of the cortex, Table 2). The second visible zone with one row of vascular canals (7% of the cortex, Table 2) can be distinguished followed by a second annulus (7% of the cortex, Table 2). The third visible zone has one row of vascular canals (7% of the cortex, Table 2) and then the third visible, thick annulus (18% of the cortex, Table 2) is laid down. The fourth visible zone (7% of the cortex, Table 2) consists of one row of vascular canals and the section ends with a comprised fourth annulus (14% of the cortex, Table 2). In all annuli numerous resting lines are visible, however, they are the most prominent in the third and fourth annulus. Sharpey's fibers are very prominent in this section, preserving long fibers that extend deep into the cortex (on the anterior side) and a second type of short fibers that are arranged in bundles and are limited to the section's outermost margin (Figs. 2G–2H).

Ulna –The cortex of the ulna sample (ISIA 200) is not completely preserved due to the fragmentary nature of the bone, however a fragment containing the outermost cortex is present (Figs. 2I–2J). A clear medullary region is not distinguishable, and the perimedullary region possesses large erosion cavities, since the remodeling process is highly advanced and has proceeded into the primary cortex. The vascular canals in the cortex are primarily longitudinal and few have become secondarily altered to reticular canals. Towards the outer cortex they become less numerous, but are arranged in rows. In general, two growth cycles are preserved (Fig. 2J). The innermost, first visible zone (59% of the cortex, Table 2) has been almost entirely remodeled and is bordered by a first visible annulus (4% of the cortex, Table 2), which is followed by the second visible, thin zone (8% of the cortex, Table 2) consisting of only one row of vascular canals. Next, a second visible, thick (29% of the cortex, Table 2) annulus with several prominent resting lines occurs. Sharpey's fibers are not abundant in this section.

Tibia –The specimen ISIA 98 consists of 95% of the maximal length of the largest known tibia (ISIA 99). It has a small and open medullary cavity with visible remains of endosteal bone. The perimedullary region is large and the remodeling is extensive. The border to the primary cortex is sharp and clearly visible, and has a low degree of remodeling. In the cortex, the vascular canals are longitudinal and sometimes circumferential (Fig. 2K). Secondary osteons are dominant in the section. In general, three growth cycles are present

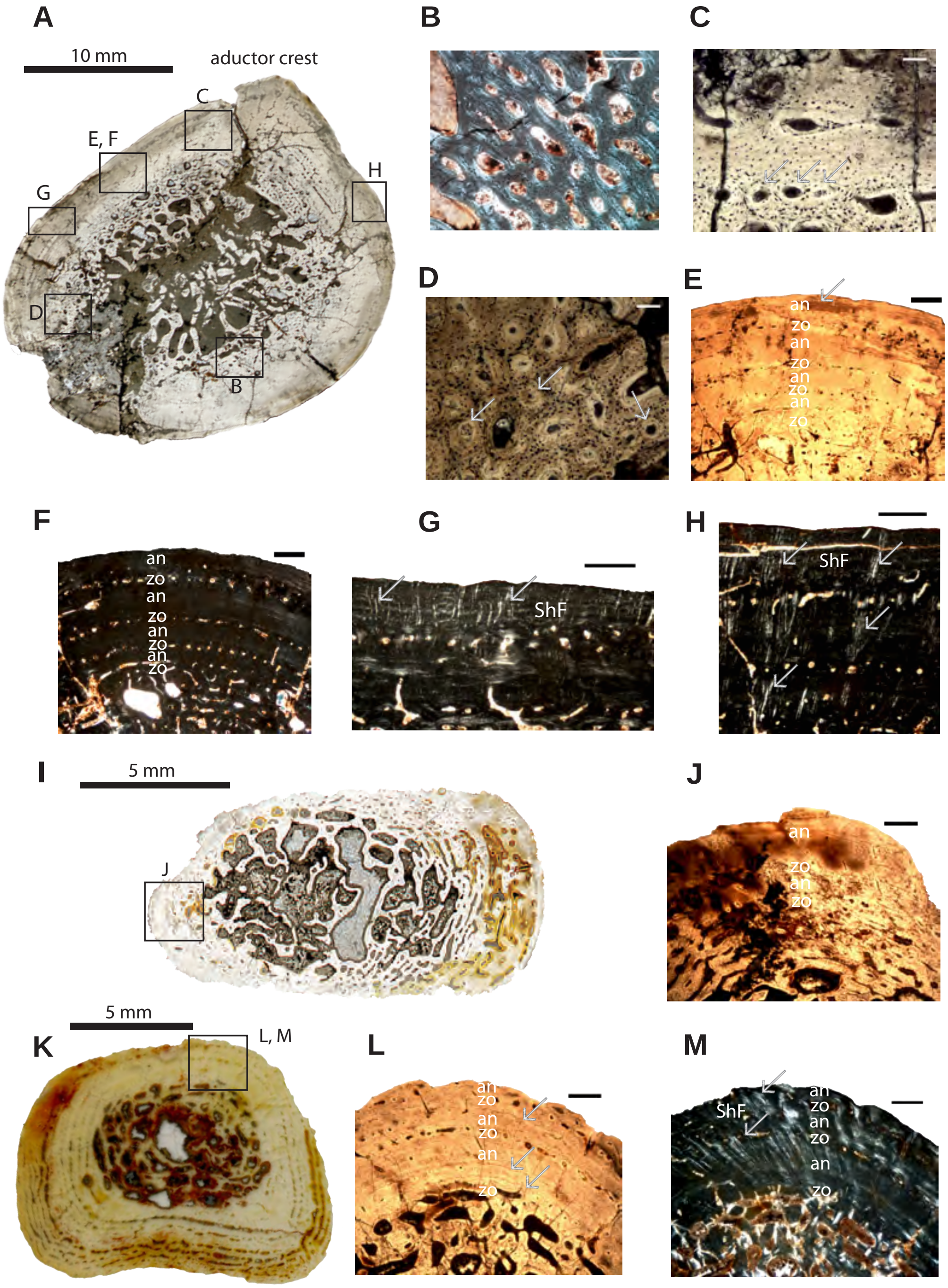

Figure 2 Microstructure and histology of the femur, ulna and tibia of *Panthasaurus maleriensis*. (A) microstructure of the femur ISA 83. (B) incipient fibro-lamellar tissue; in polarized light. (C) primary osteons embedded in the bone matrix indicated by arrows; in normal transmitted light. (D) secondary osteons embedded in the bone matrix, with a visible cementum line indicated by arrows; in normal transmitted light. (E) section showing the alternation of zones and annuli; (continued on next page...)

Full-size DOI: 10.7717/peerj.9868/fig-2

Figure 2 (...continued)
perimedullary region showing erosion cavities; towards the sections surface the zones decrease and annuli increase in width; towards the surface the vascular canals become more longitudinal with an arrangement in single rows; in normal transmitted light. (F) the same as in (E) but in polarized light. (G) short Sharpey's fibers indicated by arrows, occurring close to the cortical surface with an arrangement in bundles; in polarized light. (H) long Sharpey's fibers indicated by arrows reaching inside the cortex; in polarized light. (I) microstructure of the ulna ISA 200. (J) section showing an alternation of zones and annuli; in normal transmitted light. (K) microstructure of the tibia ISA 98. (L) section showing the alternation of zones and annuli; perimedullary region showing large erosion cavities; the zones are thin with only one row of vascular canals; the annuli are much thicker than the zones; arrow indicates a resting line in an annulus close to the sections surface; in normal transmitted light. (M) the same as in (L) but in polarized light; the arrows indicate Sharpey's fibers which are long and reach up into the cortex. Scale bar: (B, C, D), 100 µm and (E, F, G, H, J, L and M), 500; µm. Abbreviations: zo, zone; an, annulus; ShF, Sharpey's fibers.

(Figs. 2L–2M). The innermost, first visible zone is wide (54% of the cortex, Table 2), but scattered by large erosion cavities. However, the remains of the primary tissue indicate that it was once highly vascularized and low organized. Following this is a very thick, distinct annulus (19% of the cortex, Table 2) with numerous resting lines. Next, the second zone, consisting of only one row of vascular canals (5% of the cortex, Table 2), is followed by a thick annulus (12% of the cortex, Table 2), and lastly the third visible zone (5% of the cortex, Table 2) consisting again of only one row of vascular canals is deposited. The section ends with the third annulus (5% of the cortex, Table 2), which is incompletely altered (Figs. 2L–2M). All annuli possess many resting lines (Fig. 2L). Long and numerous Sharpey's fibers are very prominent in this section (Fig. 2M).

Rib –The cross-section of specimen ISIA 199 is triangular in shape (Fig. 3A). The large medullary region consisting of secondary trabeculae shows a roughly central cavity (Figs. 3B–3C). Many primary osteons are observed within the bone matrix. The sample shows three preserved growth cycles (Figs. 3B–3C). In the first innermost zone rare but large erosion cavities appear, followed by a very thin annulus comprised of highly organized tissue. The second zone is thinner than the first zone and contains only few scattered longitudinal vascular canals. Next, a second annulus of approximately the same thickness as the first annulus has been laid down. Then the third zone is preserved with again only scattered vascular canals, with a similar thickness like in the second zone, however, with distinctly lower vascularization. The difference between the following annulus is visible in the lower organization of the parallel-fibered bone. The section finishes with an annulus which possesses very prominent resting lines. Long Sharpey's fibers can be observed (Fig. 3C).

Ilium –The specimen ISIA 87 consists of 56% of the longest preserved individual. The cross-section from the midshaft is roundish in shape (Fig. 3D). The medullary region is extremely large surrounded by a perimedullary region showing extensive resorption (Figs. 3E–3F). The preserved cortex is very fibrous on the lateral side, reminiscent of a metaplastic-like bone with many structural interwoven fibers (Fig. 3G). Numerous vascular canals are limited to the outermost part of the cortex on the posteromedial and anteromedial sides (Figs. 3E–3F). No clear growth marks are visible in this section.

Intercentrum –Specimen ISIA 198 represents an intercentrum in sagittal-section (Fig. 3I). The bone histology is poorly preserved due to diagenesis. Periosteal bone is present only

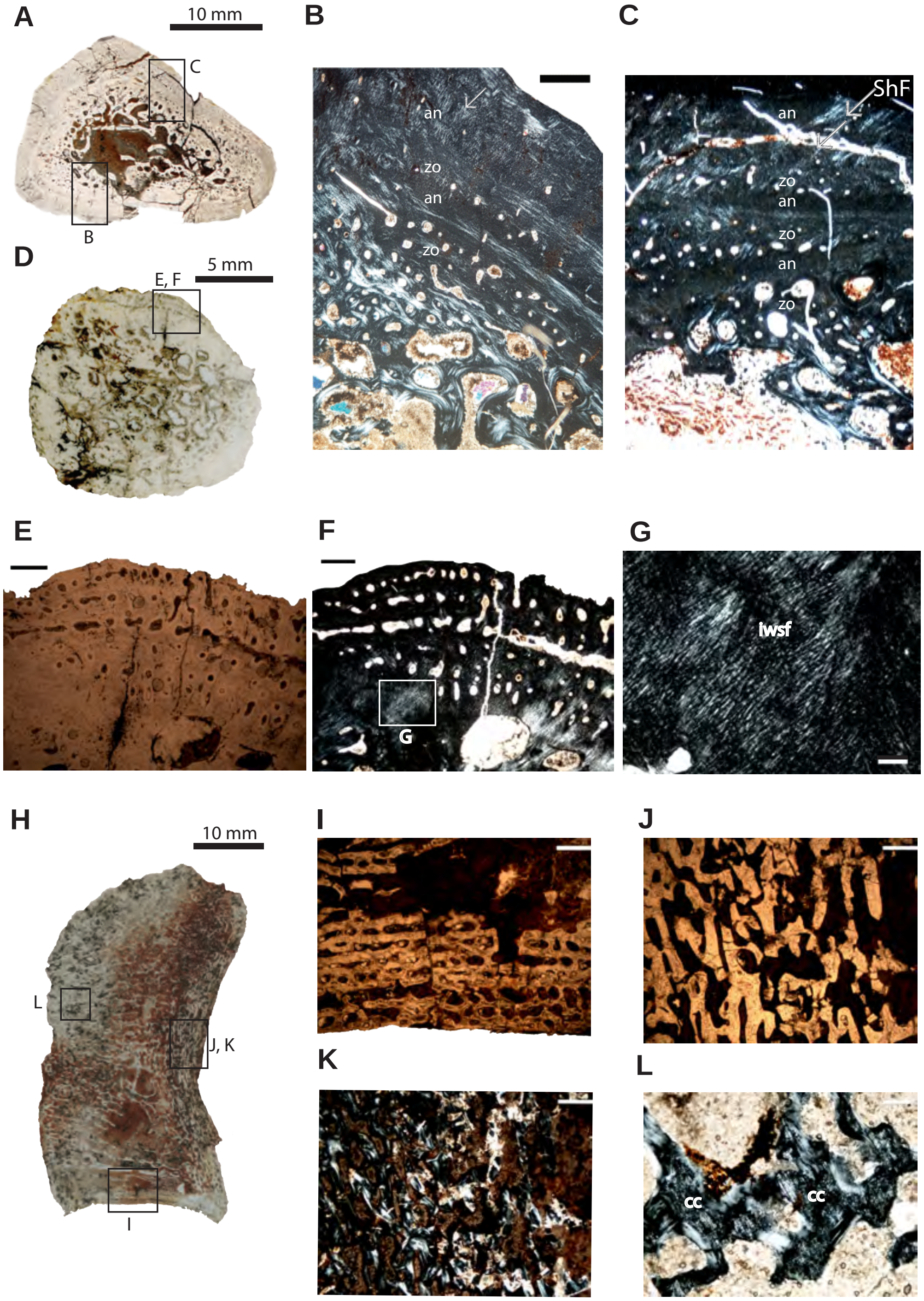

Figure 3 **Microstructure and histology of the rib, ilium and intercentrum of *Panthasaurus maleriensis*.** (A) microstructure of the rib ISA 199. (B) the section showing the alternation between zones and annuli; the vascularization is moderate; the zones in the bone's center are (continued on next page...)

Full-size DOI: 10.7717/peerj.9868/fig-3

Figure 3 (...continued)
thicker than towards the sections surface, in contrast to the annuli which increase in width towards the sections surface; in the outermost annulus metaplastic-like looking tissue occurs; these are interwoven structural fibers (iwsf). (C) the section ahows an alternation between zones and annuli and advanced remodeling; the arrow indicates Sharpey's fibers which are long and reach up into the cortex. (D) microstructure of the ilium ISA 87. (E) the section showing no zones or annuli; the vascular canals are arranged on the posteromedial side; the remodeling process is advanced; in normal transmitted light. (F) the same as in (E) but in polarized light. (G) enlargement from (F) showing metaplastic-like tissue; in polarized light (H) microstructure of the intercentrum ISA 198. (I) primary trabecular bone with vascular canals arranged in rows in periosteal bone; in normal transmitted light. (J) secondary trabeculae visible in endochondral domain; in normal transmitted light. (K) the same as in (J) but in polarized light. (L) remains of calcified cartilage (cc); in polarized light. Scale bar: (B, C, E, F, I J, K), 500 μm; (G, L), 100 μm. Abbreviations: zo, zone; an, annulus; ShF, Sharpey's fibers; iswf, interstractural woven fibers; cc, calcified cartilage.

on the ventral side forming a triangular structure (Fig. 3H). The periosteal domain consists of parallel-fibered bone with rows of longitudinal vascular canals (Fig. 3I), however, the preservation state of the bone does not allow us to distinguish any more details. The largest part of this section is built up by bone tissue of endochondral origin (Figs. 3J–3K), but eroded and thus very poorly preserved. In the endochondral domain, irregular primary or secondary, trabecular bone is observed (Figs. 3J–3K). The primary trabecular bone is visible in the middle part of the section, which is poorly ossified with a large amount of calcified cartilage that is preserved between the trabeculae (Fig. 3L). Anteriorly and posteriorly the amount of secondary remodeled trabeculae increases. Neither growth marks nor Sharpey's fibers are visible.

DISCUSSION

Intra- and interskeletal variability in *Panthasaurus maleriensis*

To answer the questions how far the environment may change the genetically conditioned histological framework, it is necessary to distinguish which characters are biologically related and/or environmentally modeled. Thus, it is important to know how bones change during ontogeny, and how the environmental signal is coded. Ontogenetic or biomechanical changes are usually visible through changes of the histological characters along the growth series (age determination or histological ontogenetic stages, see: *Klein & Sander, 2008*) whereas the environmental signal is expressed by the growth pattern (*Padian & Lamm, 2013*).

All bones studied here show lamellar-zonal tissue, with clear alternation of zones and annuli. Annuli are built from highly organized parallel-fibered bone, whereas zones represent the low organization of the same matrix type. However, along the growth series the ontogenetic change of the growth marks is visible: the older the individual, the more the growth rate decreases and the more the tissue organization increases. Only in femur ISIA 83 (Fig. 2B) in the deep part of the cortex incipient fibro-lamellar bone has been observed, which suggests a fast-initial growth (*Konietzko-Meier & Klein, 2013*). The incipient fibro-lamellar bone would be most likely deposited for gaining size fast in order to overcome predation (*Wiffen et al., 1995*; *Horner, Ricqlès & Padian, 2000*; *Steyer et al., 2004*).

In all specimens with the preserved cyclical growth (except the ilium and the intercentrum) the innermost zone is thicker than the following annulus, and, toward the surface of the cortex, the zones become very thin and consist of only one row of vascular canals, whereas the outermost annuli are thicker and increase in width towards the outer cortex (Figs. 1D–1E, 1G–1J; 2E–2F, 2J, 2L; Table 2). Moreover, no clear LAGs have been observed, although the annuli show phases of prolonged slowed-down growth with several short-lasting periods of cessation of growth indicated by multiple resting lines.

Interesting is that in all bones, except the small humerus, starting with the third cycle and moving outwards, a significant change of the growth pattern is observed (Table 2) and annuli start to have the same thickness or become even thicker than zones. The progressive decreasing of growth rate would suggest an important event in the animal's life cycle and could be related to reaching the point of sexual maturity (*Castanet, 1975*; *Steyer et al., 2001*; *Steyer et al., 2004*). *Steyer et al. (2004)* calculated the sexual maturity for *Dutuitosaurus* at the age of seven years based on the histological characters preserved in the femora (Table 3). For *P. maleriensis* the point of sexual maturity occurred earlier in the ontogeny and, based on the tested bones, should be calculated at the age of approximately three to four years (Table 3). For the taxon from Poland the age of achieving sexual maturity is not possible to determine, as all bones belong to juvenile individuals and signs of decreasing growth are not observed in the histological samples (*Konietzko-Meier & Klein, 2013*). Importantly, in none of the tested metoposaurids the age of achieving the maximal size is represented by a classical External Fundamental System (EFS) (*de Ricqlès et al., 2000*). In the two largest bones of *P. maleriensis* (femur ISIA 83 and humerus ISIA 70) in the outermost annulus, numerous and very distinct resting lines are visible (Figs. 1G–1J; 2E–2F, 2J) accompanied by the overall decreasing growth rate of the cortex. However, because similar lines occur also in deeper situated annuli it is not clear if the accumulation of the resting lines next to the cortical surface represents a structure similar to an EFS or if the well-visible resting lines are an effect of diagenetic processes. The same process of the preservation of multiple resting lines in the outer part of the cortex was observed for *M. krasiejowensis*, however in that case without a visible decreasing growth rate (*Konietzko-Meier & Sander, 2013*). Thus, we conclude that the decreasing growth rate observed in *P. maleriensis* is related to the adulthood although the animal did not achieve its maximal size.

The remodeling process has begun in all samples but is the least-advanced in the ISIA 73 humerus, contrary to the larger humerus (ISIA 70) which has undergone the most extensive remodeling. In *P. maleriensis* we observe that the bones become more porous and therefore lighter (bone mass decrease) during ontogeny. A similar pattern is shown in *D. ouazzoui* bones, where the medullary region expands and the cortex becomes thinner during ontogeny (*Steyer et al., 2004*, Fig. 6). It could be connected to the change of the ecological niche, and the adaptation to a more aquatic lifestyle (*Dutuit, 1967*; *Steyer et al., 2004*; *Gee & Parker, 2018*). The histological framework supports the observation done by *Dutuit (1976)*, who noted the taphonomic separation of adult (central basin) and juvenile (periphery of basin) specimens in the Argana Basin. This would indicate that while the animal is young and still fast growing, it would occupy a shallow water niche that would give it a safe place free of predation. As the animal matures, it might change the water

Table 3 Number of visible and estimated cycles in different skeletal elements of *Panthasaurus maleriensis*, *Metoposaurus krasiejowensis* and *Dutuitosaurus ouazzoui*.

Skeletal element	Taxon name	Total length [mm]	Visible cycles	Estimated cycles	Published as:
Humerus	*Panthasaurus maleriensis*	65	1,5	1,5	Current study
Humerus	*Metoposaurus krasiejowensis*	67.1	1	1	*Teschner, Sander & Konietzko-Meier (2018)*
Humerus	*Panthasaurus maleriensis*	120	3	4	Current study
Humerus	*Metoposaurus krasiejowensis*	82.6	2	2	*Teschner, Sander & Konietzko-Meier (2018)*
Femur	*Panthasaurus maleriensis*	140	4	5	Current study
Femur	*Metoposaurus krasiejowensis*	92	2	3-4	Konietzko-Meier & Klein (2013)
Femur	*Dutuitosaurus ouazzoui*	148	3	10	*Steyer et al. (2004)*
Ulna fragment	*Panthasaurus maleriensis*	64[a]	2	3	Current study
Ulna	*Metoposaurus krasiejowensis*	36.9	2	2	*Konietzko-Meier & Sander (2013)*
Tibia	*Panthasaurus maleriensis*	62	3	4	Current study
Tibia	*Metoposaurus krasiejowensis*	55	4	–	Current study
Rib fragm.	*Panthasaurus maleriensis*	37	3	–	Current study

Notes.

[a] estimated length.

column depth for obtaining food and overcoming predation on its own (*Wiffen et al., 1995*; *Horner, de Ricqlès & Padian, 2000*; *Steyer et al., 2004*). The same was concluded by *Gee & Parker (2018)*, based on the absence of large-sized metoposaurids in the North American localities, which might be due to an ecological separation of juveniles and adult specimens. Also, in the Polish locality preserving *M. krasiejowensis*, a taphonomic preservation of juvenile individuals is dominant over the adult specimen, however in that case it is not a result of the biological segregation, but is connected with the mass segregation during transportation of the fossil material into the Lagerstätte (*Bodzioch & Kowal-Linka, 2012*).

Sharpey's fibers occur in two different forms in both species, first type as bundles of short fibers (periosteum attachment) and second type as long fibers reaching deep into the cortex (muscle attachment). However, they are not abundant in *P. maleriensis* except in femur ISIA 83 and tibia ISIA 98. This does not correlate with the pattern in *M. krasiejowensis*, where numerous long and short Sharpey's fibers are preserved in every skeletal element. Moreover, the preservation of numerous Sharpey's fibers seems to be a typical character for temnospondyls observed also in North American *Eryops*, *Archeria* and *Diadectes* (*Konietzko-Meier, Shelton & Sander, 2016*), also visible in modern amphibians (*Kolenda et al., 2018*). Long Sharpey's fibers being most likely attachments of muscles are very prominent in the femur and tibia sections (Figs. 2G–2H, 2M), in contrast to the humeri, where they are not abundant. There might be also a biological adaptation influencing the growth pattern, and therefore a probable different usage of hind limbs over front limbs linked most likely to locomotion (*Carrier & Leon, 1990*; *Margerie de et al., 2004*). It has been proposed for *M. krasiejowensis* that it might bury in the soft substrate to overcome an unfavorable period (*Konietzko-Meier & Sander, 2013*).

Age estimation and interpretation of ontogenetic growth

A method in paleohistology which allows the retrocalculation of the lost or resorbed growth cycles to estimate the individual age of an animal is known as the superimposition method (*Leclair Jr & Castanet, 1987*; *Castanet et al., 2004*; *Bybee, Lee & Lamm, 2006*; *Sanchez et al., 2010b*). This method however, requires the application of a well-defined ontogenetic series, consisting of at least two bones from a different size range and, which in our case was only possible for the humeri. The other method to retrocalculate the number of missing cycles is by measuring the distance between the center of the medullary region and the first visible growth cycle and then dividing by the largest distance between two observed growth cycles (*Griebeler, Klein & Sander, 2013*; *Klein & Sander, 2007*; *Klein & Griebeler, 2016*).

In the current study, applying the latter method might provide a significant error, as the thickness of the growth marks varies distinctly along the sections (Table 2). The third possibility to determine the individual age of the studied bones is thus the estimation of the relative number of the growth cycles based on the comparison between closely related metoposaurids, namely *Dutuitosaurus ouazzoui* from Morocco and *Metoposaurus krasiejowensis* from Poland, which are both well sampled histologically (*Steyer et al., 2004*; *Konietzko-Meier & Klein, 2013*; *Konietzko-Meier & Sander, 2013*; *Teschner, Sander & Konietzko-Meier, 2018*). *Steyer et al. (2004)* calculated an individual age for *D. ouazzoui* by counting LAGs in femora, whereas the count of annual growth cycles (Table 3) for *M. krasiejowensis* has been performed for the femora (*Konietzko-Meier & Klein, 2013*), for the ulnae (*Konietzko-Meier & Sander, 2013*) and for the humeri (*Teschner, Sander & Konietzko-Meier, 2018*). In this method the assumption that developmental plasticity does not occur is necessary, especially if working on a small sample size. *Konietzko-Meier & Klein (2013)* compared the growth rate of *M. krasiejowensis* and *D. ouazzoui* femora and showed that both taxa had a similar growth rate and the correlation between histological framework and bone length is always constant: the longer the bone is the higher is, the number of cycles.

Application of the superimposition method was possible for the humeri of *P. maleriensis*. Therefore, the midshaft section of the smaller specimen (ISIA 73; 65 mm in length) was fitted inside the medullary region of the larger specimen (ISIA 70; 120 mm in length). The number of visible cycles in the smaller bone is one and a half and in the larger humerus it is three. Therefore, the estimation of the relative age, after the addition of the eroded cycle, is at least one and a half for the smaller specimen, and four for the larger specimen. Thus, based on the histological framework, the humerus ISIA 73 likely represents a late juvenile. The ontogenetic stage of the larger specimen (ISIA 70) based on the advanced remodeling process and expectation of achieving the sexual maturity in the fourth year of life should be determined as adult. While comparing the ISIA 73 specimen to a *M. krasiejowensis* humerus of a similar length (67.1 mm in length, one cycle visible; *Teschner, Sander & Konietzko-Meier, 2018*), the size and corresponding age are similar in both species. However, the Polish locality does not preserve bones belonging to adult specimens and the largest sampled humerus of *M. krasiejowensis* measures 82.6 mm in length and shows two growth cycles (*Teschner, Sander & Konietzko-Meier, 2018*). For *P. maleriensis* the humerus length corresponds with the histological age: the shorter the bone the ontogenetically younger the specimen and adequately, the larger the bone the older the specimen. There is no data published about the histology of *D. ouazzoui* humeri.

The femoral section (140 mm in length) is in an advanced remodeling stage and some annual growth cycles might have been resorbed. The retrocalculation method cannot be applied here as we only have one femoral section, however an age estimation can be done based on the visible cycles and comparison with *M. krasiejowensis* and *D. ouazzoui* (*Konietzko-Meier & Klein, 2013*; *Steyer et al., 2004*). The four visible growth cycles in the ISIA 83 section of *P. maleriensis* correlate to an age of at least four years, with the second cycle showing the beginning of a slowed-down growth rate. It allows to retrocalculate the amount of missing cycles as one and to estimate the age of the bone at five years. It is in contradiction to the femur of *D. ouazzoui* (*Steyer et al., 2004*), since a femur (AZA131-1; 148 mm) similar in length to the *P. maleriensis* femur is calculated to have 10 years (*Steyer et al., 2004*). From the Krasiejów locality the largest sectioned specimen of *M. krasiejowensis* is only 92 mm long (UOPB 00912) with an estimation of three to four cycles (*Konietzko-Meier & Klein, 2013*). The oldest known specimen (UOBS 02123) from the Polish locality is estimated at five years, but is shorter, having only 84 mm in length (*Konietzko-Meier & Klein, 2013*). The weak correlation between the age and the size represents developmental plasticity typical for lissamphibians and already known for Early Permian stem lissamphibian *Doleserpeton annectens* (*Gee, Haridy & Reisz, 2020*). This is in contradiction with the conclusion from *Konietzko-Meier & Klein (2013)*, where the developmental plasticity was excluded. However, in the Krasiejów locality, where only long bones of (late) juvenile individuals occur, it is possible that later in ontogeny the growth rate would start to vary, which would result with a disproportion between individual size and age.

The specimen ISIA 200 represents a fragmentary ulna which preserves a partial midshaft and the posterior head of 32 mm and was estimated to 64 mm of total bone length. The cortex is complete, although some cycles might become resorbed. Based on the number of two growth cycles visible, the minimal age corresponds with two years. A sectioned ulna of *M. krasiejowensis* with a total length of 36.9 mm shows two visible cycles (*Konietzko-Meier & Sander, 2013*). We estimate the minimal age at three years for the *P. maleriensis* ulna.

The ISIA 98 tibia (62 mm in length) shows three growth cycles, which correspond to an age of at least three years. The largest described tibia in *Konietzko-Meier & Klein (2013)* measures only 55 mm in length, however no count of the visible growth marks was published. In the section of *M. krasiejowensis*, two growth cycles are visible (E Teschner, 2020, personal observation), corresponding to a minimum age of two. For the section of *P. maleriensis* we estimated a minimal age of four years for the tibia. In the sampled ulna (ISIA 200) and tibia (ISIA 98) the sections show a large perimedullary region and secondarily widened vascular canals. Based on the amount of the counted growth cycles, both specimens would represent sub-adult individuals.

From the sampled rib specimen (ISIA 199) only a small and fragmentary bone was preserved, thus it is not possible to reconstruct the position of the bone in the skeleton or even the entire rib length. The section preserves three cycles, which indicate a minimum age of three years. The only paper studying the rib histology of *M. krasiejowensis* was published by *Gądek (2012)*, however in this article no age estimation was given. After a personal evaluation (E Teschner, 2020, personal observation) of the rib sections used in *Gądek (2012)*, based on four visible growth cycles a relative age would correspond to four years. While comparing both rib samples, the Indian specimen is ontogenetically of the same age as the Polish individual although *M. krasiejowensis* has one growth cycle more but in *P. maleriensis* the remodeling process is more advanced. It is known from dinosaurs that ribs are a very useful skeletal element for age estimation due to their relatively compact structure and slow growth (*Waskow & Sander, 2014*; *Waskow & Mateus, 2017*). On the other hand, it is important to note, that the position of the rib in the skeleton and the sectioning plane are crucial as they influence the amount of visible cycles (*Waskow & Mateus, 2017*). Therefore, the relative age estimation of the *P. maleriensis* rib is strongly doubtful. To test the expression of the growth marks and interskeletal variability among temnospondyl ribs, and especially Metoposauridae, more studies are necessary.

The ISIA 87 ilium shows no zones and annuli that could be counted. However, as the degree of resorption is very large, it could be assumed that this specimen was not at a juvenile stage anymore. No ilium has been sectioned for comparison from *M. krasiejowensis* or *D. ouazzoui*. The ilium section (ISIA 97) reveals extensive bone remodeling. We assume, that the more metaplastic-like the bone becomes, the older the specimen is. Due to its highly remodeled tissue (Fig. 3D) the ilium may represent an adult individual.

The intercentrum ISIA 198 of *P. maleriensis* has a comparable structure to the intercentrum of *M. krasiejowensis* regarding the large endochondral part, preservation of calcified cartilage in all ontogenetic stages and the periosteal bone being highly vascularized (*Konietzko-Meier, Bodzioch & Sander, 2012*). *Konietzko-Meier, Bodzioch & Sander (2012)* studied the histological variability among the intercentra of *M. krasiejowensis*, and created histological ontogenetic stages (HOS). The HOS are based on the characters of the periosteal bone in the vertebra: HOS 1 lacks periosteal ossification and shows no cortex, HOS 2 consists mostly of periosteal bone with an increasing vascularization, HOS 3 is characterized by a decrease in vascularization in the external cortex and HOS 4 shows LAGs in the external cortex (*Konietzko-Meier, Bodzioch & Sander, 2012*). The studied intercentrum of *P. maleriensis* was growing rapidly and corresponds to the late juvenile/sub-adult HOS 2-3 in comparison to *M. krasiejowensis* (*Konietzko-Meier, Bodzioch & Sander, 2012*). The only difference is that the *M. krasiejowensis* sections are less diagenetically altered. The calcified cartilage within the trabecular bone represents an intermediate state in the endochondral bone formation, and may indicate incomplete growth and bone immaturity (*Hunziker, 1994*; *Cancedda, Cancedda & Castagnola, 1995*; *Erlenbacher et al., 1995*; *Bianco et al., 1998*), suggesting the juvenile age of the sampled *P. maleriensis* specimen. However, in Stereospondyli the calcified cartilage in the vertebrae is generally preserved for a long time in the ontogenetic record (*Konietzko-Meier, Danto & Gądek, 2014*), which also seems to be the case in other vertebrate groups (squamates: *Houssaye et al., 2010*; sauropterygians: *Klein, Canoville & Houssaye, 2019*). Therefore, this is not a reliable character that can be used for an age estimation.

The Indian locality shows a wide spectrum of ontogenetic stages with a sample size based on the histological characters with the age range from one and a half to five years, with the only juvenile specimen represented by the small humerus. It is important to note that since we studied disarticulated bones originating most probably from multiple individuals, the individual growth rate of the single skeletal elements cannot be estimated here without sampling bones originating from one individual.

Climatic and environmental signal in the bones of *Panthasaurus maleriensis*

The climatic signal in osteohistology is the best represented by the growth pattern. Even though every taxon has a genetically fixed growth strategy, the climate can influence the growth pattern. The Late Triassic climate was close to todays' monsoonal climate (*Dubiel et al., 1991*; *Dickins, 1993*; *Parrish, 1993*). Therefore, the appearance of the zones and annuli in a section most likely represents an alternation of wet and dry periods in an annual cycle. This has been observed in the studied samples, as all limb bones of *P. maleriensis* show an alternation of zones and annuli. The growth in *M. krasiejowensis* is similar to *P. maleriensis*, as both taxa show an alternation of zones and annuli in the cortex. Also, in both taxa no classical LAGs are present, and a slow-down growth rate is represented only by the preservation of numerous resting lines in the annuli. In the juvenile *M. krasiejowensis* specimen, the zones are almost of the same thickness as the annuli (*Konietzko-Meier & Klein, 2013*; *Teschner, Sander & Konietzko-Meier, 2018*). In *P. maleriensis* in the inner cortex the annuli are rather thin compared to the zones, and only after achieving the sexual maturity become thicker than zones towards the cortical surface (Table 2). In both juvenile humeri (*M. krasiejowensis* vs. *P. maleriensis*) the size and corresponding age are similar. That confirms the conclusion about the lack of developmental plasticity provided by *Konietzko-Meier & Klein (2013)* based on the femoral histology observed in individuals from Poland and Morocco. For all three metoposaurid taxa the growth early in ontogeny is relatively uniform, and only after the third growth cycle the growth strategy starts to vary, with *P. maleriensis* slowing the growth rate and achieving sexual maturity and *M. krasiejowensis* continuing the juvenile pattern. In contrast to that are the sectioned femora of *D. ouazzoui* which show an alternation of thick zones and thin annuli and, most importantly, they show regularly deposited LAGs (*Steyer et al., 2004*). The different growth strategies in the femora of two different genera but of a similar length (about 148 mm) represent different ages: for *Dutuitosaurus* 10 years and for *P. maleriensis* only five years (femora of *Metoposaurus krasiejowensis* are not known in that size).

The different age of achieving sexual maturity for taxa from India and Morocco, could be on the one hand determined by genetic preconditions, however on the other hand, it is known for Lissamphibia that the age of achieving sexual maturity is highly plastic and related to environmental conditions (*Miaud et al., 2001*). Again, for the Polish taxon the age of sexual maturity is not known, but it was most likely later than in the Indian taxon.

Finally, it can be concluded, that the Polish species *M. krasiejowensis* and the Indian *P. maleriensis* show similar growth pattern, modified by developmental plasticity in later phases of ontogeny. However, common characters could still be observed between the two taxa, as evidenced by the alternation of zones and annuli and the lack of LAGs. Multiple resting lines indicate a partial stagnation of growth. Based on the histological study we assume that the climate was rather mild and not too dry in India during the Late Triassic, which is reflected in the osteohistology during the uninterrupted growth early in the ontogeny. This matches with the geological evidence in the Maleri Formation (*Dasgupta, Ghosh & Gierlowski-Kordesch, 2017*). Moreover, this would indicate harsher climatic conditions for the Moroccan metoposaurid *D. ouazzoui*, since it shows multiple LAGs in the femora (*Dutuit, 1976*; *Steyer et al., 2004*), and a milder climate in India and Poland.

CONCLUSION

The material used in this study represents a sufficient sample size including different ontogenetic stages, which allows us to draw conclusions on the growth pattern of *Panthasaurus maleriensis*. All bones consist of lamellar-zonal bone tissue and a cancellous medullary region traversed by secondary trabeculae. The border between the perimedullary region and the cortex is indistinct. A variable degree of collagen-fibers organization in the matrix has been observed resulting in an alternation of highly organized and low vascularized and lower organized and highly vascularized parallel-fibered bone. The cross-sections of the long bones always start with an innermost thick zone with a decreasing thickness of the following zones towards the cortical surface, in contrast to the annuli which increase in size toward the cortical surface and even become thicker than the zones. No clear LAGs can be observed in *P. maleriensis*. However, the annuli deposited in the outer cortex, which do not correspond to the same age, show multiple resting lines. The presence of those resting lines most likely indicates that the individual stayed active during the unfavorable season but temporarily had to cease its growth rate for exogenous reasons such as lack of nutrition or drying out of the water reservoir needed to survive. On the basis of skeletochronology, a strong developmental plasticity can be most likely excluded for *P. maleriensis*. We thus conclude that the presence of the multiple resting lines in the annuli and the absence of LAGs is linked to the environmental and/or climatic influence. Therefore, the Indian *P. maleriensis* would have lived most likely under similar climatic and environmental conditions as the Polish species *M. krasiejowensis* with rather mild climatic conditions making complete cessation of growth rate as indicated by LAGs not necessary. This contrasts with the Moroccan metoposaurid *D. ouazzoui*, where LAGs are occurring even in fast-growing juveniles, and therefore we suggest that the climate during the Late Triassic in Morocco was harsher.

ACKNOWLEDGEMENTS

We would like to thank Olaf Dülfer (University of Bonn) for preparing the thin-sections. Special thanks go to Kayleigh Wiersma-Weyand (University of Bonn) and Christina Nawrat (University of Bremen) for constructive criticism on the typescript and the linguistic improvement. We also would like to thank the editor (Christopher Noto) and the three reviewers (Jennifer Botha and two anonymous) for their comments, remarks and suggestions on the earlier version of the manuscript which helped improving this paper.

ADDITIONAL INFORMATION AND DECLARATIONS

Funding

This research has been funded by the Polish National Science Center (NCN) grant number UMO-2016/23/N/ST10/02179. The field work in the Maleri Formation and the preparation of the specimens was funded by the Indian Statistical Institute, Kolkata, India. The funders had no role in study design, data collection and analysis, decision to publish, or preparation of the manuscript.

Grant Disclosures

The following grant information was disclosed by the authors:
Polish National Science Center (NCN): UMO-2016/23/N/ST10/02179.
Indian Statistical Institute, Kolkata, India.

Competing Interests

The authors declare there are no competing interests.

Author Contributions

- Elzbieta M. Teschner conceived and designed the experiments, performed the experiments, analyzed the data, prepared figures and/or tables, authored or reviewed drafts of the paper, and approved the final draft.
- Sanjukta Chakravorti and Dhurjati P. Sengupta conceived and designed the experiments, authored or reviewed drafts of the paper, and approved the final draft.
- Dorota Konietzko-Meier conceived and designed the experiments, analyzed the data, authored or reviewed drafts of the paper, and approved the final draft.

Data Availability

The following information was supplied regarding data availability:

All listed specimens are stored at the Geological Studies Unit of the Indian Statistical Institute in Kolkata, India:

ISIA 73 –humerus
ISIA 70 –humerus
ISIA 83 –femur
ISIA 200 –ulna
ISIA 98 –tibia
ISIA 199 –rib
ISIA 87 –ilium
ISIA 198 –intercentrum

Supplemental Information

Supplemental information for this article can be found online at http://dx.doi.org/10.7717/peerj.9868#supplemental-information.

REFERENCES

Bandyopadhyay S. 2011. Non-marine Triassic vertebrates of India. In: Calvo JO, Porfiri J, Gonzalez B, Santos D, eds. *Paleontología y Dinosaurios desde América*. Latina: EDIUNC, Editorial de la Universidad Nacional de Cuyo, Mendoza, Argentina, 33–46.

Bandyopadhyay S, Ray S. 2020. Gondwana vertebrate faunas of india: their diversity and intercontinental relationships. *Episodes Journal of International Geoscience* **43(1)**:438–460 DOI 10.18814/epiiugs/2020/020028.

Bianco P, Cancedda FD, Riminucci M, Cancedda R. 1998. Bone formation via cartilage models: the 'borderline' chondrocyte. *Matrix Biology* **17(3)**:185–192 DOI 10.1016/S0945-053X(98)90057-9.

Bodzioch A, Kowal-Linka M. 2012. Unraveling origin of the Late Triassic multitaxic bone accumulation at Krasiejów (S-Poland) by diagenetic analysis. *Paleogeography, Paleoclimatology, Paleoecology* **346–347**:25–36 DOI 10.1016/j.palaeo.2012.05.015.

Branson EB. 1905. Structure and relationships of American Labyrinthodontidae. *Journal of Geology* **13**:568–610 DOI 10.1086/621258.

Brusatte SL, Butler RL, Mateus O, Steyer JS. 2015. A new species of *Metoposaurus* from the Late Triassic of Portugal and comments on the systematics and biogeography of metoposaurid temnospondyls. *Journal of Vertebrate Paleontology* **35(3)**:e912988 DOI 10.1080/02724634.2014.912988.

Bybee PJ, Lee AH, Lamm ET. 2006. Sizing the Jurassic theropod dinosaur *Allosaurus*: assessing growth strategy and evolution of ontogenetic scaling of limbs. *Journal of Morphology* **267(3)**:347–359 DOI 10.1002/jmor.10406.

Cancedda R, Cancedda FD, Castagnola P. 1995. Chondrocyte differentiation. In: *International review of cytology*. Vol. 159. Academic Press, 265–358.

Canoville A, Chinsamy A. 2015. Bone microstructure of the stereospondyl *Lydekkerina huxleyi* reveals adaptive strategies to the harsh post permian extinction environment. *The Anatomical Record* **298(7)**:1237–1254 DOI 10.1002/ar.23160.

Carrier D, Leon LR. 1990. Skeletal growth and function in the California gull (*Larus californicus*). *Journal of Zoology* **222(3)**:375–389 DOI 10.1111/j.1469-7998.1990.tb04039.x.

Case EC. 1922. *New reptiles and stegocephalians from the Upper Triassic of western Texas*. Carnegie Institution of Washington, Washington, 1–84.

Castanet J. 1975. Quelques observations sur la présence et la structure des marques squelettiques de croissance chez les amphibiens. *Bulletin de la Société zoologique de France* **100(4)**:603–620.

Castanet J, Croci S, Aujard F, Perret M, Cubo J, De Margerie E. 2004. Lines of arrested growth in bone and age estimation in a small primate: *Microcebus murinus*. *Journal of Zoology* **263(1)**:31–39 DOI 10.1017/S0952836904004844.

Chakravorti S, Sengupta D. 2019. Taxonomy, morphometry and morphospace of cranial bones of *Panthasaurus* gen. nov. *maleriensis* from the Late Triassic of India. *Journal of Iberian Geology* **45(2)**:317–340 DOI 10.1007/s41513-018-0083-1.

Chatterjee S. 1978. A primitive parasuchid (phytosaur) reptile from the Upper Triassic Maleri formation of India. *Palaeontology* **21**:83–127.

Chatterjee S. 1982. A new cynodont reptile from the Triassic of India. *Journal of Paleontology* **56**(**1**):203–214.

Chinsamy A. 1993. Bone histology and growth trajectory of the prosauropod dinosaur *Massospondylus carinatus* Owen. *Modern Geology* **18**(**3**):319–329.

Damiani RJ. 2000. Bone histology of some Australian Triassic temnospondyl amphibians: preliminary data. *Modern Geology* **24**:109–124.

Dasgupta S, Ghosh P, Gierlowski-Kordesch EH. 2017. A discontinuous ephemeral stream transporting mud aggregates in a continental rift basin: the Late Triassic Maleri Formation, India. *Journal of Sedimentary Research* **87**(**8**):838–865 DOI 10.2110/jsr.2017.47.

Datta D, Ray S, Bandyopadhyay S. 2019. Cranial morphology of a new phytosaur (Diapsida, Archosauria) from the Upper Triassic of India: implications for phytosaur phylogeny and biostratigraphy. *Papers in Palaeontology* DOI 10.1002/spp2.1292.

de Ricqlès A. 1979. Relations entre structures histologiques, ontogenèse, strategies démographiques et modalités évolutives: le cas des reptiles captorhinomorphes et des stégocéphales temnospondyles. *Comptes Rendus de l'Academie des Sciences Paris, Série D* **288**:1147–1150.

de Ricqlès A. 1983. Cyclical growth in the long limb bones of a sauropod dinosaur. *Acta Palaeontologica Polonica* **28**(**1–2**)225–232.

de Ricqlès A. 2001. Bone histology, heterochronies and the return of tetrapods to life in water: where are we?. In: Mazin JM, de Buffrenil V, eds. *Secondary adaptations of tetrapods to life in water*. München: Verlag Friedrich Pfeil, 289–310.

de Ricqlès A, Mateus O, Antunes MT, Taquet P. 2001. Histomorphogenesis of embryos of Upper Jurassic theropods from Lourinhã (Portugal). *Comptes Rendus de l'Academie des Sciences-Series IIA-Earth and Planetary Science* **332**(**10**):647–656.

de Ricqlès A, Padian K, Horner J, Francillon-Vieillot HE. 2000. Palaeohistology of the bones of pterosaurs (Reptilia: Archosauria): anatomy, ontogeny, and biomechanical implications. *Zoological Journal of the Linnean Society* **129**(**3**):349–385 DOI 10.1111/j.1096-3642.2000.tb00016.x.

Dickins JM. 1993. Climate of the late Devonian to Triassic. *Palaeogeography, Palaeoclimatology, Palaeoecology* **100**(**1–2**):89–94 DOI 10.1016/0031-0182(93)90034-G.

Dubiel RF, Parrish JT, Parrish JM, Good SC. 1991. The Pangaean megamonsoon: evidence from the Upper Triassic Chinle Formation, Colorado Plateau. *Palaios* **6**:347–370.

Dutuit JM. 1967. Gisements de vertébrés triasiques de l'Atlas marocain. *CNRS, Problémes Actuels de Paléontologie (Évolution des Vertébrés)* **163**:427–428.

Dutuit JM. 1976. Introduction à l'etude paleontologique du Trias continental marocain, Description des premiers Stegocephales recueillis dans le couloir d'Argana (Atlas occidental). *Memoires du Museum National d'Histoire Naturelle Paris Serie C* **36**:1–253.

Dutuit JM. 1978. Description de quelques fragments osseux provenant de la région de Folakara (Trias supérieur malgache). *Bulletin de Museum Nationale d'Histoire naturelle, Paris. Series III* **516**:79–89.

Erickson GM, Tumanova TA. 2000. Growth curve of *Psittacosaurus mongoliensis* Osborn (Ceratopsia: Psittacosauridae) inferred from long bone histology. *Zoological Journal of the Linnean Society* **130(4)**:551–566 DOI 10.1111/j.1096-3642.2000.tb02201.x.

Erlebacher A, Filvaroff EH, Gitelman SE, Derynck R. 1995. Toward a molecular understanding of skeletal development. *Cell* **80(3)**:371–378 DOI 10.1016/0092-8674(95)90487-5.

Fortuny J, Arbez T, Mujal E, Steyer JS. 2019. Reappraisal of 'Metoposaurus hoffmani' Dutuit 1978, and description of new temnospondyl specimens from the Middle–Late Triassic of Madagascar (Morondava Basin). *Journal of Vertebrate Paleontology* **39(1)**:e1576701 DOI 10.1080/02724634.2019.1576701.

Fortuny J, Gastou S, Escuillié F, Ranivoharimanana L, Steyer J–S. 2018. A new extreme longirostrine temnospondyl from the Triassic of Madagascar: phylogenetic and palaeobiogeographical implications for trematosaurids. *Journal of Systematic Paleontology* **16**:675–688 DOI 10.1080/14772019.2017.1335805.

Francillon-Vieillot H, de Buffrénil V, Castanet J, Géraudie J, Meunier FJ, Sire JY, Zylberberg L, de Ricqlès A. 1990. Microstructure and mineralization of vertebrate skeletal tissues. In: Carter JG, ed. *Skeletal biomineralization: patterns, processes and evolutionary trends*. Vol. I. New York: Van Nostrand Reinhold, 471–530.

Gądek K. 2012. Palaeohistology of ribs and clavicle of Metoposaurus diagnosticus from Krasiejów (Upper Silesia, Poland). *Opole Scientific Society Natural Journal* **45**:39–42.

Gee BM, Haridy Y, Reisz RR. 2020. Histological skeletochronology indicates developmental plasticity in the early Permian stem lissamphibian Doleserpeton annectens. *Ecology and Evolution* **10(4)**:2153–2169 DOI 10.1002/ece3.6054.

Gee BM, Parker WG. 2018. A large-bodied metoposaurid from the Revueltian (late Norian) of Petrified Forest National Park (Arizona, USA). *Neues Jahrbuch für Geologie und Paläontologie-Abhandlungen* **287(1)**:61–73 DOI 10.1127/njgpa/2018/0706.

Gee BM, Parker WG, Marsh AD. 2017. Microanatomy and paleohistology of the intercentra of North American metoposaurids from the Upper Triassic of Petrified Forest National Park (Arizona, USA) with implications for the taxonomy and ontogeny of the group. *PeerJ* **5**:e3183 DOI 10.7717/peerj.3183.

Griebeler EM, Klein N, Sander PM. 2013. Aging, maturation and growth of sauropodomorph dinosaurs as deduced from growth curves using long bone histological data: an assessment of methodological constraints and solutions. *PLOS ONE* **8(6)**:e67012 DOI 10.1371/journal.pone.0067012.

Gruntmejer K, Konietzko-Meier D, Bodzioch A. 2016. Cranial bone histology of *Metoposaurus krasiejowensis* (Amphibia, Temnospondyli) from the Late Triassic of Poland. *PeerJ* **4**:e2685 DOI 10.7717/peerj.2685.

Gruntmejer K, Konietzko-Meier D, Bodzioch A, Fortuny J. 2019a. Morphology and preliminary biomechanical interpretation of mandibular sutures in Metoposaurus krasiejowensis (Temnospondyli, Stereospondyli) from the Upper Triassic of Poland. *Journal of Iberian Geology* **45(2)**:301–316 DOI 10.1007/s41513-018-0072-4.

Gruntmejer K, KonietzkoMeier D, Marcé-Nogué J, Bodzioch A, Fortuny J. 2019b. Cranial suture biomechanics in Metoposaurus krasiejowensis (Temnospondyli, Stereospondyli) from the upper Triassic of Poland. *Journal of Morphology* **280(12)**:1850–1864 DOI 10.1002/jmor.21070.

Holmes R, Carroll R. 1977. A temnospondyl amphibian from the Mississippian of Scotland. *Bulletin of the Museum of Comparative Zoology* **147**:489–511.

Horner JR, de Ricqlès A, Padian K. 1999. Variation in dinosaur skeletochronology indicators: implications for age assessment and physiology. *Paleobiology* **25(3)**:295–304 DOI 10.1017/S0094837300021308.

Horner JR, de Ricqlès A, Padian K. 2000. Long bone histology of the hadrosaurid dinosaur *Maiasaura peeblesorum*: growth dynamics and physiology based on an ontogenetic series of skeletal elements. *Journal of Vertebrate Paleontology* **20(1)**:115–129 DOI 10.1671/0272-4634(2000)020[0115:LBHOTH]2.0.CO;2.

Houssaye A, Mazurier A, Herrel A, Volpato V, Tafforeau P, Boistel R, De Buffrénil V. 2010. Vertebral microanatomy in squamates: structure, growth and ecological correlates. *Journal of Anatomy* **217(6)**:715–727 DOI 10.1111/j.1469-7580.2010.01307.x.

Hunt AP. 1993. Revision of the Metoposauridae (Amphibia: Temnospondyli) and description of a new genus from western North America. In: Morales, M. (Ed.), Aspects of Mesozoic Geology and Paleontology of the Colorado Plateau. *Museum of Northern Arizona Bulletin* **59**:67–97.

Hunziker EB. 1994. Mechanism of longitudinal bone growth and its regulation by growth plate chondrocytes. *Microscopy Research and Technique* **28(6)**:505–519 DOI 10.1002/jemt.1070280606.

Klein N, Canoville A, Houssaye A. 2019. Microstructure of vertebrae, ribs, and gastralia of triassic sauropterygians—new insights into the microanatomical processes involved in aquatic adaptations of marine reptiles. *The Anatomical Record* **302(10)**:1770–1791 DOI 10.1002/ar.24140.

Klein N, Griebeler EM. 2016. Bone histology, microanatomy, and growth of the nothosauroid Simosaurus gaillardoti (Sauropterygia) from the Upper Muschelkalk of southern Germany/Baden-Württemberg. *Comptes Rendus Palevol* **15(1–2)**:142–162 DOI 10.1016/j.crpv.2015.02.009.

Klein N, Sander PM. 2007. Bone histology and growth of the prosauropod dinosaur Plateosaurus engelhardti von Meyer, 1837 from the Norian bonebeds of Trossingen (Germany) and Frick (Switzerland). *Special Papers in Palaeontology* **77**:169–206.

Klein N, Sander PM. 2008. Ontogenetic stages in the long bone histology of sauropod dinosaurs. *Paleobiology* **34(2)**:247–263 DOI 10.1666/0094-8373(2008)034[0247:OSITLB]2.0.CO;2.

Kolenda K, Najbar A, Rozenblut-Kościsty B, Serwa E, Skawiński T. 2018. Common occurrence of Sharpey's fibres in amphibian phalanges. *Zoomorphology* **137(2)**:329–336 DOI 10.1007/s00435-018-0400-4.

Konietzko-Meier D, Bodzioch A, Sander PM. 2012. Histological characteristics of the vertebral intercentra of *Metoposaurus diagnosticus* (Temnospondyli) from the Upper Triassic of Krasiejów (Upper Silesia, Poland). *Earth and Environmental Science Transactions of the Royal Society of Edinburgh* **103(3–4)**:237–250 DOI 10.1017/S1755691013000273.

Konietzko-Meier D, Gruntmejer K, Marcé-Nogué J, Bodzioch A, Fortuny J. 2018. Merging cranial histology and 3D-computational biomechanics: a review of the feeding ecology of a Late Triassic temnospondyl amphibian. *PeerJ* **6**:e4426 DOI 10.7717/peerj.4426.

Konietzko-Meier D, Klein N. 2013. Unique growth pattern of *Metoposaurus diagnosticus krasiejowensis* (Amphibia, Temnospondyli) from the Upper Triassic of Krasiejów, Poland. *Palaeogeography, Palaeoclimatology, Palaeoecology* **370**:145–157 DOI 10.1016/j.palaeo.2012.12.003.

Konietzko-Meier D, Sander PM. 2013. Long bone histology of *Metoposaurus diagnosticus krasiejowensis* (Temnospondyli) from the Late Triassic of Krasiejów (Opole, Silesia Region). *Journal of Vertebrate Paleontology* **33(5)**:1003–1018 DOI 10.1080/02724634.2013.765886.

Konietzko-Meier D, Schmitt A. 2013. A histological study of a femur of *Plagiosuchus*, a Middle Triassic temnospondyl amphibian from southern Germany, using thin sections and micro-CT scanning. *Netherlands Journal of Geosciences* **92(2–3)**:97–108 DOI 10.1017/S0016774600000020.

Konietzko-Meier D, Shelton CD, Sander PM. 2016. The discrepancy between morphological and microanatomical patterns of anamniotic stegocephalian postcrania from the Early Permian Briar Creek Bonebed (Texas). *Comptes Rendus Palevol* **15(1-2)**:103–114 DOI 10.1016/j.crpv.2015.06.005.

Konietzko-Meier D, Danto M, Gądek K. 2014. The microstructural variability of the intercentra among temnospondyl amphibians. *Biological Journal of the Linnean Society* **112(4)**:747–764 DOI 10.1111/bij.12301.

Kutty TS. 1971. Two faunal associations from the Maleri Formation of the Pranhita-Godavari valley. *Journal of Geological Society of India* **12(1)**:63–67.

Kutty TS, Chatterjee S, Galton PM, Upchurch P. 2007. Basal sauropodomorphs (Dinosauria: Saurischia) from the Lower Jurassic of India: their anatomy and relationships. *Journal of Paleontology* **81(6)**:1218–1240 DOI 10.1666/04-074.1.

Kutty TS, Sengupta DP. 1988. The Late Triassic Formations of the Pranhita-Godavari valley and their vertebrate faunal succession. *Indian Journal of Earth Sciences* **16(3–4)**:189–206.

Lamm E-T. 2013. Preparation and sectioning of specimens. In: Padian K, Lamm E-T, eds. *Bone histology of fossil tetrapods: advancing methods, analysis, and interpretation*. Los Angeles: University of California Press, 55–160.

Leclair Jr R, Castanet J. 1987. A skeletochronological assessment of age and growth in the frog *Rana pipiens* Schreber (Amphibia, Anura) from southwestern Quebec. *Copeia* **1987(2)**:361–369.

Lindeman FJ. 1991. Temnospondyls and the Lower Triassic Paleogeography of Spitzbergen. In: Kielan-Jaworowska Z, Heintz N, Nakrem HA, eds. *Fifth symposium on mesozoic terrestrial ecosystems and biota.* Oslo: Palaeontological Museum, University of Oslo, 39–40.

Margerie de ED, Robin JP, Verrier D, Cubo J, Groscolas R, Castanet J. 2004. Assessing a relationship between bone microstructure and growth rate: a fluorescent labelling study in the king penguin chick (Aptenodytes patagonicus). *Journal of Experimental Biology* **207(5)**:869–879 DOI 10.1242/jeb.00841.

McHugh JB. 2014. Paleohistology and histovariability of the Permian stereospondyl *Rhinesuchus. Journal of Vertebrate Paleontology* **34(1)**:59–68 DOI 10.1080/02724634.2013.787429.

McHugh JB. 2015. Paleohistology of *Micropholis stowi* (Dissorophoidea) and *Lydekkerina huxleyi* (Lydekkerinidae) humeri from the Karoo Basin of South Africa, and implications for bone microstructure evolution in temnospondyl amphibians. *Journal of Vertebrate Paleontology* **35(1)**:e902845 DOI 10.1080/02724634.2014.902845.

Miaud C, Andreone F, Ribéron A, De Michelis S, Clima V, Castanet J, Francillon-Vieillot H, Guyétant R. 2001. Variations in age, size at maturity and gestation duration among two neighbouring populations of the alpine salamander (*Salamandra lanzai*). *Journal of Zoology* **254**:251–260 DOI 10.1017/S0952836901000760.

Milner AR. 1990. The radiations of temnospondyl amphibians. In: Taylor PD, Larwood GP, eds. *Major evolutionary radiations. –Systematics Association Special Volume*. 42. Oxford: Clarendon Press, 321–349.

Mueller S, Krystyn L, Kürschner WM. 2016. Climate variability during the Carnian Pluvial Phase –a quantitative palynological study of the Carnian sedimentary succession at Lunz am See, Northern Calcareous Alps, Austria. *Palaeogeography, Palaeoclimatology, Palaeoecology* **441**:198–211 DOI 10.1016/j.palaeo.2015.06.008.

Mukherjee D, Ray S. 2014. A new *Hyperodapedon* (Archosauromorpha, Rhynchosauria) from the Upper Triassic of India: implications for rhynchosaur phylogeny. *Palaeontology* **57(6)**:1241–1276 DOI 10.1111/pala.12113.

Mukherjee D, Ray S, Sengupta DP. 2010. Preliminary observations on the bone microstructure, growth patterns, and life habits of some Triassic temnospondyls from India. *Journal of Vertebrate Paleontology* **30(1)**:78–93 DOI 10.1080/02724630903409121.

Mukherjee D, Sengupta DP, Rakshit N. 2020. New biological insights into the Middle Triassic capitosaurs from India as deduced from limb bone anatomy and histology. *Papers in Palaeontology* **6(1)**:93–142.

Nath TT, Yadagiri P. 2007. A new mammal-like reptile (Cynodontia) from Upper Triassic maleri formation of Pranhita-Godavari Valley, Andhra Pradesh. *Journal of the Geological Society of India* **69(1)**:57–60.

Novas FE, Ezcurra MD, Chatterjee S, Kutty TS. 2010. New dinosaur species from the Upper Triassic Upper Maleri and Lower Dharmaram formations of central India. *Earth and Environmental Science Transactions of the Royal Society of Edinburgh* **101(3–4)**:333–349 DOI 10.1017/S1755691011020093.

Padian K, Lamm ET. 2013. *Bone histology of fossil tetrapods: advancing methods, analysis, and interpretation*. University of California Press, Los Angeles, 1–285.

Padian K, de Ricqlès Ade, Horner JR. 2001. Dinosaurian growth rates and bird origins. *Nature* **4126845**:405–408.

Parrish JT. 1993. Climate of the supercontinent Pangea. *The Journal of Geology* **101**(**2**):215–233 DOI 10.1086/648217.

Patranabish-Deb S, Fukuoka M. 1998. Fe-illites in a Proterozoic deep marine slope deposit in the Penganga Group of the Pranhita Godavari Valley: their origin and environmental significance. *The Journal of Geology* **106**(**6**):741–750 DOI 10.1086/516057.

Pawley K, Warren A. 2004. Immaturity vs. paedomorphism: a rhinesuchid stereospondyl postcranium from the Upper Permian of South Africa. *Palaeontologia Africana* **40**:1–10.

Ray S, Mukherjee D, Bandyopadhyay S. 2009. Growth patterns of fossil vertebrates as deduced from bone microstructure: case studies from India. *Journal of Biosciences* **34**(**5**):661–672 DOI 10.1007/s12038-009-0055-x.

Robinson PL. 1970. The Indian Gondwana formations-a review. In: *1st international symosium on gondwana stratgraphy*, 201–268.

Roychowdhury T. 1965. A new metoposaurid amphibian from the Upper Triassic Maleri Formation of Central India. *Philosophical Transactions of the Royal Society B: Biological Sciences* **250**(**761**):1–52.

Sanchez S, Ricqlès Ade, Schoch RR, Steyer J-S. 2010a. Developmental plasticity of limb bone microstructural organization in *Apateon*: histological evidence of paedomorphic conditions in branchiosaurs. *Evolution and Development* **12**(**3**):315–328 DOI 10.1111/j.1525-142X.2010.00417.x.

Sanchez S, de Ricqlès A, Schoch RR, Steyer J-S. 2010b. Palaeoecological and palaeoenvironmental influences revealed by long-bone palaeohistology: the example of the Permian branchiosaurid *Apateon*. In: Vecoli M, Clement G, Meyer Berthaud B, eds. *The terrestrialization process: modelling complex interactions at the biosphere–geosphere interface*. London: The Geological Society, 139–149.

Sanchez S, Schoch RR. 2013. Bone histology reveals a high environmental and metabolic plasticity as a successful evolutionary strategy in a long-lived homeostatic Triassic temnospondyl. *Evolutionary Biology* **40**(**4**):627–647 DOI 10.1007/s11692-013-9238-3.

Sander PM. 2000. Longbone histology of the Tendaguru sauropods: implications for growth and biology. *Paleobiology* **26**(**3**):466–488 DOI 10.1666/0094-8373(2000)026<0466:LHOTTS>2.0.CO;2.

Sarkar S. 1988. Petrology of caliche-derived peloidal calcirudite/calcarenite in the Late Triassic Maleri Formation of the Pranhita-Godavari valley, South India. *Sedimentary Geology* **55**(**3–4**):263–282 DOI 10.1016/0037-0738(88)90134-0.

Schoch RR. 2003. Early larval ontogeny of the Permo-Carboniferous temnospondyl *Sclerocephalus*. *Palaeontology* **46**(**5**):1055–1072 DOI 10.1111/1475-4983.00333.

Schoch RR. 2013. The evolution of major temnospondyl clades: an inclusive phylogenetic analysis. *Journal of Systematic Palaeontology* **11**(**6**):673–705 DOI 10.1080/14772019.2012.699006.

Schoch RR. 2014. Frühe Tetrapoda. In: Westheide W, Rieger R, eds. *Spezielle Zoologie, 2. Wirbel- oder Schädeltiere, 3rd Edition*. München: München, Spektrum Akademischer Verlag, 305–308.

Sengupta DP. 1992. *Metoposaurus maleriensis* Roychowdhury from the Tiki Formation of Son-Mahanadi Valley of Central India. In: *Indian Journal of Geology*. 64. 300–305.

Sengupta DP. 1995. Chigutisaurid temnospondyls from the Late Triassic of India and review of the family chigutisauridae. *Palaeontology* **38**:313–339.

Sengupta DP. 2002. Indian metoposaurid amphibians revised. *Paleontological Research* **6**(**1**):41–65.

Sengupta DP. 2003. Triassic temnospondyls of the Pranhita–Godavari basin, India. *Journal of Asian Earth Sciences* **21**(**6**):655–662 DOI 10.1016/S1367-9120(02)00114-1.

Smoot JP, Olsen PE. 1988. Massive mudstones in basin analysis and paleoclimatic interpretation of the Newark Supergroup. In: *Developments in geotectonics*. 22. Elsevier, 249–274.

Stein K, Sander PM. 2009. Histological core drilling: a less destructive method for studying bone histology. In: *Methods in fossil preparation: proceedings of the first annual Fossil Preparation and Collections Symposium*. Petrified Forest National Park, 69–80.

Steyer JS, Laurin M, Castanet J, De Ricqles A. 2001. Histological evidence of rapid growth in the metoposaurian Dutuitosaurus ouazzoui from the Triassic of Morocco. *Journal of Vertebrate Paleontology* **21**(**3**):104A–105A.

Steyer JS, Laurin M, Castanet J, de Ricqlès A. 2004. First histological and skeletochronological data on temnospondyl growth: palaeoecological and palaeoclimatological implications. *Palaeogeography, Palaeoclimatology, Palaeoecology* **206**(**3**):193–201 DOI 10.1016/j.palaeo.2004.01.003.

Sulej T. 2002. Species discrimination in the Late Triassic labyrinthodont *Metoposaurus*. *Acta Palaeontologica Polonica* **47**(**3**):535–546.

Sulej T. 2007. Osteology, variability, and evolution of *Metoposaurus*, a temnospondyl from the Late Triassic of Poland. *Palaeontologia Polonica* **64**:29–139.

Teschner EM, Sander PM, Konietzko-Meier D. 2018. Variability of growth pattern observed in Metoposaurus krasiejowensis humeri and its biological meaning. *Journal of Iberian Geology* **44**(**1**):99–111 DOI 10.1007/s41513-017-0038-y.

Vijaya , Prasad GVR, Singh K. 2009. Late Triassic palynoflora from the Pranhita–Godavari Valley, India: evidence from vertebrate coprolites. *Alcheringa* **33**(**2**):91–111 DOI 10.1080/03115510902841315.

Von Meyer E. 1842. Labyrinthodonten—Genera. *Neues Jahrbuch für Mineralogie, Geographie, Geologie, Palaeontologie* **1842**:301–304.

Warren A, Rich TH, Vickers-Rich P. 1997. The last labyrinthodonts. *Palaeontographica Abteilung A-Stuttgart* **247**:1–24.

Waskow K, Mateus O. 2017. Dorsal rib histology of dinosaurs and a crocodylomorph from western Portugal: skeletochronological implications on age determination and life history traits. *Comptes Rendus Palevol* **16**(**4**):425–439.

Waskow K, Sander PM. 2014. Growth record and histological variation in the dorsal ribs of *Camarasaurus sp*, (Sauropoda). *Journal of Vertebrate Paleontology* **34(4)**:852–869 DOI 10.1080/02724634.2014.840645.

Wiffen J, de Buffrenil V, de Ricqlès A, Mazin J-M. 1995. Ontogenetic evolution of bone structure in Late Cretaceous Plesiosauria from New Zealand. *Geobios* **28**:625–640 DOI 10.1016/S0016-6995(95)80216-9.

Witzmann F. 2009. Comparative histology of sculptured dermal bones in basal tetrapods, and the implications for the soft tissue dermis. *Palaeodiversity* **2**:233–270.

Witzmann F, Soler-Gijon R. 2010. The bone histology of osteoderms in temnospondyl amphibians and in the chroniosuchian *Bystrowiella*. *Acta Zooolgica* **91**:96–114 DOI 10.1111/j.1463-6395.2008.00385.x.

Zittel KA. 1888. Vertebrata (Pisces, Amphibia, Reptilia, Aves). In: *Handbuch der Palaeontologie, Abteilung: Palaeozoologie*. vol. 13. Munich: Oldenbourg, 131–598.

CONTRIBUTIONS TO ZOOLOGY 91 (2022) 199–232
BRILL
CTOZ
brill.com/ctoz

Growth and limb bone histology of aetosaurs and phytosaurs from the Late Triassic Krasiejów locality (SW Poland) reveals strong environmental influence on growth pattern

Elżbieta M. Teschner | ORCID: 0000-0001-5961-489X
Institute of Biology, Opole University, Oleska 22, 45-052 Opole, Poland
Department of Paleontology, Institute of Geosciences, Rheinische
Friedrichs-Wilhelm-Universitat Bonn, Nussallee 8, 53115 Bonn, Germany
eteschner@uni.opole.pl

Dorota Konietzko-Meier
Department of Paleontology, Institute of Geosciences, Rheinische Friedrichs-Wilhelm-Universität Bonn, Nussallee 8, 53115 Bonn, Germany

Nicole Klein
Department of Paleontology, Institute of Geosciences, Rheinische Friedrichs-Wilhelm-Universität Bonn, Nussallee 8, 53115 Bonn, Germany
Paleontological Institute and Museum, University of Zurich, Karl-Schmid-Strasse 4,
8006 Zurich, Switzerland

RECEIVED: 8 DECEMBER 2021 | REVISED AND ACCEPTED: 3 APRIL 2022 | PUBLISHED ONLINE: 9 MAY 2022 | PUBLISHED IN ISSUE: 8 JULY 2022
EDITOR: A.A.E. VAN DER GEER

Abstract

The growth pattern of the Polish phytosaur *Parasuchus* cf. *arenaceus* and the aetosaur *Stagonolepis olenkae* (both Krasiejów; Norian) was studied. Results were compared to published data of other members of these two groups and to a new sample of the German (Heslach; Norian) phytosaur *Nicrosaurus* sp. All three herein studied taxa display lamellar-zonal bone consisting predominately of parallel-fibred tissue and on average a low to moderate vascular density. Towards the outer cortex the thickness of annuli increases in most samples and becomes distinctly wider than the zones. Therefore, most of the appositional growth in adults was achieved during phases of prolonged slow growth. All bones show a diffuse growth pattern, without well demarcated zones and annuli. Distinct lines of arrested growth (LAG) are not identified in the Krasiejów sample, only the *Nicrosaurus* femur shows one distinct LAG as do other taxa outside Krasiejów. Instead, the Krasiejów taxa display multiple rest lines and sub-cycles.

DOI:10.1163/18759866-BJA10031

Thus, identification and count of annual growth cycles remains difficult, the finally counted annual growth cycles range (two to six) is quite large despite the low size range of the samples. A correlation between age and bone length is not identified, indicating developmental plasticity. Although both are archosaurs, *Stagonolepis* and *Parasuchus* are phylogenetically not closely related, however, they show a very similar growth pattern, despite different life styles (terrestrial vs. semi-aquatic). Based on the new data, and previously histological studies from Krasiejów, the local environmental conditions were special and had a strong influence on the growth pattern.

Keywords

absence of lines of arrested growth (LAGs) – environmental influence – growth marks – growth record – microanatomy – rest lines

Introduction

Palaeohistological analyses performed on bones are a valuable source of biological information e.g., growth rate and age of extinct animals, as well as indirectly local environmental conditions (de Buffrénil et al., 2021). As an answer to adaptation in various local life conditions, vertebrates lay down cyclical (in most cases annual) growth marks (Francillon-Vieillot et al., 1990). They appear to reflect a seasonal change of the conditions, deposited as layers of fast-growing tissue (zones), created most probably during a favourable season, and slow-growing or even temporary cessed growth (annuli and/or line of arrested growth [LAG]), connected with an unfavourable phase during life (Francillon-Vieillot et al., 1990). For endothermic vertebrates the cyclicity seems to be determined genetically as showed by e.g., Köhler et al. (2012) who studied the growth pattern of wild ruminants living across different climatic zones, from polar to tropical environments, but depositing the same tissue and growth marks. This demonstrates that the annual formation of LAGs for homeothermic endotherm animals, is controlled genetically (hormonally) rather than resulting from environmental stresses (Köhler et al., 2012). In poikilotherm animals the influence of external conditions in the growth record is due to physiological constrains better visible as in homeothermic animals (see de Buffrénil et al., 2021). However, how the growth pattern of the poikilothermic animals is influenced by the environment, is understudied. Analyses of different taxa originating from the same locality and time, might shed new light on this question.

The perspective of multi-taxic histological studies

The rarity of multi-taxic osteohistological studies in palaeontology is related to the lack of enough adequate material and/or the destructive nature of histological analyses. The Krasiejów locality (southwestern Poland) provides a unique window into the Late Triassic ecosystem (Dzik & Sulej, 2007) due to a remarkable quality and the quantity of the excavated bones. Jewuła et al. (2019) studied the genesis of various Late Triassic deposits in the Upper Silesia region and proposed a gilgai (i.e., ephemeral stream system) environment for the Krasiejów deposits attributed to sedimentological evidence for semi-dry, seasonal climatic variation. The high number of skeletal elements preserved in Krasiejów presents a good opportunity to study the histology of taxa coexisting in one locality in the same horizon. The preserved tetrapod taxa include the remains of temnospondyl amphibians: *Metoposaurus krasiejowensis* (Sulej, 2007) and *Cyclotosaurus intermedius* Sulej & Majer, 2005, but also archosaurs: the aetosaur *Stagonolepis olenkae* Sulej, 2010, the phytosaur *Parasuchus* cf. *arenaceus* (Dzik, 2001; Dzik & Sulej, 2007), the 'rauisuchid' *Polonosuchus silesiacus* (Sulej, 2005), the dinosauriform *Silesaurus opolensis* Dzik, 2003, and the protorosaur *Ozimek volans* Dzik & Sulej, 2016. So far, the histology of the aquatic temnospondyl *M. krasiejowensis* from Krasiejów was studied in detail, based on almost all skeletal elements (Gądek, 2012; Gruntmejer et al., 2016, 2019, 2021; Konietzko-Meier et al., 2012, 2014, 2018; Konietzko-Meier & Klein, 2013; Konietzko-Meier & Sander, 2013; Teschner et al., 2018, 2020). The long bones of *M. krasiejowensis* show an alternating pattern of zones and annuli without LAGs, including prolonged phases of slow growth, multiple sub-cycles and rest lines. The documented growth record of *Metoposaurus* indicates a moderate, less seasonal climate at Krasiejów, after the comparison with the growth record to similarly aged (Norian) and phylogenetically related taxa from India and Morocco (Konietzko-Meier & Klein, 2013; Teschner et al., 2018). Femora, tibiae, a metatarsal, and ribs of the terrestrial dinosauriform *Silesaurus opolensis* were studied histologically (Fostowicz-Frelik & Sulej, 2010). They display a nearly uninterrupted fibro-lamellar bone (FLB) with only the outermost cortex becoming higher organized and less dense vascular, absence of LAGs, except for one tibia possessing one LAG. Fostowicz-Frelik & Sulej (2010) suggested that the lack of clear growth marks could be related with the hypothetical endothermy of that taxon, however, the sectioned material was insufficient to prove this due to a limited material sectioned.

The analysis of the two most common archosaurs in Krasiejów, an aetosaur and a phytosaur, originating from the same horizon, might contribute to answer the question, how distantly related, poikilotherm amniotes reacted to the same environmental conditions.

Taxonomy and depositional environment

Two major archosaur groups, Aetosauria (Marsh, 1884) and Phytosauria (Jäger, 1828), are a constant component of Late Triassic (Carnian to Rhaetian) faunal assemblage found on almost all continents (Buffetaut, 1993; Lucas, 1998; Desojo et al., 2013; Stocker & Butler, 2013; Barrett et al., 2020). The only exception is *Diandogosuchus* from the Middle Triassic of China (Li et al., 2012; Stocker et al., 2017), representing so far, the oldest and phylogenetically most basal phytosaur (Butler et al., 2019). Aetosauria are interpreted as being herbivorous to omnivorous in diet and occupying terrestrial habitats (Carroll, 1988; Small, 2002; Desojo & Vizcaino, 2009; Desojo et al., 2013). Phytosaurs are mostly found in lacustrine and fluviatile environments worldwide (Hungerbühler, 2000; Stocker & Butler, 2013) and their mode of life was reconstructed as semi-aquatic to aquatic (Hunt, 1989). There are also marine phytosaur representatives from Europe e.g., Austria and Italy (Buffetaut, 1993; Renesto & Paganoni, 1998; Gozzi & Renesto, 2003; Renesto, 2008; Butler et al., 2019) and China (Li et al., 2012).

The aetosaur material from Krasiejów is represented by multiple disarticulated skeletal elements for which a new species was erected within the genus *Stagonolepis*: *S. olenkae* Sulej, 2010. The validity of the discrimination of *S. olenkae* from the Scottish *S. robertsoni* was questioned by Antczak (2016), who suggested, based on the examination of new material that both belong to the same species and differences are related to individual variation and possible sexual dimorphism. Recently, an aetosaurian pes from Krasiejów was described morphologically, without a definitive assignment to *S. olenkae*, moreover, the authors could not exclude a possible co-occurrence of two aetosaur species in Krasiejów (Górnicki et al., 2021). However, the exact taxonomical assignment of our sample is not within the scope of this study and likely irrelevant as both species seem to have similar niches.

The morphology and phylogenetic relationship of the phytosaurs from Krasiejów is understudied (Butler et al., 2014) when compared to other phytosaur specimens from Europe (Hungerbühler, 2000, 2002; Brusatte et al., 2013; Mateus et al., 2014, Butler et al., 2019). Dzik (2001) first proposed affinity of the Polish material to *'Paleorhinus'* sp. and later Dzik & Sulej (2007) proposed the affinity of the material to *'Paleorhinus'* cf. *arenaceus*. However, the taxon from Krasiejów was so far not included in any phylogenetic analysis. The species from Krasiejów is considered as a basal representative within Phytosauria due to the anterior position of the nares (Dzik, 2001; Dzik & Sulej, 2007). Other *'Paleorhinus'* specimens have been reported from Germany and USA (Lees, 1907; Hunt & Lucas, 1991; Butler et al., 2014) whereas *Parasuchus* was described from India (Chatterjee, 1978). However, according to Case 3165 of the International Code of Zoological Nomenclature, the genus *Parasuchus* took priority over *'Paleorhinus'* (Chatterjee, 2001; Kammerer et al., 2016; Jones & Butler, 2018) and both taxa now represent a single taxon. Again, the exact taxonomic affiliation of the phytosaur from Krasiejów is not relevant and beyond the scope of the current study.

The age of the Krasiejów deposits is still debated due to the lack of index fossils or palynological data (Szulc, 2005). Dzik et al. (2000) favours a Carnian age based on biostratigraphy and the correlation with dated beds known from southern Germany (Lehrberg Beds; Dzik et al., 2000) and a lacustrine origin of the deposits (Dzik et al., 2000; Dzik & Sulej, 2007, 2016). However, subsequent extensive sedimentological, lithostratigraphic and taphonomic studies supported a Norian age for the deposits (Szulc, 2005; Bodzioch & Kowal-Linka, 2012; Szulc & Racki, 2015; Szulc et al., 2015, 2017) and a fluviatile origin caused by an ephemeral stream system under semi-dry climatic conditions (Szulc, 2005). Bodzioch & Kowal-Linka (2012) reconstructed a more catastrophic origin of the bone bed caused by a short-lived but high-energy flood event resulting in hydraulically segregated bone breccia, accumulating the disarticulated skeletons in the vicinity of what is today the clay pit.

Heslach, is a Late Triassic (Norian) locality in southern Germany near Stuttgart. The phytosaur *Nicrosaurus kapffi* (von Meyer, 1861), was found in fluviatile deposits of the Stubensandstein Formation (Nitsch, 2006), and is phylogenetically considered to represent a more derived specimen when compared to the Polish taxon (Hungerbühler, 2002; Kimmig, 2013). Based on the femoral morphology of *Nicrosaurus*, a semi-aquatic or even a secondarily terrestrial mode of life has been proposed (Kimmig, 2013). No sedimentological studies are known for this locality, thus no inference about the climatic conditions during the Norian in Heslach can be made.

Histology research on aetosaurs and phytosaurs to date

Histologically, the best studied elements of aetosaurs and phytosaurs are their osteoderms (Parker et al., 2008; Cerda & Desojo, 2011; Scheyer et al., 2014; Cerda et al., 2018). Both, aetosaurs and phytosaurs, preserve a diploe structure in their osteoderms (Scheyer et al., 2014). The main difference between the two clades is visible in the construction of the cortices: in phytosaurs (except for Phytosauria indet. from Germany and the *Pseudopalatus* sp. from the USA; Scheyer et al., 2014) the internal and external cortex is built from parallel-fibred bone and is highly vascularized with clearly visible and countable growth marks (LAGs, zones and annuli); whereas in aetosaurs the internal (basal) cortex consists also of parallel-fibred bone, but the external cortex is made of lamellar bone. Depending on the aetosaurian taxon sampled, the osteoderms contain also woven-fibred bone (Cerda & Desojo, 2011; Cerda et al., 2018). Moreover, vascular density is considerably lower in aetosaur osteoderms when compared to phytosaur osteoderms (Cerda & Desojo, 2011; Scheyer et al., 2014).

Seitz (1907) was the first who studied and figured femoral histology of the phytosaur *Belodon* (= *Nicrosaurus*) *kapffi* from the Stubensandstein Formation from Stuttgart. De Ricqlès et al. (2003) examined a total of seven long bones (femora, humeri and radii) of five taxa: two phytosaurs Phytosauria indet. and *Rutiodon* sp., and three aetosaurs *Stagonolepis* (= *Calyptosuchus*) sp., *Desmatosuchus* sp., and *Typothorax* sp., all originating most probably from the Placerias Quarry in Arizona, USA. Hoffman et al. (2019) sampled a partial radius and a fragmentary fibula of the aetosaur *Coahomasuchus chathamensis* originating from a locality in North Carolina, USA. Butler et al. (2019) studied a single femur of the phytosaur *Mystriosuchus steinbergeri* from the marine deposits from Austria. Recently, Heckert et al. (2021) studied a pathological femur of *Smilosuchus gregorii* from the USA, Arizona. Most recently, Ponce et al. (2022) studied a total of five long bones (femora, humeri, tibia) belonging to two individuals of *Aetosauroides scagliai* from Argentina. The main results of the available histological studies performed on aetosaurs and phytosaurs long bones are listed in table 1. In summary, all these samples show the deposition of fibro-lamellar bone (FLB) in the inner cortex with a switch to lamellar-zonal bone (LZB) in the outer cortex, the presence of an external fundamental system (EFS), and alternating distinct growth marks in form of zones, annuli and lines of arrested growth (LAGs; table 1) of both phytosaurs and aetosaurs. Due to a different origin of limb bones and osteoderms (periosteal bones vs. dermal bones), a direct comparison of the growth record of those elements is not advisable (Klein et al., 2009; Hayashi et al., 2012).

Aim of study

Microanatomy, long bone histology and growth pattern of the semi-aquatic phytosaur *Parasuchus* cf. *arenaceus* and the terrestrial aetosaur *Stagonolepis olenkae* from the Krasiejów locality are studied for the first time. Further on, femoral histology of the similarly aged (Norian) but geographically distinct phytosaur *Nicrosaurus* sp. from the German Heslach locality is studied as well. Results (i.e., growth pattern) are compared to published growth record data of aetosaurs and phytosaurs from various global localities. Moreover, the growth pattern of a temnospondyl amphibian and a dinosauromorph from Krasiejów are also compared, to test if the environmental factors had an influence on the growth pattern of those vertebrates.

Material and methods

Material

One humerus and three femora of *Parasuchus* cf. *arenaceus* from the Late Triassic (Norian) of Krasiejów are studied (table 2, figs 1–2). Humerus UOPB 00145 measures 19.4 cm (fig. 2A–D), which is 89% of the largest known

TABLE 1 Main results of the available histological studies performed on aetosaurs and phytosaurs long bones

Taxon	Provenance	Element	Bone histology	Growth rate and growth cycle count	Reference
Aetosauria					
Desmatosuchus sp.	USA, Arizona	proximal humerus	The inner cortex consists well-vascularized FLB consisting of both, woven and lamellar components; external cortex is built of more LZB and the alternating vascular zones are separated by distinctive avascular annuli associated with a LAG that can be accompanied by multiple rest lines; the external most cortex becomes lamellar and avascular; remodelling by secondary osteons	High initial growth rate for the inner cortex and a moderate growth rate for the outer cortex, 15–16 growth	de Ricqlès, Padian & Horner (2003)
Desmatosuchus sp.	USA, Arizona	distal radius	Not sampled at the midshaft plane; inner cortex consists of a homogenous bone matrix with vascularized zones separated by (almost) avascular, thin annuli with associated LAGs; towards the external cortex the zones become thinner and in the external most cortex they are almost avascular; at least 10 cycles are visible in the cortex exclusive of the very numerous LAGs in the most external cortex; remodelling by secondary osteons	Low growth rate, with a possible higher growth rate earlier in the ontogeny; >10 LAGs	de Ricqlès, Padian & Horner (2003)
Calyptosuchus (‘*Stagonolepis*’) sp.	USA, Arizona	femur	Inner cortex consists of highly vascular FLB with woven bone component and continues with an alternation with avascular, more lamellar tissue associated with at least one LAG; towards the outer cortex the tissue becomes more LZB with sequence of alternating thin and less vascularized zones and annuli; the external most cortex is lamellar and poorly vascularized, cortex stratified by multiple LAGs with no indication for an EFS;	High growth rate at the beginning and continues with low to very low growth rate; at least 10 LAGs	de Ricqlès, Padian & Horner (2003)

Typothorax sp.	USA, Arizona	proximal humerus	Longitudinal section and no information about the growth pattern visible	No estimation of the growth rate or growth cycle count are possible	de Ricqlès, Padian & Horner (2003)
Typothorax sp.	USA, Arizona	distal radius	The cortex is moderately vascularized and stratified by 10–12 LAGs resembling a LZB type; the outermost cortex is lamellar and poorly vascularized, with numerous LAGs preserved, however sheets of FLB with primary osteons oriented longitudinally and radially is also preserved; moderate remodelling by mostly circular erosion rooms and scattered secondary osteons sometimes reaching into the deep cortex	Low growth rate, 10–12 LAGs	de Ricqlès, Padian & Horner (2003)
Coahomasuchus chathamensis	USA, North Carolina	fragmentary radius	Inner cortex consists of woven-fibered bone (until the 1st LAG) and continues with progressively thinner layers of PFB; vascularity decreases towards the cortex surface; few scattered secondary osteons in the inner cortex	Fast growth rate, 7 LAGs, EFS	Hoffman, Heckert & Zanno (2019)
Coahomasuchus chathamensis	USA, North Carolina	fragmentary fibula	Innermost cortex consists of highly vascularized woven-fibered bone; the outer cortex consists of less vascularized PFB; dense remodelling by secondary osteons in the inner cortex	Fast growth rate, 7 LAGs, EFS	Hoffman, Heckert & Zanno (2019)
Aetosauroides scagliai	Argentina	humerus, femur; PVL 2073	Both elements consist of highly vascularized FLB in the inner and middle region preserving more wove bone and towards the outer cortex PFB; entire cortex stratified by LAGs with various spacing	Fast growth rate for the inner cortex and slower growth rate for the outer cortex, 10 LAGs, no EFS	Ponce, Desojo & Cerda (2022)

Taxon	Provenance	Element	Bone histology	Growth rate and growth cycle count	Reference
Aetosauroides scagliai	Argentina	humerus, femur, tibia; PVL 2052	Cortices of the femur and tibia highly vascularized, the humerus is low vascularized; all elements grow with FLB and towards the outer cortex the deposition of PFB is more pronounced; entire cortex stratified with LAGs with various spacing	Fast growth rate for the inner cortex and slower growth rate for the outer cortex, 4–5 LAGS (femur and tibia) and 8 LAGs (humerus), EFS only in femur and tibia	Ponce, Desojo & Cerda (2022)
Phytosauria					
Belodon (= *Nicrosaurus*) *kapffi*	Germany	femur	Prominent concentric growth rings reaching far into the deeper cortex with characteristic Harversian canals embedded with no order, the vascularization is present by primary vascular canals and less abundant radial canals building anastomoses; towards the inner cortex the concentric lines are becoming unorganized and larger erosion cavities are occurring in the innermost section portion; no further description of the tissue, no description of the vascular density, no description of the remodelling	No estimation of the growth rate and growth mark count was proposed and the figures are not sufficient to make an estimation approach	Seitz (1907)
Rutiodon sp.	USA, Arizona	proximal femur	Internal cortex consists of highly vascularized FLB but with a poorly developed woven component; the external cortex consists of PFB with cyclical deposition of growth marks (zones, annuli and LAGs); the annuli associated with LAGs are intercalated with thinner and less vascularized zones built of PFB; two outermost zones contain again woven component; flattened erosion cavities preserved in the inner cortex; locally scattered secondary osteons occur	Fast-growing internal cortex and a slowed-down growth rate for the outer cortex; 13–16 LAGs; no EFS	de Ricqlès, Padian & Horner (2003)

Phytosauria indet.	USA, Arizona	proximal femur	The internal cortex remodelled and the external cortex consists of LZB with a PFB component; a sequence of nearly avascular annuli built of lamellar tissue is associated with one to several LAGs, separated by vascularized, thicker zones build of lamellar periosteal tissue and some with woven bone; remodelled internal cortex with scattered, large secondary osteons	External cortex deposited at a moderate to low growth rate; At least 10 LAGs; no EFS	de Ricqlès, Padian & Horner (2003)
Mystriosuchus steinbergeri	Austria	femur	Cortex consists of LZB tissue with low vascularized zones built of PFB separated by LAGs; larger erosion cavities and secondary osteons, locally more extensively remodelled	Low bone deposition speed, 8 LAGs, no EFS	Butler et al. (2019)
Smilodon gregorii	USA, Arizona	humerus	Presence of woven bone and lamellar bone stratified with numerous LAGs; no further description of the tissue, no description of the vascular density, no description of remodelling	Low growth rate	Heckert, Viner & Carrano (2021)

Abbreviations: EFS = external fundamental system; FLB = fibro-lamellar bone; LAG = line of arrested growth; LZB = lamellar-zonal bone; PFB = parallel-fibered bone.

TABLE 2 Measurements of the sectioned long bones. Please note that, based on a complete specimen of *Parasuchus hislopi* from India, the humerus femur ratio reveals that humerus UOPB 00145 and femur UOPB 00143 correspond to the same size class when considering total body length of the individual. The humerus vs. femur range from *Stagonolepis robertsoni* reveals that the size range of the sampled humeri fits to the calculated body size revealed for the femora of the *S. olenkae*. Based on calculated maximal size and tissue all here studied individuals are regarded as adults

Specimen number	Element	Taxon	Total length (cm)	Proximal width (cm)	Distal width (cm)	Midshaft width (cm)	Total (%)	Visible growth cycles	Compactness with medullary cavity (bone %)	Compactness without medullary cavity (bone %)
UOBS 03370	femur	*Parasuchus* cf. *arenaceus*	39	8.4	–	4	100	6	90	99
UOPB 01026	femur	*Parasuchus* cf. *arenaceus*	37	8	8.2	3.5	95	6	80	96
UOPB 00143	femur	*Parasuchus* cf. *arenaceus*	25	6.1	4.7	3.3	64	5	66	97
SMNS 4381/2	femur	*Nicrosaurus* sp.	29.5	8.3	–	4.2	89	4	74	84
UOPB 00145	humerus	*Parasuchus* cf. *arenaceus*	19.4	6.9	5.3	2.1	86		79	98
UOPB 00123	femur	*Stagonolepis olenkae*	37	11.2	7.7	6.6	100	–	93	95
UOPB 00122	femur	*Stagonolepis olenkae*	33	9.6	9.6	6.5	89	–	97	97
UOPB 00137	humerus	*Stagonolepis olenkae*	24	12.4	–	3.6	100	2	93	–

UOBS 02828	humerus	*Stagonolepis olenkae*	23.8	12.2	–	3.4	99	3	95	–
UOPB 00121	humerus	*Stagonolepis olenkae*	22.8	11.3	7.1	2.8	95	4	88	98
UOPB 00142	humerus	*Stagonolepis olenkae*	22.6	10.9	7.6	3.1	94	5	87	–
UOPB 00136	humerus	*Stagonolepis olenkae*	–	–	6.7	2.5	?92	6	80	97
UOBS 01906	humerus	*Stagonolepis olenkae*	22.1	11.2	7	3.1	92	3	76	95
UOBS 02363	humerus	*Stagonolepis olenkae*	21.9	11.8	7	3	91	2	79	92
UOBS 02496	humerus	*Stagonolepis olenkae*	21.7	11.1	6.5	3	90	3	78	95
UOPB 00120	humerus	*Stagonolepis olenkae*	21.7	10.4	7.3	2.8	90	4	85	94
UOPB 00135	humerus	*Stagonolepis olenkae*	21.6	10.7	5.7	2.8	90	4	88	94

humerus from Krasiejów (ZPAL III 1516, 20.7 cm; Kimmig, 2013). As the material from Krasiejów is disarticulated and no proxy for the humerus to femur ratio is known, we used the known ratio of a closely related species and articulated specimen, *Parasuchus hislopi* from India (ISI R 42; femur length = 24 cm; humerus length = 18.2 cm; Chatterjee, 1978). This ratio reveals that humerus UOPB 00145 (19.4 cm) would correspond to a femur with a length of around 25.6 cm. Following that assumption, the sampled humerus UOPB 00145 and the femur UOPB 00143 would correspond to a similar size class (table 2). The sampled femora of *P.* cf. *arenaceus* represent a growth series ranging from 25 cm to 39 cm. This translates to 64% to 100% when considering the length of the largest known femur from Krasiejów (UOBS 03370, 39 cm; EMT, 2021, pers. obs.). The here studied femoral section of the phytosaur *Nicrosaurus* sp. originating from the German Late Triassic (Norian) locality (SMNS 4381/2; approx. length 29.5 cm; fig. 1E-G) is 89% size of the largest known femur of this taxon (SMNS 4381/1, 33 cm; EMT, 2021, pers. obs.; table 2).

From the aetosaur *Stagonolepis olenkae* from the Late Triassic (Norian) of Krasiejów, ten humeri (21.6 cm to 24 cm) and two femora (33 cm and 37 cm) were sampled (fig. 1H–K). The size of the humeri corresponds to 90% to 100% of the largest known humerus length from Krasiejów (UOPB 00137, 24 cm; EMT, 2021, pers. obs.; table 2), while the femur length corresponds to 89% to 100% of the largest known femur from Krasiejów (UOPB 00123, 37 cm; EMT, 2021, pers. obs.; table 2). Thus, all sampled bones of aetosaurs represent the upper size range. Since the aetosaur material from Krasiejów preserves only disarticulated specimens, no ratios for e.g., humerus vs. femur can be given, too. Based on the closely related *S. robertsoni* from Scotland, the humerus vs. femur ratio is 0.63 (Walker, 1961). Using this ratio, the largest preserved

FIGURE 1 Morphology of the studied femora of the phytosaurs *Parasuchus* cf. *arenaceus* UOPB 00143 (A-D), and *Nicrosaurus* sp. SMNS 4381/2 (E-G), and the aetosaur *Stagonolepis olenkae* UOPB 00122 (H-K). A, E and H in lateral view; B, F and I in medial view; C, G and J in proximal view; D and K in distal view. The arrows point to the histological plane of sectioning. Scale bars represent 5 cm for each specimen.

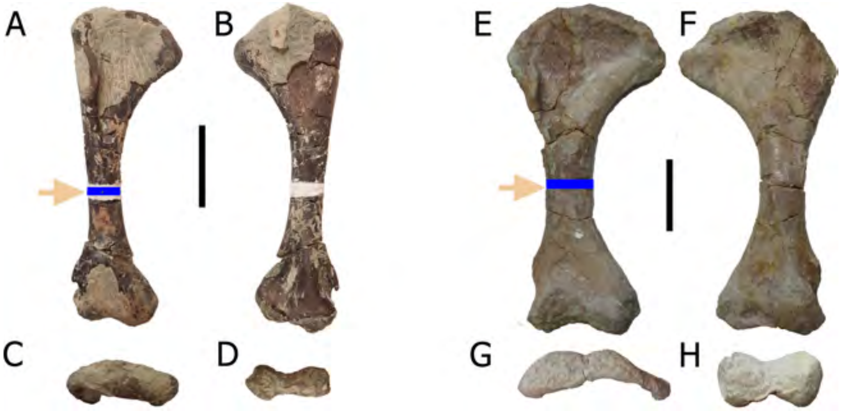

FIGURE 2 Morphology of the studied humeri of the phytosaurs *Parasuchus* cf. *arenaceus* UOPB 00145 (A-D), and the aetosaur *Stagonolepis olenkae* UOBS 01906 (E-H). A and E in ventral view; B and F in dorsal view; C and G in proximal view; D and H in distal view. The arrows point to the histological plane of sectioning. Scale bars represent 5 cm for each specimen.

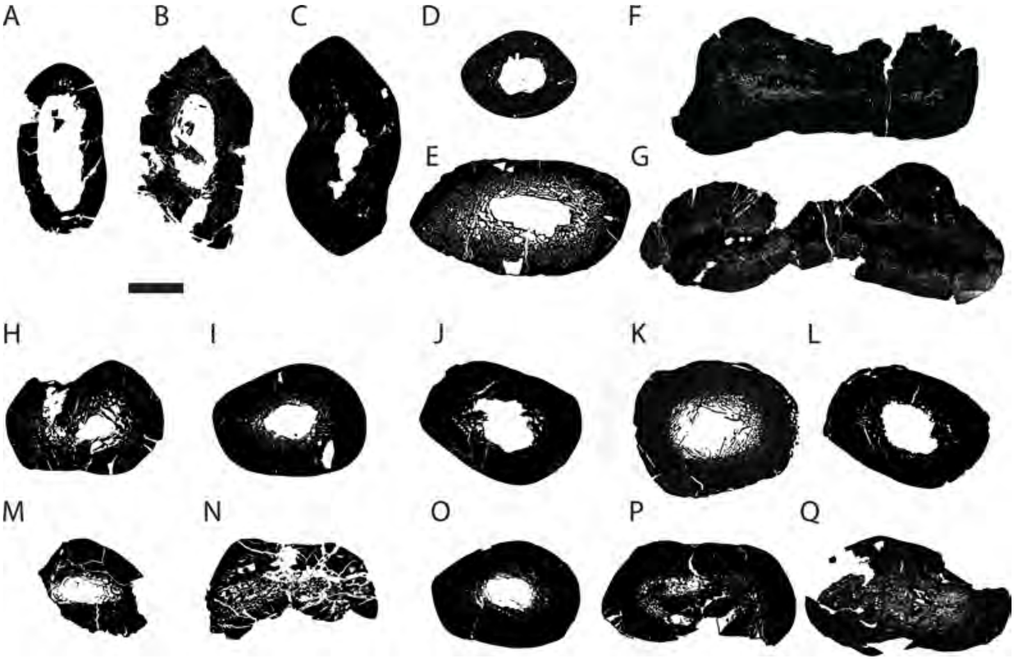

FIGURE 3 Mid-diaphyseal cross-sections of all sectioned specimens showing the bone microanatomy of the phytosaurs *Parasuchus* cf. *arenaceus* femora (A: UOPB 00143, B: UOPB 01026, C: UOBS 03370 and humerus (D: UOPB 00145), and *Nicrosaurus* sp. femur (E: SMNS 4381/2), the aetosaur *Stagonolepis olenkae* femora (F: UOPB 00122, G: UOPB 00123) and humeri (H: UOPB 00135, I: UOPB 00120, J: UOBS 02496, K: UOBS 02363, L: UOBS 01906, M: UOPB 00136, N: UOPB 00142, O: UOPB 00121, P: UOBS 02828, and Q: UOPB 00137). Taxa are arranged accordingly to their bone length. Scale bar represents 1 cm for each specimen.

femur (UOPB 00123, 37 cm) of *S. olenkae* sectioned here would correspond to a humerus of approx. 23 cm and the second femur sampled (UOPB 00122, 33 cm) would correspond with a humerus of approx. 21 cm. Thus, both femora fit to the size class of the sampled humeri.

All histological samples were taken from diagnostic humeri and femora (table 2, figs 1A–K, 2A–H). Before sampling, the taxonomical affiliation of the sampled bone either to aetosaur or to phytosaur, respectively was assured. The humeri of aetosaurs and phytosaurs can be easily distinguished: a phytosaurian humerus has a very straight medial edge of the shaft which forms almost a straight line with the proximal and distal head (fig. 2A–B, E–F; Kimmig, 2013). On the contrary, aetosaurian humeri possess a transversely wider expanded proximal head and show a more pronounced deltopectoral crest that expands laterally (Walker, 1961; Nesbitt, 2011; Roberto-Da-Silva et al., 2014; Dróżdż, 2018; fig. 2E–F). The femora of aetosaurs can be well differentiated from phytosaurs because they

TABLE 3 Thickness of zones and annuli in the phytosaurs *Parasuchus* cf. *arenaceus* and *Nicrosaurus* sp. (cycle number vs. cycle thickness)

Total length (cm)		25	37	39	29.5	19.4
Element		**femur UOPB 00143**	**femur UOPB 01026**	**femur UOBS 03370**	**femur SMNS 4831/2**	**humerus UOPB 00145**
1st	zo	–	🟨 23	–	🟩 35	🟩 22
	an	12	🟨 19	39	🟩 12	🟩 3
2nd	zo	🟥 9	🟩 10	🟩 20	🟩 23	🟩 21
	an	🟥 12	🟩 4	🟩 6	🟩 5	🟩 5
3rd	zo	🟨 7	🟥 5	🟨 3	🟥 5	🟨 8
	an	🟨 9	🟥 9	🟨 2	🟥 12	🟨 6
4th	zo	🟩 9	🟨 3	🟥 2	🟨 2	🟨 4
	an	🟩 5	🟨 5	🟥 16	🟨 6	🟨 4
5th	zo	🟥 9	🟩 11	🟥 2	–	🟩 12
	an	🟥 28	🟩 4	🟥 8	–	🟩 6
6th	zo	–	🟥 2	2	–	🟨 6
	an	–	🟥 5	–	–	🟨 3

Colours: green = zone thicker than the annulus, yellow = almost no variation in the thickness of the zones or annuli; red = annulus thicker than the zone. Abbreviations: zo = zone, an = annulus. The cycle count starts with the 1st cycle being in the innermost cortex (towards the medullary cavity) with the subsequently numbered cycles continuing towards the outer cortex (towards the bone surface)

TABLE 4 Thickness of zones and annuli in the aetosaur *Stagonolepis olenkae* (cycle number vs. cycle thickness)

Total length (cm)		21.6	21.7	21.7	21.9	22	22.1*	22.6	22.8	23.8*	24*
Element		UOPB 00135 humerus	UOPB 00120 humerus	UOBS 02496 humerus	UOBS 02363 humerus	UOBS 01906 humerus	UOPB 00136 humerus	UOPB 00142 humerus	UOPB 00121 humerus	UOBS 02828 humerus	UOPB 00137 humerus
1st	zo	🟩 40	🟨 7	🟩 32	–	🟨 19	🟩 40	🟩 37	–	🟩 19	🟩 17
	an	🟩 6	🟨 4	🟩 10	57	🟨 21	🟩 8	🟩 4	6	🟩 8	🟩 10
2nd	zo	🟩 29	🟩 21	🟩 26	🟥 14	🟨 19	🟩 30	🟩 16	🟩 19	🟩 16	🟥 33
	an	🟩 6	🟩 14	🟩 13	🟥 29	🟨 16	🟩 3	🟩 4	🟩 8	🟩 8	🟥 40
3rd	zo	🟨 6	🟥 7	🟥 5	–	🟥 9	🟨 2	🟥 3	🟩 26	🟥 10	–
	an	🟨 8	🟥 16	🟥 14	–	🟥 16	🟨 1	🟥 10	🟩 6	🟥 39	–
4th	zo	🟨 2	🟥 7	–	–	–	🟩 4	🟨 6	🟨 19	–	–
	an	🟨 3	🟥 24	–	–	–	🟩 2	🟨 8	🟨 16	–	–
5th	zo	–	–	–	–	–	🟨 2	🟨 6	–	–	–
	an	–	–	–	–	-	🟨 2	🟨 6	–	–	–
6th	zo	–	–	–	–	–	🟥 2	–	–	–	–
	an	–	–	–	–	–	🟥 4	–	–	–	–
Estimated cycles**		4	4	5	6	6	6	5	4	5	5

*estimated total bone length, **the visible growth cycles plus the estimated resorbed cycles.

Colours: green = zone thicker than the annulus, yellow = almost no variation in the thickness of the zones or annuli, red = annulus thicker than the zone. Abbreviations: zo = zone, an = annulus. The cycle count starts with the 1st cycle being in the innermost cortex (towards the medullary cavity) with the subsequently numbered cycles continuing towards the outer cortex (towards the bone surface).

are robustly built, elongated and show almost no torsion between the proximal and the distal head (fig. 1H–K). In contrast, the femora of phytosaurs are more slender and show a prominent sigmoidal curvature between the proximal and distal heads (fig. 1A–B), which is often visible in aquatic animals (Kimmig, 2013; EMT, 2021, pers. obs.).

Methods

All bone samples were processed into standard petrographic thin-sections in the laboratory of the Institute of Geosciences (IGPB) at the University of Bonn, Germany. All limb bones were sectioned transversely at the midshaft plane according to the technique described in Klein & Sander (2007). For grinding and polishing of the thin-sections wet silicon carbide (SiC) grinding powders with grit sizes of 600 and 800 were used. The osteohistological analysis was performed with a Leica DM LP polarizing light microscope (with objectives of 1.25×, 4×, 10× and 20× magnification) and the photographs were taken with a Leica DFC 420 camera attached to the microscope. The overview pictures in polarized light were stitched with the *AutoStitch* software (http://www.autostitch.net). The cross-sections for microanatomical analyses were scanned with an Epson Perfection 750V PRO scanner.

Pictures of cross sections were transformed to black (compact bone) and white (cavities) pictures to measure bone compactness. The pixel counting software then was measuring white and black pixels (©Peter Göddertz, IGPB), resulting in a ratio of compact bone to cavities (table 2, fig. 3A–Q). The compactness was measured for the complete section, including the medullary cavity and/or region and also by excluding the latter and measuring only the cortex (table 2). The histological nomenclature follows Francillon-Vieillot et al. (1990).

Growth mark count was performed under polarized light in which the differences in tissues organization of the alternating growth marks, i.e., zones and annuli, were best visible. A growth mark was identified as belonging to an annual cycle when it was followed nearly continuous over the entire cross section. Contrary, sub-cycles are defined as thin layers of high organized tissue, resembling the characteristics of annuli, that are locally restricted. The relative thickness of the zones and annuli (tables 3–4) was measured, if possible due to preservation, at the same bone area: on the posteromedial side for the femora (table 3) and on the dorsal side in the humeri (table 4).

Results

Microanatomy and histology

Parasuchus cf. *arenaceus.* All studied cross sections of femora are elliptical (fig. 3A-B), except for the large femur (UOBS 03370; fig. 3C), which was dorsoventrally compacted. The humerus section is more rounded in cross section (fig. 3D). All sections share a central, free medullary cavity, which is largest in the smallest femur (UOPB 0143, 25 cm) and smallest in the largest femur (UOPB 03370, 39 cm) (fig. 3C). The values of the bone compactness measured for the entire cross section range from 66 to 90% for the femora and it is 79% for the humerus (table 2). Based on the microanatomical analysis performed, those specimens show a tendential bone mass increase with increasing size. The cortex compactness (excluding the medullary cavity) is very high in all four specimens ranging between 96% to 99% (table 2), indicating a low vascular density. The medullary cavity is lined by a thin layer of endosteal bone in all four samples (fig. 4A–C). The primary periosteal cortex is built by parallel-fibred bone with varying degrees of collagen fibres organization in all three femora and the humerus (fig. 4D). In the femora, the vascular density is low to moderate (table 2, see bone compactness) and only the humerus is somewhat higher vascularized. Femora and humerus, show small simple vascular canals and primary osteons, the latter are more numerous but small, too. They are mostly longitudinal to reticular in shape and sometimes arranged in a plexiform system. Simple vascular canals are most numerous in the outermost cortex, whereas primary osteons are preserved throughout the entire cortex. In the humerus, the simple vascular canals are smaller and more abundant than in the femora. In the outer cortex of every specimen, the simple vascular canals are arranged in rows. Radial primary osteons occur on the medial and lateral side in the femoral sections. Vascular canals are largely restricted to the zones whereas annuli are usually avascular. Osteocyte lacunae are equally numerous throughout the cortex of all sections. They are irregular in size and shape and lack canaliculi. Sharpey's fibres are visible only in the outermost cortex of femur UOPB 01026.

The degree of remodelling in form of erosion cavities in the inner cortex and secondary osteons scattered into the primary cortex varies in the samples with no order along size. All phytosaur femora samples display small, nearly closed secondary osteons which are restricted to the inner cortex (UOPB 00143 and UOBS 03370; fig. 3A, C), except for the middle-sized femur (UOPB 01026) where they are numerous and reach far into the outer cortex (fig. 3B). The humerus UOPB 00145 shows only few, small, scattered erosion cavities restricted to the innermost cortex and no secondary osteons are observed in this specimen (fig. 4A–C). This fits with the low degree of remodelling observed in the smallest sampled femur (UOPB 00143) where only the lateral bone side shows few, scattered, small erosion cavities. In femur UOPB 01026 numerous, large erosion cavities and secondary osteons occur in the innermost cortex close to the boundary with the medullary cavity. In the middle and outer cortex, only secondary osteons occur and they are smaller and scattered. This specimen contains a well demarked and distinct concentric layer of densely packed erosion cavities and endosteal bone, resembling the content of a medullary region. However, this layer is above the thin layer of endosteal bone lining the medullary cavity i.e., outside the endosteal domain. In the largest specimen (UOBS 03370), small erosion cavities are scattered throughout the inner cortex but are less abundant, when compared to UOPB 01026.

Nicrosaurus sp. The sampled femur of *Nicrosaurus* sp. (SMNS 4381/2; table 2, fig. 4E–H) has an elliptical cross section (figs 3E, 4E). The central medullary cavity is in comparison to that of the above-described specimens relatively small (table 2, fig. 4E). It is lined by a thin layer of endosteal bone (fig. 4F). Bone compactness for the entire femur cross section is 74% and the cortex compactness (excluding the medullary cavity) is 84 % (table 2). The primary cortex consists of parallel-fibred bone with varying degree of collagen fibres organization (fig. 4G). The vascular density is moderate and is represented by longitudinal to reticular simple vascular canals and primary osteons. In the outermost cortex, simple canals are arranged in rows (fig. 4G–H). On the medial and lateral side, the simple vascular canals become radial. Numerous primary osteons occur throughout the cortex and they are mostly longitudinally oriented. Osteocyte lacunae are very numerous and are represented equally throughout the cortex. They are irregular in size and shape and show well developed canaliculi. Sharpey's fibres are not visible in this section.

The central medullary cavity is surrounded by a broad medullary region, both making 66% of the entire section. Their boundary is clear at the dorsal side where a thin layer of endosteal bone separates them, but both merge into each other at the sides. Towards the primary cortex the medullary region is also not well delineated, forming around its outer periphery a perimedullary region where erosion cavities and endosteal bone

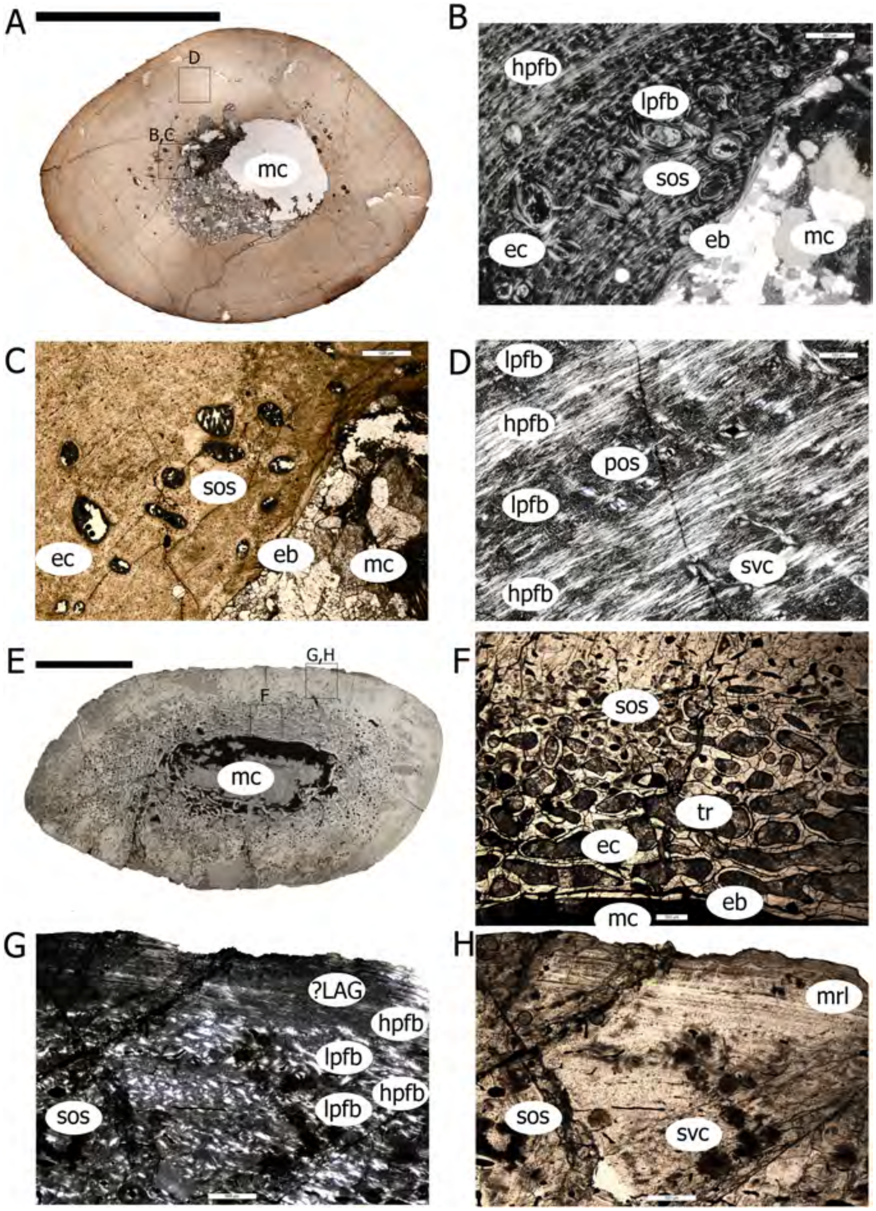

FIGURE 4 Histological growth of the phytosaurs *Parasuchus* cf. *arenaceus* on the example of the humerus UOPB 00145 (A-D) and the *Nicrosaurus* sp. femur SMNS 4381/2. Pictures A, C, E-F and H were taken under normal transmitted light and pictures B, D and G were taken under polarized light. Scale bars represent 1 cm for specimens A and E, 500 micrometres for specimens B-C, F-H and 100 micrometres for specimen D. Abbreviations: eb = endosteal bone, ec = erosion cavity, hpfb = higher organized parallel-fibered bone, LAG = Line of Arrested Growth, lpfb = lower organized parallel-fibered bone, mc = medullary cavity, mrl = multiple resting lines, pos = primary osteon, sos = secondary osteon, svc = simple vascular canal, tr = trabecular region.

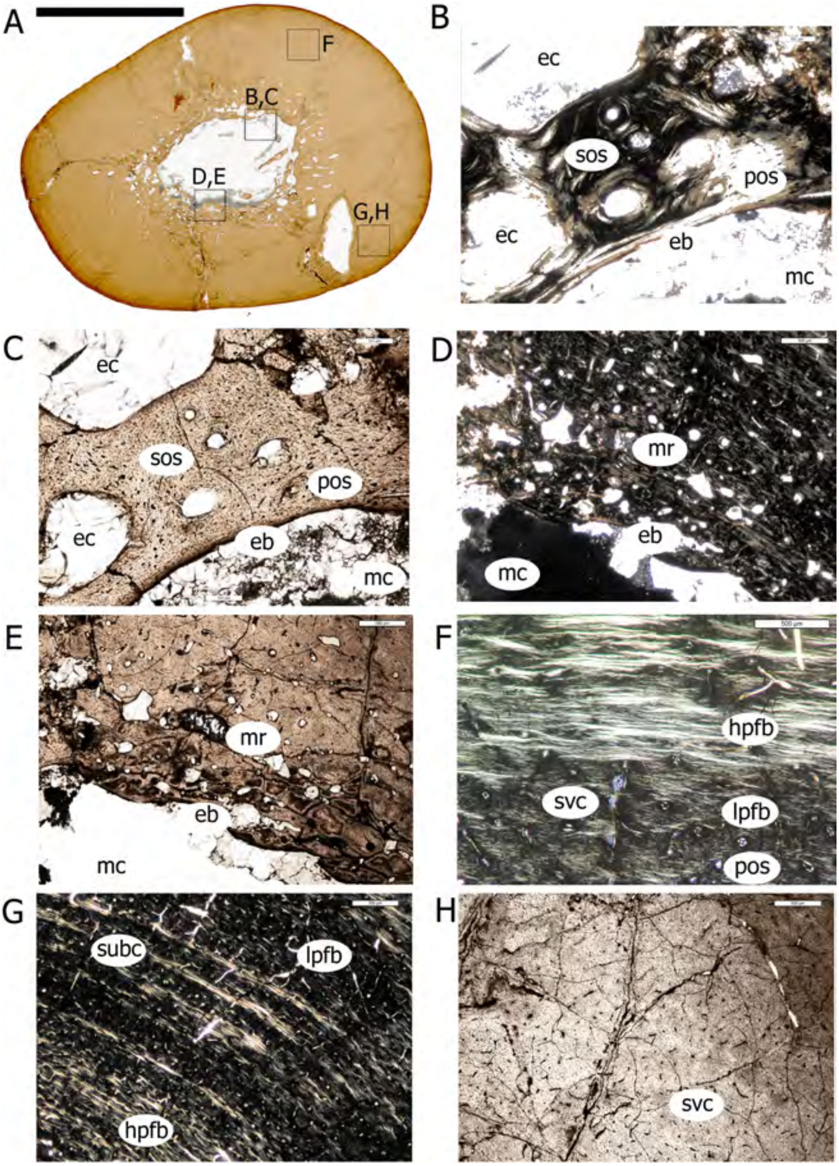

FIGURE 5 Histological growth of the aetosaur *Stagonolepis olenkae* on the example of the humerus UOPB 00120 (A-H). Pictures A, C, E and H were taken under normal transmitted light and pictures B, D, and F-G were taken under polarized light. Scale bars represent 1 cm for specimen A, 100 micrometres for specimens B-C, and 500 micrometres for specimens D-H. Abbreviations: eb = endosteal bone, ec = erosion cavity, hpfb = higher organized parallel-fibered bone, lpfb = lower organized parallel-fibered bone, mc = medullary cavity, mr = medullary region, pos = primary osteon, sos = secondary osteon, subc = sub cycles, svc = simple vascular canal.

are intermixed with scattered secondary osteons and primary cortex. Along the boundary to the medullary cavity, the medullary region consists of large rectangular shaped (dorsoventrally aligned) erosion cavities, forming a trabecular structure (fig. 4F). Towards

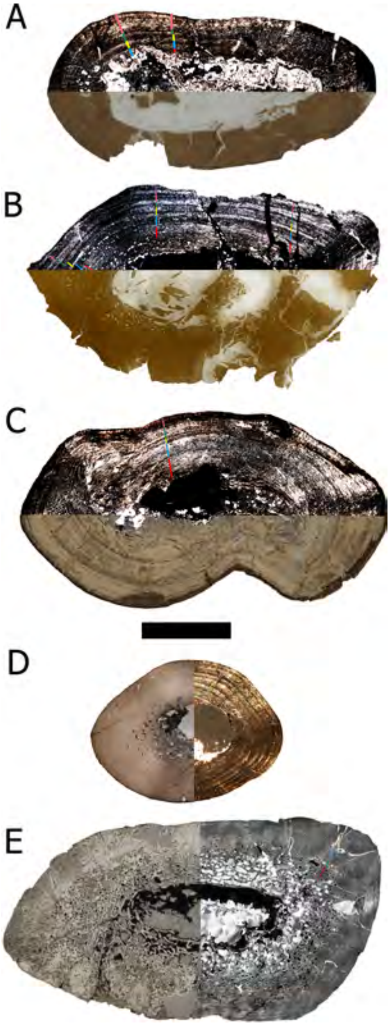

FIGURE 6 Growth pattern of the sectioned phytosaurs *Parasuchus* cf. *arenaceus* femora (A: UOPB 00143, B: UOPB 01026, C: UOBS 03370) and humerus (D: UOPB 00145) and *Nicrosaurus* sp. (E: SMNS 4381/2). Half of the picture is taken under normal transmitted light and the other picture half is taken under polarized light. Please note, that the normally transmitted picture does not show informative histological features. The coloured bars show preserved and counted cycles (zone and annulus). Specimen A preserves five growth cycles, specimen B, C and D preserve six growth cycles, and specimen E preserves four growth cycles. Taxa are arranged accordingly to their bone length. Scale bar represents 1 cm for each specimen.

the outer cortex the erosion cavities become round and are getting continuously smaller.

Stagonolepis olenkae. The aetosaur femora have an irregular but elongated cross-sectional shape (figs 3F–G, 5A). The humeri are roundish to oval (fig. 3H–K, N–Q), except for the dorsoventrally compacted specimens UOBS 02828 and UOPB 00142 (fig. 3L–M). When not compacted due to preservation, the centrally positioned medullary cavity is in all specimens surrounded by a thin layer of endosteal bone (fig. 5A–E). Bone compactness for the entire cross section ranges from 93% to 95% for the femora and between 76% to 95% for the humeri (table 2). The cortex compactness (excluding the medullary cavity) ranges between 95% to 97% for the femora, and it is between 92% to 98% for the humeri (table 2). The primary cortex is made of parallel-fibred bone tissue deposited in different degree of collagen fibres organization (fig. 5F–G). All sections show a moderate vascular density (table 2). The simple vascular canals and primary osteons are mostly longitudinal to reticular in shape. Primary osteons occur mostly in the outer cortex (fig. 5B–H). Although all humeri are of a similar size range (table 2), the number of vascular canals in the humeri is the lowest in the upper bone size range. Osteocyte lacunae are very prominent in all studied specimens. They are irregular in shape, small but numerous and are distributed throughout the entire cortex. Very short fibres are documented in the humeri UOBS 01906 and UOBS 02363, in which they are occurring sporadically in the outer cortical surface.

The broadness of the medullary region that surrounds the medullary cavity varies from narrow (e.g., UOPB 00120, UOPB 00121 and UOPB 00136) to very thick (e.g., UOBS 02363). A correlation between size of the medullary region and bone length is not identified. The erosion cavities are irregularly shaped in the

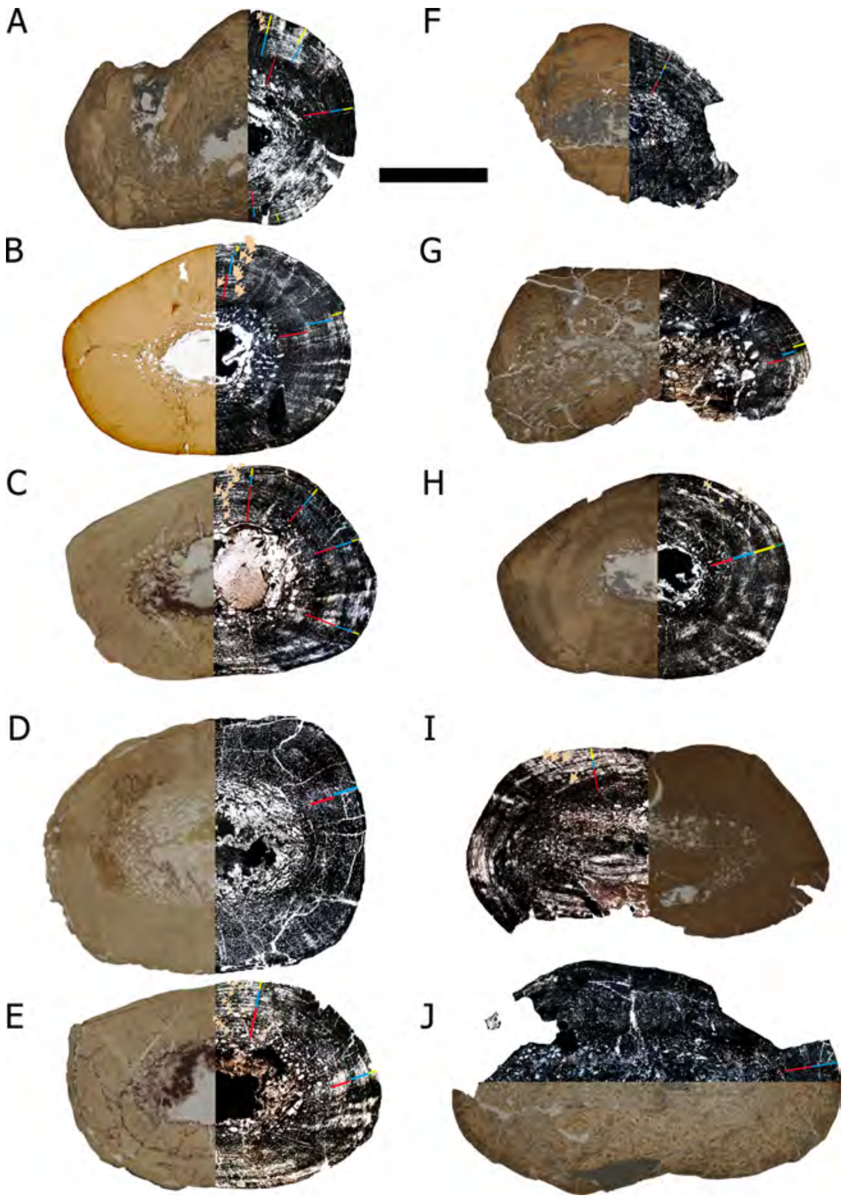

FIGURE 7 Growth pattern of the sectioned aetosaur *Stagonolepis olenkae* humeri (A: UOPB 00135, B: UOPB 00120, C: UOBS 02496, D: UOBS 02363, E: UOBS 01906, F: UOPB 00136, G: UOPB 00142, H: UOPB 00121, I: UOBS 02828, and J: UOPB 00137). Half of the picture is taken under normal transmitted light and the other picture half is taken under polarized light. Please note, that the normally transmitted picture does not show informative histological features. The coloured bars show preserved and counted cycles (zone and annulus). Specimen A-B and H preserve four growth cycles, specimen C, E, G, and I preserve three growth cycles, specimen D and J preserve two growth cycles and specimen F preserved six growth cycles. The arrows in specimens A-C, E, and H-J indicate sub-cycles. Humeri are arranged accordingly to their bone length. Scale bar represents 1 cm for each specimen.

inner medullary region and become smaller and round towards the outer cortex. The two femora (UOPB 00122 and 00123) are almost completely remodelled by secondary osteons, leaving only a small portion of primary bone visible i.e., parallel-fibred bone, in the outermost cortex.

Growth mark count and growth pattern. The entire primary cortex of *Parasuchus*, *Stagonolepis* and *Nicrosaurus* is stratified by alternating growth marks in form of zones, annuli and sometimes rest lines (tables 3–4). Zones and annuli are distinguished by a change in tissue and vascular density. Layers consisting of mostly avascular to low vascularized and high organized parallel-fibred bone partially grading into lamellar bone are interpreted as annuli. Low to moderate (in *Parasuchus*) and moderate to high (in *Nicrosaurus* and *Stagonolepis*) vascularized layers of less organized parallel-fibred bone are interpreted as zones. Under normal light growth marks are not identifiable (figs 4A, E, 5A, 6A–E, 7A–J). The distinction between zones and annuli is only possible under polarized light. Often the boundary between zones and annuli is not well delineated because they tend to merge into each other. In the aetosaurian humeri, sub-cycles are formed locally by thin layers of high organized avascular tissue (e.g., UOPB 00120, 00121, 00135, UOBS 02469, 01906; figs 5G, 6A–C, E, H–I). Multiple rest lines are documented within the annuli in all studied elements (fig. 4H). This all hampers the count of annual growth cycles. An unambiguous LAG was only identified in the outermost cortex of the *Nicrosaurus* femur (SMNS 4381/2) (fig. 4G).

In our interpretation for the current sample, an annual growth cycle consists of a zone and an annulus, which can both be followed almost all around the cross section. According to this definition, the smallest *Parasuchus* femur (UOPB 00143) shows five visible growth cycles, the middle-sized (UOPB 01026) and the largest (UOBS 03370) *Parasuchus* femur show six visible growth cycles (fig. 6A–C, table 3). The *Parasuchus* humerus shows six visible cycles (fig. 6D, table 3). Generally, the distinction of the growth cycles in the phytosaur humerus (UOPB 00145) was clearer than in the sectioned femora. The *Nicrosaurus* femur (SMNS 4381/2) shows four visible growth cycles (fig. 6E, table 3). The sampled aetosaur humeri show a slightly variable growth mark count between two and six annual growth cycles inside a small size range of 21.6 cm to 24 cm. However, bone length and number of counted cycles does not correlate (fig. 7A–J). Both aetosaur femora (UOPB 00122 and UOPB 00123) show a highly remodelled cortex making a count of annual growth cycles impossible. None of the samples document a distinct change in tissue type i.e., growth rate, for example representing the onset of sexual maturity or indicate that growth finally had ceased, as might be indicated by an EFS (Cormark, 1987).

The sequence of an annual growth cycle starts usually with a zone, except for the *Parasuchus* femora (UOPB 00143, UOBS 03370), and two *Stagonolepis* humeri (UOPB 00121, UOBS 02363). In the latter, the sequence starts with an annulus. This could either be a true signal or might be connected to the resorption of the inner growth marks. The relative thickness of an annual growth cycle is in general thicker in aetosaurs than in phytosaurs (tables 3–4). The overall thickness of growth cycles and the ratio of the thickness of zones and annuli changes from the inner to the outer cortex in both groups.

Usually, in the innermost cycles, the zone is thicker than its corresponding annulus (expect for *Stagonolepis* humerus UOBS 01906), whereas in the outermost cycles, the thickness of the annulus exceeds the thickness of the corresponding zone (tables 3–4, fig. 7E). The exception is *Stagonolepis* humerus UOPB 00136 where the annulus and the zone are of an equal thickness in the outer cortex and *Stagonolepis* humerus UOPB 00142 where the zone is still thicker than the annulus. Thus, *Stagonolepis* humeri and the *Nicrosaurus* femur show tendentially an increasing annuli thickness towards the outer cortex. The *Parasuchus* samples do not show a trend of in- or decreasing thickness of the annuli over the zones but a rather irregular change of growth mark thickness. However, around the 3rd visible cycle in the *Parasuchus* femora the zones and annuli reach a similar thickness (table 3) and, towards the outer cortex, the zones are becoming distinctly thinner. The only exception is specimen UOPB 01026 where the zones are still thicker up to the 5th cycle than the annuli. Only in the last, the 6th cycle the annulus is becoming thicker but not as significantly as in the sections UOPB 00143 and UOBS 03370 (table 3).

In spite of a low size range, the growth pattern in the humeri of *Stagonolepis* is more variable (table 4). Six out of ten specimens start the cycle sequence with a prominently thicker zone over the annulus (UOPB 00135, 00136, 00142, 00121, UOBS 02496 and 02828). The other samples (UOBP 00120, 00142, UOBS 02496 and 01906; table 4) start with a zone with an equal thickness as the annuli. As a general trend, the annuli become thicker and zones thinner towards the outermost cortex, starting from the 3rd cycle in specimens UOPB 00120, UOBS 02496, UOBS 01906, UOBS 02828, and in specimens UOBS 02363 and UOPB 00137 already from the 2nd visible cycle (table 4). Moreover, the annuli possess sub-cycles also beginning from the 3rd cycle (UOPB 00120). Specimens UOPB 00135, UOPB 00142 and UOPB 00121 died before showing a pronounced zone thinning and annuli thickening (table 4).

In addition to the growth mark count, five stages of remodelling of the periosteal cortex are identified in the aetosaur sample that might indicate aging. However, they do not correlate with bone size in the current sample. They are: 1) the lowermost remodelling degree (UOPB 00120, UOPB 00121 & UOPB 00136); 2) low remodelling degree (UOPB 00135); 3) moderate remodelling degree (UO142, UOPB 00137, UOBS 02828); 4) high remodelling degree (UOBS 01906 and UOBS 02496); and 5) the highest remodelling degree, i.e., nearly complete remodelling of the periosteal cortex (UOBS 02363) (fig. 7D).

Discussion

Microanatomy

Bone compactness can provide information about the mode of life of an animal (Germain & Laurin, 2005; Cubo et al., 2008; Kriloff et al., 2008; Canoville & Laurin, 2009, 2010; Hayashi et al., 2012). The two major microanatomical specializations are either, a bone mass increase, observed in poorly active swimmers living in shallow marine environments, or a decrease in bone mass characterized by a more spongious organization of the cortex, observed in active swimmers usually inhabiting pelagic environments (Houssaye, 2009; Houssaye et al., 2016).

The *Parasuchus* samples from Krasiejów indicate a slight bone mass increase with increasing bone size, by reducing the size of the medullary cavity (fig. 3A–C, table 2), when compared to the microanatomy of the aetosaur sample. *Nicrosaurus* also shows a bone mass increase but differs from *Parasuchus* on the basis of the presence of a broad spongious, nearly trabecular medullary region that surrounds the medullary cavity in the latter. The last character indicates a higher degree of adaptation to an aquatic lifestyle for *Nicrosaurus.* This is, however, in contradiction with the morphological reconstruction, where that taxon was proposed to be semi-aquatic or even secondarily terrestrial (Kimmig, 2013). The differences in femoral microanatomy between *Nicrosaurus* and *Parasuchus* can be related to phylogeny, intraspecific variability or might represent a true difference in lifestyle. However, due to a limited *Nicrosaurus* sample size, this remains highly speculative.

Stagonolepis humeri show some variation in overall bone compactness, which is mostly expressed by the varying size of their medullary cavities (fig. 3H–Q, table 2). Based on the humerus to femur proportions, known from *S. obertsoni* (Walker, 1961), the two large femora studied herein, are more compact, when compared to their corresponding humeri. The higher compactness of femora might be a result of different preservation or is related to biomechanical constraints (Kawano et al., 2016). The observed advanced remodelling in the femora, when compared to the humeri of aetosaurs, might also be related to biomechanics (Currey, 2002). Alternatively, a higher degree of remodelling can also be related to an older ontogenetic stage. The femora represent the maximal size for this group in this locality and thereby likely belonged to ontogenetically older individuals as the in size corresponding humeri. Interestingly, Ponce et al. (2022) studied two sets of corresponding femora and humeri belonging to a smaller *A. agliai* individual (humerus: 11 cm, femur 17.6 cm), and a larger *A. scagliai* individual (humerus: 18.9 cm, femur: 27.5 cm). Their histology displayed a still preserved primary bone, and a low degree of remodelling, which is not preserved anymore in the aetosaur sample studied herein (*S. olenkae* femur: 33 cm and 37 cm; table 2).

Aetosaurs are thought to represent terrestrial herbivores and phytosaurs are interpreted as semi-aquatic to aquatic carnivores. If both groups occupied different ecological niches, this is not reflected in the microanatomy of the Krasiejów taxa, as they cover a similar compactness spectrum. A contradiction between bone compactness values and lifestyle and/or environmental interpretations was already demonstrated for other taxa, the pseudosuchian *Batrachotomus kupferzellensis* (Klein et al., 2017), but also in chelonians (Laurin et al., 2011) and extant snakes (de Buffrénil & Rage, 1993; Houssaye et al., 2010, 2013, 2014; Canoville et al., 2016). Thus, bone compactness values alone are not always a reliable source to infer the lifestyle. A compactness study preformed on one femur of the Argentinian aetosaur *A. scagliai* (74.9 %) confirmed a terrestrial lifestyle (Ponce et al., 2022). The compactness values for the *Stagonolepis* femora (table 2) show an even higher compactness, thus, can also be reconstructed as terrestrial animals.

Growth pattern comparison between the Krasiejów taxa with taxa from other localities

All three sampled taxa, the phytosaur *Parasuchus*, the aetosaur *Stagonolepis* from Krasiejów, and the phytosaur *Nicrosaurus* from Heslach, share a similar bone tissue type throughout their entire cortex, that can be summarized as LZB. For most other so far studied aetosaurs and phytosaurs (table 1; except for *Mystriosuchus* sp.), a clear change in tissue type from FLB in the inner cortex to LZB in the outer cortex was described (table 1). This change in tissue type is usually interpreted as ontogenetic change from fast growth rates in early ontogenetic stages to slower growth rates in adults and/or sexually mature individuals (de Ricqlès et al., 2003; Hoffman et al., 2019; Heckert et al., 2021; Ponce et al., 2022; table 1). Contrary, neither the taxa from Krasiejów nor the phytosaur from Heslach show woven bone in their cortex and their vascular density is moderate to low. Thus, FLB is not documented in any of our samples. A decrease in growth rate (from moderate to low) is only observed by the increase in the thickness of annuli (tables 3–4), indicating prolonged phases of slow growth from the preserved middle cortex onwards.

The absence of fast growing, highly vascularized tissue can either be explained by the fact that the herein studied bones represent the upper size spectrum in both groups (table 2) and only late ontogenetic stages, i.e., adults had been sampled in which the change from FLB to LZB is not documented, and possibly was already resorbed by the expansion of the endosteal domain. It might also be the case, that the taxa from Krasiejów and Heslach grew in general at a lower rate, not depositing fast growing tissue even in earlier ontogenetic stages due to exogenous factors. It is possible, that due to the ontogenetically late stages the FLB was already resorbed. However, since in *Mystriosuchus* sp. from Austria, FLB was also not documented (Butler et al., 2019), it is possible, that FLB was not deposited in the studied samples, but rather became fully resorbed. In any case, the here studied individuals all represent late ontogenetic stages i.e., adult individuals, which is documented by their size range and the deposited tissue, including a certain degree of endosteal and periosteal remodelling (table 2).

The taxa from Krasiejów do not show any clear LAGs throughout their cortices nor an EFS in their outermost cortices; the phytosaur from Heslach has one LAG in its outer cortex deposited (fig. 4G). This is also contrary to the observations made in other phytosaur and aetosaur taxa where LAGs are common and an EFS is documented for several individuals (de Ricqlès et al., 2003; Hoffman et al., 2019; Butler et al., 2019; Heckert et al., 2021; Ponce et al., 2022; table 1). The two sampled *Stagonolepis* femora are nearly completely remodelled by secondary osteons, which together with their large size (table 2) indicate a late ontogenetic stage for both. However, what remains from the outermost primary cortex does not resemble an EFS. Also, the other, less remodelled samples lack an EFS or any other clear indication of a cessation in growth (i.e., avascular lamellar bone in the outer cortex). The conclusion that none of the here studied samples had stopped appositional growth and thus had not attained full size yet might be reliable. However, Late Triassic archosaurs and their kin show highly variable growth patterns and a variety of tissue types. In addition, they seem to have been highly flexible in their growth (i.e., developmental plasticity) as is also obvious from the results of the current study and seem often not to follow any clear pattern (e.g., de Ricqlès et al., 2003, 2008; Klein et al., 2017). Thus, maybe attainment of maximal body size was not always indicated by an EFS.

In former studies, growth rate was interpreted as being high in the inner cortex of most phytosaurs and aetosaurs (except for *Mystriosuchus* sp.: Butler et al., 2019), based on the deposition of FLB (i.e., highly vascularized, low organized tissue indicating fast deposition), and as low(er) in the outer cortex when tissue type had switched to LZB (de Ricqlès et al., 2003; Hoffman et al., 2019; Ponce et al., 2022; table 1). Considering the relatively high organized tissue and the low to moderate vascular density (longitudinal and reticular orientation of vascular canals), the growth rate was rather low, when compared to the growth rate in above mentioned taxa (table 1). The low growth rate applies to the samples from Krasiejów and Heslach. This is also evident from tables 3 and 4 which visualize that most of appositional growth happened during prolonged phases of slow growth. *Mystriosuchus* sp. shares with the taxa from Krasiejów and Heslach the lack of FLB and woven bone as well as the low growth rate but differs by the presence of distinct LAGs (Butler et al., 2019).

All archosaurs are likely capable of growing with woven bone/FLB (phylogenetic trajectory/precept; see Klein et al., 2017: Fig. 6) but this is not always effectuated. This is documented in modern crocodiles (e.g., Woodward et al., 2014) and possibly a similar phenomenon occurs also in the taxa from Krasiejów and Heslach as well as in *Mystriosuchus* sp. (Butler et al., 2019). Our samples confirm that the adaptational signal (i.e., exogenous factors) can be stronger than the phylogenetic signal (presence of FLB in early ontogenetic stages), as was discussed before by de Ricqlès et al. (2003, 2008). This again proofs a high developmental plasticity in early archosaurs/pseudosuchians, which might have been the key to their phylogenetic success.

Growth marks and environmental influence

The alternating growth marks in form of zones and annuli usually correspond with favourable (e.g., wet season) and unfavourable (e.g., semi-dry season) climatic conditions (Francillon-Vieillot et al., 1990). The growth record of *Stagonolepis* is more diffuse and preserves several, locally restricted sub-cycles in some humeri. The occurrence of multiple rest lines is also more common in the aetosaur than in the phytosaur samples. Fluctuating growth marks have been interpreted as evidence for unstable environmental parameters (Witzmann et al., 2012; Klein et al., 2015), which might apply to the environment in the Late Triassic of Krasiejów as well. As stated above all samples likely belong to late ontogenetic stages, i.e., adult individuals, but for none an achievement of maximal body size can be finalized. "Juvenile" tissue (i.e., highly vascularized low organized woven bone) is absent, but the onset of sexual maturity can also not be identified. Growth mark count (table 2) reveals no correlation between number of annual growth cycles and bone length (fig. 7A–J), indicating developmental plasticity. The latter is most evident by the humerus sample of *Stagonolepis*, which are all of a similar size but show a growth cycle count varying from two to six (table 4, fig. 7A–J).

The tendency of a decrease in cycle thickness from the inner to the outer cortex is however, more pronounced in *Stagonolepis* than in *Parasuchus* and *Nicrosaurus* (tables 3–4). The annuli in all three taxa increase tendentially in thickness towards the middle and outer cortex and become (partially) distinctly larger when compared to the zones (tables 3–4). Clear cessations of growth in form of LAGs are absent throughout the cortex, resulting in prolonged phases of slow growth in all individuals during which most of the recorded appositional growth was achieved.

Prolonged slow growth might be related to phylogeny (e.g., chelid turtles: Pereyra et al., 2020), endogenous, or exogenous factors (e.g., mammals: Köhler et al., 2012). If endogenous factors (e.g., diseases) are the reason usually only one individual is affected. Thus, for the prolonged slow growth phases, observed in numerous individuals of different taxa from the same locality, is best explained by exogenous factors such as climate and food availability. The pattern observed in the taxa from Krasiejów suggest a moderate climate and maybe a constant but low food availability that does not necessitate complete growth stops. A case study of wild ruminants living across different climatic zones (from polar to tropical) showed a cyclical growth (fast-growing, highly vascularized fibrolamellar bone tissue) with the deposition of LAGs (Köhler et al., 2012). This shows that the mammalian (endothermic) histological growth is not dependent on climatic conditions but rather by endogenous constraints. Hedrick et al. (2020) suggested an initial climate-induced gradient in growth patterns for ceratopsian dinosaurs, but additional sampling of closely-related taxa from geographically similar localities showed marked differences in histology, thus these patterns were most likely phylogenetically induced.

A previous approach was performed, comparing temnospondyl amphibians of the Metoposauridae family, with a similar stratigraphic distribution (Norian/Carnian) but from geographically different localities (Europe, Asia and Africa; Teschner et al., 2020). Climate of the Maleri Formation, yielding the Indian metoposaurids, was reconstructed as warm climate with seasonal rainfalls and the living niches as ephemeral and vegetated swamps or ponds (Dasgupta et al., 2017), similarly to the reconstruction of Polish Krasiejów (Jewuła et al., 2019), however, such study is lacking for the Late Triassic lacustrine deposits of Morocco. The metoposaurids from Poland, India and Morocco showed in general a comparable histology. However, the taxon from Morocco (*Dutuitosaurus ouazzoui*) displayed distinct LAGs that were absent in the Polish *Metoposaurus* and Indian *Panthasaurus*. This could suggest a rather moderate climate, without extreme fluctuations between wet/favourable and dry/unfavourable seasons preserving seasonal periods of wet but not extremely dry periods in Poland (Krasiejów) and India, but a harsher climate in Morocco (Steyer et al., 2004; Konietzko-Meier & Klein, 2013; Teschner et al., 2020), favouring here the deposition of LAGs. It is similarly observed in the herein studied sample. However, the occurrence of sub-cycles and rest lines mainly in the aetosaur sample from Krasiejów, suggests that the environmental influence mostly affected the terrestrial taxon. This corresponds well with the wet and semi-dry climatic conditions as proposed in the climatic model by using analytical methods (Jewuła et al., 2019). Based on our sample, it seemed as if the environmental conditions have had more impact on the terrestrial aetosaur than on the aquatic phytosaur. Moreover, the comparative aetosaur and phytosaur samples described from localities outside Poland (USA, Argentina and Austria), show the deposition of LAGs, absent in the samples from Krasiejów, which indicates an environmental/climatic influence rather than a phylogenetic precursor.

The uninterrupted FLB deposition observed in the dinosauromorph *Silesaurus opolensis* from Krasiejów (Fostowicz-Frelik & Sulej, 2010) would either mean, that the sampled bones represent a very young individual or the silesaurid shows already a strong phylogenetic signal. All dinosaurs, even the basal ones, grew throughout most of their life with FLB (summarized in Chinsamy-Turan, 2005; Erickson, 2014). The strong phylogenetic signal in the growth of *Silesaurus* is confirmed by a similar fast uninterrupted growth in other silesaurids (i.e., *Asilisaurus kongwe* from the Middle Triassic of Tanzania, Griffin & Nesbit, 2016; *Lewisuchus admixus* from the Late Triassic of Argentina, Marsà et al., 2017; *Sacisaurus agudoensis* from Late Triassic of Brasil, Veiga et al., 2019).

Concluding, the preserved alternating pattern of zones and annuli and the absence of LAGs is observed in the poikilotherm temnospondyl amphibian (anamniote), the aetosaur and the phytosaur (amniotes) samples, co-occurring in the Krasiejów locality. This would indicate a stronger local factor influencing the growth, rather than a biological determination of growth. As this is the first study comparing various animal groups from the same locality, it can be proposed, that the external (environmental/climatic) influence was very high on the growth of poikilotherm than on endotherm animals (dinosauromorphs).

Conclusions

The growth pattern of phytosaur *Parasuchus* cf. *arenaceus* and the aetosaur *Stagonolepis olenkae*, both sampled from the locality of

Krasiejów, is very similar and a relative distinction can be made only on the level of vascularization degree (higher in aetosaurs, lower in phytosaurs) and the growth mark expression. The German phytosaur *Nicrosaurus* sp. grew in a similar pattern when compared to the Polish phytosaur *Parasuchus*. However, the *Nicrosaurus* femur shows one LAG in the outer cortex, whereas LAGs are completely absent in sectioned material from Krasiejów. Interestingly, in spite of occupying different ecological niches, bone tissue and growth pattern as well as bone compactness is rather similar in the phytosaur and aetosaur material from Krasiejów. Bone compactness analyses reveal a similar wide spectrum for the terrestrial aetosaurs (76–97%) and the semi-aquatic or aquatic phytosaurs (66–90%), questioning the reliability of compactness data alone to address the lifestyle of a taxon.

The phytosaurs as well as the aetosaur from Krasiejów differ in growth when compared to other phytosaurs (*Rutiodon*, Phytosauria indet., and *Mystriosuchus*) and aetosaurs (*Typothorax, Calyptosuchus* (= *Stagonolepis*), *Desmatosuchus, Coahomasuchus, Aetosauroides*) described from various localities. They differ by the absence of woven bone, the absent change from FLB to LZB, due to the absence of FLB deposition, the lack of LAGs, and by prolonged phases of slow growth. The latter two differences are likely related to exogenous i.e., environmental factors. From this we conclude that the climate in Krasiejów was not very seasonal with the absence of strong fluctuations but rather moderate. Our study supports the observation made before that the environmental (= adaptational) signal can override the phylogenetic signal and that the climate/environmental conditions in Krasiejów had influenced the growth pattern of at least the temnospondyl amphibians and basal archosaurs.

Acknowledgements

We are very grateful to Adam Bodzioch (University of Opole) and to Rainer Schoch (SMNS) for the access to the specimens and the permission for sectioning the material. P. Martin Sander (University of Bonn) is thanked for fruitful discussions. Olaf Dülfer (University of Bonn) is acknowledged for the preparation of the thin sections. Feiko Miedema (SMNS) is thanked for the linguistic improvement of the earlier version of the typescript. We thank the editor Alexandra Anna Enrica van der Geer and the two anonymous reviewers for the useful comments which helped to improve the quality of this paper. This work was supported by the Polish National Science Centre (NCN) grant number: UMO-2016/23/N/ST10/02179 (awarded to EMT).

References

Antczak, M. (2016). Late Triassic aetosaur (Archosauria) from Krasiejów (SW Poland): new species or an example of individual variation? *Geological Journal* 51, 779–788.

Barrett, P.M., Sciscio, L., Viglietti, P.A., Broderick, T.J., Suarez, C.A., Sharman, G.R., Jones, A.S., Munyikwa, D., Edwards, S., Chapelle, K.E.J., Dollman, K.N., Zondo, M. & Choiniere, J.N. (2020). The age of the Tashinga Formation (Karoo Supergroup) in the Mid-Zambezi Basin, Zimbabwe and the first phytosaur from mainland sub-Saharan Africa. *Gondwana Research* 81, 445–460.

Bodzioch, A. & Kowal-Linka, M. (2012). Unravelling the origin of the Late Triassic multitaxic bone accumulation at Krasiejów (S Poland) by diagenetic analysis. *Palaeogeography, Palaeoclimatology, Palaeoecology* 346, 25–36.

Brusatte, S.L., Butler, R.J., Niedźwiedzki, G., Sulej, T., Bronowicz, R. & Satkūnas, J. (2013). First record of

Mesozoic terrestrial vertebrates from Lithuania: phytosaurs (Diapsida: Archosauriformes) of probable Late Triassic age, with a review of phytosaur biogeography. *Geological Magazine* 150, 110–122.

Buffetaut E. (1993). Phytosaurs in time and space. *Pal. Lombarda. Nuov. Ser*. 2, 39–44.

Butler, R.J., Jones, A.S., Buffetaut, E., Mandl, G.W., Scheyer, T.M. & Schultz, O. (2019). Description and phylogenetic placement of a new marine species of phytosaur (Archosauriformes: Phytosauria) from the Late Triassic of Austria. *Zoological Journal of the Linnean Society* 187, 198–228.

Butler, R.J., Rauhut, O.W., Stocker, M.R. & Bronowicz, R. (2014). Redescription of the phytosaurs *Paleorhinus* (*'Francosuchus'*) *angustifrons* and *Ebrachosuchus neukami* from Germany, with implications for Late Triassic biochronology. *Zoological Journal of the Linnean Society* 170, 155–208.

Canoville, A. & Laurin, M. (2009). Microanatomical diversity of the humerus and lifestyle in lissamphibians. *Acta Zoologica* 90, 110–122.

Canoville, A. & Laurin, M. (2010). Evolution of humeral microanatomy and lifestyle in amniotes, and some comments on palaeobiological inferences. *Biological Journal of the Linnean Society* 100, 384–406.

Canoville A., de Buffrénil, V. & Laurin, M. (2016). Microanatomical diversity of amniote ribs: an exploratory quantitative study. *Biological Journal of the Linnean Society* 118, 706–733.

Carroll, R.L. (1988). *Vertebrate Paleontology and Evolution*. W.H. Freeman, San Francisco.

Cerda, I.A. & Desojo, J.B. (2011). Dermal armour histology of aetosaurs (Archosauria: Pseudosuchia), from the Upper Triassic of Argentina and Brazil. *Lethaia* 44, 417–428.

Cerda, I.A., Desojo, J.B. & Scheyer, T.M. (2018). Novel data on aetosaur (Archosauria, Pseudosuchia) osteoderm microanatomy and histology: palaeobiological implications. *Paleontology* 61, 721–745.

Chatterjee, S. (1978). A primitive parasuchid (Phytosaur) reptile from the Upper Triassic Maleri Formation of India. *Paleontology* 21, 83–127.

Chatterjee, S. (2001). *Parasuchus hislopi* Lydekker, 1885 (Reptilia, Archosauria): proposed replacement of the lectotype by a neotype. *Bulletin of Zoological Nomenclature* 58, 34–36.

Chinsamy-Turan A. (2005). *The Microstructure of Dinosaur Bone: Deciphering Biology with Fine-Scale Techniques*. Johns Hopkins University Press, Baltimore.

Cormark, D.H. (1987). *Ham's Histology*, 9th Edition. Lippincott, New York.

Cubo, J., Legendre P., de Ricqlès, A.J., Montes, L. & de Margerie, E. (2008). Phylogenetic, functional, and structural components of variation in bone growth rate of amniotes. *Evolution & Development* 10, 217–227.

Currey, J.D. (2002). *Bones: Structure and Mechanics*. Princeton University Press, Princeton, NJ.

Dasgupta, S., Ghosh, P., & Gierlowski-Kordesch, E.H. (2017). A discontinuous ephemeral stream transporting mud aggregates in a continental rift basin: the Late Triassic Maleri Formation, India. *Journal of Sedimentary Research* 87(8), 838–865.

De Buffrénil, V., de Ricqlès, A. J., Zylberberg, L., & Padian, K. (Eds.). (2021). *Vertebrate Skeletal Histology and Paleohistology*. CRC Press.

De Buffrénil, V. & Rage, J.C. (1993). La «pachyostose» vertébrale de *Simoliophis* (Reptilia, Squamata): données comparatives et considérations fonctionnelles. *Annal. Pal.*, 79, 315–335.

De Ricqlès, A.J., Padian, K. & Horner, J.R. (2003). On the bone histology of some Triassic pseudosuchian archosaurs and related taxa. *Annal. Pal.*, 89, 67–101.

De Ricqlès, A.J., Padian, K., Knoll, F. & Horner, J.R. (2008). On the origin of high growth rates in archosaurs and their ancient relatives: complementary histological studies on Triassic archosauriforms and the problem of a "phylogenetic signal" in bone histology. *Annal. Pal.*, 94, 57–76.

Desojo, J.B., Heckert, A.B., Martz, J.W., Parker, W.G., Schoch, R.R., Small, B.J., & Sulej, T. (2013). Aetosauria: a clade of armoured pseudosuchians from the Upper Triassic continental beds. *Geological Society Special Publication* 379, 203–239.

Desojo, J.B. & Vizcaíno, S.F. (2009). Jaw biomechanics in the South American aetosaur *Neoaetosauroides engaeus*. *Paläontologische Zeitschrift* 83, 499–510.

Dróżdż, D. (2018). Osteology of a forelimb of an aetosaur *Stagonolepis olenkae* (Archosauria: Pseudosuchia: Aetosauria) from the Krasiejów locality in Poland and its probable adaptations for a scratch-digging behavior. *PeerJ*, 6, e5595.

Dzik, J. (2001). A new *Paleorhinus* fauna in the early Late Triassic of Poland. *Journal of Vertebrate Paleontology* 21, 625–627.

Dzik, J. (2003). A beaked herbivorous archosaur with dinosaur affinities from the early Late Triassic of Poland. *Journal of Vertebrate Paleontology* 23, 556–574.

Dzik, J. & Sulej, T. (2007). A review of the early Late Triassic Krasiejów biota from Silesia, Poland. *Phytopathologia Polonica* 64, 3–27.

Dzik, J. & Sulej, T. (2016). An early Late Triassic long-necked reptile with a bony pectoral shield and gracile appendages. *Acta Palaeontologica Polonica* 61, 805–823.

Dzik, J., Sulej, T., Kaim, A. & Niedźwiedzki, R. (2000). Późnotriasowe cmentarzysko kręgowców lądowych w Krasiejowie na Śląsku Opolskim. *Przegląd Geologiczny* 48, 226–235.

Erickson, G. M. (2014). On dinosaur growth. *Annual Review of Earth and Planetary Sciences* 42, 675–697.

Fostowicz-Frelik, Ł. & Sulej, T. (2010). Bone histology of *Silesaurus opolensis* Dzik, 2003 from the Late Triassic of Poland. *Lethaia* 43, 137–148.

Francillon-Vieillot, H., de Buffrénil, V., Castanet, J., Géraudie, J., Meunier, F.J., Sire, J.Y., Zylberberg, L. & de Ricql , A. (1990). Microstructure and mineralization of vertebrate skeletal tissues. Pp. 471–530 in: Carter, J.G. (ed), *Skeletal Biomineralization: Patterns, Processes and Evolutionary Trends*. Van Nostrand Reinhold, New York.

Gądek, K. (2012). Palaeohistology of ribs and clavicle of *Metoposaurus diagnosticus* from Krasiejów (Upper Silesia, Poland). *Opole Sci. Soc. Nat. J.* 45, 39–42.

Germain, D. & Laurin, M. (2005). Microanatomy of the radius and lifestyle in amniotes (Vertebrata, Tetrapoda). *Zool. Script.* 34, 335–350.

Górnicki, S., Antczak, M., & Bodzioch, A. (2021). Aetosaur pes from the Upper Triassic of Krasiejów (Poland), with remarks on taxonomy of isolated bones. In *Annales Societatis Geologorum Poloniae* 91, 389–396.

Gozzi, E. & Renesto, S. (2003). A complete specimen of *Mystriosuchus* (Reptilia, Phytosauria) from the Norian (Late Triassic) of Lombardy (Northern Italy). *Rivista Italiana di Paleontologia e Stratigrafi* 109, 475–498.

Griffin, C.T. & Nesbitt, S.J. (2016). The femoral ontogeny and long bone histology of the Middle Triassic (? late Anisian) dinosauriform *Asilisaurus kongwe* and implications for the growth of early dinosaurs. *Journal of Vertebrate Paleontology* 36, e1111224.

Gruntmejer, K., Konietzko-Meier, D. & Bodzioch, A. (2016). Cranial bone histology of *Metoposaurus krasiejowensis* (Amphibia, Temnospondyli) from the Late Triassic of Poland. *PeerJ*, 4, e2685.

Gruntmejer, K., Konietzko-Meier, D., Marcé-Nogué, J., Bodzioch, A. & Fortuny, J. (2019). Cranial suture biomechanics in *Metoposaurus krasiejowensis* (Temnospondyli, Stereospondyli) from the upper Triassic of Poland. *Journal of Morphology* 280, 1850–1864.

Gruntmejer, K., Bodzioch, A. & Konietzko-Meier, D. (2 21). Mandible histology in *Metoposaurus krasiejowensis* (Temnospondyli, Stereospondyli) from the Upper Triassic of Poland. *PeerJ*, 9, e12218.

Hayashi, S., Houssaye, A., Nakajima, Y., Chiba, K. & Ando, T. (2012). Bone inner structure suggests increasing aquatic adaptations in *Desmostylia* (Mammalia, Afrotheria). *PLoS ONE* 8, e59146.

Heckert, A.B., Viner, T.C. & Carrano, M.T. (2021). A large, pathological skeleton of *Smilosuchus gregorii* (Archosauriformes: Phytosauria) from the Upper Triassic of Arizona, U.S.A., with discussion of the paleobiological implications of paleopathology in fossil archosauromorphs. *Palaeontologia Electronica* 24, 1–21.

Hedrick, B. P., Goldsmith, E., Rivera-Sylva, H., Fiorillo, A. R., Tumarkin-Deratzian, A. R., & Dodson, P. (2020). Filling in gaps in the ceratopsid histologic database: histology of two basal centrosaurines and an assessment of the utility of rib histology in the Ceratopsidae. *Anatomical Record* 303(4), 935–948.

Hoffman, D.K., Heckert, A.B. & Zanno, L.E. (2019). Disparate Growth Strategies within Aetosauria: Novel Histologic Data from the Aetosaur *Coahomasuchus chathamensis*. *Anatomical Record* 302, 1504–1515.

Houssaye, A. (2009) "Pachyostosis" in aquatic amniotes: a review. *Integrative Zoology* 4, 325–340.

Houssaye, A., Mazurier, A., Herrel, A., Volpato, V., Tafforeau, P., Boistel, R. & de Buffrénil, V. (2010). Vertebral microanatomy in squamates: structure, growth and ecological correlates. *Journal of Anatomy* 217, 715–727.

Houssaye, A., Rage, J.C., Bardet, N., Vincent, P., Amaghzaz, M. & Meslouh, S. (2013). New highlights about the enigmatic marine snake *Palaeophis maghrebianus* (Palaeophiidae; Palaeophiinae) from the Ypresian (Lower Eocene) phosphates of Morocco. *Palaeontology* 56, 647–661.

Houssaye, A., Sander, P. & Klein, N. (2016). Adaptive patterns in aquatic amniote bone microanatomy – more complex than previously thought. *Integrative and Comparative Biology* 56, 1349–1369.

Houssaye, A., Tafforeau, P. & Herrel, A. (2014). Amniote vertebral microanatomy – what are the major trends? *Biological Journal of the Linnean Society* 112, 735–746.

Hungerbühler, A. (2000). Heterodonty in the European phytosaur *Nicrosaurus kapffi* and its implications for the taxonomic utility and functional morphology of phytosaur dentitions. *Journal of Vertebrate Paleontology* 20, 31–48.

Hungerbühler, A. (2002). The Late Triassic phytosaur *Mystriosuchus westphali*, with a revision of the genus. *Palaeontology* 45, 377–418.

Hunt, A.P. (1989). Cranial morphology and ecology among phytosaurs. Pp. 349–354 in Lucas, S.G & Hunt, A.P. (Eds.), *Dawn of the Age of Dinosaurs in the American Southwest*. New Mexico Museum of Natural History and Science.

Hunt, A.P. & Lucas, S.G. (1991). *Rioarribasaurus*, a new name for a Late Triassic dinosaur from New Mexico (USA). *Paläontologische Zeitschrift* 65, 191.

Jewuła, K., Matysik, M., Paszkowski, M., & Szulc, J. (2019). The late Triassic development of playa, gilgai floodplain, and fluvial environments from Upper Silesia, southern Poland. *Sedimentary Geology* 379, 25–45.

Jones, A.S. & Butler, R.J. (2018). A new phylogenetic analysis of Phytosauria (Archosauria: Pseudosuchia) with the application of continuous and geometric morphometric character coding. *PeerJ*, 6, e5901.

Kammerer, C.F., Butler, R.J., Bandyopadhyay, S. & Stocker, M.R. (2016). Relationships of the Indian phytosaur *Parasuchus hislopi* Lydekker, 1885. *Papers in Palaeontology* 2, 1–23.

Kawano, S.M., Economy, D.R., Kennedy, M.S., Dean, D., & Blob, R.W. (2016). Comparative limb bone loading in the humerus and femur of the tiger salamander: testing the 'mixed-chain' hypothesis for skeletal safety factors. *Journal of Experimental Zoology* 219, 341–353.

Kimmig, J. (2013). Possible secondarily terrestrial lifestyle in the European phytosaur *Nicrosaurus* *kapffi* (Late Triassic, Norian): a preliminary study. *Bulletin - New Mexico Museum of Natural History and Science* 61, 306–312.

Klein, N., & Sander, P.M. (2007). Bone histology and growth of the prosauropod dinosaur *Plateosaurus engelhardti* (von Meyer 1837) from the Norian bonebeds of Trossingen (Germany) and Frick (Switzerland). *Spec. Pap. Pal.* 77, 169–206.

Klein, N., Sander, M. & Suteethorn, V. (2009). Bone histology and its implications for the life history and growth of the Early Cretaceous titanosaur *Phuwiangosaurus sirindhornae*. *Geological Society Sspecial Publication* 315, 217–228.

Klein, N., Foth, C. & Schoch, R.R. (2017). Preliminary observations on the bone histology of the Middle Triassic pseudosuchian archosaur *Batrachotomus kupferzellensis* reveal fast growth with laminar fibrolamellar bone tissue. *Journal of Vertebrate Paleontology* 37, e1333121.

Klein, N., Houssaye, A., Neenan, J. M. & Scheyer, T. M. (2015). Long bone histology and microanatomy of Placodontia (Diapsida: Sauropterygia). *Contributions to Zoology* 84, 59–84.

Köhler, M., Marín-Moratalla, N., Jordana, X., & Aanes, R. (2012). Seasonal bone growth and physiology in endotherms shed light on dinosaur physiology. *Nature* 487(7407), 358–361.

Konietzko-Meier, D. & Klein, N. (2013). Unique growth pattern of *Metoposaurus diagnosticus krasiejowensis* (Amphibia, Temnospondyli) from the Upper Triassic of Krasiejów, Poland. *Palaeogeography, Palaeoclimatology, Palaeoecology* 370, 145–157.

Konietzko-Meier, D. & Sander, P.M. (2013). Long bone histology of *Metoposaurus diagnosticus krasiejowensis* (Temnospondyli) from the Late Triassic of Krasiejów (Opole, Silesia Region). *Journal of Vertebrate Paleontology* 33, 1003–1018.

Konietzko-Meier, D., Bodzioch, A. & Sander, P.M. (2012). Histological characteristics of the vertebral intercentra of *Metoposaurus diagnosticus* (Temnospondyli) from the Upper Triassic of Krasiejów (Upper Silesia, Poland). *Earth and Environmental Science Transactions of the Royal Society of Edinburgh* 103, 237–250.

Konietzko-Meier, D., Danto, M. & Gądek, K. (2014). The microstructural variability of the intercentra among temnospondyl amphibians. *Biological Journal of The Linnean Society* 112, 747–764.

Konietzko-Meier, D., Gruntmejer, K., Marcé-Nogué, J., Bodzioch, A. & Fortuny, J. (2018). Merging cranial histology and 3D-computational biomechanics: a review of the feeding ecology of a Late Triassic temnospondyl amphibian. *PeerJ* 6, e4426.

Kriloff, A., Germain, D., Canoville, A., Vincent, P. & Sache, M. (2008). Evolution of bone microanatomy of the tetrapod tibia and its use in palaeobiological inference. *Journal of Evolutionary Biology* 21, 807–826.

Laurin, M., Canoville, A. & Germain, D. (2011). Bone microanatomy and lifestyle: a descriptive approach. *Comptes Rendus Palevol* 10, 381–402.

Lees, J.H. (1907). The skull of *Paleorhinus*: a Wyoming phytosaur. *Journal of Geology* 15, 121–151.

Li, C., Wu, X.C., Zhao, L.J., Sato, T. & Wang, L.T. (2012). A new archosaur (Diapsida, Archosauriformes) from the marine Triassic of China. *Journal of Vertebrate Paleontology* 32, 1064–1081.

Lucas, S.G. (1998). Global Triassic tetrapod biostratigraphy and biochronology. *Palaeogeography, Palaeoclimatology, Palaeoecology* 143, 347–384.

Marsà, J.A.G., Agnolín, F.L. & Novas, F. (2017). Bone microstructure of *Lewisuchus admixtus* Romer, 1972 (Archosauria, Dinosauriformes). *Historical Biology* 31, 157–162.

Marsh, O.C. (1884). The classification and affinities of dinosaurian reptiles. *Nature* 31, 68–69.

Mateus, O., Butler, R. J., Brusatte, S. L., Whiteside, J. H. & Steyer, J.-S. (2014). The first phytosaur (Diapsida, Archosauriformes) from the Late Triassic of the Iberian Peninsula. *Journal of Vertebrate Paleontology* 34, 970–975.

Nesbitt, S.J. (2011). The early evolution of archosaurs: relationships and the origin of major clades. *Bulletin of the American Museum of Natural History* 352, 1–292.

Nitsch, E. (2006). Der Keuper. Zeitreise ins Dinosaurierland. *Biologie in unserer Zeit* 36, 374–383.

Parker, W.G., Stocker, M.R. & Irmis, R.B. (2008). A new desmatosuchine aetosaur (Archosauria: Suchia) from the Upper Triassic Tecovas Formation (Dockum Group) of Texas. *Journal of Vertebrate Paleontology* 28, 692–701.

Pereyra, M.E., Bona, P., Cerda, I.A., Jannello, J.M., De La Fuente, M.S. & Desántolo, B. (2020). Growth dynamics and body size evolution of South American long-necked chelid turtles: A bone histology approach. *Acta Palaeontologica Polonica* 65, 535–545.

Ponce, D. A., Desojo, J. B. & Cerda, I. A. (2022). Palaeobiological inferences of the aetosaur *Aetosauroides scagliai* (Archosauria: Pseudosuchia) based on microstructural analyses of its appendicular bones. *Historical Biology*. doi:10.1080/08912963.2022.2035728.

Renesto, S. (2008). Remains of a juvenile phytosaur from the Late Triassic of northern Italy. *Rivista Italiana di Paleontologia e Stratigrafia* 114, 155–160.

Renesto, S. & Paganoni, A. (1998). A phytosaur skull from the Norian (Late Triassic) of Lombardy (northern Italy). *Rivista Italiana di Paleontologia e Stratigrafia* 104, 115–122.

Roberto-Da-Silva, L., Desojo, J.B., Cabreira, S.F., Aires, A.S., Mueller, R.T., Pacheco, C.P. & Dias-Da-Silva, S. (2014). A new aetosaur from the Upper Triassic of the Santa Maria Formation, southern Brazil. *Zootaxa*, 3764, 240–278.

Scheyer, T.M., Desojo, J.B. & Cerda, I.A. (2014). Bone histology of phytosaur, aetosaur, and other archosauriform osteoderms (Eureptilia, Archosauromorpha). *Anatomical Record* 297, 240–260.

Seitz, A.L.L. (1907). Vergleichende Studien über den mikroskopischen Knochenbau fossiler und rezenter Reptilien und dessen Bedeutung für das Wachstum und Umbildung des Knochengewebes im allgemein. *Nova Acta Leop. Abh. Deu. Aka. Naturforsch.*, 37, 230–370.

Small, B.J. (2002). Cranial anatomy of *Desmatosuchus haplocerus* (Reptilia: Archosauria: Aetosauria). *Zoological Journal of the Linnean Society* 136, 97–111.

Steyer, J.S., Laurin, M., Castanet, J. & de Ricqlès, A. (2004). First histological and skeletochronological data on temnospondyl growth: palaeoecological and palaeoclimatological implications. *Palaeogeography, Palaeoclimatology, Palaeoecology* 206, 193–201.

Stocker, M.R. & Butler, R.J. (2013). Phytosauria. In: Nesbitt, S.J., Desojo, J.B.& Irmis, R.B. (Eds.), Anatomy, Phylogeny and Palaeobiology of Early Archosaurs and Their Kin. *Geological Society Special Publications* 379, 91–117.

Stocker, M.R., Zhao, L.J., Nesbitt, S.J., Wu, X.C. & Li, C. (2017). A short-snouted, Middle Triassic phytosaur and its implications for the morphological evolution and biogeography of Phytosauria. *Scientific Reports* 7, 1–9.

Sulej, T. (2005). A new rauisuchian reptile (Diapsida: Archosauria) from the Late Triassic of Poland. *Journal of Vertebrate Paleontology* 25, 78–86.

Sulej, T. (2007). Osteology, variability, and evolution of *Metoposaurus*, a temnospondyl from the Late Triassic of Poland. *Pal. Pol.*, 64, 29–139.

Sulej, T. (2010). The skull of an early Late Triassic aetosaur and the evolution of the stagonolepidid archosaurian reptiles. *Zoological journal of the Linnean Society* 158, 860–881.

Sulej, T., & Majer, D. (2005). The temnospondyl amphibian *Cyclotosaurus* from the Upper Triassic of Poland. *Palaeontology*, 48, 157–170.

Szulc, J. (2005). Sedimentary environments of the vertebrate-bearing Norian deposits from Krasiejów, Upper Silesia (Poland). *Hallesches Jahrbuch für Geowissenschaften* 19, 161–170.

Szulc, J. & Racki, G. (2015). Formacja grabowska: podstawowa jednostka litostratygraficzna kajpru Górnego Śląska. *Przegląd Geologiczny* 63, 103–113.

Szulc, J., Racki, G., Jewuła, K. & Środoń, J. (2015). How many Upper Triassic bone–bearing levels are there in Upper Silesia (southern Poland)? A critical overview of stratigraphy and facies. *Annales Societatis Geologorum Poloniae* 85, 587–626.

Szulc, J., Racki, G. & Bodzioch, A. (2017). Comment on "An early Late Triassic long-necked reptile with a bony pectoral shield and gracile appendages" by Jerzy Dzik and Tomasz Sulej. *Acta Palaeontologica Polonica* 62, 287–288.

Teschner, E.M., Sander, P.M. & Konietzko-Meier, D. (2018). Variability of growth pattern observed in *Metoposaurus krasiejowensis* humeri and its biological meaning. *Journal of Iberian Geology* 44, 99–111.

Teschner, E.M., Chakravorti, S., Sengupta, D.P. & Konietzko-Meier, D. (2020). Climatic influence on the growth pattern of *Panthasaurus maleriensis* from the Late Triassic of India deduced from paleohistology. *PeerJ* 8, e9868.

Veiga, F.H., Botha-Brink, J., Ribeiro, A., Ferigolo, J. & Soares, M.B. (2019). Osteohistology of the silesaurid *Sacisaurus agudoensis* from southern Brazil (Late Triassic) and implications for growth in early dinosaurs. *Anais. Acad. Brasil. Ciênc.*, 91, 1–17 e20180643.

Von Jäger, G.F. (1828). *Über die fossilen Reptilien, welche in Württemberg aufgefunden worden sind.* Stuttgart: Metzler.

Von Meyer, H. (1861). Reptilien aus dem Stubensandstein des oberen Keupers. *Palaeontographica* 7, 253–346.

Walker, A. D. (1961). Triassic reptiles from the Elgin area: *Stagonolepis, Dasygnathus* and their allies. *Philosophical transactions of the Royal Society of London. Series B, Biological Sciences* 244, 103–204.

Witzmann, F., Schoch, R.R., Hilger, A. & Kardjilov, N. (2012). Braincase, palatoquadrate and ear region of the plagiosaurid *Gerrothorax pulcherrimus* from the Middle Triassic of Germany. *Palaeontology*, 55, 31–50.

Woodward, H.N., Horner, J.R. & Farlow, J.O. (2014). Quantification of intraskeletal histovariability in *Alligator mississippiensis* and implications for vertebrate osteohistology. *PeerJ*, 2, e422.